

Functional characterisation of genetic variants associated with malignant hyperthermia

Alan Merritt

Submitted in accordance with the requirements for the degree of Doctor of Philosophy

The University of Leeds

School of Medicine

May 2013

The candidate confirms that the work submitted is his own and that appropriate credit has been given where reference has been made to the work of others.

This copy has been supplied on the understanding that it is copyright material and that no quotation from the thesis may be published without proper acknowledgement

© 2013 The University of Leeds and Alan Merritt

Acknowledgements

First and foremost I would like to thank my supervisors Professor Philip Hopkins, Dr. Patrick Booms and Professor Derek Steele for all they have done throughout my PhD studies. They always made themselves available to provide the advice, support and patience required to make this project a success.

Additionally I would like to thank all members past and present of the MH unit in Leeds. In particular I would like to thank Nickla Fisher and Angela Hedley who provided invaluable support both in and out of the lab. I would also like to thank Dr. Dorota Fiszer, Dr. Marie-Anne Shaw and Dr. Adrian Duke for their insight at various stages of my project. Thank you also to Dr. David Iles for his advice and encouragement to take up a PhD position.

I would also like to thank Professor Paul Allen and all the members of the Department of Anesthesiology at Brigham and Women's hospital in Boston, MA, USA who were all extremely welcoming and supportive during my three-month visit.

Thank you to Dr. Kathryn Stowell and Dr. Keisaku Sato at Massey University, New Zealand for providing the human *RYR1* cDNA construct used extensively in this project.

Thank you to the Merritts for their constant encouragement and support not only throughout the duration of my PhD studies but in everything I have done. They continuously humour me when I talk about what it is I have been doing and are always willing to provide a welcome break from all things science.

And finally thank you to Amy-Leigh Johnson for knowing exactly what I have just been through, for listening to each amended version of every presentation I have given throughout my PhD, reading countless drafts of this thesis and being an endless source of encouragement, enthusiasm and discussion even when dealing with her own PhD-related issues.

Abstract

Mutations in the skeletal muscle sarcoplasmic reticulum calcium release channel (*RYR1*) have been identified in association with malignant hyperthermia (MH) and exertional heat stroke (EHS). MH is a pharmacogenetic disorder in which hypermetabolism is triggered upon exposure to volatile anaesthetics. MH has long been linked with EHS, a life threatening increase in body temperature caused by strenuous exercise in warm climates with both conditions being caused by a deregulation of skeletal muscle calcium homeostasis. The availability of genetic testing in MH is limited to variants that have been proven to alter calcium handling *in vitro*.

In this thesis, data on the functional consequences of seven *RYR1* variants found in association with MH are presented, one of which has also been identified in an EHS patient. Site-directed mutagenesis was used to introduce the variants into a human *RYR1* cDNA clone before expressing wild type and mutant constructs in HEK293 cells. Six of the variants, including the EHS mutation, were found to have an increased sensitivity to caffeine as evidenced through a significant decrease in EC_{50} as well as exaggerated calcium release at low doses of caffeine as compared to wild type controls. For one variant, p.D3986E, an increase in *RYR1* expression was required before the phenotype resembled the other *RYR1* variants, hinting at a more complicated role in MH for this variant.

The functional data presented in this thesis is supportive of the addition of six *RYR1* variants onto the genetic diagnostic panel for MH, increasing the availability of initial genetic testing by 19%. Furthermore, the work presented further supports the link between MH and EHS through the presence of a common *RYR1* variant proven to alter calcium handling. Finally, data obtained for the p.D3986E variant lays the foundation for future studies aiming to identify genetic modifiers of the MH phenotype.

Abbreviations

4-CmC	4-chloro- <i>m</i> -creosol
AICAR	5-aminoimidazole-4-carboxamide ribonucleoside
AM	Acetoxymethyl
AMP	Adenosine monophosphate
AMPK	Adenosine monophosphate kinase
ATP	Adenosine triphosphate
AUC	Area under the curve
bp	Base pairs
BSA	Bovine serum albumin
CaCl ₂	Calcium chloride
CACNA1S	Alpha-1 subunit of the dihydropyridine receptors (gene)
Ca _v 1.1	Alpha-1 subunit of the dihydropyridine receptors (protein)
CCD	Central core disease
cDNA	Complementary deoxyribose nucleic acid
CHCT	Caffeine/halothane contracture test
CI	Confidence intervals
CICR	Calcium-induced calcium release
CMV	Cytomegalovirus
CRAC	Calcium release-activated channel

DAPI	4', 6-diamidino-2-phenylindole
DHPR	Dihydropyridine receptors
DMEM	Dulbecco's modified essential medium
DMSO	Dimethyl sulphoxide
DNA	Deoxyribose nucleic acid
dNTPs	Deoxyribonucleotide triphosphates
<i>E.coli</i>	<i>Escherichia coli</i>
EC	Excitation-contraction
EC ₁₀	10% of the maximal response
EC ₂₅	25% of the maximal response
EC ₅₀	50% of the maximal response
ECCE	Excitation-coupled calcium entry
ECL	Entactin-collagen IV-laminin
EDTA	Ethylenediaminetetraacetic acid
EHS	Exertional heat stroke
EMHG	European malignant hyperthermia group
FBS	Foetal bovine serum
FU	Fluorescence units
GFP	Green fluorescent protein
HEK	Human embryonic kidney

HEPES	4-(2-hydroxyethyl)-1-piperazineethanesulfonic acid
HRP	Horseradish peroxidase
HSV-1	Herpes simplex virus type I
IPTG	Isopropyl- β -thiogalactopyranoside
IVCT	<i>In vitro</i> contracture test
JP-45	Junctional sarcoplasmic reticulum protein 1 (protein)
JSRP1	Junctional sarcoplasmic reticulum protein 1 (gene)
kb	Kilobase
KCl	Potassium chloride
kDa	Kilodalton
LB	Luria-Bertani
LF2000	Lipofectamine-2000
LMP	Low melting point
MEGAWHOP	Mega primer polymerase chain reaction of whole plasmid
MgCl ₂	Magnesium chloride
MgSO ₄	Magnesium sulphate
MH	Malignant hyperthermia
MHAUS	Malignant hyperthermia association of the United States
MHEc	Malignant hyperthermia equivocal for caffeine
MHEh	Malignant hyperthermia equivocal for halothane

MHN	Malignant hyperthermia negative
MHS	Malignant hyperthermia susceptible
MmD	Multiminicore disease
NaCl	Sodium Chloride
NaOH	Sodium hydroxide
NEB	New England Biolabs
NGS	Normal goat serum
nm	nanometre
PBS	Phosphate-buffered saline
PCR	Polymerase chain reaction
PSS	Porcine stress syndrome
PVDF	Polyvinylidene fluoride
Recombineering	Recombinogenic engineering
RSV	Rous sarcoma virus
RYR1	Type I ryanodine receptor
SDS	Sodium dodecyl sulphate
SEM	Standard error of the mean
SERCA	Sarco(endo)plasmic reticulum calcium ATPase
shRNA	Small hairpin ribose nucleic acid
SNPs	Single nucleotide polymorphisms

SOB	Super optimal broth
SOC	Super optimal broth with catabolite repression
SOCE	Store operated calcium entry
SOICR	Store overload-induced calcium release
SR	Sarcoplasmic reticulum
T-Tubules	Transverse tubules
T/E	Trypsin/Ethylenediaminetetraacetic acid
TAE	Tris-acetic acid-ethylenediaminetetraacetic acid
TBS	Tris-buffered saline
TBST	Tris-buffered saline with tween
TE	Tris-Ethylenediaminetetraacetic acid
TG	Tris-glycine
TGS	Tris-glycine-sodium dodecyl sulphate
TM	Transmembrane
UV	Ultraviolet
v/v	Volume per volume
w/v	Weight per volume

Table of Contents

Acknowledgements	iii
Abstract	iv
Abbreviations	v
Table of Contents	x
List of Tables	xvi
List of Figures	xvii
Chapter One - Introduction	1
1.1 First reported case of malignant hyperthermia	1
1.2 Symptoms and treatment of MH	1
1.3 The <i>in vitro</i> contracture test	3
1.4 The genetics of MH	4
1.4.1 Porcine stress syndrome.....	4
1.4.2 The type 1 ryanodine receptor (<i>RYR1</i>)	6
1.4.2.1 Structure and function of <i>RYR1</i>	6
1.4.2.2 Mutations in <i>RYR1</i> associated with MH.....	9
1.4.2.2.1 Types of mutation found in <i>RYR1</i> associated with MH.....	9
1.4.2.2.2 Expression levels of <i>RYR1</i> and its role in MH pathogenesis.....	10
1.4.2.2.3 Mutation hot-spots associated with MH	11
1.5 <i>RYR1</i> variants and their role in the pathogenesis of MH.....	13
1.5.1 Structural defects in the <i>RYR1</i> protein	13
1.5.2 Physiological defects caused by mutations in <i>RYR1</i> associated with MH.....	14
1.5.2.1 Store operated calcium entry	14
1.5.2.2 Excitation-coupled calcium entry	15
1.5.2.3 Sensitivity to calcium activation and magnesium inhibition	15
1.6 Additional conditions associated with mutations in <i>RYR1</i>	18
1.6.1 Central Core Disease.....	18
1.6.2 Exertional heat stroke.....	21
1.7 Genetic heterogeneity of MH	23
1.7.1 The alpha 1 subunit of the dihydropyridine receptor (<i>Ca_v1.1</i>).....	23
1.7.2 Junctional sarcoplasmic reticulum protein (<i>JP-45</i>)	24
1.8 Genetic diagnosis of MH	25
1.8.1 EMHG guidelines for inclusion onto the genetic diagnostic panel for MH.....	28
1.8.1.1 Functional characterisation of genetic variants using <i>ex vivo</i> samples	28
1.8.1.2 Functional analysis of genetic variants in <i>in vitro</i> expression systems.....	30
1.8.1.2.1 Development of a muscle-like <i>in vitro</i> expression system for functional experiments and differences with non-native cell types.....	31
1.8.1.2.3 Knowledge gained from non-native cell types	32

1.9 Project Outline	35
1.9.1 Functional characterisation of genetic variants associated with MH.....	35
1.9.2 Evaluation of the use of non-native cell types for functional experiments of <i>RYR1</i> variants	36
1.9.3 Evaluation of <i>RYR1</i> expression level on caffeine sensitivity of transfected cells.....	36
1.9.4 Functional characterisation of a genetic variant associated with MH and EHS.....	37
1.9.5 Clinical relevance of the project goals	37
Chapter Two - Materials and Methods	39
2.1 Molecular cloning	39
2.1.1 Restriction endonuclease digests	39
2.1.1.1 Removing overhangs	40
2.1.2 Gel extraction	40
2.1.3 Ligation	40
2.1.4 Transformation of <i>E.coli</i>	41
2.1.5 Overnight cultures	42
2.1.5.1 Mini-prep overnight cultures.....	42
2.1.5.2 Maxi-prep overnight cultures	42
2.1.6 Glycerol stocks.....	42
2.1.7 Plasmid DNA extraction	43
2.1.7.1 Mini-prep plasmid DNA extraction	43
2.1.7.2 Maxi-prep plasmid DNA extraction	44
2.1.8 DNA quantification	44
2.1.9 Purification	44
2.1.10 Polymerase chain reaction	45
2.1.11 MEGAWHOP	47
2.1.12 Electrophoresis	48
2.1.13 Sequencing	51
2.2 Materials for cell culture	51
2.2.1 Defrosting the cell lines	52
2.2.2 Maintenance of cells.....	52
2.2.3 Passaging the cell lines	52
2.2.4 Freezing the cell lines	53
2.2.5 Cell counting	53
2.2.5.1 Trypan blue viability stain.....	53
2.2.6 Stable transfection of HEK293 cells	54
2.2.7 Transient transfection of HEK293 cells	55
2.2.7.1 pTUNERYR1 expression induction	56
2.2.7.1.1 Treatment with AICAR	57
2.2.8 HSV-1 viral packaging	58
2.2.8.1 Preparation of 2-2 cells and viral packaging.....	58
2.2.8.2 Harvesting HSV-1 virions	60
2.2.8.3 Preparation of 2-2 cells for HSV-1 virion titration	61

2.2.8.4 Preparation of 1B5 cells for HSV-1 virion titration	61
2.2.8.5 Immunocytochemistry assay	62
2.2.8.6 Differentiation of 1B5 cells and C2C12 cells	62
2.2.9 Transfection of 1B5 cells.....	63
2.3 Protein	63
2.3.1 Protein extraction	64
2.3.2 Protein quantification using a Bradford assay	64
2.3.3 Protein detection.....	65
2.3.3.1 Polyacrylamide gel electrophoresis.....	65
2.3.3.2 Western blotting.....	66
2.3.3.3 Western blot data analysis	67
2.4 Caffeine-induced calcium release experiments	67
2.5 Data analysis	70
2.5.1 ImageJ.....	70
2.5.2 Dose-response analysis.....	70
2.5.3 Area under the curve measurements	71
2.5.4 Statistical analysis.....	71
Chapter Three - Selection and cloning of <i>RYR1</i> variants.....	72
3.1 Introduction	72
3.1.1 EHMG guidelines	72
3.1.2 Functional analysis of <i>RYR1</i> variants using recombinant methods	73
3.1.3 Subcloning <i>RYR1</i>	73
3.1.4 Native Vs. Non-native environment	74
3.1.5 Differential expression of <i>RYR1</i> constructs in cellular systems	75
3.2 Aims of the chapter	76
3.3 Results	77
3.3.1 Selection of <i>RYR1</i> variants for this project	77
3.3.2 Cloning using <i>pcRYR1</i>	79
3.3.2.1 Creation of the 3' subclone of <i>RYR1</i>	79
3.3.2.2 Creation of the 5' subclone of <i>RYR1</i>	81
3.3.2.3 MEGAWHOP site-directed mutagenesis.....	83
3.3.2.4 Reconstruction of full-length mutant <i>pcRYR1</i> constructs using the 3' subclone.....	86
3.3.3 Cloning in pHSVPrPUC	88
3.3.4 Cloning in pTUNE	92
3.3.4.1 Removal of the <i>BspEI</i> site from pTUNE	92
3.3.4.2 Creation of the pTUNE subclone	94
3.3.4.3 Construction of full-length pTUNERYR1 constructs.....	96
3.4 Discussion	99
3.4.1 Selection of <i>RYR1</i> variants	100
3.4.2 Subcloning <i>RYR1</i>	102
3.4.3 Mutagenesis of <i>RYR1</i> subclones	103
3.4.4 The requirement of multiple expression vectors	104

3.5 Future work.....	105
3.6 Conclusions	107
Chapter Four - Functional analysis of genetic variants in the <i>RYR1</i> gene associated with malignant hyperthermia in HEK293 cells	108
4.1 Introduction	108
4.1.1 Variants in <i>pcRYR1</i>	108
4.1.1.1 p.R2336H worldwide	109
4.1.1.2 p.V4849I worldwide	110
4.1.2 The variants in the UK population	110
4.2 Aims of the chapter	111
4.3 Results	112
4.3.1 HEK293 cells stably transfected with <i>pcRYR1</i> constructs	112
4.3.1.1 Antibiotic kill curve	112
4.3.1.2 Caffeine-induced calcium release of stably transfected HEK293 cells	113
4.3.1.3 EC ₁₀ and EC ₂₅ of cells transfected with the wild type and p.D3986E constructs.....	119
4.3.1.4 Area under the curve measurements of cells stably transfected with <i>pcRYR1</i> constructs	119
4.3.2 HEK293 cells transiently transfected with <i>pcRYR1</i> constructs	121
4.3.2.1 Caffeine-induced calcium release from HEK293 cells transiently transfected with <i>pcRYR1</i> constructs	121
4.3.2.2 Area under the curve measurements of cells transiently transfected with <i>pcRYR1</i> constructs	125
4.3.2.3 Expression analysis of HEK293 cells transfected with <i>pcRYR1</i> constructs.....	126
4.3.3 Comparison of stable and transient transfection of HEK293 cells.....	128
4.4 Discussion	131
4.4.1 p.R2336H	132
4.4.2 p.E3104K.....	132
4.4.3 p.G3990V	133
4.4.4 p.D3986E	134
4.4.5 p.V4849I.....	135
4.4.6 Stable vs. Transient transfection	136
4.4.7 G418 selection of stable HEK293 cell lines expressing <i>pcRYR1</i> constructs.....	137
4.4.8 Measurement of HEK293 cell background	138
4.4.9 The calcium transient videos	139
4.5 Future work.....	139
4.6 Conclusions	141
Chapter Five - Functional analysis of genetic variants in the <i>RYR1</i> gene associated with malignant hyperthermia in 1B5 cells.	143
5.1 Introduction	143
5.1.1 EMHG Guidelines and the use of non-native cells for functional analysis	143

5.1.2 The development of a dyspedic myoblast cell line for use in functional studies of <i>RYR1</i> variants	143
5.1.2.1 Development of a viral method of transducing dyspedic myotubes with <i>RYR1</i> variants for functional studies.....	144
5.1.3 Potential differences between HEK293 cells and 1B5 cells	145
5.1.4 Variants in pHSV <i>RYR1</i>	147
5.2 Aims of the chapter	147
5.3 Results	148
5.3.1 Titration of HSV-1 virions.....	148
5.3.1.1 Titration using immunofluorescence.....	148
5.3.1.2 Titration using calcium release assays.....	149
5.3.2 Caffeine-induced calcium release of 1B5 myotubes infected with HSV-1 virions ..	152
5.3.3 Control experiments to test the ability of 2-2 cells and the cosmid set to package HSV-1 virions	154
5.3.4 Use of conventional transfection agents on 1B5 dyspedic myotubes.....	155
5.4 Discussion	157
5.4.1 Difficulties in generating a high titre of HSV-1 virions containing wild type and mutant <i>RYR1</i> constructs	157
5.4.2 The use of conventional transfection methods on dyspedic myotubes.....	159
5.5 Future work.....	160
5.6 Conclusions	161
Chapter Six - Functional analysis of genetic variants in the <i>RYR1</i> gene associated with malignant hyperthermia and exertional heat stroke using the pTUNE inducible expression vector.....	162
6.1 Introduction	162
6.1.1 p.D1056H	163
6.1.1.1 Exertional heat stroke and MH.....	164
6.1.2 p.R2355W	165
6.1.3 p.D3986E	166
6.2 Aims of the chapter	166
6.3 Results	167
6.3.1 Caffeine-induced calcium release.....	167
6.3.2 EC ₁₀ and EC ₂₅ of HEK293 cells transfected with the p.D3986E variant	172
6.3.3 Area under the curve measurements of HEK293 cells transfected with pTUNERYR1 constructs	173
6.3.4 Differential expression of pTUNERYR1 constructs.....	175
6.3.5 Area under the curve measurements of HEK293 cells expressing wild type and mutant <i>RYR1</i> at different levels.....	178
6.3.6 The effect of AICAR on the sensitivity of HEK293 cells transfected with pTUNERYR1 constructs to caffeine	181

6.3.7 Viability stain of HEK293 cells transfected with pTUNERYR1 and treated with IPTG and AICAR	183
6.3.8 Comparison between cells transfected with pcRYR1 and pTUNERYR1 cDNA constructs	185
6.3.9 Detection of RYR1 expression through western blotting	186
6.3.9 Comparison of wild type RYR1 in pcDNA and pTUNE expression vectors	188
6.4 Discussion	189
6.4.1 p.D1056H	190
6.4.2 p.R2355W	191
6.4.3 p.D3986E	192
6.4.5 The effect of AICAR on the sensitivity of RYR1 channels	193
6.4.6 Wild types and p.D3986E in pcRYR1 and pTUNERYR1	196
6.5 Future work	196
6.6 Conclusions	197
Chapter Seven - Final discussion	199
7.1 Introduction	199
7.1.1 Cloning and mutagenesis	200
7.1.2 Causative MH variants	200
7.1.3 The role of the p.D3986E variant in MH pathogenesis	201
7.1.4 p.D1056H, EHS and MH	203
7.2 Future work	204
7.2.1 Functional characterisation of further genetic variants	204
7.2.2 Native vs. non-native environment for functional studies	204
7.3 Final conclusions	205
Chapter Eight – References	207

List of Tables

TABLE 1.1 – GENETIC VARIANTS IN *RYR1* ASSOCIATED WITH EXERTIONAL HEAT STROKE AND EXERTIONAL RHABDOMYOLYSIS 22

TABLE 1.2 – LIST OF GENES AND GENETIC LOCI ASSOCIATED WITH MH 24

TABLE 2.1 – PRIMERS TO SCREEN FOR SUCCESSFUL GENERATION OF THE VARIOUS SUBCLONES CREATED IN THIS PROJECT 46

TABLE 2.2 – LIST OF PRIMERS USED FOR MUTAGENESIS AND MUTATION SITE SCREENING 49

TABLE 2.3 – RATIOS OF EACH COSMID REQUIRED FOR HSV-1 VIRAL PACKAGING 59

TABLE 2.4 – RECIPE FOR THE POLYACRYLAMIDE GELS MADE IN THIS PROJECT 66

TABLE 2.5 – AGONIST CONCENTRATIONS USED FOR THE CALCIUM RELEASE ASSAYS IN THIS PROJECT .. 69

TABLE 3.1 – DIFFERENCES BETWEEN HUMAN AND RABBIT *RYR1* SEQUENCES..... 74

TABLE 3.2 – LIST OF VARIANTS CHOSEN FOR THIS PROJECT. 77

TABLE 3.3 – AMINO ACID PROPERTIES OF THE VARIANTS SELECTED FOR STUDY IN THIS PROJECT. 78

TABLE 3.4 – MEGAWHOP MUTAGENESIS SUCCESS RATE..... 84

TABLE 5.1 – CALCULATION OF THE EFFICIENCY OF INFECTION OF WILD TYPE AND P.R2336H PHSVRYR1 VIRIONS. 150

List of Figures

FIGURE 1.1 – STATIC HALOTHANE IVCT TRACES.....	5
FIGURE 1.2 – SCHEMATIC REPRESENTATION OF ONE SUBUNIT OF THE RYR1 PROTEIN TETRAMER	7
FIGURE 1.3 – SCHEMATIC SHOWING EXCITATION-CONTRACTION COUPLING IN SKELETAL MUSCLE.....	8
FIGURE 1.4 – THE EVOLUTION OF THE <i>RYR1</i> MUTATION HOT SPOT	12
FIGURE 1.5 – SCHEMATIC OF THE STORE OPERATED CALCIUM ENTRY MECHANISM.....	16
FIGURE 1.6 – SCHEMATIC OF THE EXCITATION-COUPLED CALCIUM ENTRY MECHANISM IN SKELETAL MUSCLE.....	17
FIGURE 1.7 – MECHANISMS THAT LEAD TO THE CENTRAL CORE DISEASE PATHOGENESIS	20
FIGURE 1.8 – FLOWCHART OUTLINING THE CURRENT PROCESS FOR THE DIAGNOSIS OF MH	27
FIGURE 1.9 – SCHEMATIC OF STORE OVERLOAD-INDUCED CALCIUM RELEASE FROM THE SARCOPLASMIC RETICULUM THROUGH WILD TYPE AND MUTANT RYR1.....	34
FIGURE 2.1 – MEGAWHOP MUTAGENESIS.....	50
FIGURE 2.2 – INDUCTION OF PTUNERYR1 CONSTRUCTS.....	57
FIGURE 2.3 – STRATEGY USED TO PACKAGE PHSVRYR1 CONSTRUCTS INTO HSV-1 VIRIONS.....	60
FIGURE 2.4 – CONFOCAL MICROSCOPE SET UP FOR CALCIUM RELEASE MEASUREMENTS.....	69
FIGURE 3.1 – CREATION OF THE 3' SUBCLONE OF <i>RYR1</i>	80
FIGURE 3.2 – DIGEST AND SEQUENCE CONFIRMATION OF THE 3' SUBCLONE.....	81
FIGURE 3.3 – CREATION OF THE 5' SUBCLONE OF <i>RYR1</i>	82
FIGURE 3.4 – DIGESTION CONFIRMATION OF THE CREATION OF THE 5' SUBCLONE OF <i>RYR1</i>	83
FIGURE 3.5 – SEQUENCE CONFIRMATION OF SUCCESSFUL MUTAGENESIS.....	85
FIGURE 3.6 – RECONSTRUCTION OF FULL-LENGTH MUTANT PCRYR1 CONSTRUCTS.....	86
FIGURE 3.7 – DIGEST AND SEQUENCE CONFIRMATION OF FULL-LENGTH PCRYR1 CONSTRUCTS	87
FIGURE 3.8 – SUCCESSFUL RECONSTRUCTION OF PCRYR1 CONSTRUCTS.....	88
FIGURE 3.9 – PHSVRYR1 CLONING STRATEGY.....	89
FIGURE 3.10 – DIGEST AND SEQUENCE CONFIRMATION OF PHSVRYR1 CONSTRUCTS.....	91
FIGURE 3.11 – PHSVRYR1 CDNA CONSTRUCTS GENERATED IN THIS STUDY.....	92
FIGURE 3.12– REMOVAL OF AN ENDOGENOUS <i>BSPEI</i> RESTRICTION SITE IN PTUNE.....	93
FIGURE 3.13 – CONSTRUCTION OF THE PTUNE SUBCLONE.....	94
FIGURE 3.14 – DIGEST AND SEQUENCE CONFIRMATION OF PTUNE SUBCLONE CONSTRUCTS	95
FIGURE 3.15 – GEL IMAGE OF PTUNE SUBCLONE CONSTRUCTS SUCCESSFULLY GENERATED IN THIS PROJECT.....	96
FIGURE 3.16 – CONSTRUCTION OF FULL-LENGTH PTUNERYR1 CONSTRUCTS.....	97
FIGURE 3.17 – DIGEST AND SEQUENCE CONFIRMATION OF PTUNERYR1 CONSTRUCTS.....	98
FIGURE 3.18 – FULL-LENGTH PTUNERYR1 CONSTRUCTS DIGESTED WITH <i>ACC65I</i>	99
FIGURE 4.1 – ANTIBIOTIC KILL CURVE FOR HEK293 CELLS EXPOSED TO G418 OVER A PERIOD OF 10 DAYS.	112
FIGURE 4.2 – Ca^{2+} RELEASE FROM A HEK293 CELL UPON STIMULATION WITH 1MM CAFFEINE.....	114
FIGURE 4.3 – THE RESPONSE OF UNTRANSFECTED HEK293 CELLS TO CAFFEINE.....	115
FIGURE 4.4 – REPRESENTATIVE TRACES OF HEK293 CELLS STABLY TRANSFECTED WITH WILD TYPE AND MUTANT PCRYR1 CONSTRUCTS.....	116
FIGURE 4.5 – CAFFEINE DOSE-RESPONSE FOR HEK293 CELLS STABLY TRANSFECTED WITH WILD TYPE AND MUTANT PCRYR1 CONSTRUCTS.....	118

FIGURE 4.6 – EC ₁₀ AND EC ₂₅ CALCULATIONS FOR CELLS STABLY TRANSFECTED WITH WILD TYPE OR P.D3986E PCRYR1 CONSTRUCTS.	119
FIGURE 4.7 – AREA UNDER THE CURVE MEASUREMENTS OF HEK293 CELLS STABLY TRANSFECTED WITH PCRYR1 CONSTRUCTS.....	121
FIGURE 4.8 – REPRESENTATIVE TRACES OF CAFFEINE-INDUCED CALCIUM RELEASE OF CELLS TRANSIENTLY TRANSFECTED WITH WILD TYPE AND MUTANT PCRYR1 CDNA CONSTRUCTS.	122
FIGURE 4.9 – CAFFEINE DOSE-RESPONSE FOR HEK293 CELLS TRANSIENTLY TRANSFECTED WITH WILD TYPE AND MUTANT PCRYR1 CONSTRUCTS.	124
FIGURE 4.10 – AREA UNDER THE CURVE MEASUREMENTS OF PCRYR1 CONSTRUCTS TRANSIENTLY TRANSFECTED INTO HEK293 CELLS.	126
FIGURE 4.11 – WESTERN BLOT ANALYSIS OF HEK293 CELLS TRANSIENTLY TRANSFECTED WITH WILD TYPE AND MUTANT PCRYR1 CONSTRUCTS	127
FIGURE 4.12 – WESTERN BLOT ANALYSIS OF HEK293 CELLS TRANSIENTLY TRANSFECTED WITH WILD TYPE AND MUTANT PCRYR1 CONSTRUCTS	127
FIGURE 4.13 – COMPARISON OF THE EC ₅₀ OF HEK293 CELLS STABLY OR TRANSIENTLY TRANSFECTED WITH WILD TYPE AND P.G3990V PCRYR1 CONSTRUCTS.....	130
FIGURE 4.14 – COMPARISON OF THE AREA UNDER THE CURVE RESPONSES FOR CELLS EITHER TRANSIENTLY OR STABLY TRANSFECTED WITH WILD TYPE OR P.G3990V PCRYR1 CDNA CONSTRUCTS.	131
FIGURE 5.1 – TITRATION OF HARVESTED WILD TYPE, P.R2336H AND P.D3986E HSV-1 VIRIONS USING IMMUNOCYTOCHEMISTRY ON 2-2 CELLS.	148
FIGURE 5.2 – TITRATION OF HSV-1 VIRIONS USING 1B5 CELLS EXPOSED TO CAFFEINE.....	151
FIGURE 5.3 – TIME LAPSE IMAGE OF 1B5 MYOTUBES RELEASING CALCIUM UPON EXPOSURE TO 20MM CAFFEINE.	152
FIGURE 5.4 – CAFFEINE-INDUCED CALCIUM RELEASE EXPERIMENTS ON 1B5 CELLS INFECTED WITH HSV-1 VIRIONS CONTAINING WILD TYPE OR P.R2336H RYR1	153
FIGURE 5.5 – CONTROL EXPERIMENTS CARRIED OUT TO TEST THE 34C ANTIBODY AND THE PACKAGING PROTOCOL.....	154
FIGURE 5.6 – TRACES OF DYSPEPIC MYOTUBES TRANSFECTED WITH WILD TYPE PCRYR1 USING LF2000 AND XFECT POLYMER.....	156
FIGURE 6.1 – UNTRANSFECTED HEK293 CELLS AND UNINDUCED PTUNE CONSTRUCTS IN HEK293 CELLS.	168
FIGURE 6.2 – REPRESENTATIVE TRACES OF HEK293 CELLS TRANSFECTED WITH DIFFERENT PTUNERYR1 CONSTRUCTS RELEASING CALCIUM WHEN EXPOSED TO INCREMENTAL DOSES OF CAFFEINE.	169
FIGURE 6.3 – CAFFEINE DOSE-RESPONSE ANALYSIS OF CELLS TRANSFECTED WITH WILD TYPE, P.D1056H, P.R2355W AND P.D3986E PTUNERYR1 CONSTRUCTS.....	171
FIGURE 6.4 – EC ₁₀ AND EC ₂₅ ANALYSIS OF CELLS TRANSFECTED WITH WILD TYPE AND P.D3986E PTUNERYR1.	173
FIGURE 6.5 – AREA UNDER THE CURVE MEASUREMENTS OF HEK293 CELLS TRANSFECTED WITH PTUNERYR1 CONSTRUCTS, INDUCED WITH 25μM IPTG FOR 72 HOURS AND EXPOSED TO INCREMENTAL DOSES OF CAFFEINE.....	174
FIGURE 6.6 – THE EFFECT OF INCREASED AND DECREASED EXPRESSION ON THE EC ₅₀ OF CELLS TRANSFECTED WITH PTUNERYR1 CONSTRUCTS.	177
FIGURE 6.7 – DIFFERENTIAL EXPRESSION OF THE P.R2355W AND P.D3986E VARIANTS AND THE SUBSEQUENT EC ₅₀	178

FIGURE 6.8 – AREA UNDER THE CURVE MEASUREMENTS OF HEK293 CELLS TRANSIENTLY TRANSFECTED WITH PTUNERYR1 CONSTRUCTS AND INDUCED TO DIFFERING LEVELS OF EXPRESSION. 179

FIGURE 6.9 – THE EFFECT OF AICAR ON THE EC₅₀ OF CELLS TRANSFECTED WITH PTUNERYR1 CONSTRUCTS. 182

FIGURE 6.10 – VIABILITY STAIN OF CELLS TRANSFECTED WITH PTUNERYR1 AND TREATED WITH IPTG AND AICAR. 184

FIGURE 6.11 – A COMPARISON OF THE RESPONSE OF WILD TYPE AND P.D3986E RYR1 IN THE PCDNA AND PTUNE EXPRESSION VECTORS. 185

FIGURE 6.12 – WESTERN BLOT ANALYSIS OF HEK293 CELLS TRANSIENTLY TRANSFECTED WITH PTUNERYR1 CONSTRUCTS. 186

FIGURE 6.13 – RELATIVE QUANTITY OF RYR1 WHEN PTUNERYR1 CONSTRUCTS ARE POOLED INTO THEIR RESPECTIVE IPTG CONCENTRATIONS. 187

FIGURE 6.14 – WESTERN BLOT ANALYSIS OF HEK293 CELLS TRANSIENTLY TRANSFECTED WITH PTUNERYR1 CONSTRUCTS AND EXPOSED TO AICAR. 188

FIGURE 6.15 – A COMPARISON OF ALL WILD TYPE RYR1 CONSTRUCTS AND CONDITIONS USED IN THIS THESIS. 189

Chapter One - Introduction

1.1 First reported case of malignant hyperthermia

Malignant hyperthermia (MH) is a rare, pharmacogenetic disorder in which volatile, inhalational anaesthetics and depolarising muscle relaxants trigger a hypermetabolic reaction in susceptible individuals. The first case of MH was reported in a previously healthy 21-year-old male who underwent surgery to repair a fractured tibia and fibula (Denborough et al., 1962). The patient reported that a number of his family had died during surgery when anaesthetised using ether. The surgery went ahead cautiously using halothane instead, however, ten minutes into the operation, the patient began having what would soon become recognised as an MH crisis. The blood pressure of the patient dropped, his pulse rose and temperature increased rapidly, the surgery was concluded quickly, the use of halothane was discontinued and aggressive cooling procedures commenced resulting in the recovery of the patient over a period of 90 minutes.

1.2 Symptoms and treatment of MH

In the years since the first reported case, the pathogenesis of an MH crisis has become better defined. Early clinical features include masseter spasm, tachypnoea and tachycardia, which are often followed by an increase in temperature, cyanosis and generalised muscle rigidity. Additional symptoms include an increased creatine kinase level, rhabdomyolysis, hyperkalaemia, hypoxaemia, metabolic and respiratory acidosis and, if not treated promptly, death (Hopkins, 2000). The number, severity and onset of symptoms that manifest during an MH crisis vary between patients and are partly dependent on the duration of anaesthesia, type of anaesthetic used and the patient themselves. Additionally, previous, uneventful anaesthesia is not an indicator of being unsusceptible to MH; in some instances an MH reaction occurs after several anaesthetics with triggering drugs. During an MH crisis, the most frequently observed

sign is respiratory acidosis. There are a median of four clinical signs present with hypercarbia, masseter spasm and tachycardia the most common first signs of a reaction, which, in many cases, begin less than a minute after the induction of anaesthesia (Larach et al., 2010).

The symptoms triggered by an MH episode can be attributed to a deregulation of calcium homeostasis in skeletal muscle (MacLennan and Phillips, 1992, Ryan et al., 1994, Hopkins, 2000). MH-inducing anaesthetics trigger uncontrolled calcium release from the sarcoplasmic reticulum (SR) of the muscle cells resulting in muscle contracture and the associated muscle rigidity observed in MH patients. Cellular systems for the sequestration of calcium are eventually overwhelmed. Adenosine triphosphate (ATP) is required to pump intracellular calcium back into the SR stores. As this happens, it is broken down into adenosine diphosphate and inorganic phosphate which stimulates glycolysis and oxidative phosphorylation. The depletion of ATP during this process also stimulates the respiratory systems to produce more ATP, further increasing metabolism. Hypermetabolic activity results in respiratory and lactic acidosis and an excess of heat production which feeds back causing a further increase in metabolic activity.

To date, the only commercially available drug to tackle an MH reaction during anaesthesia is dantrolene (Kolb et al., 1982). Dantrolene dramatically reverses the symptoms of patients undergoing an MH crisis during anaesthesia whilst possessing relatively little side effects. Dantrolene prevents an MH reaction through the reduction of the baseline resting calcium level of muscle fibres, which in MH susceptible muscle is elevated above a wild type level (Lopez et al., 1985a, Lopez et al., 1985b, Lopez et al., 1988). Following the introduction of dantrolene, mortality rates from MH dropped from 75% of patients experiencing an MH crisis to around 2-3% (Jurkat-Rott et al., 2000). Nevertheless, a reliable way of screening patients preoperatively for MH is not available, unless the family is already under investigation

by an MH unit and MH therefore, still presents a serious threat to otherwise healthy patients undergoing general anaesthesia.

1.3 The *in vitro* contracture test

The *in vitro* contracture test (IVCT) is the current gold standard method used to diagnose susceptibility to MH in which muscle biopsy specimens are exposed to incremental doses of caffeine and halothane as a diagnostic indicator of probands and their families who have suffered an MH crisis (Kalow, 1970, Ellis et al., 1971). The European Malignant Hyperthermia Group (EMHG) uses a standardised protocol for three procedures carried out on viable muscle specimens of patients under investigation for MH (Ellis, 1984). Static tests for both caffeine and halothane are performed by exposing muscle specimens to incremental concentrations of the stimulant (0.25mM to 4mM for caffeine and 0.5% volume per volume (v/v) to 2% v/v for halothane). Successive concentrations are added after the specimen has reached a contracture plateau from the previous stimulation (Figure 1.1). In the dynamic halothane test, a muscle specimen is exposed to the same incremental concentrations of halothane but they are added at the end of a cycle consisting of stretching the muscle at a rate of 4mm per minute for 90 seconds, holding the muscle at this tension and releasing at the same speed. A positive diagnosis of an MH susceptible (MHS) individual is made on the basis of the muscle samples giving a sustained contracture of 0.2g at or below 2mM caffeine or 2% halothane for all tests. An MH normal (MHN) diagnosis is given if this criterion is not met. A third diagnosis of MH equivocal is given if the contracture is met for only one of the caffeine or halothane tests (MHEc and MHEh respectively).

The malignant hyperthermia association of the United States (MHAUS) uses a different protocol for the diagnosis of MH termed the caffeine/halothane contracture test (CHCT) but still takes advantage of the sensitivity of MH muscle to halothane and caffeine (Rosenberg, 1989, Melton et al., 1989, Larach, 1989). The CHCT involves a

single exposure to 3% halothane as well as incremental doses of caffeine similar to the EMHG IVCT. A positive diagnosis is given when the muscle specimen reacts with a minimal contracture of 0.5g at a concentration of 3% for halothane or 0.2g at 2mM caffeine.

An additional test, which can be optionally included as part of the EMHG IVCT protocol, is the ryanodine test (Hopkins et al., 1991b). This involves the exposure of fresh muscle specimens to ryanodine, a plant alkaloid that shows dose dependent responses in normal skeletal muscle from both rats and pigs (Sutko et al., 1997). The muscle specimen is held in a bath containing 1 μ M of Krebs solution. A positive test is one in which a contraction is observed in the presence of ryanodine.

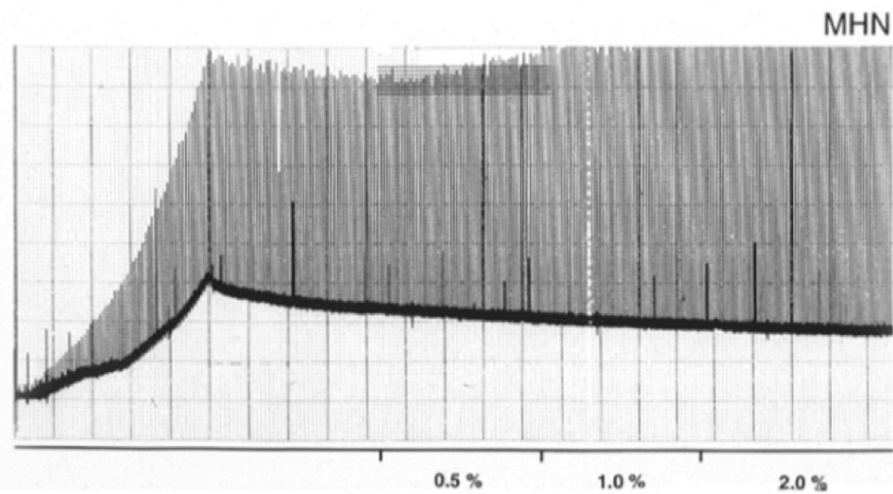
1.4 The genetics of MH

1.4.1 Porcine stress syndrome

Pigs suffer a similar reaction to human MH, called porcine stress syndrome (PSS) when exposed to high levels of stress encountered before slaughter as well as with MH-triggering drugs (Otsu et al., 1994, Mitchell and Heffron, 1982). Similarly to MH, PSS is caused by a deregulation of calcium homeostasis in skeletal muscle, more specifically a hypersensitive gating of the calcium release channel of skeletal muscle (O'Brien, 1986b, O'Brien, 1986a). Isolation of a partial fragment of the skeletal muscle calcium release channel, the type 1 ryanodine receptor (*RYR1*) mapped the gene to porcine chromosome 6p11-q21 (Harbitz et al., 1990), a region of synteny with human chromosome 19. Linkage studies from multiple human multi-generation MH families with markers across chromosome 19 and within *RYR1* itself located the disease gene to chromosome 19q12-13.2 firmly establishing *RYR1* as the primary candidate locus for MH (McCarthy et al., 1990, MacLennan et al., 1990). Similarly to the search for the disease loci, the first MH mutation was identified in PSS (Fujii et al., 1991, Otsu et al., 1991). A C>T transition at nucleotide residue 1843 resulting in an amino acid substitution of arginine to cysteine is, to date, the only *RYR1* variant associated with

PSS. The human equivalent mutation was found to cosegregate with MH susceptibility in a large Canadian family (Gillard et al., 1991).

A



B

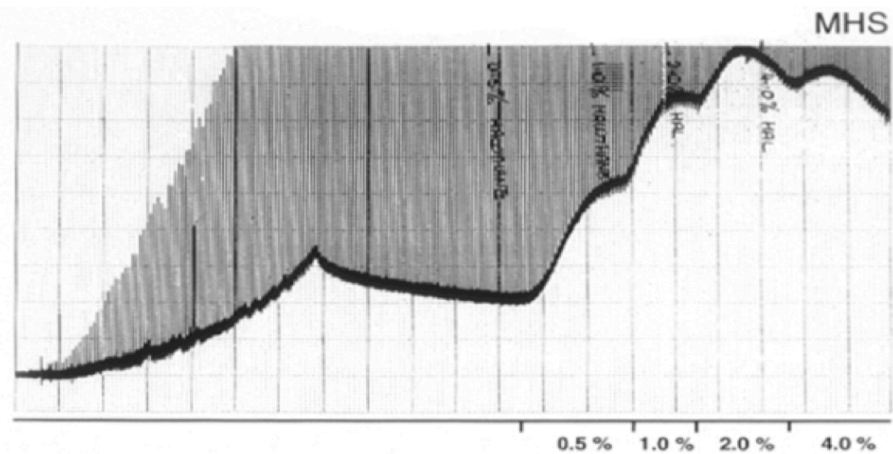


Figure 1.1 – Static halothane IVCT traces

(A) Representative trace of a negative diagnosis for MH. Upon the addition of 0.5%-2% halothane (indicated on the x-axis), no increase in muscle tension is observed. (B) Representative trace of a positive diagnosis for MH. Upon the addition of 0.5%-2% halothane (indicated on the x-axis), a continuous increase in muscle tension is observed. The next dose of halothane is added as the muscle tension begins to plateau after the addition of the previous dose. Image of diagnostic traces kindly provided by Dr. P. J. Halsall.

1.4.2 The type 1 ryanodine receptor (*RYR1*)

1.4.2.1 Structure and function of *RYR1*

RYR1 is the SR calcium release channel in skeletal muscle and is one of three ryanodine receptor isoforms in humans, with *RYR2* being the primary isoform of smooth muscle and *RYR3* being expressed in the brain. The *RYR1* gene spans 160 kilobase pairs (kb) of deoxyribose nucleic acid (DNA) on chromosome 19q13.2 and contains 106 exons with a total of 15,391 base pairs (bp) of coding sequence (Phillips et al., 1996). The resultant 5,038 amino acid *RYR1* protein functions as a homotetramer with each subunit having a mass of 563 kilodaltons (kDa), making it the largest ion channel known and one of the largest proteins in the human body. Early predictions based on sequence motifs of the *RYR1* protein suggested a structure that is primarily cytoplasmic at the N-terminal end followed by 8 transmembrane domains and a much smaller C-terminal cytoplasmic region (Figure 1.2) (Du et al., 2002). Subsequent cryo-electron microscopy experiments revealed a mushroom-like structure with over 80% of the mass in the cytoplasm (Ludtke et al., 2005, Serysheva et al., 2005, Samsó et al., 2005). Upon activation, *RYR1* undergoes a large conformational change resulting in channel opening. Protein structures of open and closed states of the *RYR1* protein indicate that upon activation, the inner helices of the transmembrane domains undergo a conformational change by rotating to expand the diameter of the calcium pore, allowing calcium release (Serysheva et al., 1999, Samsó et al., 2009).

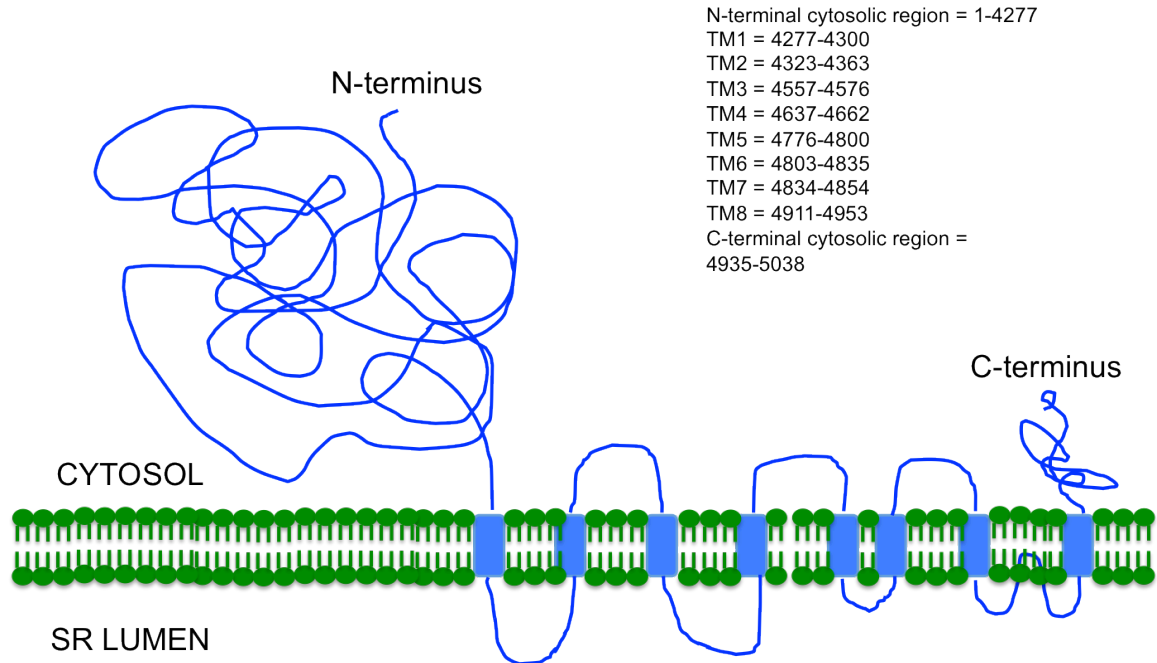


Figure 1.2 – Schematic representation of one subunit of the RYR1 protein tetramer
 The majority of RYR1 is in the cytoplasm followed by a total of 8 transmembrane (TM) regions between amino acids 4277 and 4953 before another, much smaller cytosolic region at the C-terminus of the protein. The calcium pore is predicted to lie between TM7 and 8. Based on information in Du et al. (2002).

Allosteric gating of RYR1 during excitation-contraction (EC) coupling is primarily triggered through interactions of the N-terminal cytoplasmic region with the skeletal muscle voltage sensors, the alpha-1 subunit ($Ca_v1.1$) of the dihydropyridine receptors (DHPRs) (Figure 1.3). After transmission of an action potential from the motor end plate of a neuron to the sarcolemmal membrane, a wave of depolarisation travels along the membrane and down the transverse tubules (T-Tubules) to the DHPRs. $Ca_v1.1$ detects the voltage change, which causes a conformational change in the protein, in particular a projection of a region called the II-III loop to into the cytoplasm of the muscle fibre to directly interact with RYR1 causing channel opening and subsequent muscle contraction (Cherednichenko et al., 2004).

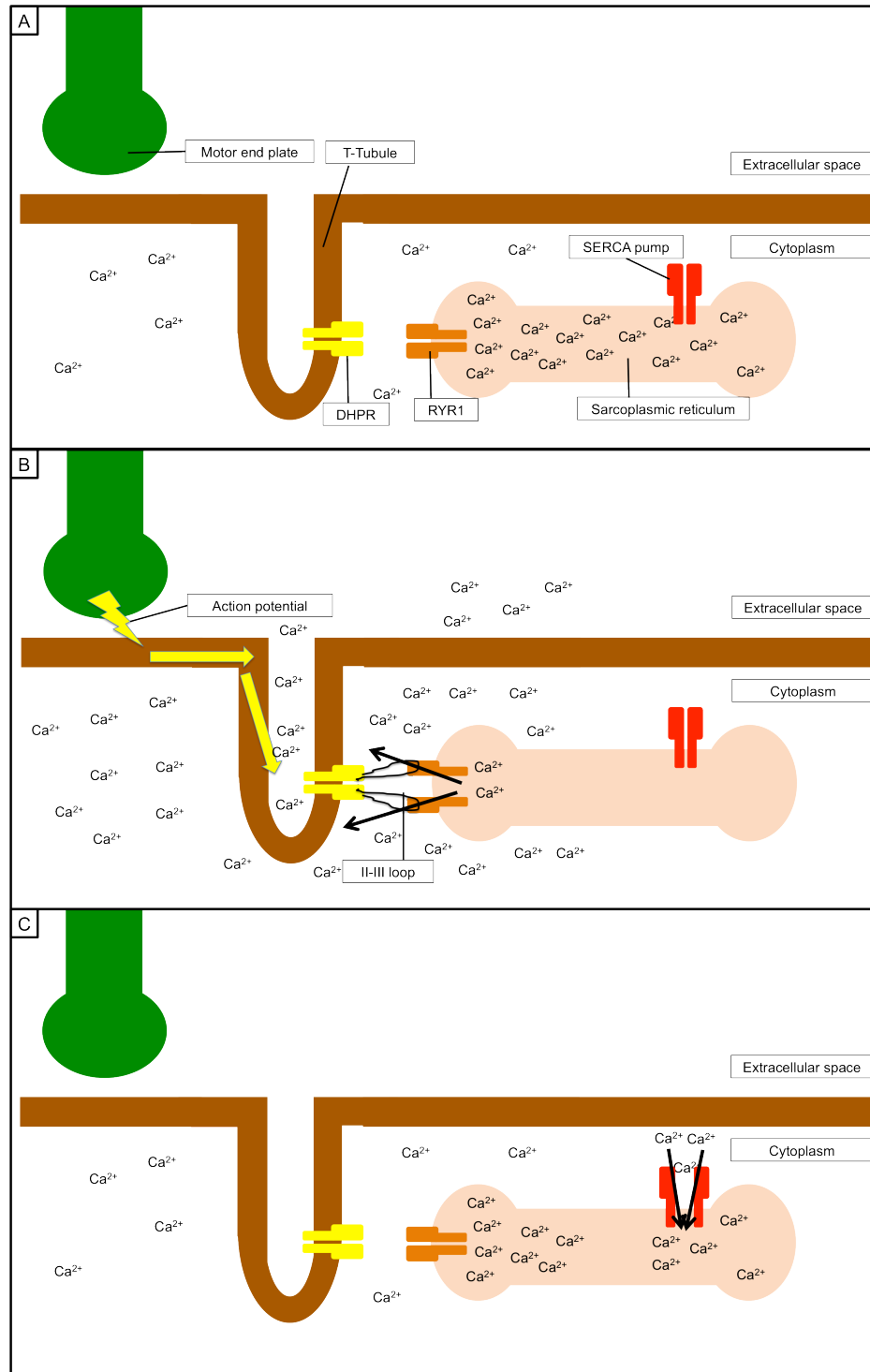


Figure 1.3 – Schematic showing excitation-contraction coupling in skeletal muscle.
(A) Skeletal muscle at rest. The majority of cellular calcium (Ca^{2+}) is in the sarcoplasmic reticulum stores. **(B)** When an action potential arrives at the motor end plate the signal is transmitted to the sarcolemmal membrane and travels down the T-Tubules to the DHPR. Electrical stimulation of the DHPR causes the II-III loop to project across the cytoplasm to interact with RYR1 in the sarcoplasmic reticulum membrane. This interaction results in the opening of RYR1 allowing calcium to flood into the cytosol, subsequently leading to muscle contraction. **(C)** After stimulation the sarco(endo)plasmic reticulum calcium ATPase (SERCA) pump actively transports calcium ions back into the sarcoplasmic reticulum stores.

1.4.2.2 Mutations in RYR1 associated with MH

Whilst only one mutation to date has been found in association with PSS, 244 variants in *RYR1* are currently listed on the EMHG website (www.emhg.org). Of these variants approximately 36% are unique to the family in which they were found, however, in the UK the p.G2434R variant accounts for almost half of MH cases and is also recurrent in the US (Sei et al., 2004, Robinson et al., 2006). The frequency of particular *RYR1* variants varies throughout the world with the second most common UK variant, p.T2206M, being particularly prevalent in Germany (Brandt et al., 1999), whereas the p.R2336H and p.V2168M variants are common in Switzerland (Girard et al., 2001b) and the p.R614C variant recurrent in Italy and Canada (Gillard et al., 1991, Robinson et al., 2003b). Whilst in these countries many of the MH cases can be attributed to these variants, in Japan, China, Taiwan, Australia and New Zealand the majority of reported cases of MH are due to variants unique to the families (Davis et al., 2002, Oyamada et al., 2002, Yeh et al., 2005). Despite there being 106 reported cases in which the *RYR1* variant identified is unique to that family, half of all MH cases reported up to 2006, for which an *RYR1* variant has been identified, have been found to be associated with the p.R164C, p.G341R, p.R614C, p.R2163H, p.V2168M, p.T2206M, p.R2434H and p.R2458H variants (Robinson et al., 2006). However, with MH being a rare disease, only a few centres in the world specialise in mutation screening for MH and the frequencies of certain variants may be biased by centres that have established thorough screening programmes. As diagnostics of MH moves into next generation sequencing to identify *RYR1* variants, variants previously thought to be unique to certain families may be identified at a higher frequency.

1.4.2.2.1 Types of mutation found in *RYR1* associated with MH

The overwhelming majority of genetic variants in *RYR1* associated with MH are missense mutations present in heterozygous form (Robinson et al., 2006). There are, however, a number of cases in which patients are reported to be homozygous for the

same variant as well several cases of compound heterozygous individuals, in which two mutant alleles were inherited from two MHS parents (Lynch et al., 1997, Monnier et al., 2002). As well as missense variants, there have been two reports of deletions in *RYR1* associated with MH, one resulting in the absence of one amino acid from the protein and the other resulting in a premature stop codon 150 amino acids before the end of the protein (Sambuughin et al., 2001a, Robinson et al., 2006). The single amino acid deletion results in a larger than normal electrically evoked contracture during IVCT diagnosis hinting at a disruption of normal EC coupling. There are no functional data available for the deletion mutation that results in a premature stop codon, however, as it has been identified in conjunction with MH it appears to suggest that the level of *RYR1* expression is critical for normal function and a defect in the level of wild type *RYR1* expression may be pathogenic in some instances of MH.

1.4.2.2 Expression levels of *RYR1* and its role in MH pathogenesis

The exact effect of a differential level of wild type and mutant *RYR1* expression on susceptibility to MH is not known. Evidence from other *RYR1* related myopathies such as central core disease (CCD) and multimimicore disease (MmD) has suggested that a decrease in *RYR1* expression may be responsible for the associated muscle weakness. In core myopathies, monoallelic expression of a paternal *RYR1* variant has been associated with a severe form of CCD (Zhou et al., 2006a). Additionally, a cryptic splice site mutation in *RYR1*, which results in a drastic decrease of *RYR1* in skeletal muscle, has been found in association with a severe form of MmD (Monnier et al., 2003). To date, there is limited data on MH cases with *RYR1* expression level defects. There has been a suggestion that in patients carrying *RYR1* variants associated with MH, an upregulation of the wild type allele is evident, possibly as a compensatory mechanism against the hypersensitivity and leakiness of the mutant *RYR1* channel (Grievink and Stowell, 2010). Recently, it has been suggested that epigenetic allelic silencing may play a role in the overall inheritance of MH as affected fathers have significantly fewer

affected daughters than sons however, there is no evidence to suggest that MH pathogenesis is a result of allelic silencing of wild type *RYR1* in susceptible individuals (Robinson et al., 2009).

Increasing the expression level of wild type *RYR1* in myotubes does not significantly alter the caffeine sensitivity of the cells, nor does it have an impact on the baseline resting calcium level present in the cytoplasm of the cells (Perez et al., 2005). Interestingly however, a similar increase in *RYR3* expression results in a significant increase in sensitivity to caffeine that is in line with an increase in resting calcium level. MHS individuals have an elevated baseline resting calcium level associated with MH mutations (Yang et al., 2007, Eltit et al., 2012a), which, upon correction to wild type levels, reduces the sensitivity of mutant cells to channel activators (Lopez et al., 2005). Although there is no data to date examining the effect of the expression level of wild type or mutant *RYR1* on a higher resting calcium background, fluctuations in expression of these alleles may, at least in part, explain the variability of the penetrance and severity of an MH crisis in susceptible individuals upon exposure to anaesthesia. Recently, a gene dosage effect has been observed in p.T4826I *RYR1* mice with a clear rank order in severity of the observed phenotype (Barrientos et al., 2012). Homozygous muscle fibres were significantly more affected than heterozygous fibres suggesting that, for at least some variants, expression levels and gene dose of mutant *RYR1* alleles may contribute to the severity of an MH reaction.

1.4.2.2.3 Mutation hot-spots associated with MH

Since the discovery of the first mutation in *RYR1*, screening projects of MH patients have continued to add to the list of potentially causative variants. Early in this search, the idea of mutation hot spots focussed screening projects onto small sections of *RYR1* as a means to offset the difficulties of screening a 15kb gene. Initially, two mutation hot spots were described, one at the N-terminal region spanning from the cysteine at residue 35 to the arginine at residue 614 and one in the central region of *RYR1*

covering a region of 315 amino acids between two arginine residues at positions 2163 and 2458 (Jurkat-Rott et al., 2000) (Figure 1.4). A third hot spot was proposed after the discovery of an *RYR1* variant in the C-terminal region of the gene from the valine residue at position 4583 to the glutamine at position 4934 (Lynch et al., 1999, Davis et al., 2003). As sequencing technologies have improved, screening projects of the *RYR1* gene have begun to identify a vast number of variants associated with MH, causing the boundaries of the three mutation hot spots to expand to cover almost 40% of the *RYR1* coding sequence (Carpenter et al., 2009c). Robinson et al. (2006) outlined the spread of mutations across *RYR1* indicating that no particular hot spot existed and that the original theory was based on sequencing bias.

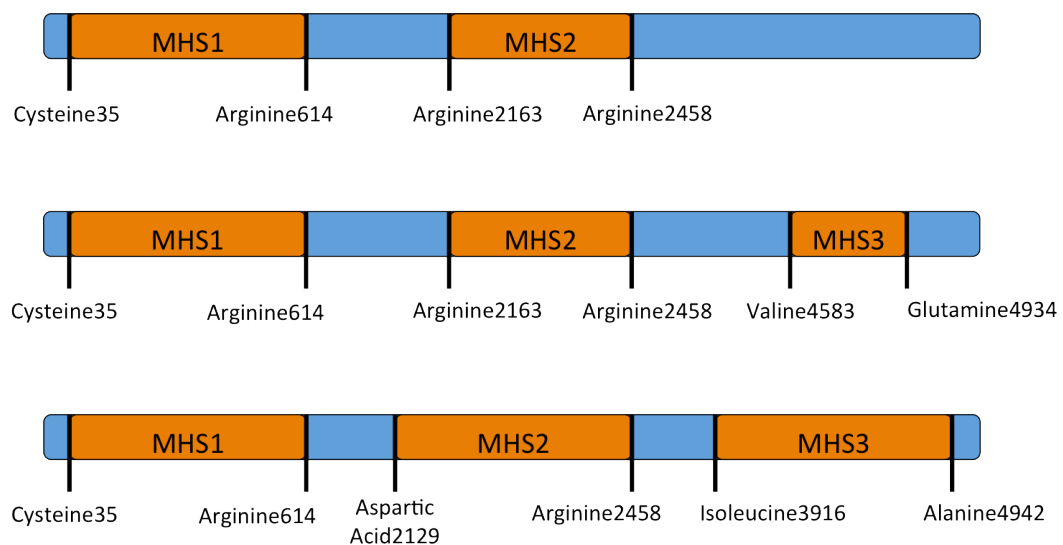


Figure 1.4 – The evolution of the *RYR1* mutation hot spot

Since the discovery of the first *RYR1* variant, screening projects were focussed on the areas in which variants had already been found. This led to the postulation of a hot spot theory of MH. Originally only two hot spots (MHS1 and MHS2) at the N-terminal region and central region of *RYR1* were proposed. This was subsequently expanded to three hot spots upon the discovery of a variant in the C-terminal portion of *RYR1* (MHS3). The proposed hot spots have grown and now encompass almost 40% of the entire coding sequence.

1.5 *RYR1* variants and their role in the pathogenesis of MH

1.5.1 Structural defects in the *RYR1* protein

Variants in *RYR1* confer a hypersensitivity to activation and a passive calcium leak resulting in a higher baseline resting calcium level (Tong et al., 1997, Tong et al., 1999a, Yang et al., 2007, Yang et al., 2003). The mechanism by which missense mutations in the large calcium channel can result in hypersensitive gating upon stimulation is not entirely known. Early theories based on the idea of interacting domains of the *RYR1* protein suggested that mutations result in a reduced stability of these interactions leading to hypersensitivity and calcium leak (Yamamoto et al., 2000). The hypothesis states that the gating of *RYR1* is dependent on the stability of interacting domains in the large cytoplasmic N-terminal region and central regions of *RYR1*, roughly corresponding to the mutation hot spots suggested to exist in *RYR1*.

The advancement of protein structure technologies has enabled several mutations to be mapped onto the structure of *RYR1* and caused an expansion of the early theories of interdomain interactions. Mutations in *RYR1* appear to cluster around known phosphorylation sites, regions of both intra- and interdomain interactions and regions that result in thermal instability of the native protein (Lobo and Van Petegem, 2009, Tung et al., 2010, Yuchi et al., 2012). Whilst the effect of a number of mutations may be accounted for through the breakdown of internal interactions within *RYR1* it appears unlikely that there is a model that fits all variants associated with MH. There is evidence to suggest that certain mutations may not only affect the basic stability of *RYR1* but also affect the proper functioning of $\text{Ca}_v1.1$ (Esteve et al., 2010, Bannister et al., 2010). Mutations in *RYR1* not only result in hypersensitivity of *RYR1* but also have consequences for signalling to the DHPR for calcium entry into the muscle fibre. Furthermore, the increased open probability of *RYR1* results in a retrograde interaction with the DHPR, priming it for activation at lower voltages through depolarisation.

1.5.2 Physiological defects caused by mutations in *RYR1* associated with MH

As well as resulting in structural defects in *RYR1* that affect signalling to and from regulatory proteins involved in EC coupling, variants in *RYR1* appear to affect normal skeletal muscle physiological processes that, when defective, may result in an exacerbation of the MH phenotype upon triggering.

1.5.2.1 Store operated calcium entry

Store operated calcium entry (SOCE) is the process by which calcium enters the cell after prolonged SR store depletion (Smyth et al., 2010) and works through the interaction of two proteins, Orai1 and STIM1. Orai1 is a calcium release-activated channel (CRAC) localised in the plasma membrane that allows calcium entry upon depletion of the SR stores. Activation of the Orai1 CRAC is mediated through a redistribution of STIM1 in the SR membrane as a response to store depletion. STIM1 is a calcium sensing protein that is normally localised throughout the SR membrane, however, upon depletion of the SR stores translocates to form punctate structures at areas of the SR close to the plasma membrane allowing interaction with Orai1 and subsequent calcium entry (Figure 1.5).

When MHN muscle fibres are exposed to MH-triggering anaesthetics little or no calcium is released from the SR stores, however, when MHS muscle fibres are exposed to clinically relevant concentrations of halothane, sufficient calcium depletion from the SR is achieved to activate SOCE (Duke et al., 2010). The additional calcium entry from the intracellular space coupled with exaggerated calcium release from the SR may contribute to the pathological increase in calcium associated with MH and partly explain how an MH episode is maintained during anaesthesia.

1.5.2.2 Excitation-coupled calcium entry

Excitation-coupled calcium entry (ECCE) is a second mode of calcium entry in skeletal muscle and occurs as a response to prolonged membrane depolarisation but, unlike SOCE, ECCE is not dependent on store depletion for activation (Rosenberg, 2009). ECCE requires the interaction of RYR1 and DHPR to permit the entry of calcium, most likely through $Ca_v1.1$ (Cherednichenko et al., 2004, Hurne et al., 2005, Bannister et al., 2009) (Figure 1.6). Mutations in *RYR1* associated with MH and in particular CCD show an increase in ECCE which can be reversed with treatment with dantrolene, which, similarly to SOCE may contribute to the prolonging of the MH phenotype (Cherednichenko et al., 2008, Treves et al., 2011).

1.5.2.3 Sensitivity to calcium activation and magnesium inhibition

It has long been established that calcium has the ability to induce further calcium release from ryanodine receptors. Whilst this calcium-induced calcium release (CICR) has a more prominent role in cardiac and smooth muscle EC coupling through RYR2 (Collier et al., 2000), RYR1 is also sensitive to CICR (Endo, 2009). In the presence of physiological amounts of magnesium in the intracellular environment, CICR through RYR1 is inhibited. A reduction in magnesium and an increase in cytosolic calcium have the ability to activate wild type RYR1. Additionally, reducing the amount of magnesium causes normal muscle to be more sensitive to known MH triggers caffeine, halothane and sevoflurane. MHS muscle has a more dramatic sensitivity to all these activators in the presence of reduced magnesium but also when exposed to physiological concentrations of magnesium (Kawana et al., 1992, Owen et al., 1997, Duke et al., 2004, Duke et al., 2006, Duke et al., 2003, Duke et al., 2002). Furthermore, a reduction in magnesium also makes MHN muscle more sensitive to store depletion and the associated calcium entry through the SOCE mechanism, a reaction that is once again more exaggerated in MHS fibres (Duke et al., 2010).

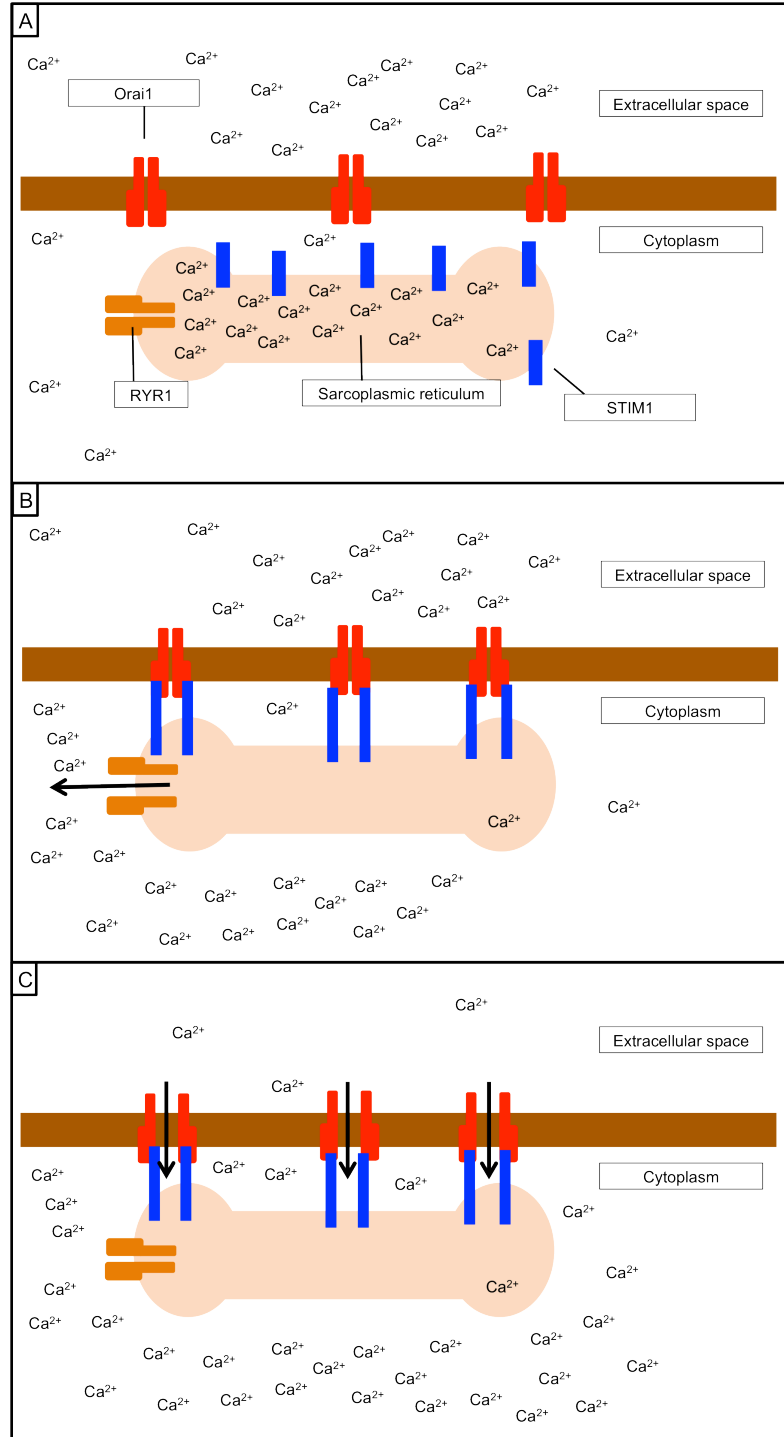


Figure 1.5 – Schematic of the store operated calcium entry mechanism.

(A) Skeletal muscle at rest. STIM1 molecules are present throughout the sarcoplasmic reticulum and Orai1 channels are present in the sarcolemmal membrane. (B) Store depletion triggers the rearrangement of STIM1 molecules to distinct regions close to the sarcolemmal membrane to allow interaction with Orai1 channels that undergo a similar rearrangement. STIM1 molecules under oligomerisation and elongate to allow the interaction with Orai1. (C) Interaction of STIM1 and Orai1 facilitates calcium entry from the extracellular space. Based on information from Lewis (2007), and Smyth et al. (2010)

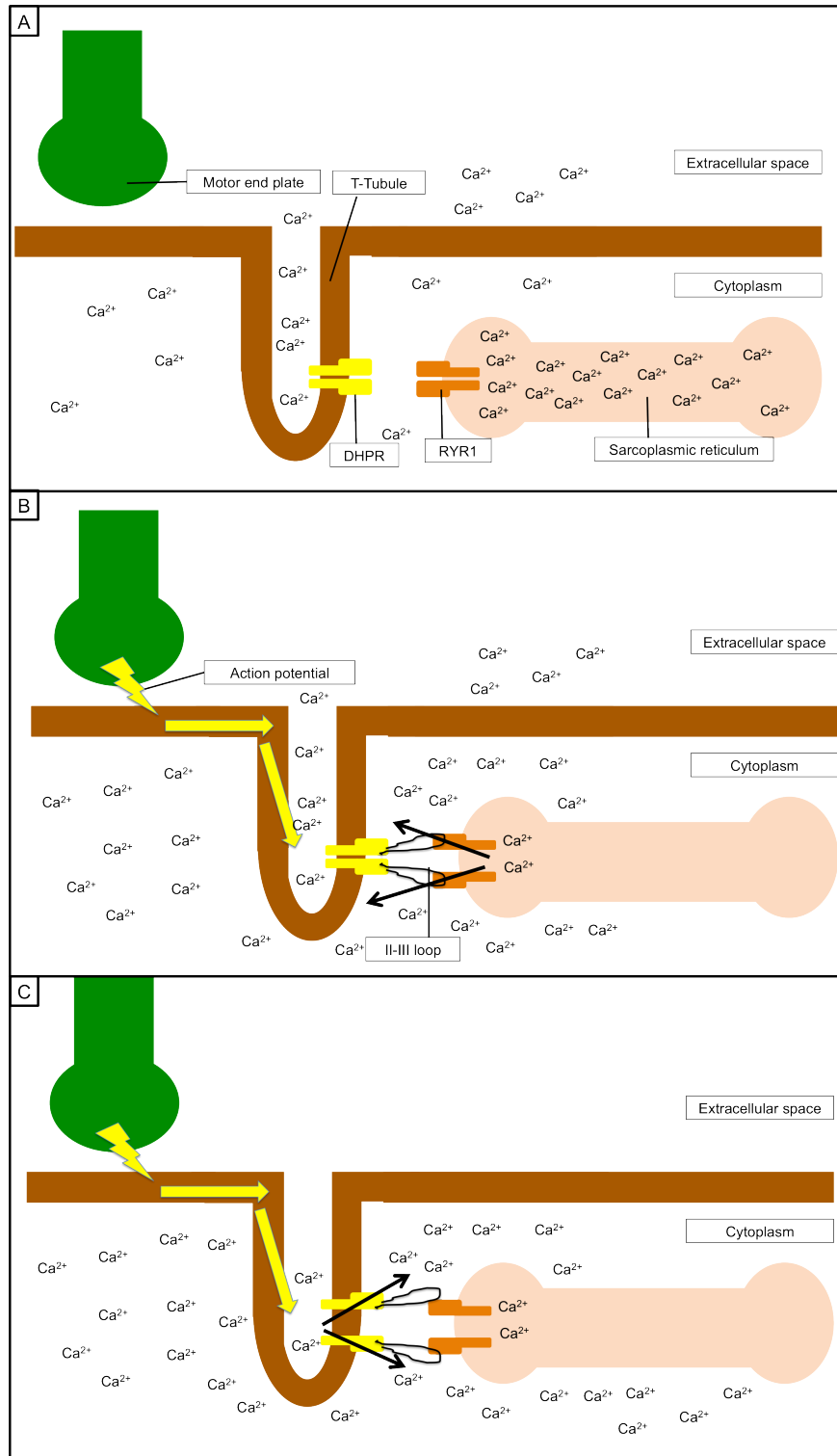


Figure 1.6 – Schematic of the excitation-coupled calcium entry mechanism in skeletal muscle.
(A) Skeletal muscle at rest. The majority of the cellular calcium is in the sarcoplasmic reticulum stores. There is also calcium present both in the cytoplasm and in the extracellular space. **(B)** Depolarisation of the sarcolemmal membrane results in excitation-contraction coupling through interaction between the DHPR and RYR1 calcium channels. **(C)** Prolonged depolarisation results in calcium entry through the DHPR from the extracellular space. Based on information from Rosenberg (2009).

1.6 Additional conditions associated with mutations in *RYR1*

As well as MH, mutations in *RYR1* have been associated with a number of neuromuscular disorders including MmD (Ferreiro et al., 2002), nemaline rod myopathy (Monnier et al., 2000), King-Denborough syndrome (Dowling et al., 2011) and centronuclear myopathy (Jungbluth et al., 2012, Wilmshurst et al., 2010). Whilst the contribution of *RYR1* to these conditions appears to be largely heterogeneous, *RYR1* is the main locus responsible for CCD and is increasingly being associated with a physiological episode that shares many common features with MH; exertional heat stroke (EHS).

1.6.1 Central Core Disease

CCD is a minimally progressive, congenital myopathy characterised histopathologically through the presence of amorphous areas known as cores that lack oxidative enzymes and mitochondria (Robinson et al., 2006). Common clinical features include muscle atrophy, generalised lower limb weakness and floppy infant syndrome however, the spectrum of clinical features of CCD is wide, with some patients being largely asymptomatic despite the presence of cores and others being severely affected through acute muscle weakness (Shuaib et al., 1987, Quinlivan et al., 2003).

Despite the seemingly contrasting symptoms associated with the two disorders, the link between CCD and MH has long been established (Denborough et al., 1973). A number of *RYR1* mutations have been associated with CCD either in conjunction with MH or, in some cases, independent of MH (Quane et al., 1993, Zhang et al., 1993, Lynch et al., 1999, Robinson et al., 2006). Whilst the hot-spot theory of MH has largely been quashed it does appear as though the third mutation hot spot at the C-terminal region of *RYR1* is the main area for mutations in CCD (Monnier et al., 2001, Davis et al., 2003). This is perhaps not surprising as mutations in the calcium pore of *RYR1* may explain the large amount of calcium leak associated with CCD and the resultant

myopathy, however, similarly to MH, mutations associated with CCD are being identified across *RYR1* (Shepherd et al., 2004).

Like MH, CCD is associated with elevated resting calcium attributed to passive leak through RYR1. In CCD patients this leak appears to be more severe, leading to myopathy, however, the hypersensitivity of RYR1 is maintained leading to both phenotypes (Tong et al., 1997). This calcium leak is attributed to an increased hypersensitivity of RYR1 to activation when not challenged with traditional agonists and when exposed to volatile anaesthetics an MH reaction is still triggered. An alternative molecular mechanism for the onset of CCD has also been established for cases not linked to MH termed excitation-contraction uncoupling (Dirksen and Avila, 2002) (Figure 1.7). In a number of cases of CCD that have not been linked to MH, there is an apparent uncoupling of the DHPRs and RYR1 during EC coupling leading to severe myopathy. In homozygous form *in vitro*, RYR1 mutations associated with this mechanism results in completely abolished EC coupling which is only partially restored by heterozygous expression of wild type RYR1.

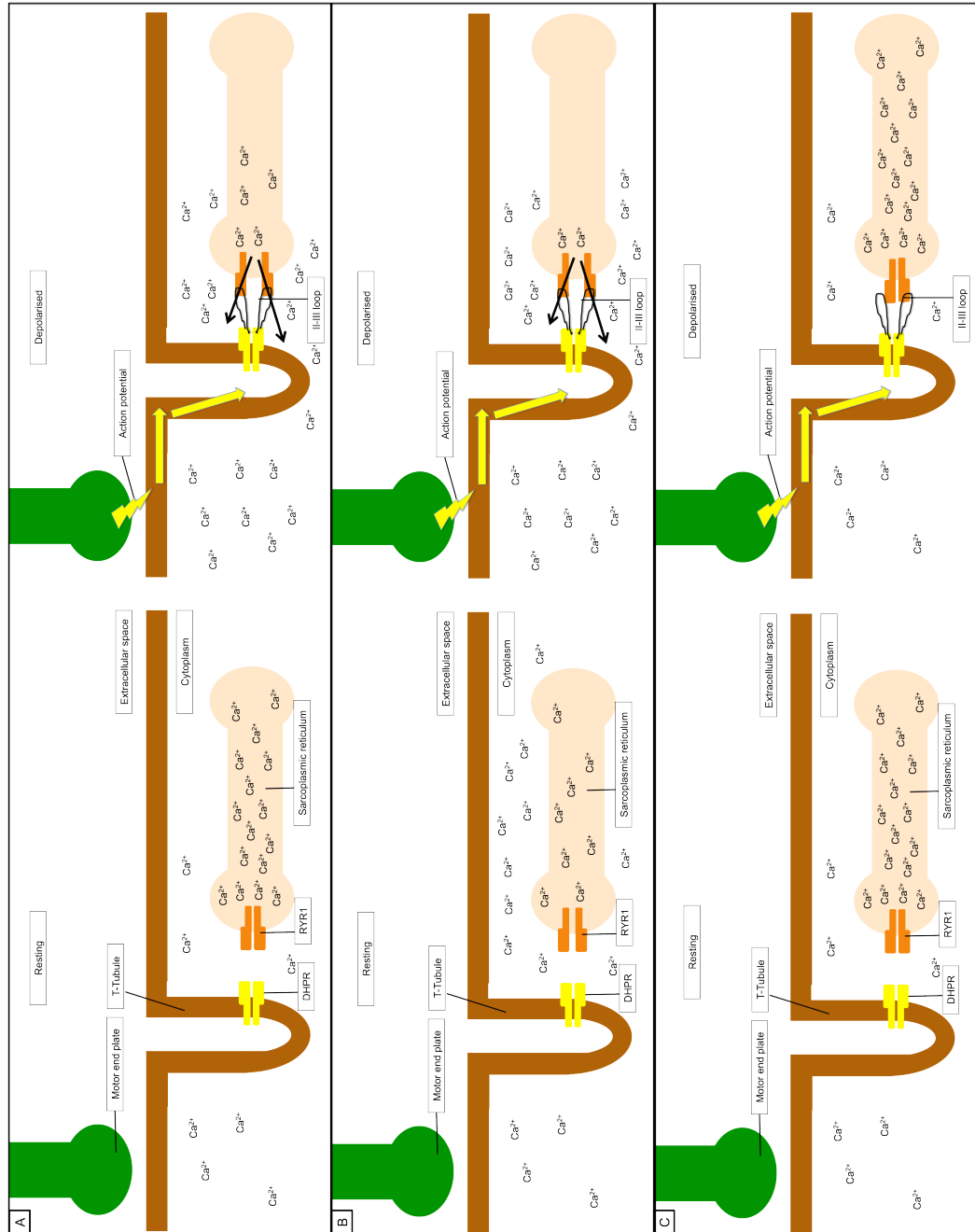


Figure 1.7 – Mechanisms that lead to the central core disease pathogenesis

(A) Normal skeletal muscle at rest (left) and during depolarisation (right). At rest, the majority of cellular calcium is in the sarcoplasmic reticulum stores. Upon depolarisation, interaction between RYR1 and the DHPR causes calcium release from the sarcoplasmic reticulum stores. (B) Leaky RYR1 channels at rest (left) and during depolarisation (right). Leaky RYR1 channels causes there to be a higher cytoplasmic calcium level resulting in a reduced amount of calcium release upon depolarisation resulting in muscle weakness and myopathy. (C) Excitation-contraction uncoupling. Upon depolarisation, no calcium release is observed as coupling between the DHPR and RYR1 is abolished. This phenotype is less severe when in heterozygous form. Based on information from Avila et al. (2001).

1.6.2 Exertional heat stroke

EHS is a form of heat stroke associated with vigorous exercise in warm climates such as military training programmes and mass participant events such as marathons (Hopkins, 2007). When triggered, susceptible individuals experience excessive increases in body temperature as well as significant central nervous system dysfunction. There has long been a suggested link between MH and EHS based on the similarity in the symptoms of both conditions as well as reports of several individuals who suffer an EHS reaction and are subsequently tested MHS through the IVCT (Hopkins et al., 1991a, Hackl et al., 1991, Kochling et al., 1998, Hopkins, 2007, Muldoon et al., 2007, Muldoon et al., 2008). Currently, members of the British military who suffer repeated EHS episodes and fail heat tolerance tests are referred to the UK MH diagnostic centre for testing. Furthermore, both porcine (Mitchell and Heffron, 1982, Otsu et al., 1994) and murine models of MH (Chelu et al., 2006, Yang et al., 2006) are induced into the hypermetabolic reaction associated with MH through exposure to an increase in ambient temperature to 42°C

The phenotypic link has, in recent years been supported through genetic data emerging in EHS cases as well as other heat-related illnesses such as exertional rhabdomyolysis (Table 1.1). Davis et al. (2002) and Wappler et al. (2001) reported a total of six independent families possessing *RYR1* variants associated with exertional rhabdomyolysis and MH. Furthermore, there have been recent reported cases of fatal stress-induced MH associated with *RYR1* variants in two children (Groom et al., 2011). Whilst these conditions are related to MH and EHS, there has, to date, been only one-reported case where an EHS reaction has been categorically linked to an *RYR1* mutation and previous MH family history (Tobin et al., 2001). A 12-year old boy had suffered an MH reaction during anaesthesia and subsequently recovered without any further complications. However, the boy died several months later of a clear EHS episode whilst playing football. Genetic analysis of the boy and his family revealed the presence of the p.R163C variant that has been previously associated with MH as well

as being proven causative in functional experiments (Tong et al., 1997, Yang et al., 2003).

Nucleotide change	Amino acid change	Reference
487 C>T	R163C	Tobin et al. (2001)
487 C>T	R163C	Wappler et al. (2001)
1021 G>A	G341R	
7297 G>A	L2433I	
1201 C>T	R401C	Davis et al. (2002)
11947 C>T	R3983C	Groom et al. (2011)
13513 G>C	D4505H	

Table 1.1 – Genetic variants in *RYR1* associated with exertional heat stroke and exertional rhabdomyolysis
The number of *RYR1* variants associated with exertional heat illnesses is steadily increasing. To date, only one variant, the p.R163C has been definitively linked to both an MH and EHS episode in the same family.

Whilst there is no treatment available for EHS aside from aggressive cooling measures, recently a compound has been shown to protect against EHS in *RYR1* mutant mice (Lanner et al., 2012). 5-aminoimidazole-4-carboxamide ribonucleoside (AICAR) is an adenosine analogue that is readily taken up into cells and mimics the effect of adenosine monophosphate (AMP) in the activation of AMP kinase (AMPK). AMPK is an energy sensor that is activated upon an increase in AMP and inhibited in the presence of high ATP (Merrill et al., 1997). Activation of AMPK increases the amount of metabolic enzymes present in skeletal muscle, specifically GLUT-4 and hexokinase (Holmes et al., 1999, Winder and Hardie, 1999, Winder et al., 2000). AMPK activity is elevated in individuals who have undergone endurance exercise training but it has recently been shown that when AICAR is administered over a period of time, exercise endurance and the associated increase in mitochondrial enzymes is increased even in sedentary mice (Corton et al., 1995, Pold et al., 2005, Narkar et al., 2008).

Prophylactic treatment of an MH mouse expressing an *RYR1* variant with AICAR is fully protective against the EHS phenotype. Whilst AMPK is known to be protective of cells against heat shock, the actual method by which AICAR protects against the EHS

episode is through a direct interaction with *RYR1* resulting in a reduction of calcium leak from the mutant channel (Lanner et al., 2012). Treatment with AICAR was unable to protect against anaesthesia induced MH suggesting that the volatile anaesthetic overwhelms the ability of AICAR to reduce calcium leak from *RYR1*.

1.7 Genetic heterogeneity of MH

Despite the number of missense variants in *RYR1* associated with MH, there are a number of families in which no mutation has been identified. Furthermore, initial studies searching for the genetic locus responsible for MH, as well as identifying *RYR1* as the primary locus for MH, found several families in which no linkage was observed to chromosome 19 through microsatellite and single nucleotide polymorphisms (SNPs) (Deufel et al., 1992, Levitt et al., 1992, Iles et al., 1992). Additionally, 5% of MH cases in which a previously identified variant is present show genotype/phenotype discordance when correlated with IVCT data (Deufel et al., 1995, Fagerlund et al., 1997, Robinson et al., 2003b), suggesting the possibility of further genetic loci associated with MH as potential modifiers of the MH phenotype. This is supported through the work of Robinson et al. (2003a) who showed that multiple interacting gene products contribute to the MH phenotype in patients with and without identified *RYR1* mutations.

1.7.1 The alpha 1 subunit of the dihydropyridine receptor (Ca_v1.1)

Aside from *RYR1*, six additional loci have been associated with MH in various linkage studies and mutation screens and two strong additional candidate genes have been proposed (Table 1.2). The most important of these is the gene encoding the alpha 1 subunit of the DHPR (*CACNA1S*) coding for the Ca_v1.1 protein (Robinson et al., 1997). Screening of *CACNA1S* in MH patients has, to date, identified two potentially causative variants (Monnier et al., 1997, Carpenter et al., 2009b) and functional analysis of these variants in dysgenic (*CACNA1S* null) myotubes show an increased sensitivity to caffeine

and potassium chloride (KCl) as well as causing a decrease in the ability of Ca_v1.1 to negatively regulate RYR1 indicating the functional relevance of these variants to the MH reaction (Weiss et al., 2004, Eltit et al., 2012a).

Chromosome position	Gene
19q13.1	Type I ryanodine receptor (<i>RYR1</i>)
1q32	Alpha 1 subunit of the dihydropyridine receptor (<i>CACNA1S</i>)
19p13.3	Junctional sarcoplasmic reticulum protein (<i>JSRP1</i>)
17q	Unknown
7q	Unknown
3q	Unknown
5p	Unknown

Table 1.2 – List of genes and genetic loci associated with MH

A total of 7 genetic loci have been linked to MH. Mutations have been identified in three genes have been identified as potential causative factors in MH. The most important of these genes is *RYR1*, which accounts for half of all MH cases. Two variants have been found in *CACNA1S* and proven to alter calcium homeostasis. Two mutations have been identified in *JSRP1* but their functional consequences still remain unclear. Four loci in the genome have also been identified in linkage studies but with no candidate gene or mutations identified to date.

1.7.2 Junctional sarcoplasmic reticulum protein (JP-45)

A third candidate gene was identified through a sequencing screen of a number of genes known to be involved in EC coupling and calcium regulation in skeletal muscle (Althobiti et al., 2009). Two variants have been identified in the junctional sarcoplasmic reticulum protein (*JSRP1*), coding for an integral membrane protein (JP-45) that co-localises with RYR1 at the junctional triad and interacts with Ca_v1.1 and calsequestrin, a calcium binding protein in the terminal cisternae of the SR (Anderson et al., 2003, Althobiti et al., 2009). Unpublished observations from our laboratory in human embryonic kidney (HEK293) cells co-transfected with *RYR1* and wild type and mutant *JSRP1* constructs suggest the variants confer an increased sensitivity to caffeine, however, expression of the variants in *JSRP1* null myotubes resulted in a decreased sensitivity to KCl (Yasuda et al., 2013). The conflicting functional data emphasises that the role of these variants in MH pathogenesis is unclear, however,

having been identified in a large number of MHN individuals it is likely that if these variants do contribute to MH it is only in a modifier role to a more severe MH-causing variant.

As well as distinct candidate genes, linkage studies have identified several genetic loci for which no obvious candidate gene has been identified (Levitt et al., 1991, Iles et al., 1994, Sudbrak et al., 1995, Robinson et al., 1997). Regions of chromosome 3q, 5p, 7q and 17q have all been identified in linkage studies as regions that may possess genes of interest for MH. The alpha sub unit of the skeletal muscle sodium channel was a putative candidate for the 17q region due to its function in skeletal muscle EC coupling; however, no mutation was identified in the families linked to this region (Olckers et al., 1992). Similarly, the alpha 2-delta subunit of the DHPR was localised to 7q but with no mutation present in the linked family (Schleithoff et al., 1999).

1.8 Genetic diagnosis of MH

One of the main focuses of MH research in recent years has been the development of a genetic diagnostic panel for MH. The IVCT involves an invasive muscle biopsy that leaves patients in discomfort for several weeks after the procedure and permanently scarred. Furthermore, in the UK, there is only one national diagnostic centre at which the IVCT can be carried out meaning that patients have to travel, in some instances, hundreds of miles to be tested. On occasion this has to be done as a matter of emergency to ascertain the risk of MH before the patient can undergo another urgent operation. Additionally, the IVCT is not universally available to all patients at risk of MH as the biopsy can only be carried out on patients 10 years old and over. In such cases, testing of the parents can only rule out the possibility of MH if both the mother and father test negative. Studies aimed at elucidating the functional consequences of missense variants identified in MH patients have demonstrated that, at least in some cases, the use of genetic testing is a plausible method of diagnosis. The process by which genetic diagnosis can be used is outlined in Figure 1.8.

Treves et al. (1994) were the first to engineer the swine MH mutation into recombinant *RYR1* and ascertain the effect on calcium homeostasis in an *in vitro* system. Mutant RYR1 was proven to cause an abnormal increase in calcium transients when challenged with the channel agonist 4-chloro-*m*-creosol (4-CmC). Tong et al. (1997) subsequently expanded this study into a comprehensive pharmacological analysis of 15 MH-associated *RYR1* variants in HEK293 cells. All variants under investigation were found to possess an increased sensitivity to caffeine, 4-CmC and halothane. Furthermore, MHS myotubes have been shown to have an increased affinity of [3H] Ryanodine binding when exposed to channel agonists indicating an increased open-state channel in MHS patients (Richter et al., 1997).

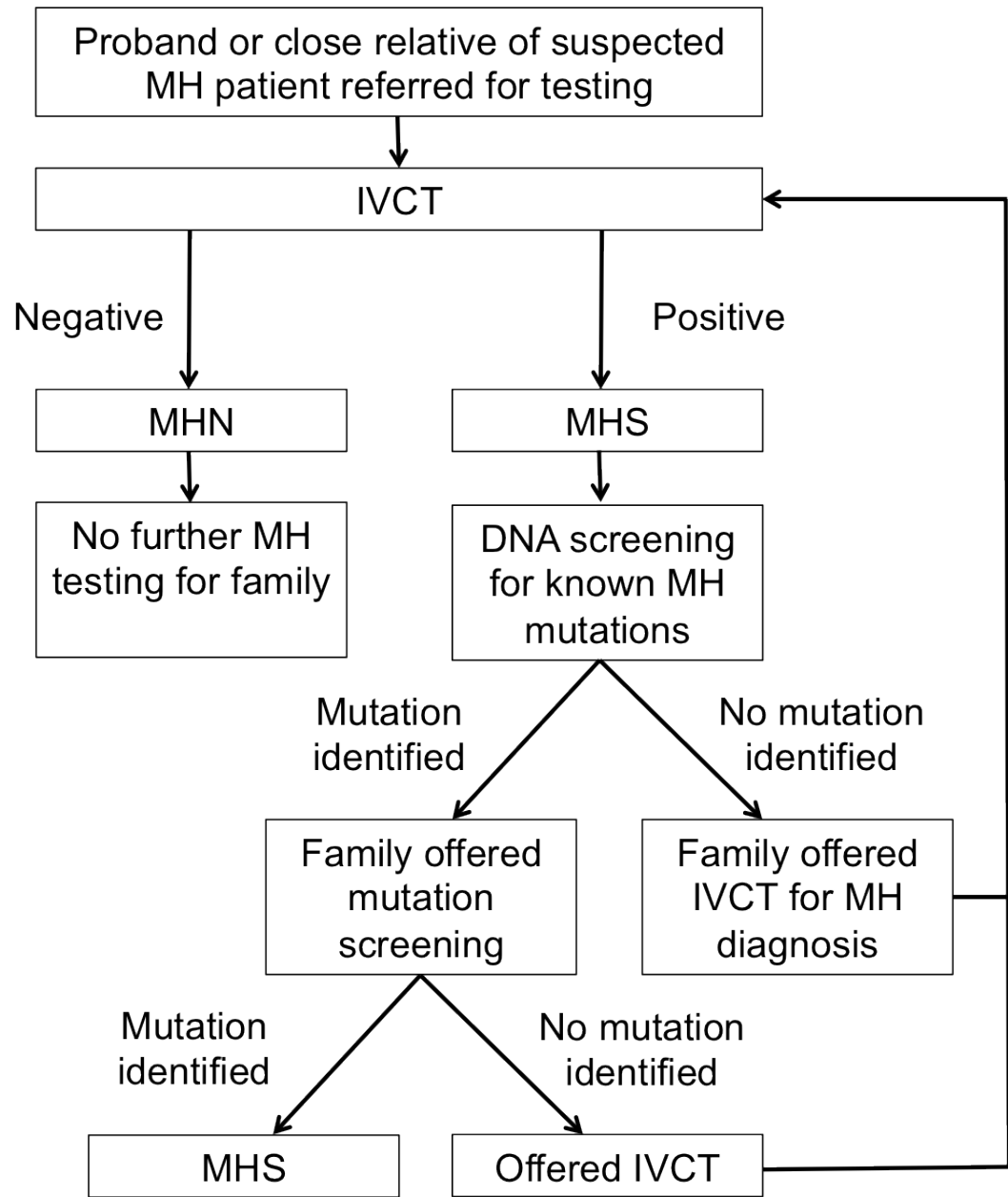


Figure 1.8 – Flowchart outlining the current process for the diagnosis of MH

Upon referral for MH testing, the proband that experienced a suspected MH reaction is offered the IVCT to confirm the MH diagnosis. If the proband died or is too young for MH testing a close relative is offered the IVCT to confirm the MH diagnosis. If the MH diagnosis is confirmed, the patient is added to the genetic screening panel to test for the presence of known causative MH-associated mutations in RYR1. If no mutation is identified all family members are offered an IVCT for MH diagnosis. If a mutation is identified, all subsequent family members are offered genetic screening for MH before the need for an IVCT. If the mutation is not identified in the family members MH is not ruled out and the IVCT is required to confirm the MHN diagnosis. If the familial mutation is identified an MHS diagnosis can be made without the need for the IVCT. Based on information in Urwyler et al. (2001)

1.8.1 EMHG guidelines for inclusion onto the genetic diagnostic panel for MH

With this molecular genetic data in mind, the EMHG developed a set of guidelines that need to be fulfilled for missense mutations in *RYR1* to be added to a genetic diagnostic panel (Urwyler et al., 2001, Robinson and Hopkins, 2001). Genetic variants identified in *RYR1* must be characterised on a genetic and functional level. Genetic characterisation involves examining the change at both a DNA and protein level by considering any aspects of evolutionary conservation in the region of the gene affected and any potential structural or protein charge differences that may occur as a result of the amino acid substitution. In practice this involves aligning *RYR1* DNA sequences from different species and the different human *RYR* isoforms to see if the base and amino acid affected lies in an evolutionary conserved region. The variant must be found to co-segregate with MH in at least two pedigrees as well as being absent from at least 200 control chromosomes to ensure that the variant is a non-pathogenic polymorphism. Other attempts to characterise potential MH mutations involve the use of various bioinformatic resources to predict what, if any, change of protein structure may occur as a result of the variant. Prediction software must be used with caution. Due to the size of *RYR1*, there is limited structural data available and predictions are based on computer algorithms based on motifs from other genes. Generating a reliable prediction of where exactly an *RYR1* variant lies on the overall protein structure and also predicting what effect, if any that will have on function may not be possible. Genetic characterisation is a first step in evaluating the potential seriousness of any change in *RYR1* found in MH patients; however, the genetics of MH has been proven to be, at times, extremely complex so until functional assays are carried out, genetic information is just auxiliary.

1.8.1.1 Functional characterisation of genetic variants using *ex vivo* samples

Functional characterisation of *RYR1* variants can be performed in one of two ways. The first of which is the use of *ex vivo* samples of known genotypes obtained from

patients undergoing MH testing. The majority of such experiments have utilised primary myoblasts obtained from muscle biopsy specimens surplus to diagnostic requirements. Additionally, some groups have obtained B-lymphocytes from the blood of patients under investigation (Wehner et al., 2002, Sei et al., 1999). When using such methods, members of the family under investigation both with and without the *RYR1* variant must be tested to assign causality to the variant. However, because the genetic background in these cases is not defined, the contribution of an unknown genetic variant cannot be ruled out. To counteract this, the guidelines state that such experiments must be performed on material obtained from at least two independent families with the same mutation, however, recent evidence has hinted at the possibility of patients carrying the same *RYR1* variant possessing a shared high-risk MH haplotype (Carpenter et al., 2009a). It is unknown whether in these circumstances the shared haplotype of MH patients would possess a second, potentially causative variant which could diagnose the wrong mutation in the family.

Additionally, the use of such material for functionally characterising MH mutations essentially provides no new information on top of the IVCT. The assay can ascertain whether the cells are responding in an MHS or MHN manner but to conclude that this is because of the presence of one *RYR1* variant may not be accurate. The identification of the first *RYR1* variants prompted mutation-screening experiments to focus on 'hot spots' of the coding sequence in which variants had previously been identified. Currently, most MH centres genotype patients by focussing on these regions to screen for previously identified variants. Very few studies have carried out comprehensive sequencing of *RYR1* to rule out the presence of any other variants in the patients. This is highlighted in several reported cases of patients carrying more than one missense variant potentially responsible for MH. Patients have been identified carrying two mutant alleles of *RYR1* as either homozygous for the same variant, compound heterozygous for two *RYR1* variants inherited from two unrelated MHS parents and compound heterozygous with a variant in both *RYR1* and *CACNA1S* (Lynch et al., 1997, Monnier et al., 2002). If *ex vivo* experiments are to be used in

functional experiments it is vitally important that it is certain that the variant under investigation is the only potentially causative MH variant in the patient. Having this knowledge is highly unlikely unless the patient has undergone whole genome sequencing meaning that *ex vivo* experiments are still problematic.

1.8.1.2 Functional analysis of genetic variants in *in vitro* expression systems

The second method described in the EMHG guidelines is the use of recombinant complementary DNA (cDNA) clones transfected into *in vitro* systems such as HEK293 cells. The defined genetic background of the cellular systems employed in such experiments ensures that the results obtained can only be accredited to the variant under investigation. The difficulties associated with producing recombinant mutant *RYR1* clones are offset with the power of the analysis to confirm the causative nature of the variant under investigation. To date, the majority of variants approved for genetic diagnosis of MH have been functionally characterised using these methods with HEK293 cells being the primary expression system used (Tong et al., 1997, Tong et al., 1999a, Sato et al., 2010). Whilst HEK293 have consistently shown an increased sensitivity of MH variants to channel agonists such as caffeine and halothane, questions remain over their suitability as a functional system for MH. The lack of expression of any of the *RYR* isoforms in HEK293 cells is one of the reasons for their use in functional studies (Rossi et al., 2002), however, such non-muscle cell systems also lack the expression of key triadic proteins such as the DHPR subunits that *RYR1* relies on for normal function in skeletal muscle (Nakai et al., 1996). Additionally, HEK293 cells do not possess the highly organised cellular structure and specialised organelles of skeletal muscle such as the T-tubules and SR.

The primary reason for the use of non-native cell types such as HEK293 cells for functional studies of *RYR1* variants is the ease of which they are transfected with cDNA constructs compared with muscle cells. It is widely acknowledged that as the size of the plasmid being transfected increases, the overall efficiency drops dramatically

(Kreiss et al., 1999, Yin et al., 2005). In spite of this, transfection efficiencies of over 20kb plasmids containing *RYR1* into HEK293 cells remain sufficiently high for the reliable analysis of *RYR1* variants. Muscle cells, specifically differentiated myotubes are difficult to transfect with small plasmids and, as the size of the construct increases, transfection efficiencies have been seen to rapidly decline to efficiencies approaching 0% (Wang et al., 2000, Campeau et al., 2001, Neuhuber et al., 2002).

1.8.1.2.1 Development of a muscle-like *in vitro* expression system for functional experiments and differences with non-native cell types

A highly efficient system of carrying out *in vitro* studies in muscle-like cells has been developed utilising type 1 human herpes simplex virus (HSV-1) (Cunningham and Davison, 1993, Fraefel et al., 1996, Moore et al., 1998, Wang et al., 2000, Yang et al., 2003). A set of five cosmids representing the entire HSV-1 genome minus the packaging and cleavage signals required to produce virions was produced and paired with a modified pUC vector containing the missing signals and a gene of interest. The co-transfection of the cosmids and expression vector resulted in HSV-1 virions containing only the gene of interest and has been used to deliver *RYR1* at efficiencies of up to 90% into dyspedic (*RYR* functional knock-out) muscle cells. The functional consequences of 6 previously characterised *RYR1* variants were assessed using this system. In addition to an increase in sensitivity to caffeine, halothane and 4-CmC, mutant myotubes also displayed defects in EC coupling when depolarised using KCl. Whilst there were no differences observed between HEK293 cells and 1B5 cells in terms of the sensitivity of expressed *RYR1* variants, evidence suggests there may be some differences in the resting intracellular calcium level generated when variants are expressed.

Muscle fibres from both MH swine (Lopez et al., 1987a) and MHS patients (Lopez et al., 1987b, Lopez et al., 1992) have a statistically significantly increased resting calcium when compared to wild type controls. The elevated resting calcium has been

implicated as a causative factor of the MH episode and a reduction in which results in a decrease in sensitivity of muscle fibres to MH-triggering drugs (Lopez et al., 2000, Lopez et al., 2005). In spite of this, the resting calcium of MH variants expressed in HEK293 cells appears to be no different to that of wild type transfected cells (Tong et al., 1999b). Whilst this hints at a fundamental difference in the cellular environment of myotubes and HEK293 cells, the discrepancy may be due to the method employed.

The experiments involving muscle fibres and dyspedic myotubes utilise calcium-sensitive microelectrodes that are calibrated before and after each measurement to ensure the maximum possible sensitivity and accuracy of the measurements. The use of the electrodes requires a large cytoplasmic region for injection, which is not readily visible in HEK293 cells, which are largely nuclear. Resting calcium measurements on HEK293 cells and other non-muscle cell types have used the ratiometric calcium dye fura-2. The overall sensitivity of fura-2 is much lower than calcium-sensitive microelectrodes and, in some cases, MH variants that have been proven to confer a higher resting calcium level in myotubes have been found to be no different to wild type in HEK293 cells. Similarly, when fura-2 has been used in myotubes, not all MH variants have been shown to have a higher resting calcium level (Wehner et al., 2002). In HEK293 cells, only resting calcium levels with CCD associated mutations are detectable as being higher than wild type (Tong et al., 1999b). Whilst it cannot be ruled out that the variation observed is due to discrepancies between individual *RYR1* variants, the likelihood is that the differences observed are due to either an inherent difference between the two expression systems or methods utilised. Whatever the reason, resting calcium data obtained in HEK293 cells remains unreliable and problematic.

1.8.1.3 Knowledge gained from non-native cell types

Despite the potential limitations associated with carrying out functional experiments in non-native cell types, HEK293 cells and B-lymphocytes have been used to generate

useful information on the pathogenesis of MH. Additionally, the majority of the 31 listed causative variants on the EMHG website have been functionally characterised in non-native cellular systems. HEK293 cells expressing wild type *RYR1* have a greater propensity of store overload induced calcium release (SOICR) when luminal calcium concentrations are increased (Jiang et al., 2008). This effect, however, is more severe in HEK293 cells expressing a mutant *RYR1* construct (Figure 1.9). As discussed previously, *RYR1* mutations confer a higher baseline resting calcium level, coupled with the exaggerated calcium entry mechanisms associated with an MH phenotype, the high levels of calcium being pumped back into the SR could be the reason for this SOICR. Furthermore, there is evidence to suggest that the sarco(endo)plasmic reticulum calcium ATPase (SERCA) pump, responsible for calcium reuptake after calcium release is overactive in cells expressing *RYR1* variants (Tong et al., 1999b).

B-lymphocytes isolated from patients known to be carrying *RYR1* variants have previously been used for *ex vivo* functional experiments as they express *RYR1* and respond to channel agonists such as caffeine and 4-CmC (Sei et al., 1999). The exaggerated calcium release associated with the MHS phenotype induces a higher level of $\text{IL-1}\beta$, a pyrogenic cytokine that induces temperature increases, which may partly explain the rapid increase in temperature observed during an MH crisis (Girard et al., 2001a).

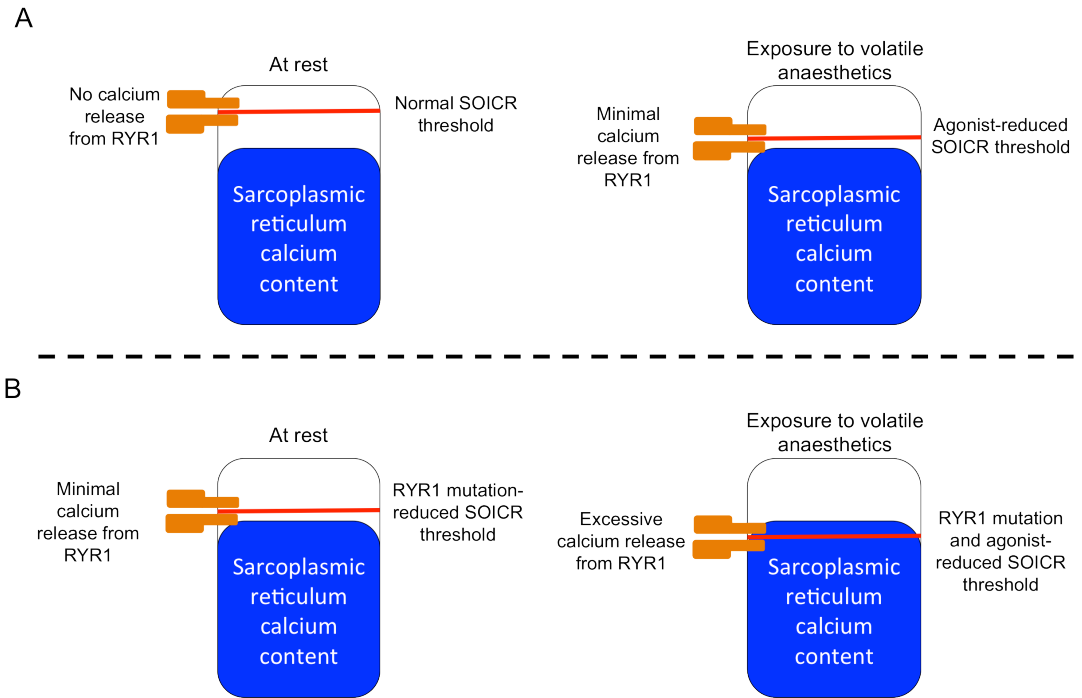


Figure 1.9 – Schematic of store overload-induced calcium release from the sarcoplasmic reticulum through wild type and mutant RYR1

(A) The amount of calcium present in the sarcoplasmic reticulum is indicated in blue. At rest, wild type RYR1 has a high threshold for store overload-induced calcium release that, although lowered when exposed to volatile anaesthetics, does not cause a significant amount of calcium release. (B) Conversely, mutant RYR1 lowers the resting threshold for store overload-induced calcium release to a level similar to that of wild type RYR1 during exposure to volatile anaesthetics. This threshold is further reduced through exposure to triggering anaesthetics resulting in an MH crisis being triggered. Redrawn and modified from Jiang et al. (2008)

1.9 Project Outline

The primary goals of this research project are as follows:

- To functionally characterise six common variants in the *RYR1* gene associated with MH;
- To develop a robust and reliable method of creating variants in *RYR1* cDNA;
- To express the genetic variants generated in this project in both HEK293 cells and 1B5 cells to evaluate the use of non-native cell types in functional studies;
- To examine the effect of increased or decreased *RYR1* expression on the sensitivity of the wild type and mutant channels to activation;
- To functionally characterise a genetic variant identified in *RYR1* associated with both MH and EHS.

1.9.1 Functional characterisation of genetic variants associated with MH

Despite the large number of genetic variants in the *RYR1* gene associated with MH and found in patients known to be susceptible to MH, only 31 are available for genetic diagnosis worldwide. This means that the majority of patients undergoing testing for MH are still reliant on the IVCT, an invasive procedure that leaves the patients in discomfort for several weeks and permanently scarred. Furthermore, St James's Hospital in Leeds is the only certified MH diagnostic centre in the UK meaning that patients often have to travel hundreds of miles for diagnosis. The expansion of the genetic diagnostic panel is vitally important to MH patients not only in the UK but worldwide. The primary goal of this research project is to assess the functional consequences of several common variants in *RYR1* that have been found in association with MH. The functional data obtained on the genetic variants in this project will be used to support their inclusion onto the genetic diagnostic panel for MH as per the EMHG guidelines.

1.9.2 Evaluation of the use of non-native cell types for functional experiments of *RYR1* variants

The most ideal method for performing these experiments is in recombinant *in vitro* systems using cDNA clones. In this project, a human *RYR1* cDNA clone will be used for functional studies. Due to the size of the *RYR1* cDNA, subclones will be made to make plasmid sizes more suitable for site-directed mutagenesis. Upon confirmation of the successful introduction of the mutation, full-length *RYR1* cDNA constructs will be reassembled and expressed in HEK293 cells for functional experiments. Currently, the use of these non-native cell types is acceptable in the EMHG guidelines for functionally assessing the consequences of genetic variants in *RYR1* despite the lack of the highly specialised cellular structure of myotubes or the expression of key, regulatory proteins of *RYR1*. Therefore, the *RYR1* variants generated in this project will also be expressed in dyspedic myotubes, simulating a more native cellular environment for *RYR1*. Directly comparing the results obtained in HEK293 cells and 1B5 dyspedic myotubes will form the framework for a thorough evaluation of the use of non-native cell types for functional studies of *RYR1* variants.

1.9.3 Evaluation of *RYR1* expression level on caffeine sensitivity of transfected cells

There is evidence to suggest that, at least in core myopathies, there is a decrease in wild type *RYR1* expression through allelic silencing (Zhou et al., 2006a, Zhou et al., 2006b). Silencing of wild type *RYR1* effectively increases the expression of the mutant allele resulting in a severe core myopathy phenotype. In MH patients, it has been found that there is an upregulation of the wild type *RYR1* allele as a compensatory mechanism to counteract the hypersensitivity of the mutant allele as well as the passive calcium leak associated with MH mutations (Grievink and Stowell, 2010). There is no evidence to suggest that an upregulation of the wild type *RYR1* allele is a contributor to the MH phenotype however, experiments increasing the expression of *RYR3* resulted in both an increase in the baseline resting calcium level and caffeine

sensitivity. It has been shown that reducing the resting calcium level of cells expressing RYR1 mutations also results in a reduction in sensitivity to caffeine and other triggering agents. To date, there have been no studies aimed at examining the effect of an increase in mutant *RYR1* expression on the caffeine sensitivity of transfected cells. In this project, the *RYR1* variants generated will be shuttled into a pTUNE inducible expression vector allowing tight regulation of *RYR1* expression.

1.9.4 Functional characterisation of a genetic variant associated with MH and EHS

It is becoming increasingly apparent that the link between MH and EHS is more than just phenotypic similarities. A number of *RYR1* variants are emerging associated with multiple exertional heat illnesses such as exertional rhabdomyolysis and EHS. Recently, our laboratory exome sequenced a number of families in which no genetic variant had been identified as potentially causative of MH. One of the *RYR1* variants identified was also found in an EHS patient that had previously tested negative for MH through the IVCT. In this project, functional analysis will be carried out on this variant to examine its association with both the MH and EHS phenotype observed in the patients. Furthermore, experiments will be performed using AICAR, the compound recently found to be entirely protective of heat-induced MH in murine models.

1.9.5 Clinical relevance of the project goals

Functional analysis of the genetic variants in *RYR1* as part of this thesis will increase the availability of mutations approved for genetic diagnosis for MH by 22.5%. The variants selected for functional analysis have been found in a total of 43 families in the UK and make up 27% of the families that have an as yet uncharacterised *RYR1* variant in the UK MH population. A number of individuals in these families are yet to be tested for MH, approval of these variants for genetic diagnosis would negate the need for these individuals and any future identified families to undergo the IVCT.

It is becoming increasingly evident that the link between MH and EHS is strengthening. Both phenotypic and genotypic data provide a strong argument for MH and EHS being different manifestations of the same molecular defects in patients with one or both of these conditions. Functional analysis of the EHS variant will contribute to the understanding of the two disorders and support the current standard of MH testing for all EHS sufferers. Expanding the knowledge of the molecular causes of an EHS episode is of particular importance to the armed services due to the volume of EHS patients identified whilst on active duty in warm climates.

Chapter Two - Materials and Methods

2.1 Molecular cloning

During this project an extensive cloning strategy was designed to facilitate the introduction of missense mutations into the *RYR1* coding sequence. The starting material was human *RYR1* cDNA in a pcDNA3.1 + expression vector (*pcRYR1*) which was a gift from Dr. Kathryn Stowell's laboratory in New Zealand (Sato et al., 2010). Subclones were created from *pcRYR1* for mutagenesis and the entire coding sequence was shuttled into two additional expression vectors for further experiments. Subclones of *RYR1* were constructed in pBluescript II SK + (Agilent technologies; Wokingham, UK). Due to the limited number of unique restriction sites in *pcRYR1*, non-directional cloning was required to shuttle *RYR1* into a pHSVPrPUC expression vector (Wang et al. (2000); Vector was a gift from Professor Paul Allen's laboratory in Boston, MA, USA) to facilitate the packaging of *RYR1* into HSV-1 virions and subsequent expression in myotubes. Furthermore, a two-step cloning strategy was developed to shuttle *RYR1* into a pTUNE inducible expression vector (Deans et al. (2007); OriGene; Wembley, UK) to examine the effect of expression level of *RYR1* mutants on caffeine sensitivity. The cloning strategies are described in more detail in chapter 3 but the various molecular biology techniques used to carry out the strategy are described below. All plasmids used in this project contained an ampicillin resistance gene for bacterial selection. All the expression vectors used also possessed a neomycin resistance gene conferring resistance to the antibiotic G418 for eukaryotic cell line selection.

2.1.1 Restriction endonuclease digests

Restriction endonuclease digestion was used to obtain cDNA fragments for subcloning and a diagnostic means to confirm successful ligation and starting plasmid material. One or multiple enzymes (New England Biolabs (NEB); Hitchin, UK or Fermentas;

Loughborough, UK) were used according to manufacturer's instructions or, in the case of double digests, reactions were set up as recommended by the NEB and Fermentas double digest calculator websites (available at <http://www.neb.com/nebecomm/DoubleDigestCalculator.asp#.T8Nk8-2KPKc> and <http://www.fermentas.com/en/tools/doubledigest> respectively).

2.1.1.1 Removing overhangs

DNA overhangs generated by restriction digestion were removed using DNA polymerase I (Klenow fragment) (NEB). Digested DNA was gel purified (see section 2.1.3) before incubation of purified DNA with 1 unit of the Klenow fragment per microgram of DNA and 33 μ M each dNTP (NEB) for 15 minutes at 25°C. The reaction was stopped with ethylenediaminetetraacetic acid (EDTA) at a final concentration of 10mM. Additionally, the Klenow fragment was heat inactivated at 75°C for 20 minutes.

2.1.2 Gel extraction

Gel extraction was performed to retrieve cDNA fragments with the intention of subcloning into shuttle vectors or for the reconstruction of full-length cDNA clones. The bands of interest were separated by electrophoresis (see section 2.2.13) excised from a 0.7% low melting point (LMP) agarose (Fisher Scientific; Loughborough, UK) gel using an individual sterile scalpel each before purifying the DNA using the QIAGEN QIAEX II kit (Manchester, UK) according to manufacturer's instructions.

2.1.3 Ligation

Fragments to be subcloned were ligated with T4 DNA ligase (NEB). Purified DNA fragments were incubated with 200 units of ligase at 16°C overnight at a molar ratio of 3:1 (insert:vector) in which the total amount of DNA never exceeded 100ng. Ligation

mixes were heat inactivated at 65°C for 15 minutes. If only one restriction enzyme was used to generate the DNA fragments or the two enzymes produced compatible overhangs, the vector sample was pre-treated with Antarctic phosphatase (NEB) to prevent religation of the fragments. Restriction endonuclease enzymes that produced a 5' extension were incubated with 2.5 units of Antarctic phosphatase for 15 minutes at 37°C. For enzymes that produced blunt ends, digested fragments were incubated for 1 hour at 37°C.

2.1.4 Transformation of *E.coli*

XL10 Gold ultracompetent *Escherichia coli* (*E.coli*) (Agilent technologies) were used for bacterial transformation. Cells and DNA were defrosted on ice before adding β -mercaptoethanol to a final concentration of 4% v/v to a 100 μ l aliquot of cells. 50ng of plasmid DNA was mixed gently with 50 μ l of XL10 Gold cells in a pre-chilled 14ml falcon tube and placed on ice for 30 minutes. The mixture was heat shocked for 30 seconds at 42°C in a water bath and placed back on ice for 2 minutes. 900 μ l of super optimal broth with catabolite repression (SOC) medium (1% w/v tryptone, 0.25% w/v yeast extract, 4.28mM sodium chloride (NaCl), 2.5mM, 10mM magnesium chloride (MgCl₂), 20mM magnesium sulphate (MgSO₄), 20mM glucose, pH 7) was added to the mixture before placing them in a 37°C shaking incubator for 1 hour. 100 μ l of the *E.coli* and SOC mixture was then plated onto Luria-Bertani (LB) agar plates (0.5% w/v tryptone, 0.25% w/v yeast extract, 171mM, 0.75% w/v agar) containing 50 μ g/ml ampicillin and incubated overnight at 37°C.

When transforming XL10 Gold cells after ligation, the same procedure was carried out, however, after incubation with SOC medium, the *E.coli* were pelleted and resuspended in 100 μ l of SOC medium and plated onto the LB agar plates containing 50 μ g/ml ampicillin.

2.1.5 Overnight cultures

Overnight bacterial cultures were established for a number of bacterial colonies on plates containing potentially successfully ligated subclones and full-length plasmid constructs. Initially, mini-prep cultures were set up to screen for successful ligation followed by maxi-prep cultures to produce large quantities of plasmid DNA for the transfection experiments.

2.1.5.1 Mini-prep overnight cultures

Single bacterial colonies were picked for overnight cultures using an individual sterile inoculation loop. Colonies were placed into 14ml falcon tubes with 4ml of LB medium containing 50µg/ml ampicillin. Tubes were placed in a shaking incubator overnight at 37°C .

2.1.5.2 Maxi-prep overnight cultures.

A single bacterial colony was picked using an individual sterile inoculation loop and placed into 4ml of LB broth containing 50µg/ml ampicillin as a starter culture. The tubes were placed in a shaking incubator at 37°C for 8 hours. For cDNA constructs 200µl of the starter culture was diluted into 100ml of LB broth containing 50µg/ml ampicillin and placed in a 37°C shaking incubator. For cosmid DNA, 500µl of starter culture was used to inoculate 250ml of super optimal broth (SOB) broth (1% weight per volume (w/v) tryptone, 0.25% w/v yeast extract, 4.28mM NaCl, 2.5mM, 10mM MgCl₂, pH 7) containing 50µg/ml ampicillin.

2.1.6 Glycerol stocks

Glycerol stocks were made of all cultures of interest. 500µl of bacteria taken from the overnight cultures was mixed 1:1 with 30% glycerol in a 2ml cryo-tube to create 15% glycerol stocks. Cultures were flash frozen in liquid nitrogen and stored at -80°C. Any

stocks that were tested and proved negative for the plasmid of interest were allowed to defrost before being treated with 1% virkon overnight according to the local biological safety regulations.

2.1.7 Plasmid DNA extraction

As discussed in section 2.1.6, overnight cultures were established for bacterial colonies of interest. The mini-prep plasmid DNA extraction was performed to an in-house protocol whereas maxi-prep plasmid DNA extractions were performed using a QIAGEN EndoFree maxi-prep kit. Both protocols used an alkaline lysis method for plasmid DNA extraction.

2.1.7.1 Mini-prep plasmid DNA extraction

Bacterial cultures grown overnight in 14ml falcon tubes were centrifuged at 1,500 x g for 10 minutes at 4°C. The supernatant was discarded. Pellets were resuspended in 200µl of ice-cold resuspension buffer (50mM glucose, 20mM Tris, 10mM EDTA, pH 8) by vortexing. 400µl of room temperature lysis buffer (0.2M sodium hydroxide (NaOH) 1% w/v Sodium dodecyl sulphate (SDS)) was added. The tubes were inverted several times to ensure thorough mixing and placed on ice for no more than 5 minutes. After the incubation time 300µl of neutralisation buffer (3M potassium acetate, pH 5.5) was added. The tubes were inverted several times to ensure thorough mixing to neutralise the reaction. All samples were centrifuged at full speed in a microcentrifuge at 4°C for 10 minutes. The supernatant was transferred to a fresh 1.5ml centrifuge tube containing 0.7 volumes of 100% isopropanol. The samples were mixed gently and centrifuged at full speed in a microcentrifuge at 4°C for 45 minutes. The supernatant was discarded and the pellet was washed with 1ml of 70% ethanol by centrifuging at full speed in a microcentrifuge at 4°C for 10 minutes. The supernatant was again discarded and the pellet was allowed to air dry for 10 minutes. Once the pellet was a

bright white colour it was redissolved in 50µl of Tris EDTA (TE) buffer (10mM Tris, 1mM EDTA). DNA pellets were allowed to dissolve at 4°C before being quantified and stored at -20°C long term.

2.1.7.2 Maxi-prep plasmid DNA extraction

Maxi-prep plasmid DNA extraction was carried out using the QIAGEN EndoFree plasmid maxi kit with a modified protocol. DNA eluted from the QIAGEN tip was precipitated with 0.7 volumes of room temperature isopropanol and centrifuged at 1,500 x g for 90 minutes at 4°C followed by washing the DNA pellet with 5ml 70% ethanol and centrifuging at 1,500 x g for 90 minutes at 4°C. The DNA pellet was allowed to dry for 30 minutes before being resuspended in 100µl TE buffer.

2.1.8 DNA quantification

DNA was quantified using either gel electrophoresis or a Nanodrop 1000 spectrophotometer. For gel electrophoresis quantification samples were run on a 1% agarose gel (see section 2.1.13). Linear DNA samples were run with a DNA MassRuler ladder of known band concentrations for comparison. For the Nanodrop 1µl of the DNA to be measured was placed on the spectrophotometer stage and absorbance reads were taken. DNA quantity was measured as compared to a blank sample and DNA quality read was measured by dividing the absorbance at 260 nanometres (nm) by the absorbance at 280nm. A value close to 1.8 indicated high purity of the DNA sample.

2.1.9 Purification

When plasmid DNAs were linearised for stable transfection of HEK293 cells (see section 2.2.6) or after *PacI* digestion of the cosmid DNA set for HSV-1 packaging (see section 2.2.8), they were purified of protein using a phenol:chloroform method. The

restriction digest reaction was made up to 600µl using TE buffer. An equal volume of 25:24:1 phenol:chloroform:isoamyl alcohol (Fisher Scientific) was added and mixed thoroughly. Samples were centrifuged at full speed in a microcentrifuge for 1 minute. The aqueous phase was gently removed ensuring that the interphase was not disturbed and placed into a fresh 1.5ml centrifuge tube. 0.1 volumes of 3M sodium acetate (pH 5.5) and 0.7 volumes of 100% isopropanol were added to the samples and mixed gently. Samples were stored at -80°C for 2 hours or -20°C overnight to precipitate the DNA. The precipitated samples were centrifuged at full speed in a microcentrifuge at 4°C for 30 minutes. The supernatant was discarded and the DNA pellet was washed with 1ml of 70% ethanol by centrifugation at full speed in a microcentrifuge at 4°C for 15 minutes. The supernatant was again discarded and the pellet was allowed to air dry for 10 minutes before redissolving in 20µl of TE. As phenol is toxic to the cells being used, purity of the samples were analysed using a Nanodrop 1000 (see section 2.1.9). Phenol and protein contamination produced a characteristic shift to the left on the Nanodrop plots resulting in a decrease in the 260/280 ratios. If this shift was seen the DNA was reprecipitated using 0.1 volumes of 3M sodium acetate (pH 5.5) and 0.7 volumes of 100% isopropanol overnight at -20°C before washing the pellet again as before. This process was repeated until no phenol contamination was seen on the Nanodrop plots.

2.1.10 Polymerase chain reaction

Polymerase chain reaction (PCR) was used to amplify regions of *RYR1* cDNA for confirmation of successful ligations and mutagenesis. PCR products were sent for DNA sequencing (see section 2.1.14). PCR cycling reactions were carried out using Thermoprime Taq polymerase (Thermo Scientific; Loughborough, UK) on a GeneAmp 2700 thermocycler. The PCR reactions contained 10x Taq reaction buffer, 20pmol each primer, 0.25mM each dNTP, 1mM MgCl₂, 2.5 units of Taq polymerase and 100ng of template DNA in a total reaction volume of 25µl. Oligonucleotide primers were

designed using Primer 3 (<http://frodo.wi.mit.edu/>) to be between 15 and 25 nucleotides long with a melting temperature of 60°C and obtained from IDT technologies (Leuven, Belgium). Cycling conditions were specifically optimised for each reaction with an annealing temperature of 58°C as a starting point. On rare occasions when 58°C was an unsuitable annealing temperature for PCR, an optimisation reaction was carried out on a DNAEngine Peltier gradient thermocycler with a gradient of annealing temperatures ranging from 50°C to 58°C to obtain the optimal annealing temperature. A list of primers used in this project for the screening of the various subclones is given in Table 2.1

Primer name	Primer sequence (5'-3')	Target
pBSrev	ATTAATGCAGCTGGCACGAC	5' subclone <i>SpeI</i> restriction site
SC11	ATGGCATGGCCATACAGG	
5scHindfor	GGCCTCTTCGCTATTACGC	5' subclone <i>HindIII</i> restriction site
5scHindrev	AGGACATCGAGGAGATGGTG	
pBSfor	GTCCCATTCGCCATTCAG	3' subclone <i>Acc65I</i> restriction site
SC31	GCGGTTCTCACCAAAGTG	
pBSrev	ATTAATGCAGCTGGCACGAC	3' subclone <i>XbaI</i> restriction site
SC42	CATGGCTTCGAGACTCAC	
pTUNE_BspEifor	GCATCAGAGCAGCCGATT	pTUNE plasmid endogenous <i>BspEI</i> site
pTUNE_BspEirev	GCGCCACCTTCTACTCTC	
pTUNEfor	TCGCTGATTTGTGTAGGGGA	<i>XhoI/Acc65I</i> restriction site in pTUNE subclone
pTUNESCrev	GGATGGCCTCTTCGATGG	
pTUNESCFLfor	CCAAGTGCTTCATCTGTGGA	<i>Sall/BsiWI</i> restriction site in pTUNE subclone
pTUNESCrev	CGGGAATTCGTCGACTGG	
pTUNEFLfor	ACATTCTGCGCGTTGCTAGT	<i>SpeI/NheI</i> restriction in full-length pTUNERYR1
pTUNESCrev	CGGGAATTCGTCGACTGG	
pHSVfor	GTCCTCGTCGATAAGCTTGC	5' end of <i>RYR1</i> in full-length pHSVRYR1
RYR1HSVrev	GGCGGAGTTGTTACGACATT	
RYR1HSVfor	AGCACAACCTGGCCAATTAC	3' end of <i>RYR1</i> in full-length pHSVRYR1
pHSVrev	GGGCATCTCTACCTCAGTGC	

Table 2.1 – Primers to screen for successful generation of the various subclones created in this project
Listed are all the primers used to screen potential subclones generated for the various cloning steps in this project. Primers were designed to create a PCR product over the restriction sites used for ligation. A PCR product would only be generated if ligation had been successful.

2.1.11 MEGAWHOP

Mega primer PCR of whole plasmid (MEGAWHOP) was used for site-directed mutagenesis to introduce specific single nucleotide missense mutations into *RYR1* cDNA constructs. MEGAWHOP mutagenesis utilises a mega primer system in conjunction with the QuikChange mutagenesis protocol (Figure 2.1). MEGAWHOP was originally developed for the introduction of random mutations into cDNA libraries but has been successfully used in the site-directed mutagenesis of large plasmid constructs (Miyazaki, 2003, Sato et al., 2010, Sato et al., 2013). Forward mutagenic primers between 20 and 35 nucleotides long were designed with the desired mutation in the middle, allowing strong binding to the template DNA at either side of the missense change. This was partnered with a reverse wild type primer between 15 and 20 nucleotides long, resulting in a PCR product of 200 to 800 bp. This first round of PCR generated a mutated double stranded PCR product, which, after confirmation of successful introduction of the missense change via sequencing (see section 2.1.14) was used as a pair of mutagenic mega primers. Whole plasmid DNA replication was carried out using *Pfu* ultra DNA polymerase (Agilent Technologies) according to the QuikChange system but with the mega primers generated in the first mutagenesis step. The PCR reaction was digested with the *DpnI* restriction enzyme, removing the *Dam*⁺ methylated template DNA, leaving only unmethylated, replicated PCR product. The PCR product was then transformed into XL10 Gold *E.coli* and grown on LB plates containing ampicillin (see section 2.1.5) before plasmid DNA extraction (see section 2.1.8.1) and PCR screening for successful mutagenesis. The primers used for mutagenesis and subsequent screening are listed in Table 2.2.

The mega-primer generating PCR was carried out using 10x Taq polymerase reaction buffer, 20pmol of each primer, 0.25mM each dNTP, 1mM MgCl₂, 2.5 units of Taq polymerase, 100ng of template DNA in a total volume of 25µl. The cycling conditions were an initial denaturation step of 95°C for 5 minutes followed by 25 cycles of 95°C for 30 seconds, 58°C for 30 seconds and 72°C for 45 seconds followed by a final extension step of 72°C for 7 minutes.

Whole plasmid PCR followed using 5x *Pfu ultra* polymerase reaction buffer, 200ng of mega primers, 0.25mM each dNTP, 2mM MgCl₂, 2.5 units of *Pfu ultra* DNA polymerase and 100ng of template DNA in a total volume of 50µl. The reaction included a final concentration of 6% (v/v) of Quiksolution from the Agilent mutagenesis kit. Cycling conditions consisted of an initial denaturation step of 95°C for 1 min followed by 18 cycles of 95°C for 50 seconds, 53°C for 50 seconds and 68°C for 2 minutes per kb of template DNA followed by a final extension step of 7 minutes at 68°C.

2.1.12 Electrophoresis

DNA gel electrophoresis was performed using 0.7%-2% agarose depending on the product sizes expected containing 0.5µg/ml ethidium bromide. Gels were made and run in 1x Tris-acetic acid-EDTA (TAE) buffer (40mM Tris, 20mM acetic acid, 1mM EDTA) and allowed to set before loading samples and subjecting it to an electric current. DNA samples were electrophoresed for between 20 minutes and 1 hour at 100-150v depending on the product sizes expected. Products were visualized using ultra violet (UV) light in a UGenius Gene Flash gel doc system. When PCR products or digest fragments were required for gel extraction, DNA samples were run on a 0.7% LMP agarose gel made from 1x TAE buffer at 4°C.

	Primer sequence (5'-3')	Target subclone
Mutation	p.D1056H (c.3166 G>C)	
Mutagenic primer (forward)	AACATCGAGCCTCCT C ACCAGGAGCCCAGT	5'
PCR screening primer (forward)	AGAAAATGGGCACAACGTG	
Reverse primer (both reactions)	GTCGATCATACAGCCAACGA	
Mutation	p.R2336H (c.7007 G>A)	
Mutagenic primer (forward)	TACCTGGACTTCCTGCA C CTTTGCTGTCTTCGTCAA	3'
PCR screening primer (forward)	GAGCTGGCCTTGGCATT	
Reverse primer (both reactions)	TGCCGGCTTGGATTAGAT	
Mutation	p.R2355W (c.7063 C>T)	
Mutagenic primer (forward)	ACGCCAATGTGGTGGT G TGGCTGCTCATCCGGAA	3'
PCR screening primer (forward)	GAGCTGGCCTTGGCATT	
Reverse primer (both reactions)	TGCCGGCTTGGATTAGAT	
Mutation	p.E3104K (c.9310 G>A)	
Mutagenic primer (forward)	CTCGGAGGACATCA A AGAAGATGGTGGAGAA	3'
PCR screening primer (forward)	GAGTCTCTCTTTGGGACA	
Reverse primer (both reactions)	CAGCTCGGCTCCAGGAA	
Mutation	p.D3986E (c.11958 C>G)	
Mutagenic primer (forward)	AGTCGCCTATGGGA G GCAGTGGTGGGATT	3'
PCR screening primer (forward)	CTACTCGGGCAAGGATGTCATT	
Reverse primer (both reactions)	CTTCTGGAAGTCCTTCTTGGAGAT	
Mutation	p.G3990V (c.11969 G>T)	
Mutagenic primer (forward)	ACGCAGTGGTGG T ATTCCTGCACGTGTT	3'
PCR screening primer (forward)	CTACTCGGGCAAGGATGTCATT	
Reverse primer (both reactions)	CTTCTGGAAGTCCTTCTTGGAGAT	
Mutation	p.V4849I (c.14545 G>A)	
Mutagenic primer (forward)	GGCGGTGGTCA T CTACCTGTACA	3'
PCR screening primer (forward)	TACCTGGGCTGGTATATGGTGATGT	
Reverse primer (both reactions)	GCACTTGGTCTCCATATCCTCCTT	

Table 2.2 – List of primers used for mutagenesis and mutation site screening

Primers used for mutagenesis are listed in the table. A total of seven *RYS1* variants were targeted in the subclones. Mutagenic forward primers (with the missense change highlighted in red) were paired with a reverse primer to generate mutagenic mega primers that were subsequently used for whole plasmid mutagenesis. Upon screening for successful mutagenesis the PCR screening primers were paired with the same reverse primer used for the generation of the mega primers to screen over the mutation site.

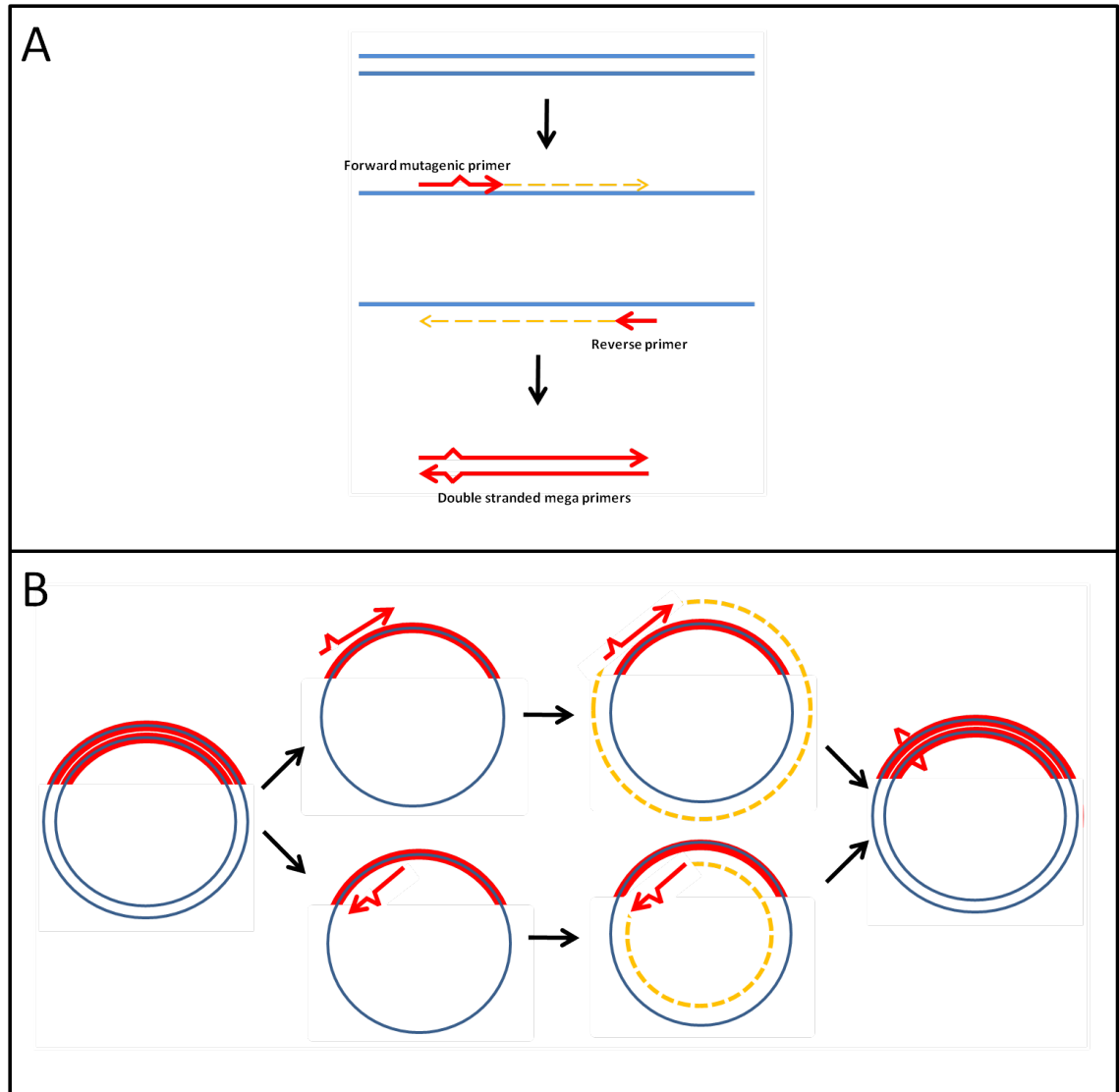


Figure 2.1 – MEGAWHOP mutagenesis.

(A) Mutagenic mega primers were created using a mutagenic forward primer of around 30 nucleotides in length which was paired with a wild type reverse primer of 20 nucleotides to create a mutated PCR product of between 200 and 800bp. The mega primers were sent for sequencing to confirm the presence or absence of the desired mutation. (B) Mutagenic mega primers were used for whole plasmid PCR to introduce the desired mutation into the subclone of *RYR1*.

2.1.13 Sequencing

DNA sequencing was performed on PCR products generated spanning mutation and ligation sites to confirm successful mutagenesis and cloning respectively. PCR products to be sequenced were purified by incubating with exosap-IT (Affymetrix; High Wycombe, UK) at 37°C for 30 minutes using the manufacturers recommended concentration and then heat inactivated at 80°C for 15 minutes. Samples were sequenced using the BigDye Terminator kit (Applied Biosystems). Purified PCR product was mixed with 1.6pmol of the primer used to generate the PCR product and the BigDye components according to manufacturers recommendations. The sequencing reaction was carried out on an Applied Biosystems Gene Amp 2700 thermocycler with cycling conditions consisting of an initial denaturation step of 96°C for 5 minutes followed by 30 cycles of 96°C for 30 seconds, 58°C for 20 seconds and 60°C for 4 minutes. Sequenced products were precipitated with 3M sodium acetate (pH 5.5) and resuspended in Hi-Di formamide (Life Technologies; Paisley, UK). Resuspended pellets were sent to the Leeds Institute of Molecular Medicine in-house sequencing service for sequence reading using an ABI3103xl genetic analyser (Life Technologies). Base calling was performed by the service using Sequence Analysis v5.2 and sequencing results were examined in 4peaks sequencing software (available to download at <http://nucleobytes.com/index.php/4peaks>).

2.2 Materials for cell culture

In this project, various cell lines were used. HEK293 cells were the primary *in vitro* expression system used for functional experiments (LGC Standards; Teddington, UK). 1B5 Myoblasts were differentiated into myotubes for functional experiments in muscle-like cells. 2-2 cells were used for HSV-1 viral packaging (see section 2.2.8) (The 1B5 and 2-2 cell lines were a gift from Professor Paul D Allen's laboratory in Boston, MA, USA as was the cosmid set used for viral packaging). A C2C12 mouse myoblast cell

line was used as a positive control for immunocytochemistry (Sigma-Aldrich; Poole, UK) (see section 2.2.8.3.1).

2.2.1 Defrosting the cell lines

2ml cryo tubes containing a frozen aliquot of the cells required were defrosted quickly by placing the tubes into a 37°C water bath. Defrosted cells were placed into a 50ml falcon tube containing preheated growth medium and centrifuged for 5 minutes at 400 x g. The cell pellet was resuspended in 10ml of growth medium (see section 2.2.2 for the growth medium of each cell line) and plated onto a 10cm tissue culture dish.

2.2.2 Maintenance of cells

Cells were maintained in the growth medium recommended by the supplier or lab of origin (Life Technologies). HEK293 cells and C2C12 cells were maintained in Dulbecco's Modified Essential Medium (DMEM) containing 4.5g/L glucose, for stably transfected HEK293 cells, the growth medium was supplemented with 0.5mg/ml G418. 1B5 cells were maintained in DMEM containing 1g/L D-glucose and pyruvate. 2-2 Cells were maintained in DMEM containing 4.5g/L glucose, 25mM 4-(2-hydroxyethyl)-1-piperazineethanesulfonic acid (HEPES) and 0.5mg/ml G418 (Sigma-Aldrich). All growth media was supplemented with 10% fetal bovine serum (FBS) (Biosera; Uckfield, UK) and 10-units/ml penicillin and 10µg/ml streptomycin solution (Life Technologies).

2.2.3 Passaging the cell lines

Growth medium was removed from the plates containing cells. The cells were washed with phosphate-buffered saline (PBS) (Life Technologies) pre-heated to 37°C before a thin covering of 0.25% Trypsin-EDTA (T/E) (Life Technologies) was applied. The plates were incubated at 37°C for 5 minutes. Confirmation that the cells were detached from the plate was seen under the light microscope. 5ml of PBS was used to gently detach

any remaining cells before transferring the cells to a 50ml tube that contained 15ml PBS. Tubes were centrifuged at 400 x g for 5 minutes to pellet the cells. The supernatant was discarded and the pellet was resuspended in 10ml of growth medium. The desired amount of suspension was added to new plates with fresh growth medium in.

2.2.4 Freezing the cell lines

When cells were required for freezing the same procedure was carried out as for passaging the cells up until they were pelleted and the supernatant discarded. Cells were resuspended in the desired amount of freezing medium (full growth medium with 10% dimethyl sulphoxide (DMSO; Sigma Aldrich). 2ml aliquots were placed into cryotubes. The tubes were put in a 'cool cell' freezing device (Sanyo-Biomedical; Loughborough, UK) and stored overnight at -80°C to allow the cells to freeze slowly at 1°C per minute. The following day cells were taken to liquid nitrogen stores for long-term storage.

2.2.5 Cell counting

Cells were counted using a haemocytometer. Cells were passaged as described above until the pelleting step. The cell pellets were resuspended in the required amount of growth medium. 10µl was added to the haemocytometer and all cells within the 4 large corner squares were counted. The average cell number from the 4 squares was equivalent to the amount of cells x 10⁴ per ml of medium. The desired number of cells was then plated onto the next tissue culture vessel.

2.2.5.1 Trypan blue viability stain

An antibiotic kill curve was established to determine the correct amount of selection pressure to add to transfected cells. 5 x 10⁴ HEK293 cells were plated in TC25 flasks

and allowed to adhere to the vessel. 24 hours later, growth medium containing varying levels of G418 antibiotic were added to the cells (0mg/ml, 0.5mg/ml, 1mg/ml and 1.5mg/ml). Trypan blue viability staining was carried out every 2 days after the addition of antibiotics to see how effectively G418 was killing the cells.

Cells were passaged as described in section 2.2.3 up until the pelleting step. The cell pellets were resuspended in 200µl of PBS. An equal volume of 0.4% w/v trypan blue (Acros Organics; Geel, Belgium) was added to each cell suspension and allowed to incubate at room temperature for 5 minutes. After incubation, 10µl of the mixture was added to a haemocytometer and visualised under a light microscope. Dead cells took up the dye and therefore appeared dark blue whereas living cells remained white. The total numbers of cells were counted and the percentage of dead cells was calculated and plotted in a graph. When carrying out stable transfection of HEK293 cells, trypan blue viability staining was carried out after the initial selection of 10 days to ensure that mock-transfected cells were dead and transfected cells showed resistance to the antibiotic (see section 2.2.6).

2.2.6 Stable transfection of HEK293 cells

Stable transfection of pcRYR1 constructs into HEK293 cells was performed to establish cell lines expressing RYR1 at high levels for caffeine-induced calcium release experiments. Prior to transfection, cells were plated into 24-well tissue culture plates in antibiotic-free growth medium and were allowed to grow to 90% confluence. Purified, linear plasmid DNA was diluted in 50µl of Opti-MEM (Life Technologies) ensuring that 800ng of DNA was present per transfection. 2µl of Lipofectamine-2000 (LF2000; Life Technologies) was also diluted in 50µl of Opti-MEM. The two mixtures were allowed to incubate at room temperature for 5 minutes before combining the two. The tubes were mixed gently and incubated at room temperature for 20 minutes to allow the formation of DNA-lipid complexes. After the incubation time, 100µl of the complexes were dropped into each well. The plate was gently rocked several times

and placed in a 37°C incubator with 5% CO₂. 24 hours post-transfection cells were split 1:10 and plated into 10cm plates containing fresh growth medium. 48 hours after transfection, antibiotic selection pressure was added to the growth medium (1mg/ml G418).

Cells were allowed to grow in the high selection growth medium for 10 days before carrying out trypan blue viability staining (see section 2.2.5.1). If mock transfected cells had a much higher dead cell count than transfected cells they were discarded and the transfected cells were transferred to a new, lower selection pressure (0.8mg/ml G418) and allowed to grow for a further 10 days. If mock transfected cells had a similar dead cell count to transfected cells, high selection pressure was maintained for a further 10 days and tested again using trypan blue. Cells were always split 1:10 when 70% confluence was reached.

After 20 days of selection the fastest growing cells were selected to take forward with the remaining plates being frozen as back ups (see section 2.2.4). The selection pressure was dropped to 0.5mg/ml G418. The cells were split and diluted enough to ensure that individual colonies of cells had space to grow. Colonies were allowed to grow for 7 days before the fastest growing were individually picked using a 10ml pipette and placed into a well each in a 6-well plate. The cells were allowed to grow for a further 7 days before the fastest growing well was selected as the stable clone.

2.2.7 Transient transfection of HEK293 cells

Transient transfection of *pcRYR1* constructs was also performed. Additionally, transient transfection of *pTUNERYR1* plasmids was carried out due to the absence of a suitable antibiotic selection gene after cloning. Transient transfection of plasmids into HEK293 cells was carried out prior to calcium release measurements (48 hours for *pcRYR1* constructs and 72 hours for *pTUNERYR1* constructs). The 96-well opti-clear plates used for transfection and calcium release measurements were pre-coated with

Entactin-Collagen IV-Laminin (ECL) (Millipore; Watford, UK) extracellular matrix proteins to allow greater adhesion to the plate during the calcium release experiments. The wells that would eventually contain cells were coated with ECL at a final concentration of 20µg/ml for 1 hour at 37°C. 5×10^4 HEK293 cells were plated into each well of a 96-well plate and allowed to adhere overnight. The following day DNA transfection was carried out. 200ng of the desired construct and 0.5µl of LF2000 was diluted with 25µl of Opti-MEM each and allowed to incubate at room temperature for 10 minutes. Following the incubation period the DNA and LF2000 were combined and mixed gently and left at room temperature for 20 minutes to allow DNA:lipid complex formation. After the incubation period, 50µl of DNA:lipid complexes were added to each well to be transfected. The plate was rocked gently several times and placed in a 5% CO₂ incubator for 48 hours prior to calcium release measurements.

2.2.7.1 pTUNERYR1 expression induction

The pTUNE expression vector allows for inducible expression through a process based on the lac operon (Figure 2.2). In the switched off state, expression of *RYR1* is inhibited by the constitutive expression of LacI proteins that bind to operator sites directly upstream of a cytomegalovirus (CMV) promoter and Rous sarcoma virus (RSV) promoter blocking transcription from both. The RSV promoter drives expression of the gene of interest which, when blocked by LacI proteins results in limited, if any, expression of the gene of interest. The CMV promoter drives expression of TetR proteins which, when blocked results in the expression of a small hairpin ribose nucleic acid (shRNA) that binds to the 3' untranslated region of the gene of interest blocking any residual gene expression. In the presence of Isopropyl-β-thiogalactopyranoside (IPTG) (Cell Signalling Technology; Hitchin, UK), LacI expression is blocked preventing the binding of these proteins upstream of the CMV and RSV promoters. This results in expression of the gene of interest and absence of expression of the shRNA. Expression can be fine tuned depending on the amount of IPTG added to the cell culture medium.

HEK293 cells transfected with pTUNERYR1 constructs were allowed to sit in the transfection mix for 6 hours before changing the medium to standard HEK293 cell growth medium containing the desired amount of IPTG. Fresh medium was added to the transfected cells every 24 hours until caffeine-induced calcium release measurements or cell viability assays were carried out, in the case of pTUNERYR1 transfected cells, experiments were performed 72 hours post-transfection. For standard dose-response experiments, an IPTG induction level of 25 μ M was selected based on information from Deans et al. (2007). A higher (250 μ M) and lower (2.5 μ M) dose of IPTG was used to tune *RYR1* expression in later experiments.

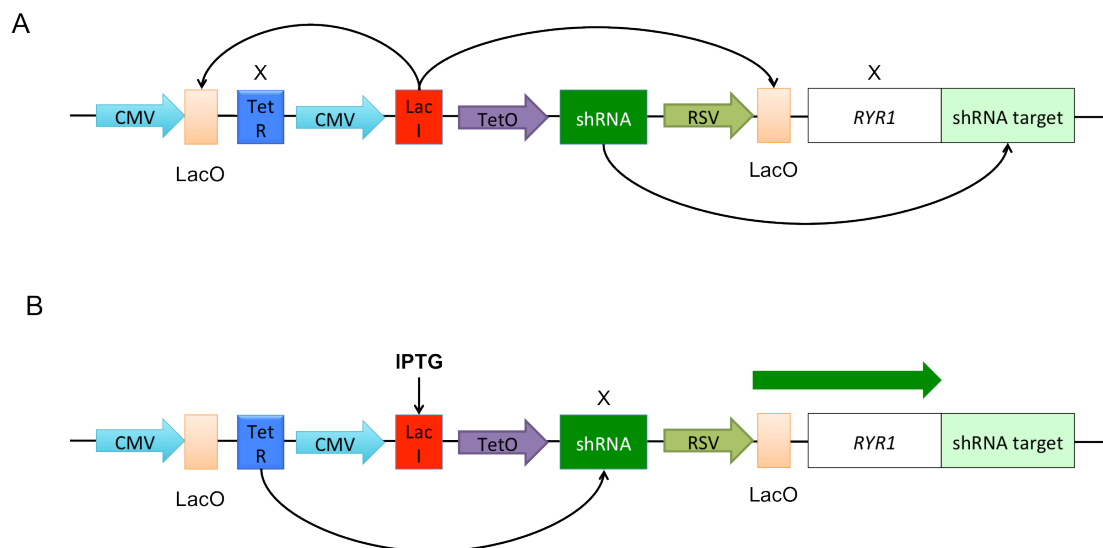


Figure 2.2 – Induction of pTUNERYR1 constructs

(A) Repression of *RYR1* expression. A constitutively expressed LacI protein binds to LacO sites preventing the transcription of the TetR protein as well as preventing *RYR1* expression from the RSV promoter. The TetO promoter is free to transcribe a shRNA that binds to a target in the 3' untranslated region of *RYR1* preventing any expression that may pass through the initial LacI block. (B) Activation of gene expression using IPTG. IPTG prevents the LacI proteins binding to LacO sites allowing expression of the TetR protein, which prevents the shRNA binding to its target. Without a LacI protein bound to the LacO site and shRNA to its target, *RYR1* expression can occur without being blocked. Redrawn from Deans *et al* 2008.

2.2.7.1.1 Treatment with AICAR

Some HEK293 cells transfected with pTUNERYR1 constructs were pre-treated with AICAR (Cell Signalling Technology) to examine its effect on caffeine sensitivity. In these

experiments cells were incubated with 1mM AICAR in the normal growth medium containing the desired amount of IPTG to maintain *RYR1* expression. Cells were treated with AICAR overnight prior to the caffeine-induced calcium release experiments or cell viability assays.

2.2.8 HSV-1 viral packaging

pHSV*RYR1* constructs generated through the cloning steps in this project were packaged into HSV-1 virions according to previously reported protocols (Wang et al., 2000, Yang et al., 2003), which are described below.

2.2.8.1 Preparation of 2-2 cells and viral packaging

Monkey Vero 2-2 cells were passaged in cell culture until there were ten 10cm dishes reaching confluence per pHSV*RYR1* construct to be packaged. The day before viral packaging, 3×10^6 cells were plated onto each plate to be transfected. Viral packaging was carried out on 10 plates for each construct. Co-transfection of plasmid DNA and cosmid DNAs containing the entire HSV-1 genome minus the viral packaging signal was carried out to produce HSV-1 virions (Figure 2.3 A). The cosmid DNA set was produced by Fraefel et al. (1996) and then modified by Wang et al.,(2000). Each of the 5 cosmid DNAs were transfected at an equal molar ratio based on the size of each cosmid with no more than 1.2 μ g of any cosmid being used. 1.2 μ g of the largest cosmid was added to each plate. The concentration of each other cosmid in the mix was based on their size relative to the largest cosmid as outlined in Table 2.3.

Cosmid	Size (bp)	% of the largest cosmid	Amount of DNA per plate transfected (μg)
6	39,165	98%	1.176
14	36,032	90.7%	1.08
28	39,706	-	1.2
48	35,977	90.6%	1.08
56	35,710	89%	1.07
			Total: 5.4

Table 2.3 – Ratios of each cosmid required for HSV-1 viral packaging.

Each of the five cosmids used for HSV-1 viral packaging needed to be co-transfected at equal molar ratios.

Because each cosmid is different in size the amount of DNA in μg required to reach an equal molar ratio is different. A maximum of $6\mu\text{g}$ of cosmid DNA was required for each 10cm dish transfected. Cosmid 28 was the largest and the rest were calculated as a percentage of the largest to calculate the amount of DNA required compared to the largest. $1.2\mu\text{g}$ of DNA was used as the maximum amount of DNA for each cosmid.

For each plate to be transfected the following reactions were set up; $1.5\mu\text{g}$ of the plasmid DNA construct (containing the HSV-1 packaging signals) was diluted with $750\mu\text{l}$ of Opti-MEM. Cosmid DNA (containing the rest of the HSV-1 genome) mix totalling $5.4\mu\text{g}$ of cosmid DNA containing the entire HSV genome minus the packaging signals were added. An equal volume of μl of PLUS reagent (Life Technologies) to μg of DNA was added to the mixture, mixed gently and incubated at room temperature for 10 minutes. At the same time, for each plate to be transfected, $50\mu\text{l}$ of LF2000 was diluted in $750\mu\text{l}$ of Opti-MEM and incubated for 10 minutes at room temperature. After the incubation period, the LF2000/Opti-MEM mixture was added drop-wise to each plasmid DNA construct, mixed by inversion several times before an incubation period of 45 minutes at room temperature. Each plate to be transfected was washed 3 times with Opti-MEM before the addition of 8ml of transfection mix to each plate. Plates were placed in a 37°C and humidified 5% CO_2 incubator for 2.5 days before harvesting of the HSV-1 virions.

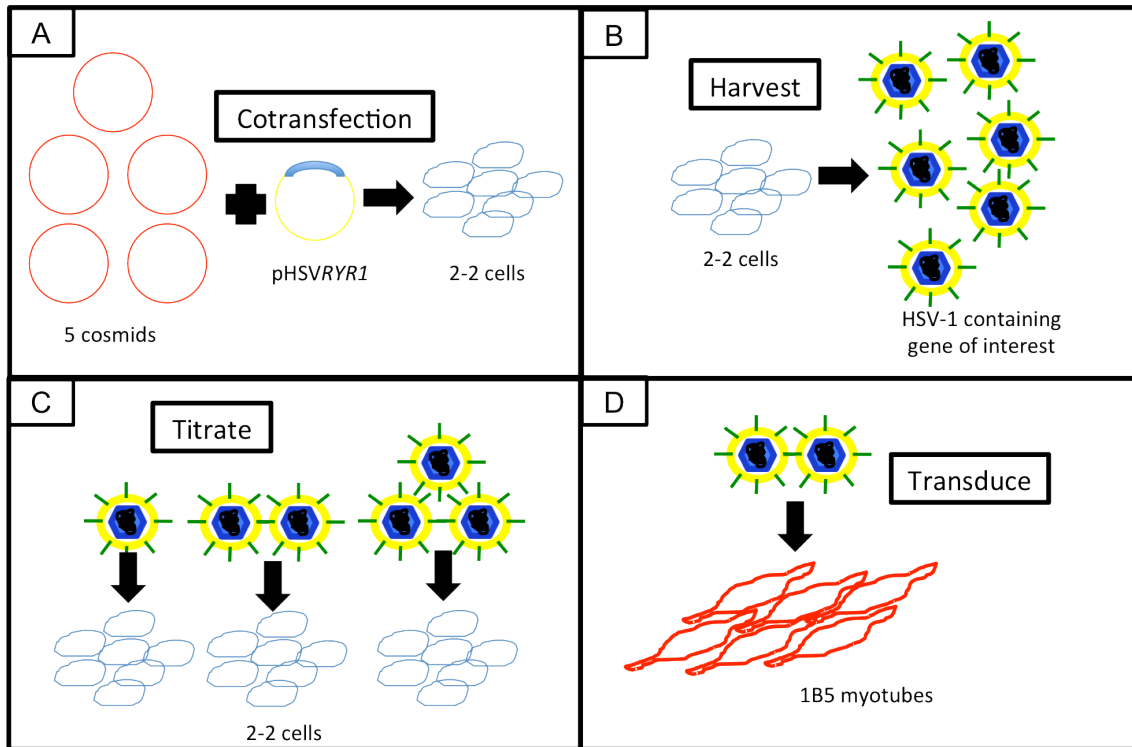


Figure 2.3 – Strategy used to package pHSVRYR1 constructs into HSV-1 virions

(A) Co-transfection of the 5 cosmids and pHSVRYR1 plasmid into 2-2 cells. Cells are transfected and allowed to remain in culture for 2.5 days to ensure high levels of HSV-1 within the cells upon harvesting. (B) Harvesting the HSV-1 virions. Cells are pooled and harvested using a combination of freeze thawing and sonication to break open the cells, freeing the HSV-1 virions. (C) Titration of the HSV-1 virions using 2-2 cells to determine the viral titre obtained in the 2.5 days of viral packaging. (D) After the viral titre has been determined, suitable amounts of virions can be used to transduce dyspedic 1B5 cells to allow the expression of *RYR1* and subsequent calcium release experiments.

2.2.8.2 Harvesting HSV-1 virions

The following harvesting procedure was carried out for each construct being packaged (Figure 2.3 B). Cells from each of the plates that were co-transfected with the cosmid DNA set and pHSVRYR1 constructs were harvested with a cell scraper. Cells transfected with each pHSVRYR1 construct were pooled into a 50ml falcon tube and placed on ice for 10 minutes. Each tube was centrifuged at 1,400 x g for 10 minutes. All but 2ml of the supernatant was transferred to a fresh 50ml falcon tube and flash frozen in a dry-ice ethanol bath. The majority of the packaged virions are contained within the cells but the supernatant contains some virions and was frozen as back up stock of virions. The remaining cell pellet was resuspended in the 2ml supernatant left

over and transferred into a 14ml tube. The suspended cells were put through three freeze/thaw cycles in a dry-ice ethanol bath followed by thawing in a 37°C water bath. After the 3 cycles, cells were subjected to sonication at 20% output for a total period of 20 seconds in 2-second bursts. Sonicated cells were then centrifuged at 1,400 x g for 15 minutes. The supernatant was transferred into 100µl aliquots of virions and flash frozen in a dry-ice ethanol bath. Frozen virions and supernatants were stored at -80°C until needed.

2.2.8.3 Preparation of 2-2 cells for HSV-1 virion titration

1 X 10⁵ Vero 2-2 cells were plated onto a 24-well plate and cultured overnight. The following day, 1µl, 5µl and 20µl of harvested virions were diluted in DMEM containing 2% FBS to a total volume of 250µl. The Vero 2-2 cell growth medium was removed and replaced with the 250µl virion mixture and cultured overnight at 37°C and 5% CO₂. The following day, the virion mixture was replaced with standard 2-2 cell growth medium and cultured for a further 24 hours before being fixed with ice cold methanol for 20 minutes at -20°C. Fixed cells were washed with 4°C PBS and stored at 4°C until required for titration using immunostaining (see section 2.2.8.5) (Figure 2.3C).

2.2.8.4 Preparation of 1B5 cells for HSV-1 virion titration

1B5 Cells were differentiated on a 96-well Opti-clear plate as described in section 2.2.8.6. Midway through the 4-day differentiation period, the differentiation medium was removed and replaced with one containing either 20µl, 50µl or 100µl virions in growth medium with DMEM containing 2% FBS to a total volume of 150µl. Cells were incubated in this medium overnight in an incubator at 37°C and 5% CO₂ before replacing the medium with differentiation medium and incubation in the hypoxic incubator for a further 24 hours prior to titration using caffeine-induced calcium release (Figure 2.3D).

2.2.8.5 Immunocytochemistry assay

Fixed cells were washed with 4°C PBS and blocked overnight in PBS with 5% normal Goat serum (NGS) (Life Technologies) at 4°C. The following day, cells were washed three times in PBS before the primary anti-RYR1 antibody (34C) (Sigma Aldrich) was incubated with the cells at a concentration of 1µg/ml diluted in PBS with 5% NGS for 2 hours at 4°C. The cells were then washed with 4°C PBS three times before adding a goat-anti-mouse secondary antibody with Cy3 conjugate (Jackson ImmunoResearch; Newmarket, UK) at a dilution of 1:3000 in PBS with 5% NGS for 1 hour at 4°C. After secondary antibody staining, the cells were washed three times in 4°C PBS before being covered with 300mM 4', 6-diamidino-2-phenylindole (DAPI; Life Technologies) nucleic acid stain for 5 minutes and washing a further three times in 4°C PBS. The cells were then coated in 4°C PBS prior to detection.

Fluorescence was detected using the Delta Vision wide field deconvolution microscope in the University of Leeds, Faculty of Biological Sciences bio-imaging facility. A 60x oil immersion lens was used to detect Cy3 fluorescence using a filter set with excitation at 555/28nm and detection at 617/73. DAPI staining was detected using a filter set with excitation at 360/40nm and emission at 457/50nm. Images were overlaid together and saved to file using SoftWoRx v3.3.6 image acquisition software.

2.2.8.6 Differentiation of 1B5 cells and C2C12 cells

1B5 and C2C12 cells were plated onto a 96-well Opti-clear plate pre-coated with ECL as described in section 2.2.7 and allowed to grow to 70% confluence before switching to a differentiation medium containing 2% heat-inactivated horse serum (Sigma-Aldrich) as well as transferring the plate to a hypoxic incubator containing 5% CO₂ and 5% O₂ at 37°C. Cells were allowed to grow for 4 days in the hypoxic incubator to fully differentiate myoblasts into myotubes. Complete differentiation was observed through the presence of elongated and multinucleated myotubes under the light microscope.

2.2.9 Transfection of 1B5 cells

Conventional transfection of 1B5 cells was also performed using LF2000 and Xfect polymer (Clontech; Paris, France). LF2000 transfections were performed using the same reaction as described in section 2.2.7. Transfections with the Xfect polymer were performed to manufacturer's instructions; briefly, 400ng of DNA per well to be transfected was diluted to 25 μ l with the Xfect buffer. 0.2 μ l per transfection of the Xfect polymer was diluted to 25 μ l with the Xfect buffer. Both tubes were combined and vortexed at a medium speed for 10 seconds before a 10-minutes room temperature incubation. Following the incubation, the 50 μ l mix was added to each well to be transfected.

Transfections using each method were performed at different differentiation stages. Transfections were performed before a 3-day and 4-day differentiation step. For these transfections, 1B5 cells were plated onto a 96-well Opti-clear plate pre-coated with ECL 24 hours prior to transfection. Transfections were performed as described above. Cells were allowed to sit in the transfection mixes for 6 hours before having the medium changed to 1B5 differentiation medium (see section 2.2.8.6) and being placed in the hypoxic incubator for the desired differentiation period. Alternatively, cells were transfected midway through a 4-day differentiation period. In this case, 1B5 cells were plated onto a 96-well Opti-clear plate pre-coated with ECL. 24 hours after plating, the plate was transferred to the hypoxic incubator for 2 days. Transfections were then performed as described above. Cells were allowed to sit in the transfection mixes for 6 hours in the 5% CO₂ incubator before having the medium changed and being placed back into the hypoxic incubator for a further 2 days of differentiation.

2.3 Protein

HEK293 cells were seeded onto a 6-well plate to perform transient transfections to obtain cells expressing RYR1 for protein extraction and subsequent detection. When the cells reached 80% confluence they were transfected with the various cDNA

constructs used in this project. Transfections were performed using the same procedure described in section 2.2.7 however, 4 μ g of each plasmid was transfected and diluted in 250 μ l of Opti-MEM. Similarly, the amount of LF2000 was increased to 10 μ l per transfection diluted in 250 μ l of Opti-MEM. For the *pcRYR1* transient experiments, cells were transfected and allowed to grow for 48 hours before protein extraction. For the *pTUNERYR1* transfections, cells were transfected and induced to the desired level using IPTG (see section 2.2.7.1) before protein was harvested after a total incubation time of 72 hours. These culture times were consistent with the times allowed before calcium measurements were carried out (see section 2.2.7.1). For stable HEK293 cell lines, cells were plated onto a 10cm tissue culture dish and allowed to grow to sub-confluence prior to protein extraction.

2.3.1 Protein extraction

Cells were cooled on ice and washed once with 4°C PBS. Cells were covered in 4°C PBS for a second time and loosened from the plate surface using a cell scraper. Cells were collected and placed in a 50ml falcon tube and cooled on ice for 5 minutes. Following the cooling step the cells were centrifuged at 1,600 rpm for 15 minutes to pellet the cells. Cell pellets were resuspended in 100 μ l of cell lysis buffer (100mM Tris, 0.5% v/v triton x-100, 1% protease cocktail inhibitor). Resuspended cell pellets were incubated at 37°C for 10 minutes before centrifuged at 10,000 x g for 15 minutes. The supernatant was transferred to a fresh 1.5ml centrifuge tube and stored at -20°C until needed.

2.3.2 Protein quantification using a Bradford assay

A Bradford assay to quantify the protein samples was performed on the Nanodrop 1000 machine. Protein standards were made from bovine serum albumin (BSA) (BioFX; Cambridge, UK) powder at concentrations of 0.1mg/ml, 0.5mg/ml, 1mg/ml, 4mg/ml and 8mg/ml by diluting the appropriate amount of BSA in distilled water. 10 μ l

of each of the protein standards and samples to be measured were mixed with 200 μ l of Bradford reagent (Bio-Rad) and incubated at room temperature for 10 minutes. The Nanodrop machine was blanked using 2 μ l of Bradford reagent containing no BSA before measuring 2 μ l each of the protein standards in triplicate to generate a standard curve. Following the generation of the standard curve, 2 μ l of each sample extracted was measured on the Nanodrop with concentrations being calculated relative to the standard curve.

2.3.3 Protein detection

2.3.3.1 Polyacrylamide gel electrophoresis

4%-8% polyacrylamide gels were made according to the recipe given in Table 2.4. 50 μ g of each protein sample was diluted to 15 μ l in deionised water. A mixture of 10% β -mercaptoethanol (Sigma-Aldrich) in Laemmli loading buffer (v/v) (Bio-Rad) was made, mixed 1:1 with the protein sample and incubated at 95°C for 10 minutes. After the boiling step, the samples were placed on ice for 10 minutes before loading onto the polyacrylamide gel. A mini-protean protein electrophoresis tank was set up according to the manufacturers instructions (Bio-Rad). The internal chamber was filled with 1x tris-glycine-SDS (TGS) buffer (25mM Tris, 190mM glycine 0.1% w/v SDS) as was half of the external tank. A total of 30 μ l of the protein sample mix was added to each well with one well possessing a Precision Plus protein ladder (Bio-Rad). All samples were electrophoresed for 2 hours at 100v or until the dye front had reached the end of the gel.

	4% stacking gels	8% resolving gels
Deionised water	2.816ml	10.584ml
Polyacrylamide mix (40%)	400µl	4ml
Tris (pH 8.8) (1.5M)	700µl	-
Tris (pH 6.8) (0.7M)	-	5ml
SDS (10%)	40µl	200µl
Ammonium persulphate (10%)	40µl	200µl
Tetramethylethylnediamine	4µl	16µl

Table 2.4 – Recipe for the polyacrylamide gels made in this project

8% resolving gels were made and poured into the gel cast and allowed to set for 30 minutes with an overlay of 0.1% SDS before the addition of the 4% stacking gel mix. The stacking gel was allowed 30 minutes to set with a comb in prior to electrophoresis.

2.3.3.2 Western blotting

Prior to the completion of electrophoresis, a total of 6 squares of 3mm Whatman blotting paper were cut to the same size as the gel. A piece of polyvinylidene fluoride (PVDF) membrane was also cut to the same size as the gel. The membrane was activated in 100% methanol for 2 minutes before being washed in TGS buffer. The western blot was set up so that the gel and the membrane were sandwiched between 3 pieces of Whatman paper each and blotted overnight at 4°C and 30 volts with gentle mixing of the buffer with a magnetic flea. The blot was run in tris-glycine (TG) buffer (25mM Tris, 190mM glycine). The following day, the membrane and gel was checked for complete protein transfer as indicated by the largest band of the pre stained ladder being visible on the membrane but absent from the gel. The membrane was blocked for 1 hour in 5% milk in tris-buffered saline (TBS) with tween (TBST) buffer (50mM Tris, 150mM NaCl 1% v/v tween) with gentle agitation. For RYR1 detection a 34C mouse anti-RYR1 primary antibody was diluted 1:5000 in 5% milk in TBST. For alpha-tubulin detection a mouse primary anti-alpha-tubulin antibody (Sigma-Aldrich) was also diluted 1:5000 in 5% milk in TBST. The membrane was incubated with the primary antibodies for 2 hours at room temperature with constant agitation. Following incubation with the primary antibodies the membrane was washed 3 times for ten minutes each in 5% milk in TBST before incubation with the secondary antibody. A goat-anti-mouse secondary antibody with horseradish peroxidase (HRP) conjugate

(Bio-Rad) was diluted 1:5000 in 5% milk in TBST and incubated with the membrane at room temperature for 1 hour with constant agitation. Following the incubation, the membrane was washed 2 times with 5% milk in TBST and a final wash in 5% milk in TBS.

Chemiluminescence was detected using the North2South HRP detection kit (Thermo Scientific). Equal volumes of the luminol enhancer and peroxide solutions were mixed and placed onto the membrane and incubated at room temperature for 5 minutes before protein detection in a ChemiDoc MP imaging system (Bio-Rad). Exposure times were calibrated for each sample to ensure that overexposure was avoided.

2.3.3.3 Western blot data analysis

Western blotting images were analysed in ImageLab software. RYR1 expression was quantified relative to the alpha-tubulin expression and compared across all samples to examine differences in RYR1 expression in each of the transfected cell samples and untransfected controls. Two-tailed unpaired student's *t*-tests were performed on the data obtained for each construct.

2.4 Caffeine-induced calcium release experiments

HEK293 cells transiently transfected with pcRYR1 and pTUNERYR1 constructs were prepared on 96-well Opti-clear plates suitable for caffeine-induced calcium release experiments as described above (see section 2.2.7). Similarly, 1B5 cells either infected with HSV-1 virions or transfected using LF2000 or Xfect were also prepared on the 96-well plates (see section 2.2.9 and 2.2.10 respectively). For stably transfected HEK293 cells, 24 hours prior to the caffeine-induced calcium release assays, cells were transferred onto 96-well Opti-clear plates.

Plates destined for caffeine-induced calcium release assays were washed three times in imaging buffer (125mM NaCl, 5mM KCl, 2mM calcium chloride (CaCl₂), 1.2mM

MgSO₄, 6mM glucose, 25mM HEPES, pH 7.4). After the washing steps the cells were incubated with 20µM Fluo-4 acetoxymethyl (AM) (Life Technologies), a fluorescent calcium indicator, for 20 minutes at room temperature. Fluo-4 AM 1mM stocks were diluted to 20µM in imaging buffer. During the incubation with Fluo-4 AM, a caffeine dilution series was created as described in Table 2.5. The reason for the differences in caffeine series was due to the availability of the injection channels at the time of the experiments. The incremental doses of caffeine were loaded into a syringe each starting with the lowest concentration and working up to the maximum caffeine concentration. For the 1B5 cell transfection experiments, 20mM caffeine and 40mM KCl were used as agonists to examine the transfection efficiency. After incubation with Fluo-4 AM, cells were washed a further three times in imaging buffer before the commencement of the caffeine-induced calcium release assay. The syringes were attached to a central Perspex column via narrow tubing. The column was specifically designed to fit in the well of a 96-well plate (Duke and Steele, 2008) (Figure 2.4). Each syringe was individually primed to deliver a small, but excess amount of caffeine upon activation to the cells. The syringes were under computer control so that a standardised dose was delivered every 40 seconds, however, the delivery of the next caffeine dose was manually delayed until the previous calcium release event triggered by the caffeine had finished. The cells being measured were constantly perfused with imaging buffer meaning applied caffeine doses were instantly removed to eliminate the possibility of multiple calcium release events due to prolonged exposure to caffeine. The apparatus was set up and the plate placed on the stage of a Nikon Eclipse TE3000 inverted confocal microscope and visualised with a 40x oil immersion Fluor objective. Upon stimulation with caffeine, cells responded by releasing calcium, which was visualised as a temporary increase in fluorescence that was ultimately sequestered back into the cellular stores through excitation at 488nm and detection at 520nm. The entire duration of the experiment was recorded as a Z-stack with Image Pro Plus software with 1 image taken per second.

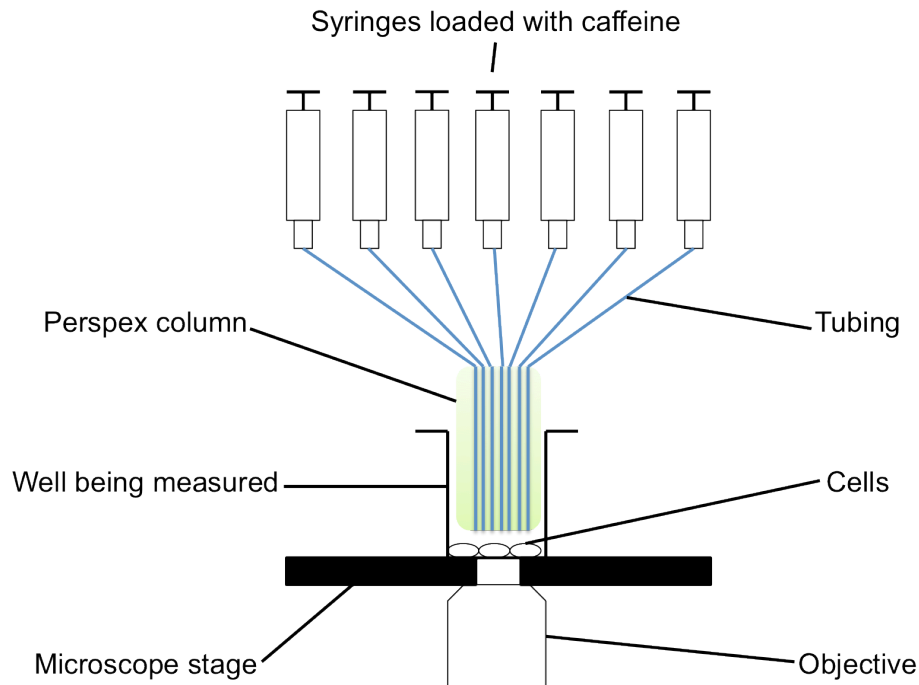


Figure 2.4 – Confocal microscope set up for calcium release measurements.

A maximum of seven syringes were loaded with incremental doses of caffeine. The syringes were attached to a central Perspex column via narrow tubing. The column was specifically designed to fit into the well of the 96-well plates used in this project. The syringes are under computer control so that the caffeine doses are added sequentially to the cells in a standardised fashion. A constant perfusion of imaging buffer means that as soon as the caffeine has been added to the cells it is removed. Increases in fluorescence associated with calcium release is detected via confocal microscopy and recorded as a z-stack.

	Experiment					
	Initial HEK293 transient transfection (caffeine)	Extended HEK293 transient transfection (caffeine)	HEK293 stable transfection (caffeine)	1B5 titration (caffeine)	1B5 extended experiments (caffeine)	1B5 transfection experiments (caffeine and KCl)
Agonist conc.	0.2mM 0.5mM 1mM 2mM 5mM 10mM 20mM	0.5mM 1mM 2mM 4mM 8mM 20mM	0.5mM 1mM 2mM 5mM 20mM	1mM 5mM 20mM	0.5mM 1mM 2mM 4mM 8mM 20mM	20mM (caffeine) 40mM (KCl)

Table 2.5 – Agonist concentrations used for the calcium release assays in this project

Various caffeine concentrations were used throughout the project based on the availability of the injection channels attached to the confocal microscope. For the 1B5 titration experiment, only three caffeine concentrations were selected to get induced calcium release at low and high concentrations of caffeine to ascertain the infection efficiency. For the 1B5 cell transfection experiments, KCl was also used as an agonist. A single high dose (40mM) of KCl was used with 20mM caffeine to induce calcium release.

2.5 Data analysis

The videos generated from confocal microscopy were analysed in ImageJ software. The fluorescence data obtained from ImageJ analysis was imported into the Prism 6 statistical package for subsequent statistical analysis and graph production.

2.5.1 ImageJ

The z-stack videos created were analysed using ImageJ software (available to download at <http://rsbweb.nih.gov/ij/>). Any uneven background fluorescence was removed using the software. To remove any effects of cell density adding to the fluorescence data, regions of interest were selected by highlighting areas that responded to low doses (1mM-2mM) of caffeine, as untransfected cells did not produce a calcium release event at these concentrations. This was particularly important for transient transfection experiments where not all cells were expected to respond to caffeine. Cells seen to be reacting to caffeine stimulation were highlighted, creating a data sheet of their levels of fluorescence over time. All the cells reacting in the given field of view were highlighted and measurements were taken. Each of the dose-response experiments were measured and the fluorescence data was imported into Prism 6 statistics package (available to download at <http://www.graphpad.com/prism/>).

2.5.2 Dose-response analysis

The fluorescence data was imported to Prism and normalised with 0% defined as the fluorescence level before the addition of any caffeine and 100% as the peak fluorescence achieved during the dose-response experiments. The fluorescence level achieved after each dose of caffeine was taken for each experiment and plotted on a log x-axis to construct a dose-response curve. The non-linear regression function in Prism 6 was used to fit a curve. The dose required to produce half of the maximum response (the EC₅₀) was taken from the fitted dose-response curve. In some cases, the

dose required to produce 10% and 25% of the maximum response was also calculated (the EC₁₀ and EC₂₅ respectively).

2.5.3 Area under the curve measurements

Each dose-response experiment was also subjected to area under the curve (AUC) measurements for each caffeine concentration that produced a calcium release event. The baseline for measurements was independently set for each caffeine concentration and each experiment.

2.5.4 Statistical analysis

Unpaired Student's *t*-tests were carried out between each construct measured to determine if there were any statistically significant differences between the dose-responses and AUC measurements taken. As there is evidence to suggest some *RYR1* variants result in a decrease in caffeine sensitivity as well as the more common increase in caffeine sensitivity, two-tailed statistical tests were performed for the dose-response and AUC experiments. For the experiments involving pre-treatment with AICAR, one-tailed statistical tests were performed as a decrease in caffeine sensitivity was expected in these cases. Similarly, for experiments aimed at examining the effect of *RYR1* expression, one-tailed statistical tests were performed.

Chapter Three - Selection and cloning of *RYR1* variants.

3.1 Introduction

3.1.1 EHMG guidelines

Since the introduction of the EMHG guidelines in 2001 that outlined the process by which missense variants in the *RYR1* gene can be added to a genetic diagnostic panel, only 31 mutations have been functionally characterised (Urwyler et al., 2001). This is, at least in part, due to the difficulties associated with cloning and manipulating a gene the size of *RYR1*. The guidelines outline two methods by which functional studies can be carried out. The first of these is to utilise *ex vivo* samples from patients who have previously undergone a muscle biopsy to diagnose MH status. Whilst this is of no benefit to the patients who have already been diagnosed, functional data obtained from samples of known genotype can contribute to their inclusion on the genetic diagnostic panel for MH. However, due to potential problems with having samples of an unknown genetic background, the presence of additional causal variants contributing to the functional results cannot be ruled out. Multiple variants have been found in some patients including two variants on the same allele, compound heterozygosity and variants in two different genes (*RYR1* and *CACNA1S*) (Monnier et al., 2002). Because of these complications, the guidelines require the studies to be carried out in two independent families to rule out the contribution of genetic background on the functional results. Although this eliminates the issue of genetic background, some variants are found uniquely in one family meaning that there would be no hope of these families ever having their MH status diagnosed genetically. Worldwide, 36% of all MH families possess a unique *RYR1* or *CACNA1S* variant, meaning that these families would be unsuitable for genetic diagnosis using this method.

3.1.2 Functional analysis of *RYR1* variants using recombinant methods

By far the most reliable method of functionally characterising genetic variants in *RYR1* is to carry out experiments using cDNA clones. Such experiments remove the issue of an unknown genetic background affecting the functional results and also allow the possibility of families with unique genetic variants to have their variant characterised, potentially leading to diagnosis before the need for a muscle biopsy. This method, however, is not without difficulties itself. *RYR1* is one of the largest genes in the human genome, spanning 106 exons and including over 15kb of coding sequence making molecular cloning extremely challenging. Conventional methods of working with cDNA clones, in general, are not applicable to a construct of *RYR1*'s size. Although some studies claim to be able to carry out site-directed mutagenesis on constructs of 20kb, these are difficult to replicate in the laboratory. To improve the efficiency of these experiments, *RYR1* first needs to be subcloned using unique restriction sites to produce a plasmid of a reasonable size to facilitate successful mutagenesis. The larger the gene, the fewer unique restriction sites are available for subcloning and in the *RYR1* cDNA there are only 14 unique restriction sites, a number that is further reduced when incorporated into an expression vector. Experiments involving subcloning and mutagenesis of *RYR1* cDNA constructs to date, have required elaborate cloning strategies to obtain the desired mutant constructs.

3.1.3 Subcloning *RYR1*

The earliest attempt at functionally characterising *RYR1* variants utilised a cloning strategy involving the production of eleven subclones to introduce new unique restriction sites for further subcloning and subsequent mutagenesis (Tong et al., 1997). The mutations involved in this study were only separated by 2kb of DNA. Subsequent studies have all had similarly complicated cloning strategies to facilitate the construction of wild type and mutant *RYR1* constructs (Du et al., 2001, Sambuughin et al., 2001b, Yang et al., 2003). One of the primary aims of the work described in this

chapter was to develop a cloning strategy that is as simplistic as possible given the size of *RYR1* and the inherent complications involved in such cloning experiments. To do this, a human *RYR1* clone was used that was kindly provided by Dr. Kathryn Stowell (Sato et al., 2010). The majority of the previous functional work has been carried out using a rabbit *RYR1* (*RyR1*) cDNA construct that, although having a high level of homology with the human gene, is not identical (Table 3.1).

	DNA	Protein
Identity	91.3%	96.5%
Mismatches	1,322	175
Gaps	39	17

Table 3.1 – Differences between human and rabbit *RYR1* sequences.

The majority of functional work on *RYR1* variants has been carried out using a rabbit *RyR1* cDNA clone in spite of the coding sequence being only 91.3% identical to the human equivalent. When aligned using ClustalW2 (available at <http://www.ebi.ac.uk/Tools/msa/clustalw2/>) 1,322 mismatches are present between the human and rabbit sequences with 39 gaps in the sequence. This is translated into a 96.5% identity in the protein sequence with 175 mismatched amino acids and 17 gaps in the sequence.

ClustalW2 alignment of the protein and cDNA sequences for both the human and rabbit constructs reveals 96.5% and 91.3% identity respectively. Although there is a high percentage of identity between the sequences, the rabbit sequence has a total of 1,322 mismatched nucleotides, which translates to 175 different amino acids in the protein sequence with a total of 17 gaps in the sequence where amino acids in the rabbit sequence are missing. In studies using rabbit clones, mutations ‘corresponding’ to the same mutation in the human gene are introduced. The use of a human clone in these experiments makes the experiments more representative of the human condition.

3.1.4 Native Vs. Non-native environment

In spite of being structurally and functionally different to the native environment of *RYR1*, HEK293 cells have been the primary cellular system to carry out functional

studies to date. HEK293 cells do not have the structural architecture of mature myotubes such as the T-Tubules, which are a uniquely muscle cell structure essential for excitation-contraction coupling. Furthermore, the SR in myotubes is a highly specialised version of the endoplasmic reticulum found in other cell types. HEK293 cells have traditionally been used due to the fact that they are easy to culture and easy to transfect when compared to muscle cells, which are extremely difficult to work with. Myoblasts need to be differentiated into myotubes to be functionally active. Transfection of myoblasts has a low efficiency, which is exacerbated when trying to transfect differentiating myoblasts or mature myotubes (Neuhuber et al., 2002). Recently, a method of viral transduction using HSV-1 has been developed, which boasts an extremely high efficiency of gene transfer when infecting differentiating myotubes (Fraefel et al., 1996, Wang et al., 2000). To facilitate this method of expression in myotubes, a specialised expression vector containing the HSV-1 packaging signal and a viral promoter driving gene expression was developed. In this study, wild type and mutant constructs will be transferred into this pHSVPrPUC vector to allow viral packaging and expression of our constructs in myotubes.

3.1.5 Differential expression of RYR1 constructs in cellular systems

Maintaining expression of *RYR1* is of paramount importance when examining the functional consequences of different genetic variants. Transfection efficiencies of large cDNA constructs are inevitably much lower than that of smaller constructs (Campeau et al., 2001). This means that maintaining a consistently high level of *RYR1* expression in cells successfully transfected is essential. A recent study has demonstrated the importance of the expression levels of *RYR1*. Allele specific PCR revealed that patients carrying known *RYR1* mutations had a higher level of expression from the wild type allele, possibly as a compensatory mechanism for the mutated allele (Grievink and Stowell, 2010). This difference in expression was postulated to be a partial explanation for the variability seen in patients with MH. Recent work looking

at the increased expression of *RYR1* and *RYR3* in dyspedic myotubes has suggested that an increased expression of wild type channels does not affect the sensitivity of the channels to activating agents such as caffeine and KCl. Although an increased *RYR1* expression had no effect on the excitability of the cells, an increase in *RYR3* resulted in a statistically significant decrease in EC_{50} of the cells. This was, in part, put down to the increase in resting calcium associated with an increased *RYR3* expression. It has been long established that mutants in *RYR1* cause an increase in the resting intracellular calcium level of cells carrying these variants; however, no studies have examined the increased expression of mutant *RYR1* alleles in cellular systems. Shuttling *RYR1* into an inducible expression system will allow us to examine the effect of an increased or decreased expression of *RYR1* on the excitability of the cells to channel agonists.

3.2 Aims of the chapter

The aims of this chapter are to select *RYR1* variants for functional studies in this thesis based on the frequency at which they have been identified in the UK and worldwide population. To facilitate the functional studies of these variants an additional goal is to develop a robust, efficient and relatively simple cloning strategy that will allow for the introduction of missense variants into a human *RYR1* cDNA construct. Furthermore, wild type and mutant *RYR1* constructs will be shuttled into a pHSVPrPUC expression vector that will allow *RYR1* to be packaged into HSV-1 virions for expression in dyspedic myotubes. The constructs will also be transferred into an inducible expression vector, allowing us to examine the effect of expression levels of wild type and mutant *RYR1* on the excitability of the channels when exposed to triggering agents.

3.3 Results

3.3.1 Selection of *RYR1* variants for this project

There are currently 158 *RYR1* variants identified in the UK population that are uncharacterised and therefore unavailable for genetic diagnosis of MH. The primary selection criteria for variants used in this project was the frequency at which they have been identified in the UK population apart from for the p.D1056H variant which was added to the project after it was identified in an EHS patient who tested negative for MH. The variant was found to segregate with disease in one additional MH family. The seven variants listed in Table 3.2 account for 35% of all families in the UK that possess an as yet uncharacterised *RYR1* variant.

Nucleotide change	Amino acid change	Families in the UK	Total global families
c.3166 G>C	p.D1056H	1 (+1 EHS)	1 (+1 EHS)
c.7007 G>A	p.R2336H	8	15
c.7063 C>T	p.R2355W	7	9
c.9310 G>A	p.E3104K	4	4
c.11958 C>G	p.D3986E	4	4
c.11969 G>T	p.G3990V	10	10
c.14545 G>A	p.V4849I	8	12

Table 3.2 – List of variants chosen for this project.

The variants chosen for functional characterisation in this project account for 43 of the UK MH families that possess an as yet uncharacterised variant. An additional 13 families worldwide have been found carrying one of the variants in association with MH. The c.3166 G>C, p.D1056H variant was added to the project after it emerged it was identified in an EHS patient who had tested negative for MH. The variant was also found to segregate with the MH phenotype in one additional family. Functional characterisation of these variants will increase the genetic diagnostic panel for MH by 22.5%.

All of the variants selected in this project are missense mutations resulting in a change of amino acids in the *RYR1* protein chain (Table 3.3). The potential severity of these changes varies between each variant. The p.D3986E variant has the mildest amino acid change with aspartic acid and glutamic acid both being acidic, polar and hydrophilic meaning the substitution may be a mild one. Additionally, the p.V4849I variant results in a similar substitution despite being found in 12 families worldwide. The remaining variants all cause amino acid property changes meaning that the overall

structure and function of the protein may be altered as a result of the substitution. Furthermore, there is a high level of evolutionary conservation of all variants under investigation in this project. The base mutated in human MH is maintained across a number of species known to undergo similar MH reactions as well as closely related species indicating the importance of the residue. The only discrepancy is that in mouse *RYR1*, the cytosine residue that is mutated in the p.D3986E variant is a thymine, however this does not effect the amino acid coded for in the wild type sequence. The same difference is seen in human *RYR2*, however once again the amino acid is maintained. Additionally, in human *RYR3*, the arginine residue that is effected in the p.R2355W variant is a lysine residue.

Residue	Starting amino acid	Substituted amino acid	Charge	Acid/basic	Hydrophobic/hydrophilic
1056	Aspartic acid (D)	Histidine (H)	Negative to positive	Acidic to basic	Hydrophilic to neutral
2336	Arginine (R)	Histidine (H)	No change (positive)	No change (basic)	Hydrophilic to neutral
2355	Arginine	Tryptophan (W)	Positive to neutral	Basic to neutral	Hydrophilic to hydrophobic
3104	Glutamic acid (E)	Lysine (K)	Negative to positive	Acidic to basic	No change (hydrophilic)
3986	Aspartic acid	Glutamic acid	No change (negative)	No change (acidic)	No change (hydrophilic)
3990	Glycine (G)	Valine (V)	No change (neutral)	No change (neutral)	Neutral to hydrophobic
4849	Valine	Isoleucine (I)	No change (neutral)	No change (neutral)	No change (hydrophobic)

Table 3.3 – Amino acid properties of the variants selected for study in this project.

Five of the missense variants under investigation in this project result in a substitution of amino acid that has significantly different properties. These substitutions may result in a change in the structure and therefore function of the overall protein. Of the 7 selected variants, 2 possess no major changes (p.D3986E and p.V4849I). However, these two variants have been identified in 16 families worldwide. Patients carrying the p.D3986E variant have been found to have a significantly higher caffeine contracture compared to other *RYR1* variants during the IVCT and the p.V4849I variant has been identified in a large number of both MH and CCD families worldwide making both variants of interest in this project.

An additional criterion for selection in this project is the co-segregation of the variant under investigation with the disease phenotype. All the variants selected for this project segregate with the MH phenotype in all individuals available for genetic testing and are therefore not considered to be polymorphisms. Finally, all of the variants selected in this project have been found to be absent from a panel of 200 MHN control UK chromosomes through routine diagnostic screening at the Leeds MH testing centre, further reducing the possibility of the variants being non-pathogenic.

3.3.2 Cloning using *pcRYR1*

The *RYR1* cDNA sequence in a pcDNA3.1 expression vector results in a 20,649bp plasmid. This is too large for conventional methods of mutagenesis. To be able to introduce missense variants into *RYR1* associated with MH and EHS *pcRYR1* needed to be subcloned. The variants selected for functional experiments in this project are mainly clustered in the 3' half of *RYR1*, however, the p.D1056H variant is within the 5' end. Generating a 3' subclone containing all of the sites for the six variants in this half of *RYR1* was possible due to the unique restriction sites *Acc65I* and *XbaI*. However, the creation of a 5' subclone for the introduction of the p.D1056H variant into *RYR1* was made more difficult due to the absence of any suitable restriction sites in the 5' end of *RYR1*. Cloning this variant required the shuttling of *RYR1* into a new expression vector.

3.3.2.1 Creation of the 3' subclone of *RYR1*

pcRYR1 was digested with *Acc65I* and *XbaI* resulting in a DNA fragment of 8,248bp which was gel purified. The larger 12,401bp fragment remaining from *XbaI* and *Acc65I* digestion was also gel purified and saved for later reconstruction of full-length mutant *pcRYR1* constructs. pBluescript II SK + was also digested with *XbaI* and *Acc65I* and gel purified. The 8,248bp *RYR1* fragment was ligated into the linear 2,880bp pBluescript sample to create a 3' subclone of *RYR1*, 11,128bp in length (Figure 3.1).

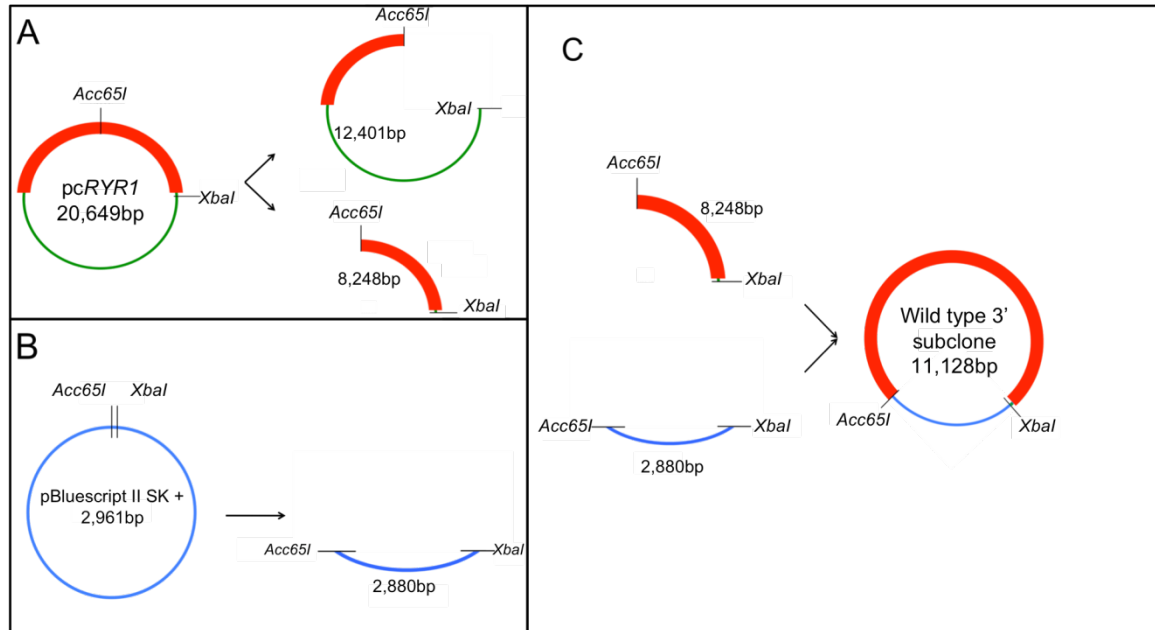


Figure 3.1 – Creation of the 3' subclone of RYR1.

(A) The unique restriction sites *Acc65I* and *XbaI* were used to cut *pcRYR1* resulting in two fragments. One large fragment of 12,401bp containing the pcDNA expression vector and the 5' end of RYR1 was produced as well as a smaller fragment of 8,284bp containing the 3' end of RYR1. Both fragments of DNA were gel purified; the smaller fragment for subcloning and the larger fragment for reconstruction of full-length *pcRYR1* constructs. (B) pBluescript II SK+ was cut with *Acc65I* and *XbaI* resulting in a linear product of 2,880bp which was gel purified. (C) The 8,248bp fragment of RYR1 from (A) was inserted into pBluescript to create the 3' subclone of RYR1.

Ligation mixes were transformed into XL10 Gold ultracompetent *E.coli* and bacterial colonies were allowed to form on LB agar plates containing ampicillin. Bacterial colonies were cultured for mini prep plasmid DNA extraction and were screened using *EcoRI* restriction digestion for successful ligation. Positive samples produced DNA bands at 7,592bp, 1,986bp and 1,550bp (Figure 3.2). PCR products were generated over the *Acc65I* and *XbaI* cloning sites and sent for sequencing. The TCTAGA *XbaI* and GGTACC *Acc65I* cloning sites were identified as well as the RYR1 and pBluescript sequence immediately flanking each site were confirmed from reference sequences

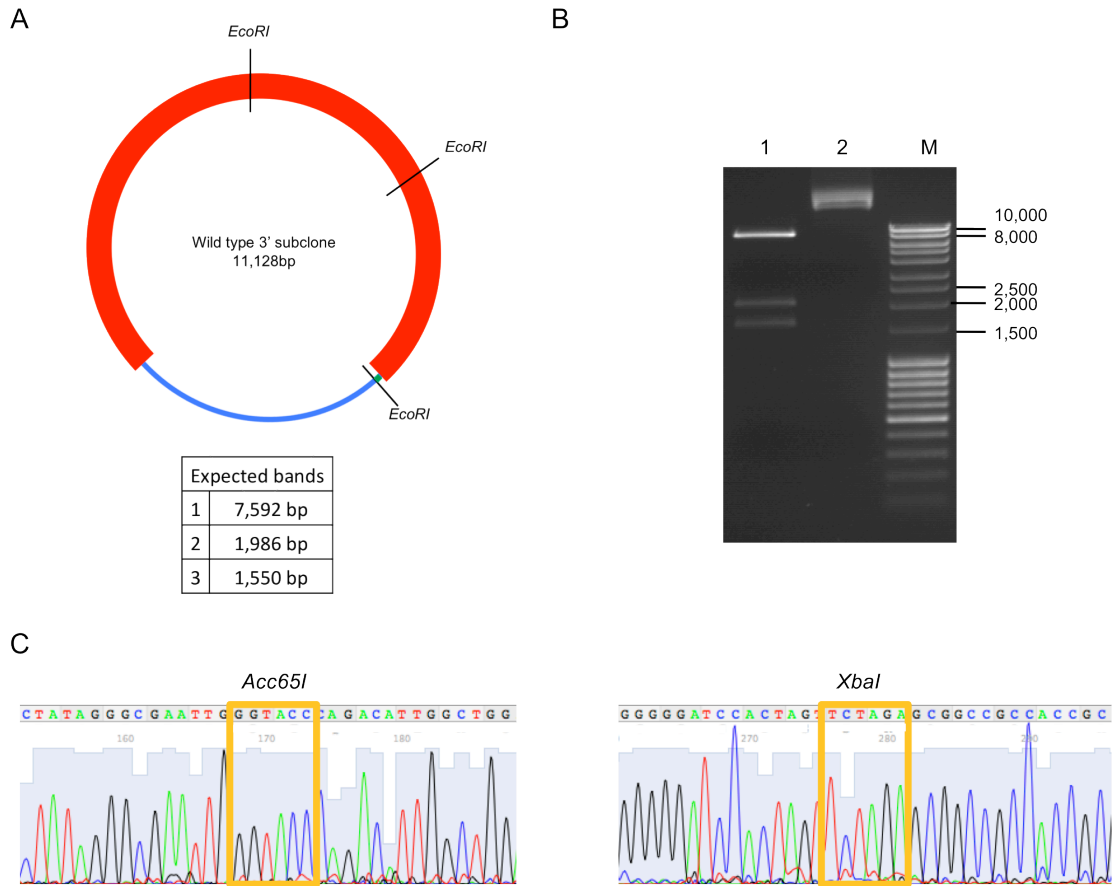


Figure 3.2 – Digest and sequence confirmation of the 3' subclone.

(A) Plasmid map of the 3' subclone with *EcoRI* sites marked and expected DNA bands in the table below the map. (B) Gel image of the 3' subclone. Lane 1 is a 3' subclone sample digested with *EcoRI*. DNA bands at 7,592bp, 1986bp and 1,550bp indicate successful ligation and creation of the 3' subclone. Lane 2 is an undigested 3' subclone sample. Lane M is a DNA MassRuler ladder with relevant DNA band sizes marked. (C) PCR products created with primers at either side of the ligation sites were sequenced. The GGTACC *Acc65I* and TCTAGA *XbaI* sites are marked with the gold boxes. Sequences generated were aligned to reference sequence samples to confirm successful ligation.

3.3.2.2 Creation of the 5' subclone of *RYR1*

There were no unique restriction sites at the 5' end of the *RYR1* in *pcRYR1* meaning that a 5' subclone could not be created that would be able to be inserted back into *pcRYR1*. However, a 5' subclone of *RYR1* was created using one of three *SpeI* and *HindIII* restriction sites that left the 5' end of *RYR1* intact (Figure 3.3). *pcRYR1* digested with *SpeI* and *HindIII* produced DNA bands at 9,601bp, 4,692bp, 4,292bp, 1,311bp, 717bp and 36bp. The 9,601bp fragment produced when cutting *pcRYR1* with *SpeI* and *HindIII* was gel purified. All the remaining DNA bands produced with this digestion

were not purified as no reconstruction could be made from their products. pBluescript II SK + was also cut with *SpeI* and *HindIII*, resulting in a linear product of 2,922bp and was gel purified. Both purified fragments were ligated together to produce a 5' subclone of *RYR1*, 12,523bp in size. Ligation mixes were transformed into XL10 Gold ultracompetent cells and colonies potentially containing the 5' subclone were cultured for mini prep plasmid DNA extraction and screened using *XhoI* restriction endonuclease to test for successful ligation (Figure 3.4). Positive samples created DNA bands at 5,396bp, 4,019bp, 2,086bp and 1,022bp. A PCR product was generated over the two cloning sites and sent for sequencing to confirm successful ligation. Sequence analysis confirmed the presence of the ACTAGT *SpeI* and AAGCTT *HindIII* restriction sites as well as the *RYR1* and pBluescript sequence immediately before and after the cloning sites.

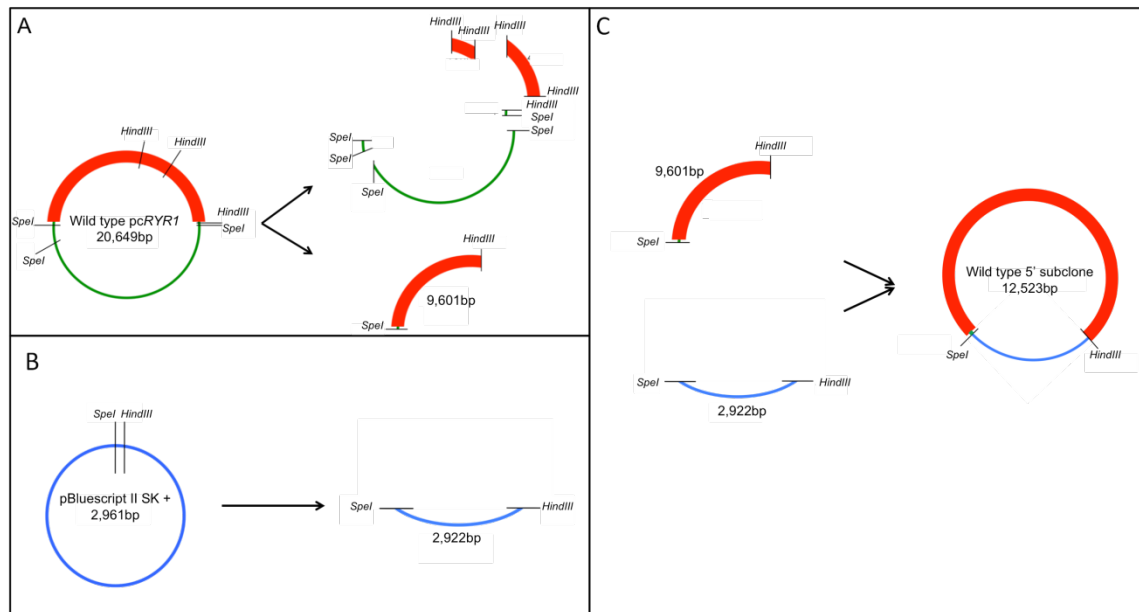


Figure 3.3 – Creation of the 5' subclone of *RYR1*.

(A) *pcRYR1* was cut with *SpeI* and *HindIII* resulting in 8 DNA bands. The largest band of 9,601bp contained the 5' end of *RYR1* and was gel purified. The remaining bands were not gel purified, as it was not possible to reconstruct full-length *pcRYR1* from these pieces. **(B)** pBluescript II SK + was cut with *SpeI* and *HindIII* which produced a linear product of 2,922bp that was gel purified. **(C)** Both gel-purified fragments were ligated together to form a 12,523bp plasmid resulting in the 5' subclone of *RYR1*.

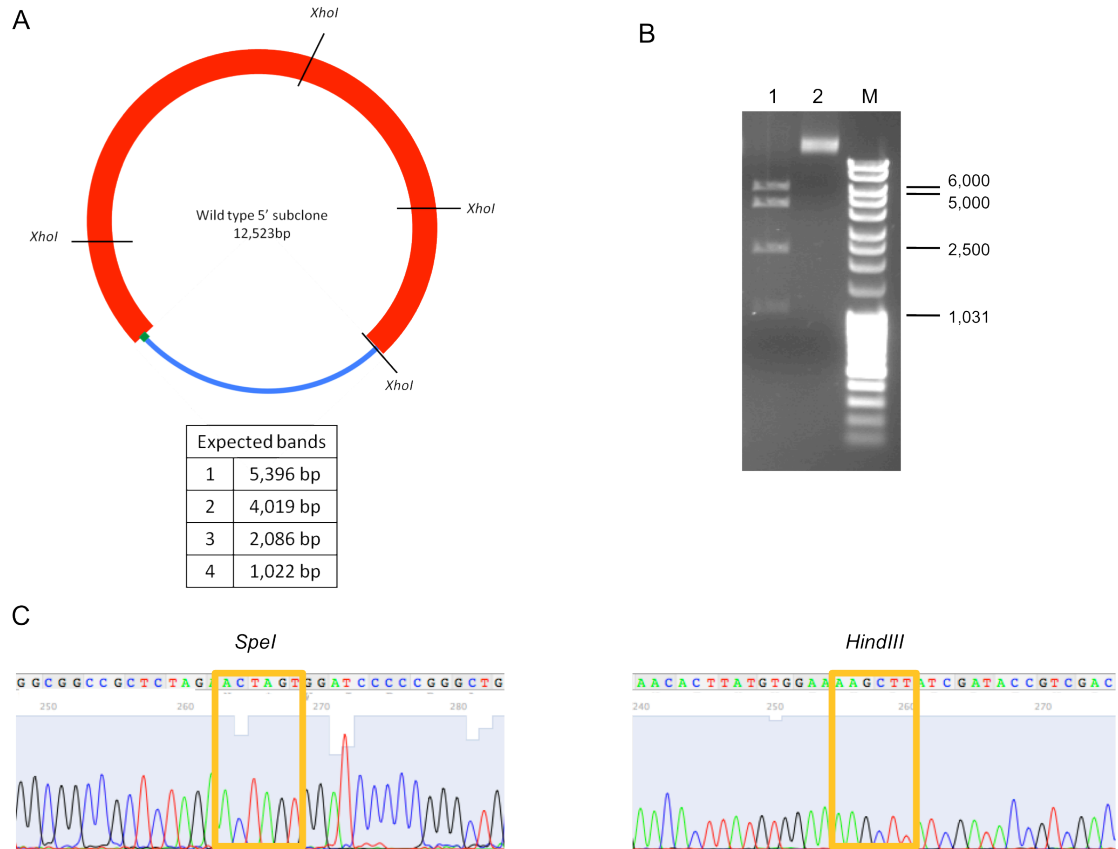


Figure 3.4 – Digestion confirmation of the creation of the 5' subclone of *RYR1*.

(A) Plasmid map of the 5' subclone with *XhoI* sites labelled. The expected DNA bands are indicated in the table below the map. (B) Gel image of the 5' subclone cut with *XhoI* resulting in DNA bands at 5,396bp, 4,019bp, 2,086bp and 1,022bp indicating successful ligation. Lane 2 is an undigested 5' subclone sample. Lane M is a MassRuler DNA ladder with the relevant DNA band sizes indicated. (C) Sequence confirmation of the successful creation of the 5' subclone. PCR products generated over the cloning sites were sequenced in both directions to confirm ligation. The ACTAGT *SpeI* site and AAGCTT *HindIII* sites were identified (gold boxes). The sequence immediately flanking these cloning sites was aligned to reference sequences for *RYR1* and pBluescript to confirm successful ligation.

3.3.2.3 MEGAWHOP site-directed mutagenesis

The 5' and 3' *RYR1* subclones were used as templates for MEGAWHOP site-directed mutagenesis. Mega primers between 200bp and 800bp in length were generated and sequenced in both directions to ensure that the desired mutation was introduced successfully. After successful generation of the mega primers, mutagenic PCR was performed followed by *DpnI* digestion and transformation into XL10 Gold ultracompetent cells. Colonies generated were counted and cultured overnight in LB

broth for mini prep plasmid DNA extraction. Primers flanking the mutation sites were designed and used to generate a PCR product that was sequenced to confirm successful mutagenesis (Figure 3.5). A total of 34 colonies were produced throughout the mutagenesis experiments, 18 of which contained the mutation of interest resulting in an overall mutagenesis efficiency of 52.9% (Table 1). The success of the introduction of individual mutations ranged from 100% of colonies screened (1/1 for p.D1056H and p.V4849I) to 20% of colonies screened (1/5 for p.R2336H).

Mutation	Colonies screened	Colonies positive	% Success
p.D1056H	1	1	100
p.R2336H	5	1	20
p.R2355W	12	6	50
p.E3104K	6	4	66.6
p.D3986E	4	2	40
p.G3990V	5	3	60
p.V4849I	1	1	100
TOTAL	34	18	52.9

Table 3.4 – MEGAWHOP mutagenesis success rate.

An overall success rate of 52.9% was observed. Individual mutagenesis success ranged from between 20% and 100%. The number of bacterial colonies produced after the mutagenesis protocol ranged from 1 to 12.



Figure 3.5 – Sequence confirmation of successful mutagenesis.

PCR products were generated over each mutation site and sent for sequencing to confirm the introduction of the desired mutation into the subclone of *RYR1*. Wild type sequences are in the right hand column; mutant sequences are in the left hand column. The amino acid altered is indicated with a gold box.

3.3.2.4 Reconstruction of full-length mutant pcRYR1 constructs using the 3' subclone

After confirmation of successful mutagenesis, the mutant 3' subclone was cut with *Acc65I* and *XbaI* producing a large DNA band, 8,248bp in length containing the mutated 3' end of *RYR1* and a smaller band of 2,880bp. The larger band was gel purified. The 12,401bp DNA fragment that was saved during the construction of the 3' subclone was used as the vector for ligation of the 3' end of *RYR1* back into pcRYR1 (Figure 3.6).

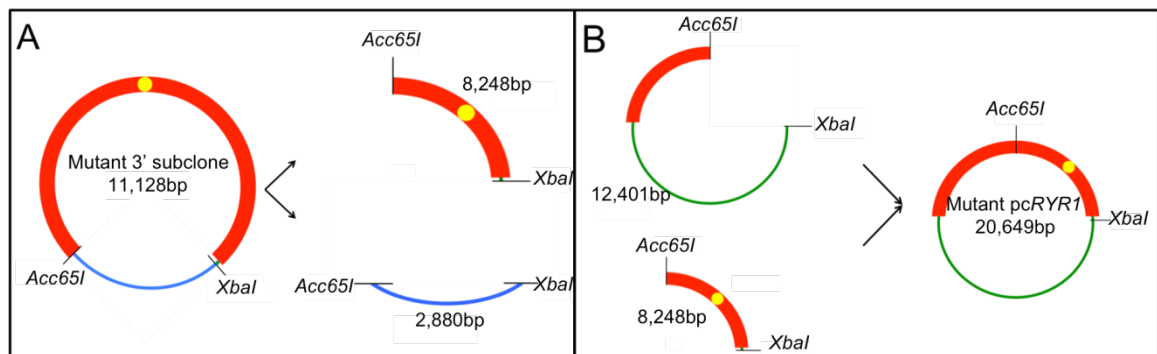


Figure 3.6 – Reconstruction of full-length mutant pcRYR1 constructs.

(A) Mutant 3' subclones were digested with *Acc65I* and *XbaI*. The mutation site is indicated with the yellow circle. The 8,248bp fragment corresponding to the 3' end of *RYR1* was gel purified. The 2,880bp pBluescript vector DNA was discarded. (B) The 3' end of *RYR1* was re-ligated back into pcRYR1 using the 12,401bp 'vector' sequence saved from the construction of the 3' subclone to create a mutant pcRYR1 construct.

The ligation products were transformed into XL10 Gold Ultracompetent cells and cultured overnight on LB agar plates containing ampicillin. Individual colonies were selected and cultured overnight in LB broth for mini prep plasmid DNA extraction. Extracted DNA samples were screened using *HindIII* to test for successful ligation and reconstruction of pcRYR1 constructs. Positive samples produced DNA bands at 15,046bp, 4,292bp and 1,311bp (Figure 3.7). Full-length mutant pcRYR1 constructs were generated for the variants p.R2336H, p.3104K, p.D3986E, p.G3990V and p.V4849I (Figure 3.8). PCR products were generated over the *Acc65I* and *XbaI* cloning sites and

sequenced in both directions. The presence of the GGTACC *Acc65I* restriction site and TCTAGA *XbaI* restriction site were confirmed as well as the presence of the sequence of *RYR1* or pcDNA3.1 immediately flanking both sites was from reference sequences. In addition to this, the presence of the desired mutation was also confirmed in the full-length constructs.

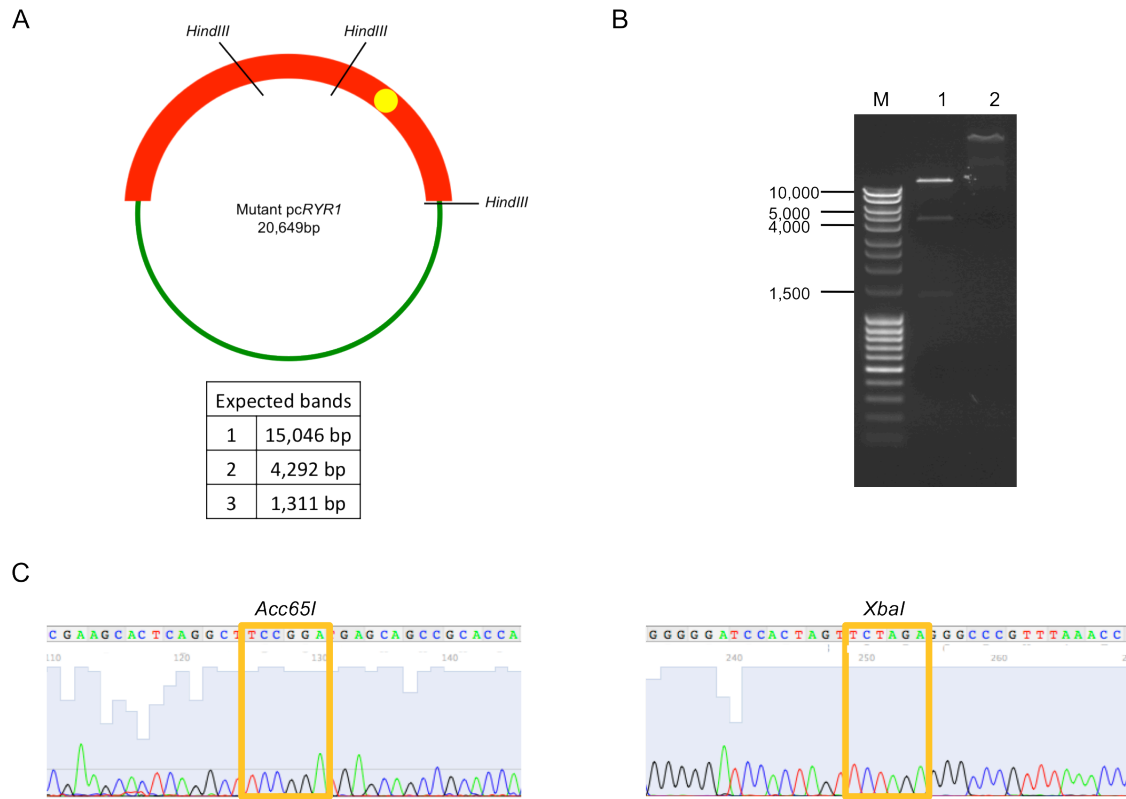


Figure 3.7 – Digest and sequence confirmation of full-length pcRYR1 constructs

(A) Plasmid map of mutant pcRYR1 with *HindIII* sites marked. The expected DNA bands produced through *HindIII* digestion are marked in the table below the map. (B) Gel image of pcRYR1 cut with *HindIII*. Lane 1 is a mutant pcRYR1 construct digested with *HindIII*. Lane 2 is an undigested mutant pcRYR1 construct. Lane M is a MassRuler DNA ladder with the relevant DNA band sizes marked. (C) PCR products were generated over both cloning sites and sequenced to confirm successful ligation. The presence of the TCCGGA *Acc65I* site and TCTAGA *XbaI* site was identified and aligned to reference sequences to confirm successful ligation.

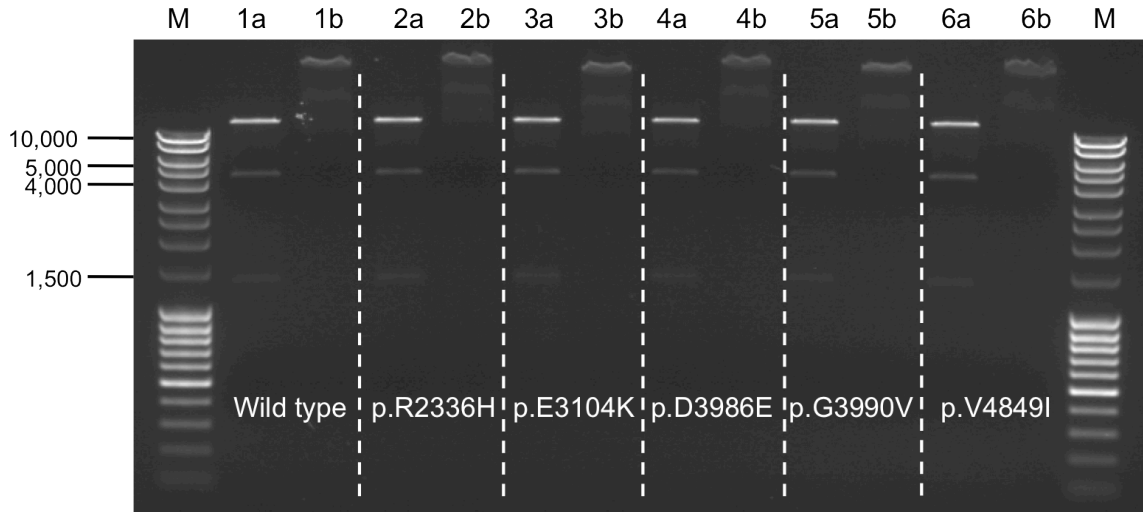


Figure 3.8 – Successful reconstruction of *pcRYR1* constructs.

Gel image showing *pcRYR1* constructs digested with *HindIII*. Lanes 1a and 1b are wild type controls for *HindIII* digestion of *pcRYR1* (a lane) and an undigested sample of *pcRYR1* (b lane). Lanes 2-6 follow the same pattern and represent the successfully reconstructed mutant *pcRYR1* samples generated. Lane M is a MassRuler DNA ladder with the relevant DNA band sizes marked.

3.3.3 Cloning in pHSVPrPUC

To use the HSV-1 method of infecting dyspedic myotubes the *RYR1* cDNA constructs needed to be transferred from the pcDNA3.1 expression vector into pHSVPrPUC. Due to the large size of *RYR1* there were limited unique restriction sites in the plasmid and there were no unique restriction sites at the 5' end of the cDNA construct. The only usable restriction sites to shuttle the *RYR1* cDNA sequence into pHSVPrPUC were two *SpeI* restriction sites that flanked either side of the insert. The *SpeI* recognition site (ACTAGT) produces a 5' overhang of CTAG that is compatible with the *XbaI* (TCTAGA) restriction site in the pHSVPrPUC polylinker. The limited number of restriction sites in the pHSVPrPUC polylinker meant that there was no suitable method available for transferring *RYR1* into the vector in subclone steps.

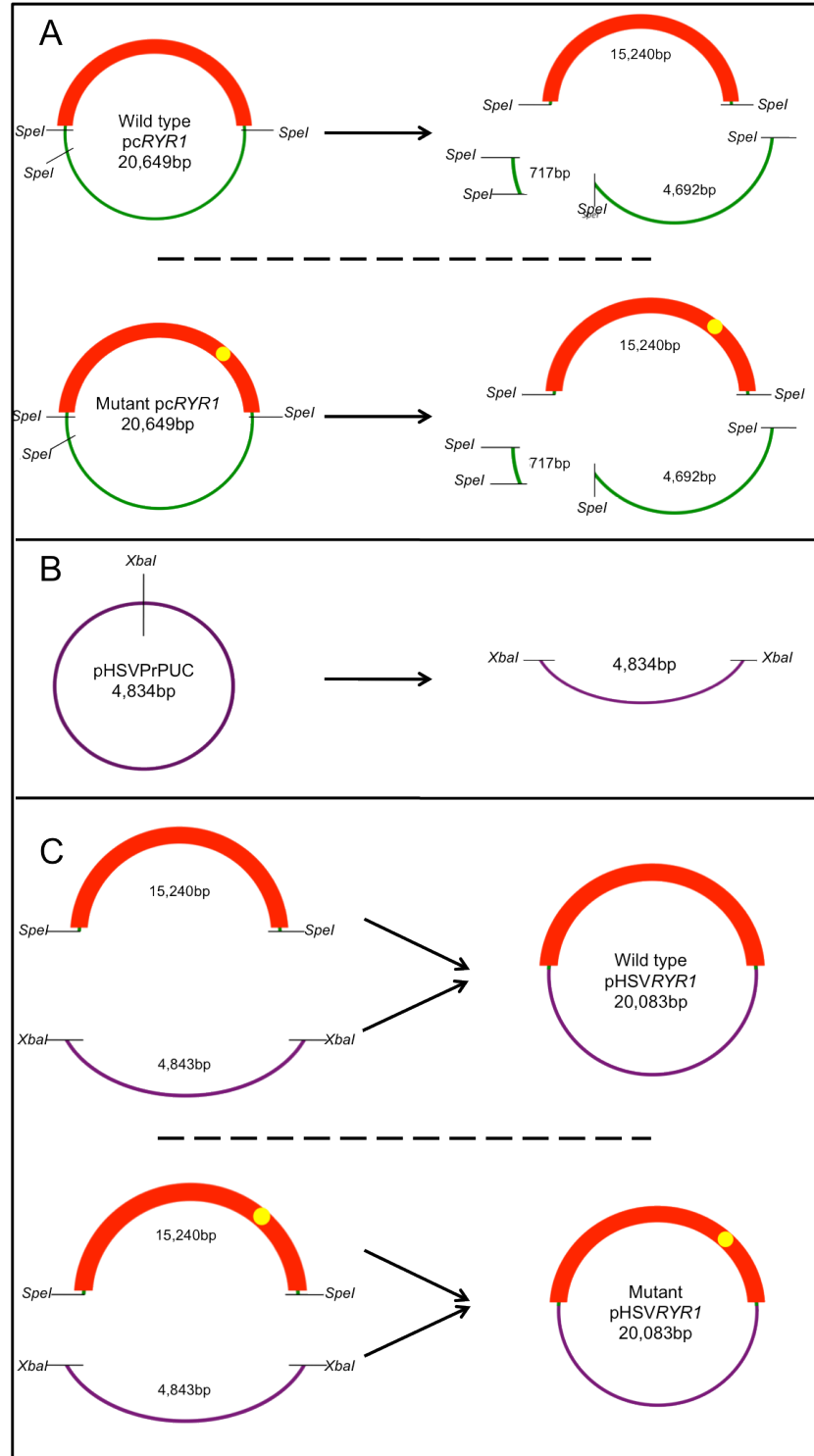


Figure 3.9 – pHSVRYR1 cloning strategy.

(A) Wild type and mutant full-length pcRYR1 constructs were digested with *SpeI* producing DNA bands 15,240bp, 4,692bp and 717bp in length. The 15,240bp fragment contained the entire RYR1 coding sequence. The RYR1 cDNA fragment was gel purified. (B) pHSVPrPUC was linearised with *XbaI* and treated with Antarctic phosphatase to prevent religation. The treated sample was gel purified. (C) Gel purified RYR1 cDNA and pHSVPrPUC vector were ligated together to produce a 20,083bp plasmid for full-length wild type or mutant pHSVRYR1.

Wild type and mutant *pcRYR1* constructs were digested with *SpeI* producing three DNA fragments (Figure 3.9). The largest was 15,240bp in length and contained the entire *RYR1* coding sequence. This fragment was gel purified with the remaining bands being discarded. *pHSVPrPUC* was linearised using an *XbaI* site in the polylinker, treated with Antarctic phosphatase to prevent religation and gel purified. The *RYR1* cDNA fragment and linear *pHSVPrPUC* samples were ligated together to produce either wild type or mutant *pHSVRYR1* samples. The ligation products were transformed into XL10 Gold Ultracompetent cells and cultured overnight on LB agar plates containing ampicillin. Individual bacterial colonies were selected for overnight cultures in LB broth. Mini prep plasmid DNA extraction was carried out before screening the DNA samples with a *HindIII* digest to test for successful ligation of the *pHSVRYR1* samples (Figure 3.10). Positive samples produced DNA bands at 9,625bp, 4,855bp, 4,292bp and 1,311bp. Because a non-directional cloning method was used it was possible for the *RYR1* cDNA to ligate in either orientation into *pHSVPrPUC* however, *HindIII* was able to successfully discriminate between the two orientations. *RYR1* in the reverse orientation produces DNA bands at 14,420bp, 4,292bp, 1,311bp and 60bp.

PCR products were generated over both cloning sites and sequenced in both directions. Both the *SpeI* and *XbaI* sites were destroyed by the ligation resulting in a TCTAGT site at the 5' end of *RYR1* and a ACTAGA site at the 3' end of *RYR1*. The presence of these sites was confirmed via sequencing as well as aligning the immediately flanking sequences of *RYR1* and *pHSVPrPUC* to reference sequences. Positive bacterial colonies were identified for three constructs ligated into *pHSVPrPUC* (wild type, p.R2336H and p.D3986E) (Figure 3.11).

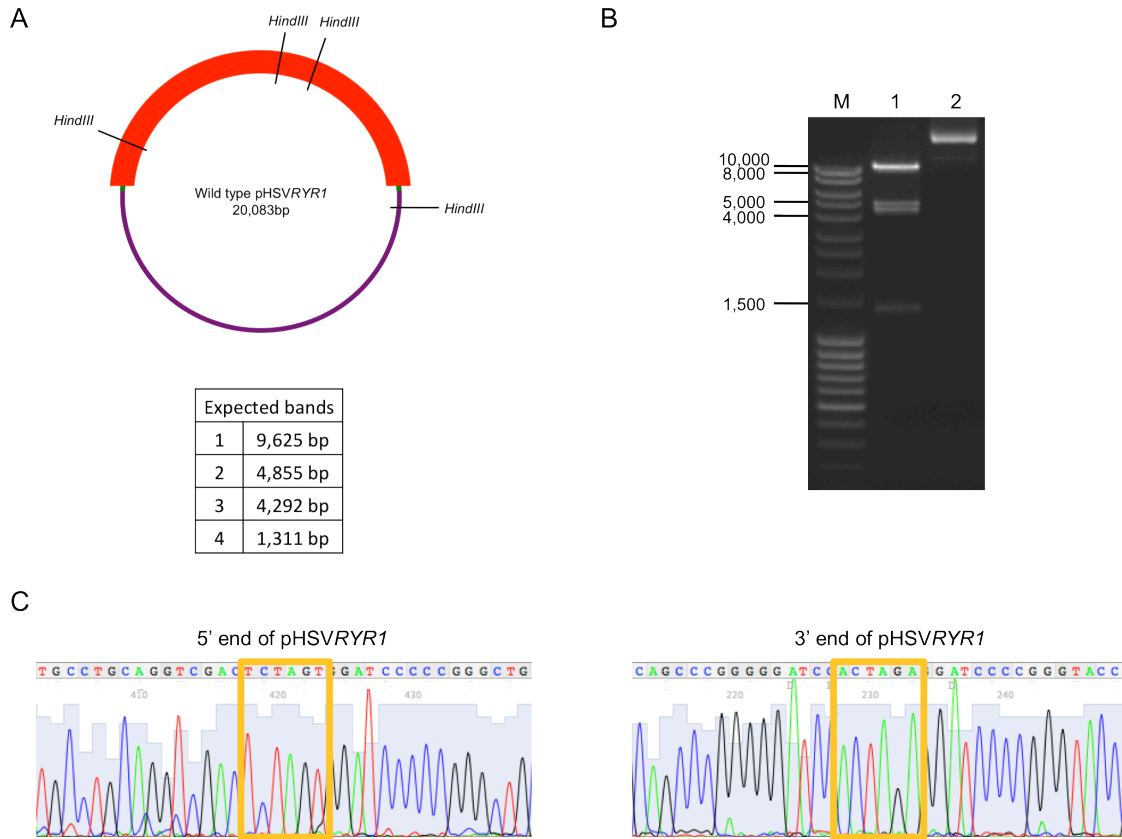


Figure 3.10 – Digest and sequence confirmation of pHSVRYR1 constructs.

(A) Plasmid map of pHSVRYR1 with *HindIII* sites labelled and the expected DNA bands indicated in the table below the map. (B) Gel image of wild type pHSVRYR1 cut with *HindIII*. Lane 1 is a wild type pHSVRYR1 construct digested with *HindIII*. Lane 2 is an undigested pHSVRYR1 sample. Lane M is a MassRuler DNA ladder with the relevant DNA band sizes marked. The presence of the 9,625bp, 4,855bp, 4,292bp and 1,311bp fragments in lane 1 indicate positive ligation and the successful generation of a pHSVRYR1 construct. (C) The ligation of *SpeI* into the compatible *XbaI* site produced an TCTAGT sequence at the 5' end of *RYR1* and a ACTAGA site at the 3' end of *RYR1*. These sequences were identified and are marked with a gold box. The sequences immediately flanking these sites were confirmed to be *RYR1* and pHSVPrUC through aligning the sequences to reference samples.

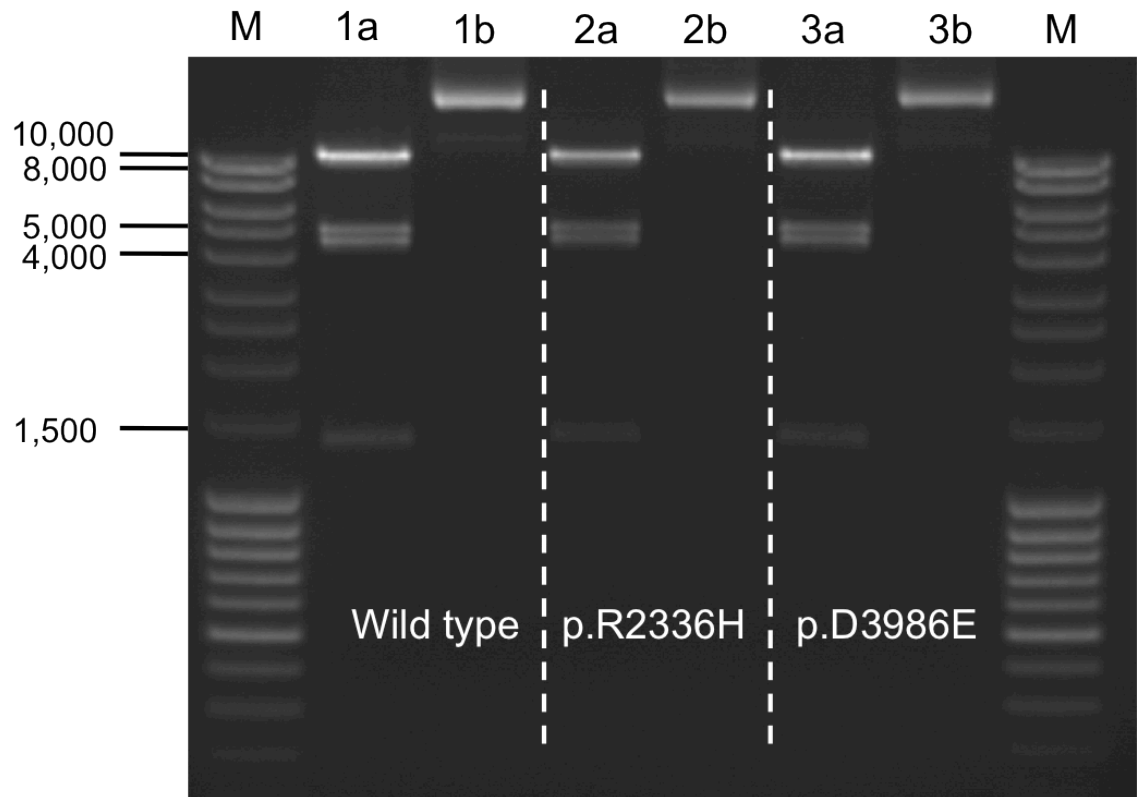


Figure 3.11 – pHSVRYR1 cDNA constructs generated in this study.

Wild type, p.R2336H and p.D3986E RYR1 cDNA constructs were successfully ligated with pHSVPrPUC. Each 'a' lane is a pHSVRYR1 construct digested with *HindIII*. Each 'b' lane is an undigested pHSVRYR1 sample. The 'M' lanes are MassRuler DNA ladders with the appropriate DNA band sizes marked on the left.

3.3.4 Cloning in pTUNE

3.3.4.1 Removal of the *BspEI* site from pTUNE

Unlike the cloning strategy for pHSVRYR1, there were sufficient restriction sites available to shuttle RYR1 from the two subclones in pBluescript II SK + to pTUNE using a two-step and directional cloning strategy. However, for this to work, an endogenous *BspEI* restriction site first needed to be removed from pTUNE (Figure 3.12). pTUNE was digested with *BspEI* before blunting with Klenow fragment and religation of the newly blunt ends.

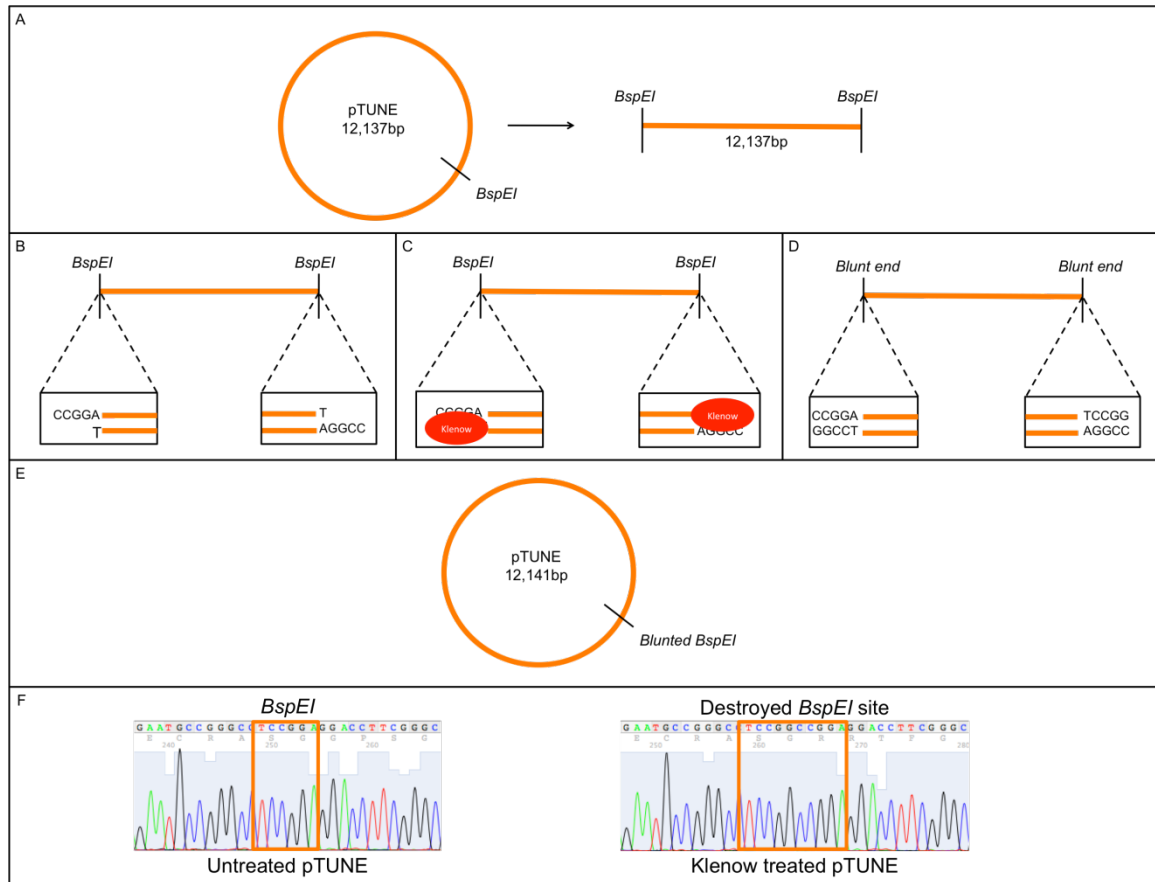


Figure 3.12– Removal of an endogenous *BspEI* restriction site in pTUNE.

(A) pTUNE was linearised with *BspEI* and gel purified. (B-D) Purified, linear DNA was incubated with Klenow fragment at a concentration of 1 unit per microgram of DNA. Klenow fragment blunts the 5' overhang created by *BspEI* by filling in the 3' recessed end with dNTPs supplied in the reaction resulting in a blunt TCCGG sequence at one end and a CCGGA sequence at the other end. (E-F) Blunt end ligation is carried out resulting in a plasmid that has lost its *BspEI* restriction site. Sequence confirmation confirmed the successful blunting of *BspEI* with the presence of a TCCGCCGGA site where the *BspEI* site originally was.

Primers were designed flanking the endogenous *BspEI* restriction site. A PCR product was generated and sequenced in both directions to confirm the successful blunting of the *BspEI* site. The original TCCGGA *BspEI* site was filled in to form a TCCGCCGGA site.

3.3.4.2 Creation of the pTUNE subclone

The 3' subclone generated for MEGAWHOP mutagenesis was used to shuttle the 3' end of *RYR1* into pTUNE (Figure 3.13). The 3' subclone was cut with *Acc65I* and *Sall* which generated DNA fragments 8,168bp and 2,960bp in length. The larger fragment contained the entire 3' end of *RYR1* and was gel purified. The smaller, pBluescript fragment was discarded. pTUNE was double digested with *BsiWI* and *XhoI* which produce compatible 5' overhangs for *Acc65I* (CATG overhang) and *Sall* (AGCT overhang) respectively. The linear pTUNE DNA was gel purified. The 8,168bp fragment representing the 3' end of *RYR1* was ligated into the purified linear pTUNE sample to create a 20,297bp plasmid termed the pTUNE subclone.

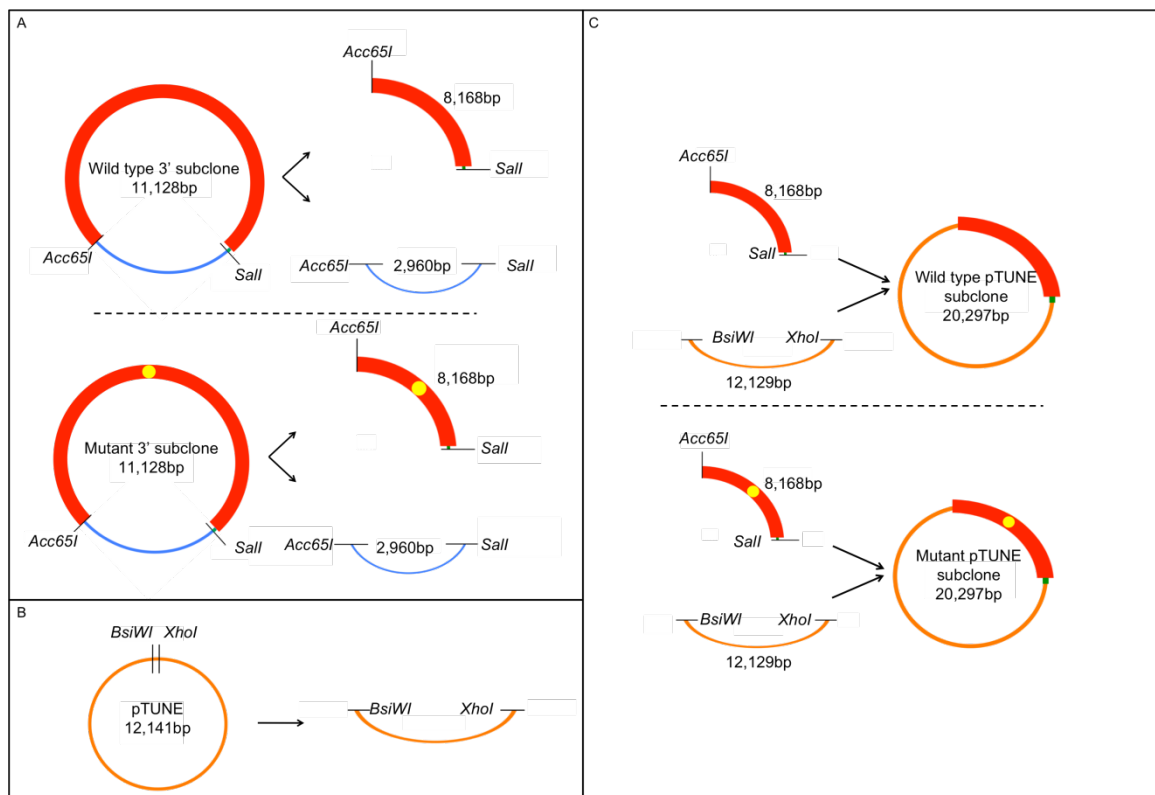


Figure 3.13 – Construction of the pTUNE subclone.

(A) The 3' subclone of *RYR1* was cut with *Acc65I* and *Sall* to produce an 8,168bp fragment of *RYR1*. This fragment was gel purified. The 2,960bp fragment of pBluescript was discarded. (B) pTUNE was cut with *BsiWI* and *XhoI* which produce compatible overhangs with *Acc65I* and *Sall* respectively and gel purified (C) These two fragments were ligated together to produce the pTUNE subclone. This entire process was repeated for each mutant construct present in the 3' end of *RYR1*.

Ligation products were transformed into XL10 Gold Ultracompetent cells and cultured overnight on LB agar plates containing ampicillin. Individual bacterial colonies were selected and screened using the restriction enzyme *XhoI* (Figure 3.14). Positive samples produced a DNA band at 16,005bp and 4,292bp. Additionally, primers were designed flanking the two cloning sites so that a PCR product could only be generated if successful ligation had occurred. PCR products were generated over the cloning sites of samples that tested positive with *XhoI* digestion and were sequenced to confirm successful ligation.

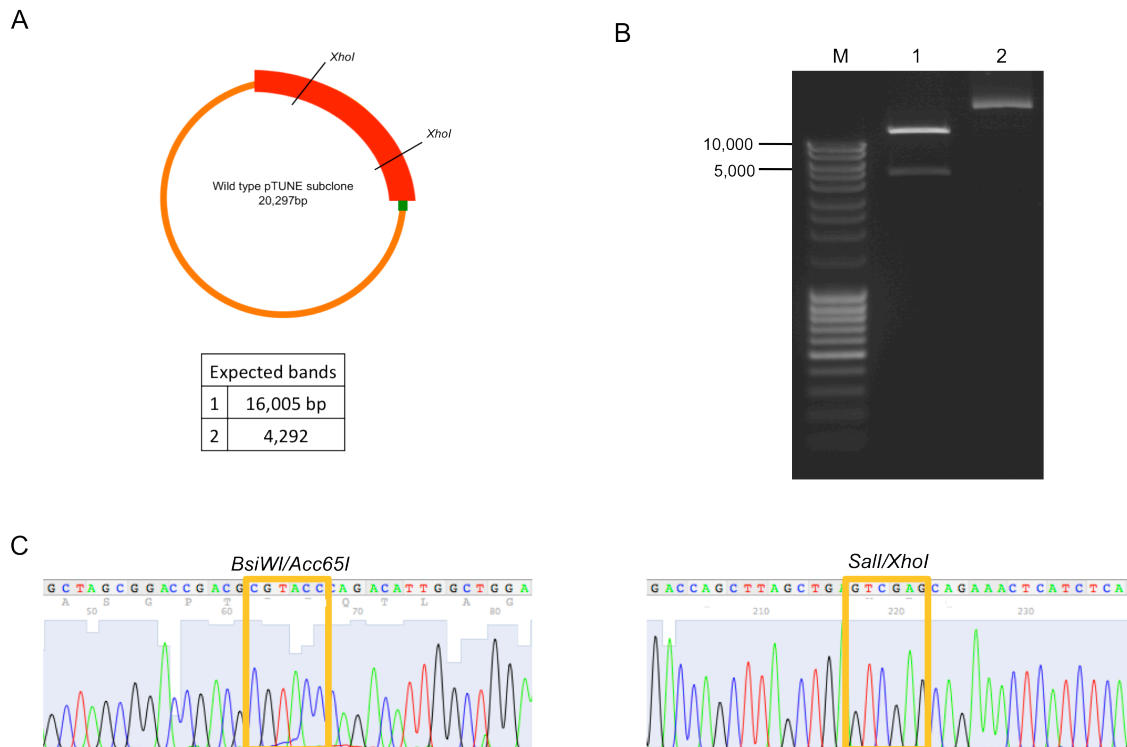


Figure 3.14 – Digest and sequence confirmation of pTUNE subclone constructs

(A) Plasmid map of the pTUNE subclone with *XhoI* restriction sites marked. Expected DNA bands are indicated in the table below the map. (B) Gel image of a positive sample for wild type pTUNE subclone. Lane 1 is the wild type pTUNE subclone digested with *XhoI*. Lane 2 is undigested pTUNE subclone. Lane M is a DNA MassRuler marker with the relevant DNA band sizes marked. The presence of 16,005bp and 4,292bp bands in lane 1 indicates successful ligation and creation of the pTUNE subclone. (C) The *BsiWI* and *Acc65I* restriction sites were both destroyed to produce a CGTACC sequence. The *Sall* and *XhoI* restriction sites were both destroyed to produce a GTCGAG sequence. The new sites are indicated with a gold box.

Ligating together the *BsiWI* and *Acc65I* sites together destroyed both sequences to produce a CGTACC site and ligating together the *Sall* and *XhoI* sites destroyed both sequences to produce a GTCGAG sequence. These sites were identified in the sequence files. The sequence immediately flanking each cloning site was aligned to reference sequences to confirm successful ligation. Positive samples identified through digestion and sequencing were identified for wild type, p.R2355W and p.D3986E constructs (Figure 3.15).

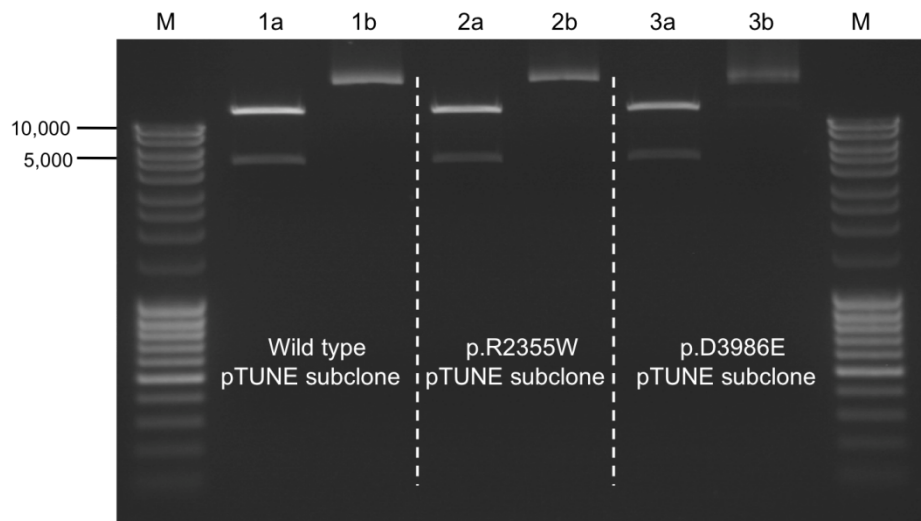


Figure 3.15 – Gel image of pTUNE subclone constructs successfully generated in this project. Wild type, p.R2355W and p.D3986E pTUNE subclones were successfully generated. The 16,004bp and 4,292bp fragments indicate positive digests. 'a' lanes are pTUNE subclone samples digested with *XhoI*. 'b' lanes are undigested pTUNE subclone samples. The 'M' lanes are MassRuler DNA ladders with the appropriate DNA band sizes indicated.

3.3.4.3 Construction of full-length pTUNERYR1 constructs

Wild type and mutant pTUNE subclone samples were digested with *NheI* and *BspEI* to produce a linear 20,158bp DNA product that was gel purified. Digestion with *BspEI* removed the small section of *RYR1* that contained the *Acc65I* site that had been lost due to ligation into the compatible *BsiWI* restriction site. The 5' subclone that was

generated for MEGAWHOP mutagenesis was digested with *SpeI* and *BspEI* which produced a DNA fragment of 7,121bp and that included the entire 5' end of *RYR1* not represented in the pTUNE subclone as well as a 5,402bp fragment containing the rest of the 5' end of *RYR1* and the pBluescript vector. The 7,121bp fragment was gel purified and the other fragment was discarded. The 7,121bp gel purified sample was ligated into the linear pTUNE subclone samples to generate 27,279bp full-length wild type and mutant pTUNERYR1 constructs (Figure 3.16).

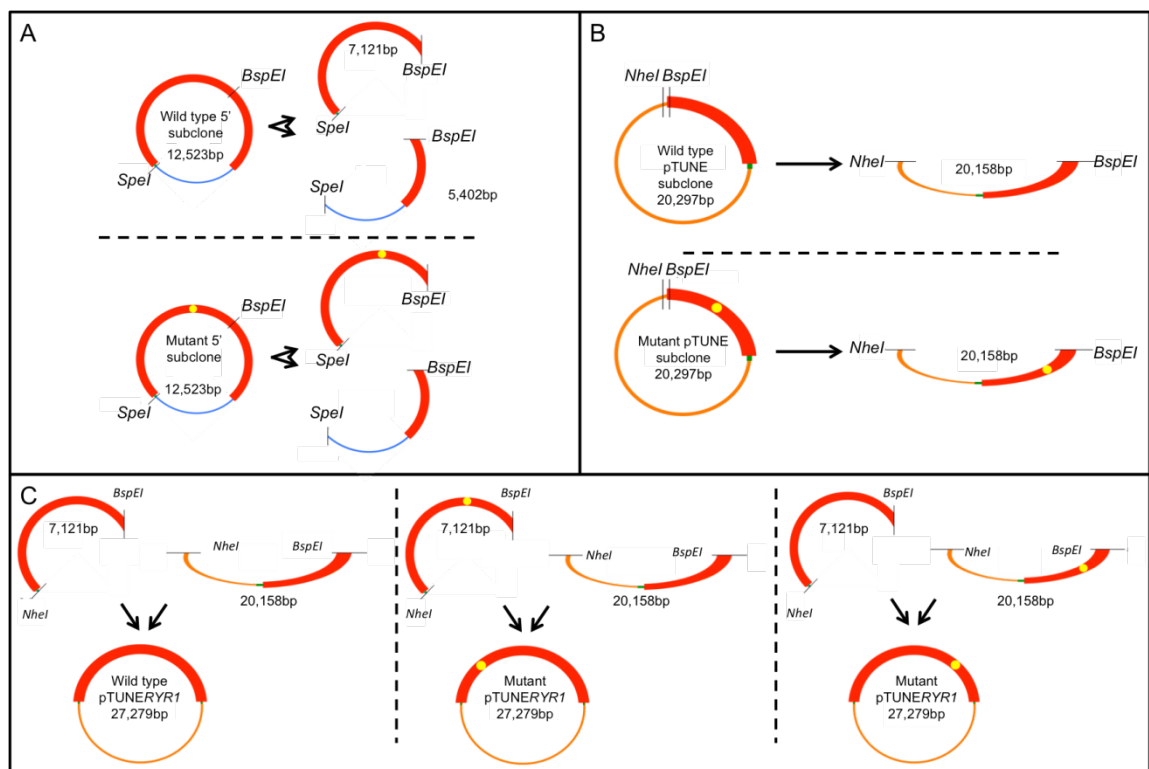


Figure 3.16 – Construction of full-length pTUNERYR1 constructs.

(A) Wild type and mutant 5' subclone samples were digested with *SpeI* and *BspEI* to remove the first 7kb of *RYR1* and was gel purified. (B) Wild type and mutant pTUNE subclones were cut with *NheI* and *BspEI* and gel purified. (C) 3 different pTUNERYR1 constructs were produced. The wild type 5' subclone fragment was ligated into the wild type pTUNE subclone to create wild type pTUNERYR1. The mutant 5' subclone fragment was ligated into the wild type pTUNE subclone to create the p.D1056H pTUNERYR1 construct and the wild type 5' subclone fragment was ligated into the mutant pTUNE subclone to create the p.R2355W and p.D3986E pTUNERYR1 constructs.

The wild type 5' subclone was used to produce p.R2355W and p.D3986E pTUNERYR1 constructs and the p.D1056H mutated 5' subclone was ligated into the wild type pTUNE subclone to generate p.D1056H pTUNERYR1. Ligation products were transformed into XL10 Gold Ultracompetent cells and cultured overnight on LB agar plates containing ampicillin. Individual bacterial colonies were selected for overnight cultures and were subject to mini prep plasmid DNA extraction. Potential full-length pTUNERYR1 DNA samples were digested with *Acc65I* which, when positive produced DNA bands at 20,220bp and 7,054bp (Figure 3.17).

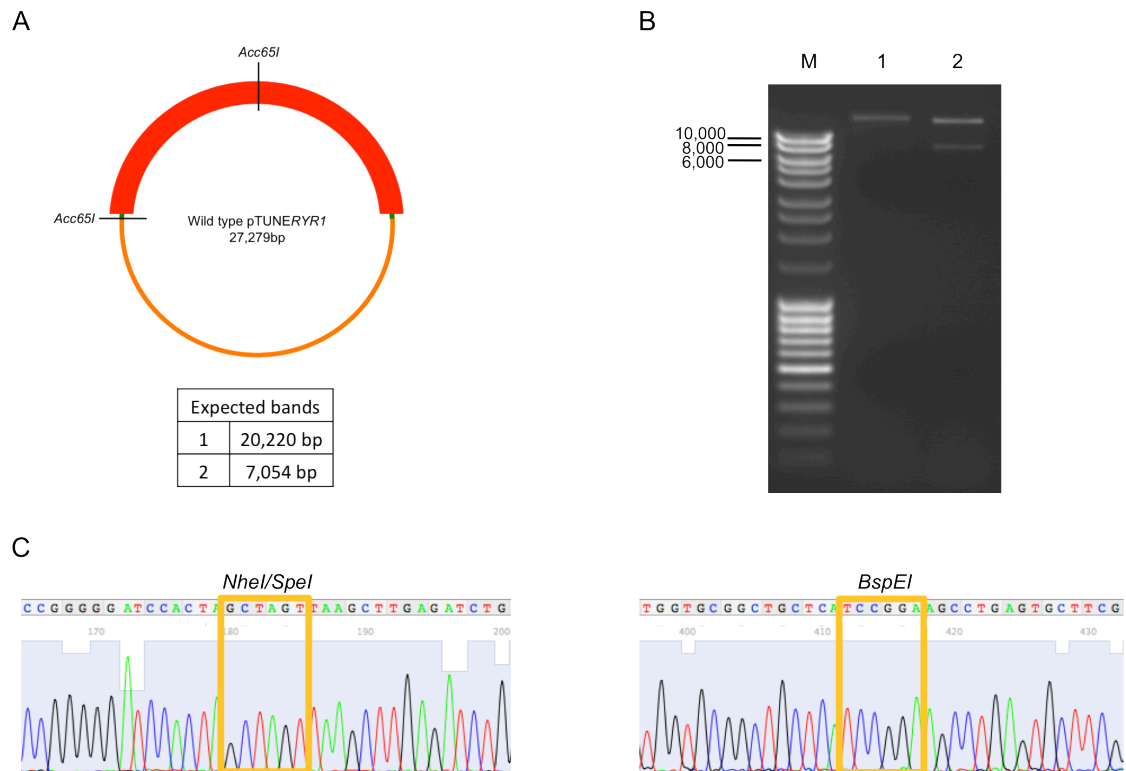


Figure 3.17 – Digest and sequence confirmation of pTUNERYR1 constructs.

(A) Plasmid map of pTUNERYR1 with *Acc65I* sites marked and expected DNA bands indicated in the table below the map. (B) Gel image of pTUNERYR1 digested with *Acc65I*. Lane 1 is an undigested pTUNERYR1 sample. Lane 2 is pTUNERYR1 digested with *Acc65I*. Lane M is a DNA MassRuler ladder with the relevant DNA band sizes marked. The presence of 20,220bp and 7,054bp DNA bands in lane 1 indicates successful creation of full-length pTUNERYR1. (C) The *NheI* and *SpeI* sites were ligated together to produce a GCTAGT site, resulting in the destruction of both original restriction sites. The *BspEI* site was left intact. Sequences immediately flanking each cloning site were aligned to RYR1 and pTUNE reference sequences to confirm ligation.

Additionally, primers were designed that flanked each cloning site so that a PCR product could only be generated if successful ligation had occurred. A PCR product was generated over both cloning sites and sequenced in both directions to confirm ligation. Ligation of compatible *NheI* and *SpeI* sites resulting in the destruction of both restriction sites and the presence of a GCTAGT sequence. This sequence and the TCCGGA *BspEI* sequence were identified. The sequences immediately flanking each cloning site were also aligned against *RYR1* and pTUNE plasmid DNA reference sequences. Full-length pTUNERYR1 constructs were successfully generated for wild type, p.D1056H, p.R2355W and p.D3986E (Figure 3.18).

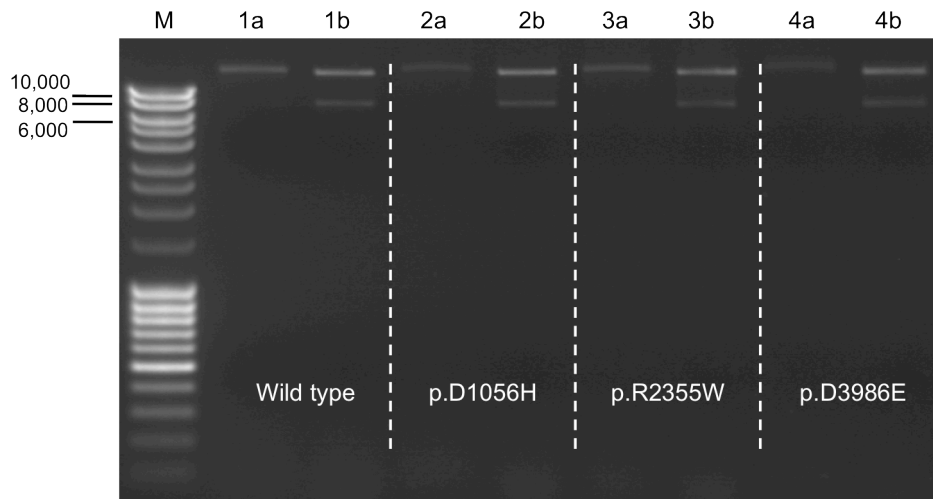


Figure 3.18 – Full-length pTUNERYR1 constructs digested with *Acc65I*. Wild type, p.D1056H, p.R2355W and p.D3986E pTUNERYR1 constructs were successfully generated. ‘a lanes’ are undigested full-length pTUNERYR1 constructs and ‘b lanes’ are constructs digested with *Acc65I*.

3.4 Discussion

In this chapter, seven *RYR1* variants were selected for experiments aimed at elucidating their functional consequences. As part of this project, a comprehensive cloning strategy needed to be devised coupled with a mutagenesis protocol as robust and reliable as possible for such large plasmids. The work presented above meets

these criteria with all seven variants successfully introduced into subclones of *RYR1* before full-length plasmid reconstructions in several eukaryotic expression vectors.

3.4.1 Selection of *RYR1* variants

Seven variants were selected that have been identified in over a third of the UK MH population that possess an as yet uncharacterised *RYR1* variant. A total of 46 families have been found to possess one of these variants and the successful functional characterisation of these variants would increase the availability of initial genetic diagnosis by 22.5% worldwide, negating the need for the invasive muscle biopsy associated with IVCT testing for MH.

Amongst the seven variants are two which might be predicted to have minimal function consequences based on the properties of the amino acids that are substituted in the MH patients. The p.D3986E variant has an extremely mild amino acid substitution of glutamic acid to aspartic acid. Both amino acids are polar, hydrophilic and acidic and differ only in the presence of an additional methylene group in glutamic acid. Despite the seemingly mild change, the p.D3986E variant has been found in association with MH in 4 UK families which, when the IVCT results are taken together produce a significantly larger caffeine contracture than specimens carrying other *RYR1* variants meaning it is still a good candidate for MH testing (Carpenter et al., 2009c).

The second variant, p.V4849I, again maintains acidity and hydrophobicity. However, this variant, has been found in a large number of families worldwide in conjunction with both MH and CCD. Data obtained from lymphoblastoid cells indicates that this variant produces an elevated resting calcium concentration in cells expressing the variant, consistent with both MH and CCD phenotypes (Ducreux et al., 2006). Based on the frequency at which the variant has been identified as well as data obtained in patient cells, the functional consequences of the p.V4849I variant are still of interest in this project.

Evolutionary conservation of the nucleotide and amino acid affected is also of interest when selecting *RYR1* variants that may potentially be causative of MH. Across a number of species that are closely related to humans or have been reported to undergo a similar reaction to MH, all amino acids affected in the variants selected are maintained indicating at least some importance of the residue in question. Interestingly, the p.D3986 and p.V4849 residues that appeared to have a mild change when mutated have been fully maintained not only across different species but also across the three RYR isoforms in humans suggesting that the amino acid present is important for the normal function of the protein.

The only residue that shows any form of variation between different RYR proteins is the p.R2355 residue that in human RYR2 is a lysine residue. The change from arginine to lysine is a relatively mild one with both amino acids being positively charged and basic however, as discussed above this does not negate the possibility of a change of function. However, as these two residues are present in the two wild type sequences, it suggests that the change is a functional one relating to the slightly different roles of RYR1 and RYR2 in the tissue in which they are primarily expressed. The p.R2355 residue is maintained across all the RYR1 isoforms examined indicating the importance of this residue and therefore its inclusion in this project.

The primary selection criterion for inclusion in this project was the frequency at which the variant has been found in the UK MH population. The exception to this is the p.D1056H RYR1 variant, which was chosen for study in this project due to its association with both MH and EHS. The variant was identified to co-segregate with disease in an MH family but upon subsequent screening of the UK MH population it was also identified in an individual who suffered an EHS reaction and was subsequently referred for MH testing. However, the EHS individual tested negative for MH through the IVCT. There has long been a link between MH and EHS through a shared phenotype and with increasing evidence of a genotypic link, experiments on

the p.D1056H variant are of particular interest (Tobin et al., 2001, Hopkins, 2007, Muldoon et al., 2007, Muldoon et al., 2008).

3.4.2 Subcloning *RYR1*

The cloning work presented above represents a significant step forward in simplifying the processes by which functional studies can be carried out using *RYR1* cDNA clones. It is unfeasible to carry out conventional mutagenesis on a full-length *RYR1* cDNA construct and so the necessity to subclone certain sections of *RYR1* is unavoidable. The first work aimed at functionally assessing a number of genetic variants in *RYR1* associated with MH constructed eleven separate subclones of *RYR1* to carry out mutagenesis on (Tong et al., 1997). This, however, was a large undertaking that first needed the introduction of five new unique restriction sites into the cDNA sequence of *RYR1*. Three large subclones of *RYR1* were created for the introduction of the new restriction sites, one of which was then subcloned further after the introduction of a new restriction site. The shuttle vectors used for these manipulations were themselves modified to allow the subcloning of certain regions of *RYR1*. After the introduction of the new restriction sites, an expression vector also had to be manipulated to allow the full-length *RYR1* construct to be inserted. Furthermore, this work was carried out to facilitate the introduction variants that were only separated by 2kb of DNA.

Subsequent work has also required the creation of multiple step cloning strategies to allow the introduction of genetic variants in *RYR1*. Sambuughin et al. (2001b) removed one piece of *RYR1* directly from a full-length construct but needed to insert the mutated piece of DNA into one of three subclones which were then combined to recreate a full-length *RYR1* cDNA construct. Sato et al. (2010) used a similar strategy in which full-length *RYR1* was split into two large subclones before each being halved again to create a total of four constructs. Mutagenesis was performed on one of the

four smaller constructs before going through two reconstruction steps to create full-length mutants.

The cloning strategies used were in part necessary to produce a small enough subclone to carry out site directed mutagenesis. The original functional study used plasmids no larger than 4.5kb in size. As mutagenesis protocols have advanced, the size of the plasmid used as a template for mutagenesis has increased but never above 10kb. The MEGAWHOP mutagenesis protocol utilised in this study has allowed us to carry out mutagenesis on plasmids 12.5kb in size. This increase in size of template DNA has facilitated the use of a one step subcloning strategy in which *RYR1* was split in half to create a 5' and a 3' subclone. The possibility of carrying out mutagenesis on these subclones means that individual strategies do not need to be developed for individual genetic variants in *RYR1*. The mutation site will be present in either of the two subclones and can be used for mutagenesis. The 5' subclone has an overlap into the 3' subclone meaning that no area of *RYR1* is missed. Mutations in the 3' end of *RYR1* can be reconstructed into *pcRYR1* to create full-length constructs however, due to the lack of a unique restriction site at the 5' end of *RYR1*, mutations in this subclone had to be reconstructed into a new vector (pTUNE). The wild type 3' end of *RYR1* was inserted into pTUNE meaning that the need for only a one step cloning strategy is maintained.

3.4.3 Mutagenesis of *RYR1* subclones

The mutagenesis protocol had an overall efficiency of 52.9% but ranged from 20%-100% of colonies screened for individual mutations. This discrepancy is likely due to variability in the stringency of the mutagenesis procedure. One such example would be inconsistencies in *DpnI* digestion of the original template DNA. For variants in which there were more colonies after transformation the success percentage was lower. For both variants where only one colony formed after transformation (p.D1056H and p.V4849I), that colony was positive for the mutation. Previous studies fail to report their mutagenesis efficiency however it is widely accepted that as

plasmid size increases the efficiency for any enzymatic process is reduced. A success rate of over 50% is considered good for a cDNA construct of the size of *RYR1*. The development of a simple and robust method of generating mutant *RYR1* constructs is not only of use to our group but other groups working on characterising mutations identified in the MH population. Many variants identified in patients are unique to their family. EMHG guidelines only allow variants to be added to the genetic diagnostic panel of MH if experiments have been carried out on *ex vivo* samples from two independent families meaning some variants may never be characterised using this method. Making recombinant experiments more accessible to other laboratories would aid the increase of the genetic diagnostic panel in the global MH population.

3.4.4 The requirement of multiple expression vectors

For simple functional experiments involving easily transfectable cells such as HEK293 cells the use of the pcDNA expression vector is sufficient. However, in this study we wanted to be able to compare the functional consequences of variants in *RYR1* in HEK293 cells as well as in the more native 1B5 muscle-like cells. Conventional transfection methods are unsuitable for experiments in muscle cells. Small plasmids have low transfection efficiency in muscle cells (Campeau et al., 2001) and when coupled with a plasmid over 20kb in size, the efficiency drops further. A method to virally transduce the dyspedic 1B5 cells has been developed which allows functional experiments to be carried out in a more native environment for *RYR1* (Yang et al., 2003). The method involves packaging *RYR1* into HSV virions. To do this, the *RYR1* cDNA needed to be transferred to the pHSVPrPUC vector that contains the packaging signal for HSV capsid formation. Due to the size of *RYR1*, there are limited unique restriction sites for shuttling over the cDNA sequence to the pHSVPrPUC vector. The only method available in this study was to cut with *SpeI* which had three sites in the pc*RYR1* vector. There were no *SpeI* sites in the *RYR1* cDNA sequence but one at either end of the sequence and a further one in the vector sequence. *SpeI* produces

compatible overhangs with *XbaI*. pHSVPrPUC was linearised using *XbaI* and *RYR1* was non-directionally cloned into pHSVPrPUC. This method was far from ideal as ligations of such size are extremely inefficient. This was exacerbated by the fact that the *RYR1* cDNA could insert into pHSVPrPUC in either direction further reducing the ligation efficiency. Nevertheless, three constructs were successfully generated. Wild type, p.R2336H and p.D3986E *RYR1* were introduced into the pHSVPrPUC vector. Getting the wild type construct into pHSVPrPUC was essential for any subsequent comparisons with mutant constructs.

Recent evidence has hinted at the importance of expression levels of *RYR1* alleles in patients with MH (Grievink and Stowell, 2010). This coupled with the desire to reliably obtain specific levels of *RYR1* expression in cellular systems led to the idea to place *RYR1* constructs into the pTUNE inducible expression vector (Deans et al., 2007). Unlike most other inducible expression vectors, pTUNE functions as a single vector which, when dealing with a construct the size of *RYR1* is ideal. The polylinker of pTUNE had several restriction sites that had complimentary overhangs to several sites in pc*RYR1* making the shuttling of *RYR1* into pTUNE easier than it was for pHSVPrPUC. The strategy depended on *BspEI* to be a unique restriction site within *RYR1* meaning an endogenous *BspEI* site needed to be removed before *RYR1* could be cloned into pTUNE. The pTUNE *BspEI* site resided in the neomycin resistance gene meaning that no stable pTUNER*RYR1* clones would be able to be created. However, with the added complication of needing to induce expression, only transient transfections of HEK293 cells were planned for these constructs.

3.5 Future work

The cloning work presented here represents a substantial step forward in increasing the ease at which functional experiments for *RYR1* variants can be carried out. The development of a highly efficient and robust mutagenesis method coupled with a one step reassembly strategy means that the speed at which mutant *RYR1* constructs can

be created is greatly increased. There are currently over 200 uncharacterised *RYR1* variants that need to be functionally tested before they can be included on a genetic diagnostic panel and decrease the need for a muscle biopsy. The development of a production line of mutant *RYR1* variants would increase the efficiency at which the variants can be added to the genetic diagnostic panel.

In spite of this, work can still be done to further improve the efficiency of the production of mutant *RYR1* constructs. Currently, any variants in the 5' end of *RYR1* need to be reconstructed into the pTUNE inducible vector. Ideally, there would be a unique restriction site at the 5' end of *RYR1* that would facilitate the possibility of introducing the mutated 5' end of *RYR1* straight back into the pcDNA vector. Although placing the 5' end of *RYR1* into pTUNE is still a one step cloning strategy, the plasmid is much larger than pcDNA and along with the need to induce the cells with high doses of IPTG to generate expression of *RYR1* it would be less technically demanding to place the variants into the pc*RYR1* construct. Future work could introduce a new, unique restriction site into the pcDNA expression vector as well as at the 5' end of *RYR1* in the 5' subclone meaning that the subclone could be recreated using the new site and *Acc65I*. This would allow the introduction of the 5' subclone directly into pc*RYR1*.

Another area that could be improved is the mutagenesis method. MEGAWHOP site-directed mutagenesis, although efficient and suitable for large plasmids, is still a PCR based method that holds inherent risks of introducing additional, unwanted mutations into the plasmid targeted. A technique, which could be used in such experiments, is recombinogenic engineering (recombineering). This method is based on lambda Red-mediated homologous recombination. The technique was first developed to study the gene functions of recently sequenced genes of unknown function derived from the human genome project. The method has been used extensively in studying gene function and expression patterns in the nematode worm, *Caenorhabditis elegans* through the insertion of reporter constructs at the end of C-terminal end of target genes (Dolphin and Hope, 2006). One of the biggest advantages of this technique is its

potential for limitless size of constructs manipulated and although recombineering has been primarily used for the addition of reporter constructs to genes the potential is there to introduce single point mutations in a similar fashion to the MEGAWHOP protocol developed here. The use of recombineering would eliminate the need for unique restriction sites and laborious 'cut and paste' methods of subcloning to facilitate site-directed mutagenesis as well as limit the amount of error introduced through PCR based mutation strategies.

3.6 Conclusions

The work presented here provides a large step forward in the production of full-length, mutant *RYR1* cDNA constructs. By far the best ways of functionally characterising *RYR1* variants are recombinant methods. Therefore, developing a robust, efficient and simple cloning strategy that allows the relatively rapid creation of *RYR1* variants is essential. In the 10 years prior to this work, only 31 *RYR1* variants have been accepted as causative of MH and placed onto the genetic diagnostic panel. This is in no small part due to the difficulties associated with working with large cDNA constructs. The methods developed here have created 7 full-length mutant *RYR1* constructs that, after subsequent functional analysis can potentially increase the genetic diagnostic panel by 22.5%. These variants represent a total of 46 families in the UK that possess an as yet uncharacterised missense *RYR1* variant. The addition of these variants to the diagnostic panel for MH will improve the diagnostic procedure for people within these families and new families referred to the MH diagnostic centre carrying these variants.

Chapter Four - Functional analysis of genetic variants in the *RYR1* gene associated with malignant hyperthermia in HEK293 cells

4.1 Introduction

Since the introduction of the EMHG guidelines for the inclusion of *RYR1* and *CACNA1S* variants onto the genetic diagnostic panel for MH, by far the most frequently used method has been expressing recombinant *RYR1* variants in HEK293 cells. Out of the 31 mutations listed as causative on the EMHG website, 85% have been tested in HEK293 cells. Recently, experiments involving dyspedic muscle-like 1B5 cells have been developed but currently they have only been used to confirm the causative nature of MH mutations already on the diagnostic panel (Yang et al., 2003). Work on *ex vivo* samples struggle to make it to the diagnostic panel for MH due to the limited number of samples and families available for such studies and due to the problems associated with working on a non-defined genetic background they possess relatively little scientific merit as a method of functionally assessing *RYR1* variants.

4.1.1 Variants in *pcRYR1*

Several of the most frequent *RYR1* variants found in association with MH in the UK population were selected as candidates to be functionally characterised as described in chapter 3. Five of the variants, p.R2336H, p.E3104K, p.D3986E, p.G3990V and p.V4849I were introduced into *pcRYR1* and account for a total of 34 UK families with an as yet uncharacterised *RYR1* variant. The p.E3104K, p.D3986E and p.G3990V variants have been identified exclusively in the UK whereas the p.R2336H and p.V4849I variants have been found worldwide.

4.1.1.1 p.R2336H worldwide

The p.R2336H variant is particularly prevalent in the MH population of Switzerland with one report suggesting it may be present in a similar frequency to the p.V2168M variant which is the most common in Switzerland (Treves et al., 2011). Interestingly, immortalised lymphoblastoid cells isolated from patients carrying this variant only showed an increased sensitivity to 4-CmC but not caffeine (Levano et al., 2009). In this case, cells from seven separate families were analysed, potentially removing any worries of the genetic background playing a part in the seemingly wild type phenotype when the cells were exposed to caffeine. However, lymphocytes are not a cell type in which RYR1 would carry out its primary function and questions remain over the use of these cells as a representative system for these experiments, especially considering the fact that this variant has been identified to cosegregate with the MH phenotype in 14 families worldwide. The p.R2336H variant has also been implicated in a form of non-anaesthesia induced MH. A patient carrying both the p.R2336H variant and a p.E209K variant experienced almost 100 episodes of generalised body rigidity and muscle spasms in the absence of anaesthesia (Loke et al., 2007, Muldoon et al., 2008). The p.E209K variant was dismissed as the causative factor in this case based on the prediction of an *in silico* protein prediction program and p.R2336H accepted as the cause. Whereas the p.R2336H variant has been implicated in a non-anaesthesia reaction, an additional variant at this codon, p.R2336C, has been found in association with a recessive myopathy (Bevilacqua et al., 2011). A patient carrying a p.R2336C and p.D4911L displayed axial and proximal muscle weakness along with impaired respiratory function and poor spontaneous movements. It is not known whether this variant has any link to MH but highlights the broad range of conditions associated with RYR1 variants.

4.1.1.2 p.V4849I worldwide

The p.V4849I variant has been identified in cases of CCD as well as MH. Monnier et al. (2005) reported a case where only MH was found in the family carrying the p.V4849I variant whereas, in the UK, 6 out of the 8 families that possess the p.V4849I variant have CCD segregating with the variant in addition to MH. Jungbluth et al. (2002) reported a family in which the p.V4849I variant had been identified in the heterozygous state in both parents of a CCD affected child who carried the variant in homozygous form. The parents were asymptomatic of CCD but unfortunately, no family members were tested for MH susceptibility via the IVCT. Similarly to the p.R2336H variant, immortalised lymphoblastoid cells isolated from both parents and the CCD affected daughter did not display an increased sensitivity to 4-CmC (Ducreux et al., 2006). This was, however, just one family tested using a non-defined genetic background and in a cellular system far removed from the normal environment of *RYR1*. An elevated resting calcium level was seen, however, in the patients indicating that this variant may, at least in part, contribute to the myopathy phenotype.

4.1.2 The variants in the UK population

Carpenter et al. (2009c) presented data for each of the variants under investigation in this chapter in correlation with IVCT data obtained at the St James's Hospital MH diagnostic centre. All variants correlated with a strong MHS IVCT response. There was some variability between the variants within the different parameters of the IVCT procedure and the MH reaction experienced by patients carrying these variants. Patients carrying the p.D3986E and p.G3990V variants were found to have a significantly higher static caffeine contracture in the IVCT as compared to patients carrying a known causative MH variant. Patients carrying the p.G3990V variant were also associated with a more severe dynamic halothane IVCT response. Both the p.R2336H and the p.D3986E variants were associated with a higher creatine kinase value in MH probands. The p.E3104K variant was associated with a ryanodine binding

response close to wild type and an overall weaker response throughout the IVCT. Although the p.V4849I variant was associated with both MH and CCD, the IVCT response was not significantly different to any of the other variants under investigation.

This variability observed between patients known to be carrying these variants and their IVCT responses may represent one reason why some patients have a more severe MH reaction, a quicker onset time and why some patients can undergo more than one anaesthesia before experiencing an MH reaction. However, each of the patients included in such studies also have unknown genetic factors contributing to this variability. Comprehensive functional analysis of these genetic variants in recombinant systems will allow greater conclusions to be drawn on the inherent variability of different *RYR1* variants.

4.2 Aims of the chapter

The aims of this chapter were to functionally characterise common *RYR1* variants that have consistently been identified in association with MH in the UK population. The functional studies carried out will be the final step for placing these variants onto the genetic diagnostic panel for MH, expanding the current availability for genetic diagnosis by 16.1% and reducing the need for a muscle biopsy for patients. HEK293 cells were selected as the expression system in this chapter to allow a robust, reliable and reproducible method of transfection and subsequent measurements to be established. The aim of this was to develop a protocol that can be readily used for many other *RYR1* variants found associated with MH in the UK and worldwide populations. Furthermore, obtaining data in HEK293 cells is the first step of evaluating their use in functional studies as a comparison point to data obtained in dyspedic myotubes.

4.3 Results

4.3.1 HEK293 cells stably transfected with pcRYR1 constructs

4.3.1.1 Antibiotic kill curve

To determine the correct concentration of the selective antibiotic, G418, to use in selecting stable HEK293 cell lines transfected with wild type or mutant pcRYR1 constructs, an antibiotic kill curve was established (Figure 4.1).

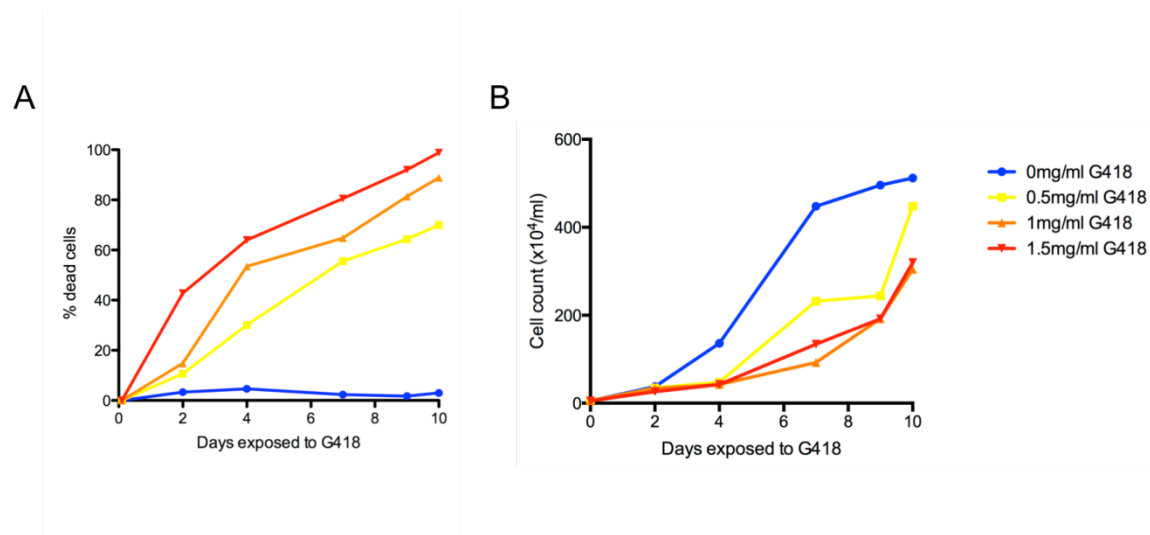


Figure 4.1 – Antibiotic kill curve for HEK293 cells exposed to G418 over a period of 10 days.

(A) The percentage of cells that died after up to 10 days of exposure to G418. Measurements were taken every 2 days. The higher the concentration of G418, the higher the percentage of cells that took up the trypan blue viability stain and were therefore dead. After 10 days, 98% of cells exposed to 1.5mg/ml G418 were dead. No more than 5% of cells were dead at any time point when the growth medium was free of antibiotics. (B) Cell count of cells after exposure to G418. Cells with no antibiotic continued to grow freely. The higher the antibiotic concentration, the slower the cells were able to proliferate.

Panel A shows the percentage of cells that took up the trypan blue dye and were therefore dead. The higher the concentration of G418 in the growth medium, the more cells died throughout the 10-day experiment. After 10 days, 98% of cells exposed to 1.5mg/ml G418 took up the trypan blue viability stain indicating cell death compared with 89% and 70% for cells exposed to 1mg/ml G418 and 0.5mg/ml G418, respectively. No more than 5% of cells were dead when no antibiotic was in the growth medium. Based on this, 5% was taken as the background death, presumably

caused by the resuspension procedure to mix the cells with trypan blue. Panel B shows the cell count in each of the flasks measured throughout the experiment. Cells exposed to no antibiotics grew the most prolifically. As the concentration of antibiotic increased, the cell count at each time point measured decreased. The tissue culture flasks were initially seeded with 5×10^4 HEK293 cells. The flasks that were not exposed to any G418 reached a cell count of 512×10^4 . Cells exposed to 0.5mg/ml of G418 grew to a cell count of 448×10^4 . Cells exposed to 1mg/ml of G418 reached 304×10^4 cells/ml and cells exposed to 1.5mg/ml similarly only managed to reach 320×10^4 cells per ml over the 10-day time period. 1mg/ml G418 was the recommended starting antibiotic concentration and based on the results obtained here, there was no reason to diverge from this concentration for the stable transfection experiments.

4.3.1.2 Caffeine-induced calcium release of stably transfected HEK293 cells

Data obtained from confocal microscopy was saved as a z-stack video and analysed in ImageJ and fluorescence traces were plotted in Prism 6 statistics package (Figure 4.2). Cells were loaded with Fluo-4 AM as described in section 2.4. Upon stimulation with caffeine, calcium release was observed as a temporary increase in fluorescence followed by a return to baseline as the Ca^{2+} ions were sequestered back into the stores. All cells responded at caffeine concentrations of between 1mM and 20mM. A small proportion of untransfected HEK293 cells responded to high doses of caffeine (8-20mM) (Figure 4.3A). Because of this, ten independent experiments were analysed to calculate a background rate of cells responding to caffeine that were untransfected resulting in an average background rate of 4.02% being calculated (Figure 4.3B). Based on the responses of untransfected cells, only cells that responded to low doses of caffeine (1mM-5mM) were selected on the videos for analysis. Any cells that only responded to caffeine doses above 5mM were not used for subsequent analysis.

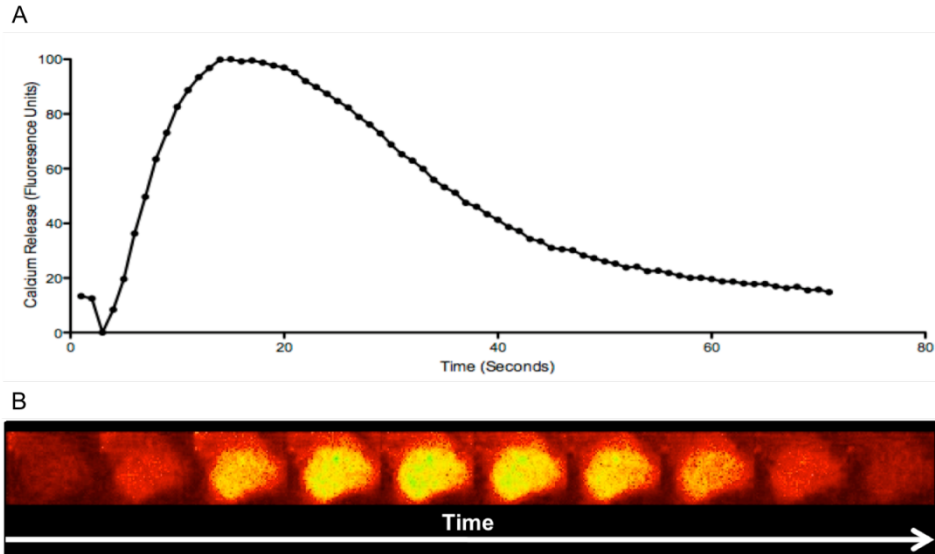
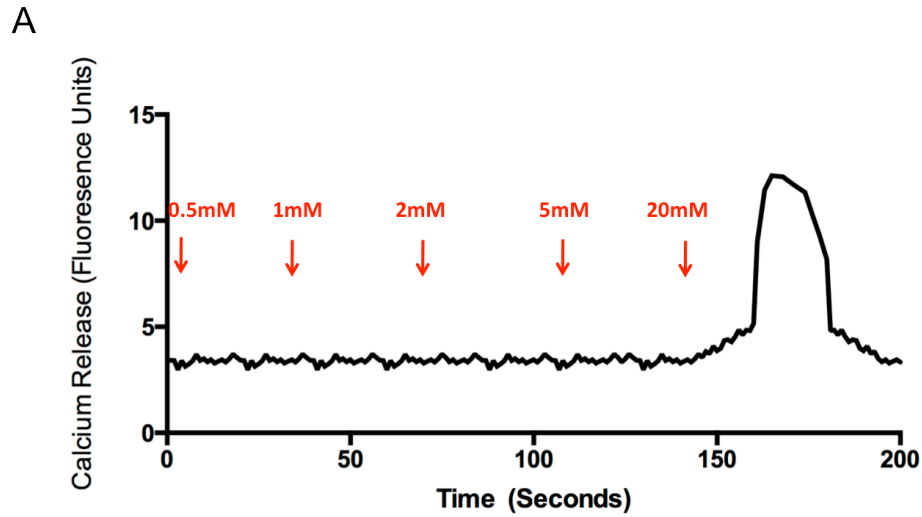


Figure 4.2 – Ca^{2+} release from a HEK293 cell upon stimulation with 1mM caffeine. (A) Fluorescence trace generated from a HEK293 cell releasing Ca^{2+} . (B) Time lapse image showing the same HEK293 cell releasing Ca^{2+} upon stimulation with caffeine. Ca^{2+} release is visualised as a temporary increase in fluorescence before being sequestered back into intracellular stores, resulting in a decrease in fluorescence.



B

Total cells	Responding cells	Background
214	6	2.8%
116	6	5.2%
143	9	6.3%
43	1	2.3%
61	2	3.3%
55	2	3.6%
312	21	6.7%
320	10	3.1%
256	9	3.5%
208	7	3.4%
Average		4.02%

Figure 4.3 – The response of untransfected HEK293 cells to caffeine.

(A) Untransfected cells only responded to high doses of caffeine as seen by the temporary increase in fluorescence observed after the addition of 20mM caffeine in the above trace. (B) Ten independent experiments were analysed giving an estimated background rate of 4.02% of HEK293 cells that responded to high doses of caffeine (8mM-20mM).

Wild type cells never responded to 0.5mM caffeine and only on rare occasions did the mutants (Figure 4.4). Each experiment was plotted as a normalised response with 100% being the peak fluorescence for each video and 0% being the baseline fluorescence before the addition of any caffeine. A maximum response was usually observed at 5mM caffeine for all constructs. On occasion, wild type and p.D3986E

transfected cells only achieved a maximum response at 20mM caffeine. p.R2336H and p.G3990V often reached a maximum response at concentrations of caffeine as low as 2mM. Dose-response curves were plotted on a log x-axis. The peak fluorescence produced from each caffeine concentration was taken before non-linear regression was used to fit a representative curve for all experiments (Figure 4.5A-C).

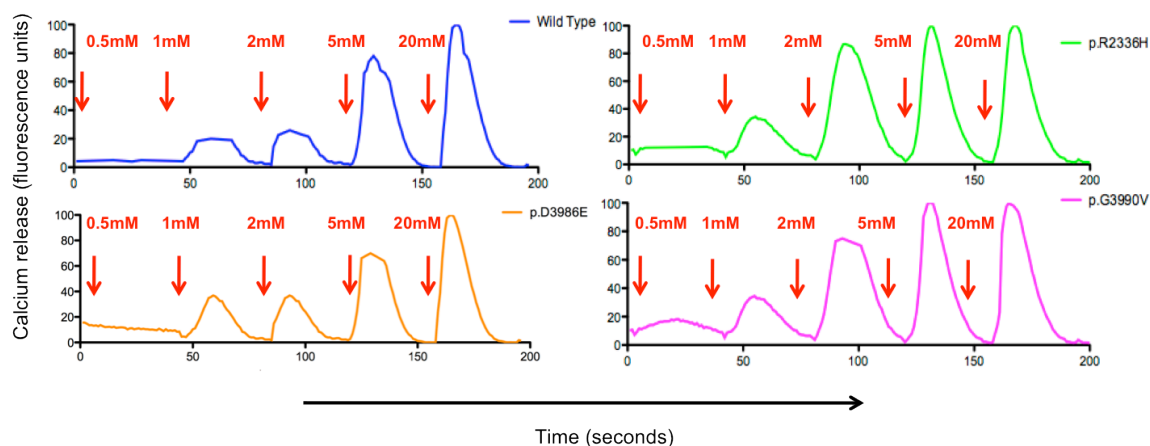


Figure 4.4 – Representative traces of HEK293 cells stably transfected with wild type and mutant pcRYR1 constructs.

The response at each caffeine concentration is seen as a temporary increase in fluorescence. The red arrows mark the time that each caffeine concentration was added to the well and instantly perfused off. Wild type transfected cells never reached a maximum response before the addition of 5mM caffeine. This was the same for cells transfected with the p.D3986E variant, however, cells transfected with both the p.R2336H and p.G3990V variants often reached a maximum response at caffeine concentrations as low as 2mM.

For cells transfected with p.R2336H and p.G3990V constructs, the fitted curve was shifted to the left, indicating an increase in sensitivity to caffeine. Cells transfected with p.D3986E had a curve that was very similar to the curve produced by wild type cells. The dose at which half of the maximum response (EC_{50}) was produced was calculated from the curves generated in the Prism software package (Figure 4.5D-E). Compared to cells stably transfected with the wild type pcRYR1 construct where the EC_{50} was 3.209mM (standard error of the mean (SEM) = 0.259, 95% confidence intervals (CI) = 2.443-3.774), p.R2336H and p.G3990V transfected cells had an EC_{50} that was statistically significantly reduced to 0.9101mM (SEM = 0.092, 95% CI = 0.801-1.274; $p=0.0003$) and 1.414mM (SEM = 0.098, 95% CI = 1.118-1.694; $p=0.0001$)

respectively (n=6). The EC₅₀ of cells transfected with the p.D3986E construct was only slightly reduced to 2.857mM, which was not statistically significantly different from that of wild type (SEM = 0.1865, 95% CI = 2.225-3.184; p=0.2339) (n=6).

The percentage of the maximum response was plotted for each construct at each caffeine concentration (Figure 4.5F). At 1mM caffeine, cells transfected with p.R2336H produced a response that was statistically significantly higher than any other construct (wild type (p=0.001), p.D3986E (p=0.0004) and p.G3990V (p=0.0004).). p.D3986E transfected cells produced a response that was statistically significantly higher than wild type at 1mM caffeine (p=0.046) whereas, as a percentage of its maximum, p.G3990V produced a response that was not significantly different from wild type at 1mM caffeine (p=0.1554). At 2mM all variants produced a statistically significantly higher response as a percentage of their maximum as compared to wild type (p.R2336H p<0.0001, p.D3986E p=0.0033, p.G3990V p<0.0001). However, the p.D3986E response was significantly smaller than the p.R2336H and p.G3990V variants (p<0.0001 for both constructs). At 5mM and 20mM caffeine a maximum response had been achieved for all constructs meaning that there were no significant differences observed. For all analyses n=6.

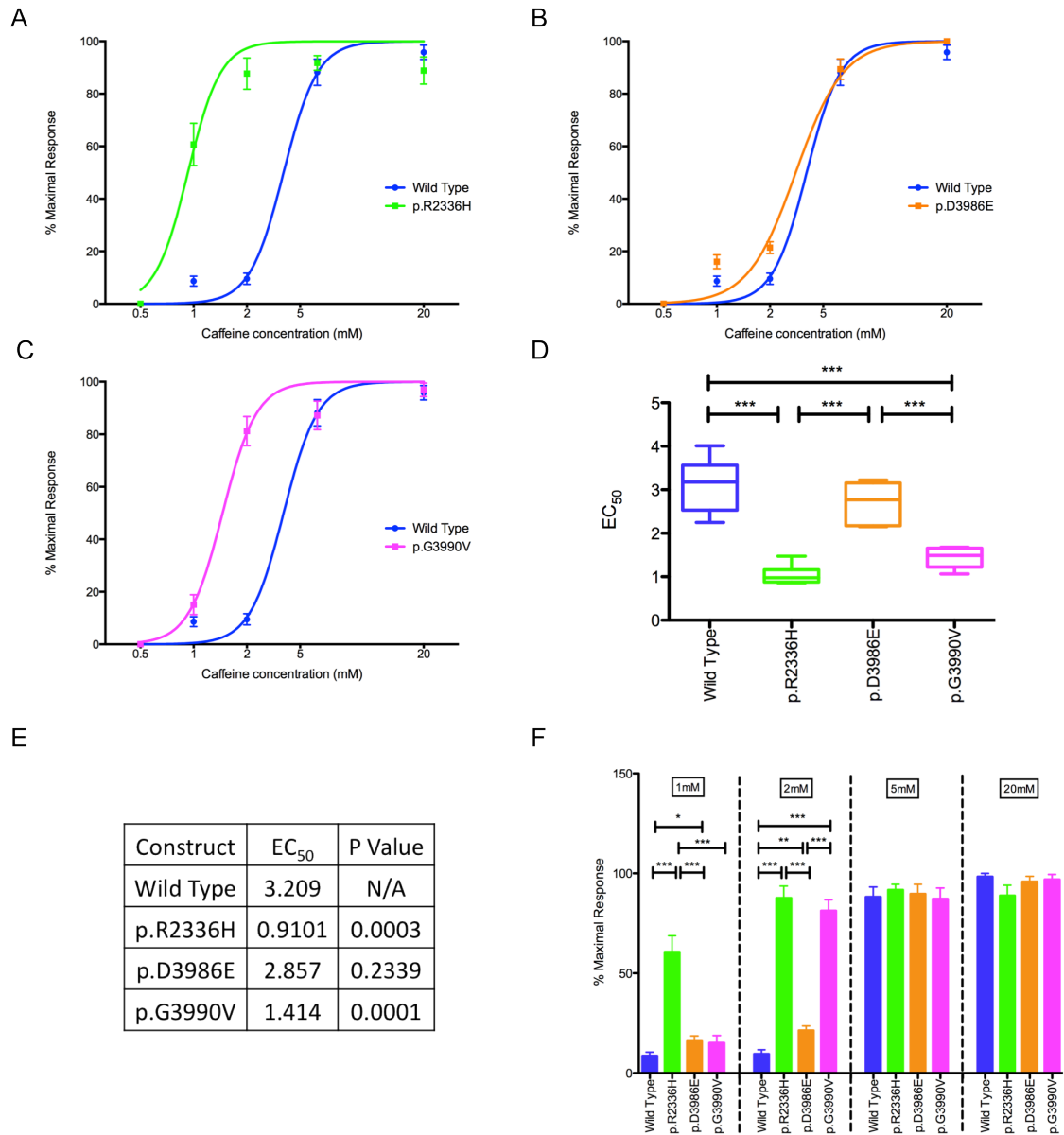


Figure 4.5 – Caffeine dose-response for HEK293 cells stably transfected with wild type and mutant *pcRYR1* constructs.

(A-C) Dose-response curve for each variant stably transfected into HEK293 cells plotted with wild type. Data points are shown as the mean plus and minus the standard error of the mean. The curves for p.R2336H and p.G3990V variants are shifted to the left indicating an increase in sensitivity to caffeine. The p.D3986E curve is very similar to the wild type curve. (D-E) EC₅₀ for each experiment. A two-tailed student's *t*-test showed a statistically significant reduction in EC₅₀ as compared to wild type for p.R2336H and p.G3990V. No statistical significance was seen between wild type and p.D3986E. Box plots are shown as median, upper and lower quartiles and the maximum and minimum data points. (F) Graph showing the % maximal response produced at each dose of caffeine for each construct. Data is presented as mean plus or minus the standard error of the mean. A two-tailed student's *t*-test showed a statistically significant increase in % of maximal response produced at 1mM caffeine for p.R2336H and p.D3986E. At 2mM all variants had a significant increase in the % of the maximal response produced. No significant difference was seen at 20mM caffeine. **p*<0.5, ***p*<0.01, ****p*<0.001

4.3.1.3 EC₁₀ and EC₂₅ of cells transfected with the wild type and p.D3986E constructs

Due to cells transfected with p.D3986E constructs having an EC₅₀ similar to wild type transfected cells but still producing a statistically significantly higher response as a percentage of it's maximum at 1mM and 2mM caffeine, EC₁₀ and EC₂₅ measurements were taken from the same dose-response curve generated in Figure 4.5 B (the dose required to produce 10% and 25% of the maximum response respectively). p.D3986E transfected cells had a statistically significantly lower EC₁₀ (1.58mM) as compared to wild type (2.19mM; p=0.04). The EC₂₅ of p.D3986E transfected cells (2.15mM) was considerably lower than wild type transfected cells (2.68mM) but this did not reach statistical significance (p=0.07) (Figure 4.6). For each measurement n=6.

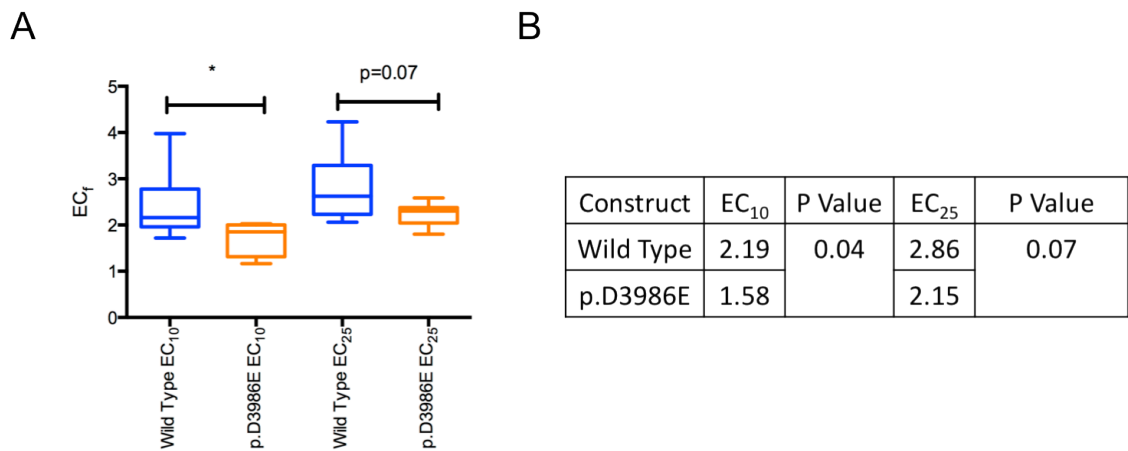


Figure 4.6 – EC₁₀ and EC₂₅ calculations for cells stably transfected with wild type or p.D3986E pcRYR1 constructs. (A) Box plots representing EC₁₀ and EC₂₅ measurements for both constructs. Cells transfected with p.D3986E constructs had a lower EC₁₀ and EC₂₅ compared to wild type. Box plots are shown as the median, the upper and lower quartiles and the maximum and minimum data points. (B) The EC₁₀ of p.D3986E transfected cells (1.58mM) was statistically significantly lower than that of wild type transfected cells (2.19mM; p=0.04) The EC₂₅ measurement for p.D3986E (2.15mM) was considerably lower than wild type (2.68mM) but this was not significant (p=0.07). * p<0.05

4.3.1.4 Area under the curve measurements of cells stably transfected with pcRYR1 constructs

AUC measurements were taken as an indirect measure of the quantity of calcium being released at each caffeine concentration. To account for the variable baseline

produced in each dose-response experiment, AUC measurements were specifically tailored for each individual experiment. No measurements were taken at 0.5mM caffeine as only a few experiments produced a response at that dose and wild type did not respond at all (Figure 4.7). At 1mM caffeine, wild type transfected HEK293 cells produced 24.81 ± 8.357 fluorescence units (FU) (measurements were taken as mean plus or minus the standard error of the mean). p.R2336H and p.G3990V transfected cells produced 587.1 ± 135.1 FU and 938.6 ± 180.7 FU respectively which was statistically significantly higher than the wild type response ($p=0.0089$ and $p=0.0039$ respectively). Cells transfected with p.D3986E constructs produced a small response that was not statistically significantly higher than wild type (237.6 ± 34.19 FU; $p=0.1712$). Similar responses were observed at 2mM caffeine with wild type producing a response of 124.1 ± 57.1 FU and p.R2336H and p.G3990V transfected cells producing statistically significant increases in calcium releases of 930.5 ± 122.5 FU ($p=0.0172$) and 1326 ± 334.4 FU ($p=0.0165$) respectively. Cells transfected with p.D3986E constructs again responded in a similar way to wild type with a total calcium release of 350.5 ± 47.34 FU which was not statistically significant. Furthermore, cells transfected with p.R2336H and p.G3990V constructs produced a statistically significantly higher response than cells transfected with the p.D3986E variant at both 1mM ($p=0.0145$ and $p=0.0054$) and 2mM caffeine ($p=0.0176$ and $p=0.0055$). At 5mM and 20mM caffeine no significant differences were observed between any of the constructs under investigation. For each comparison $n=6$.

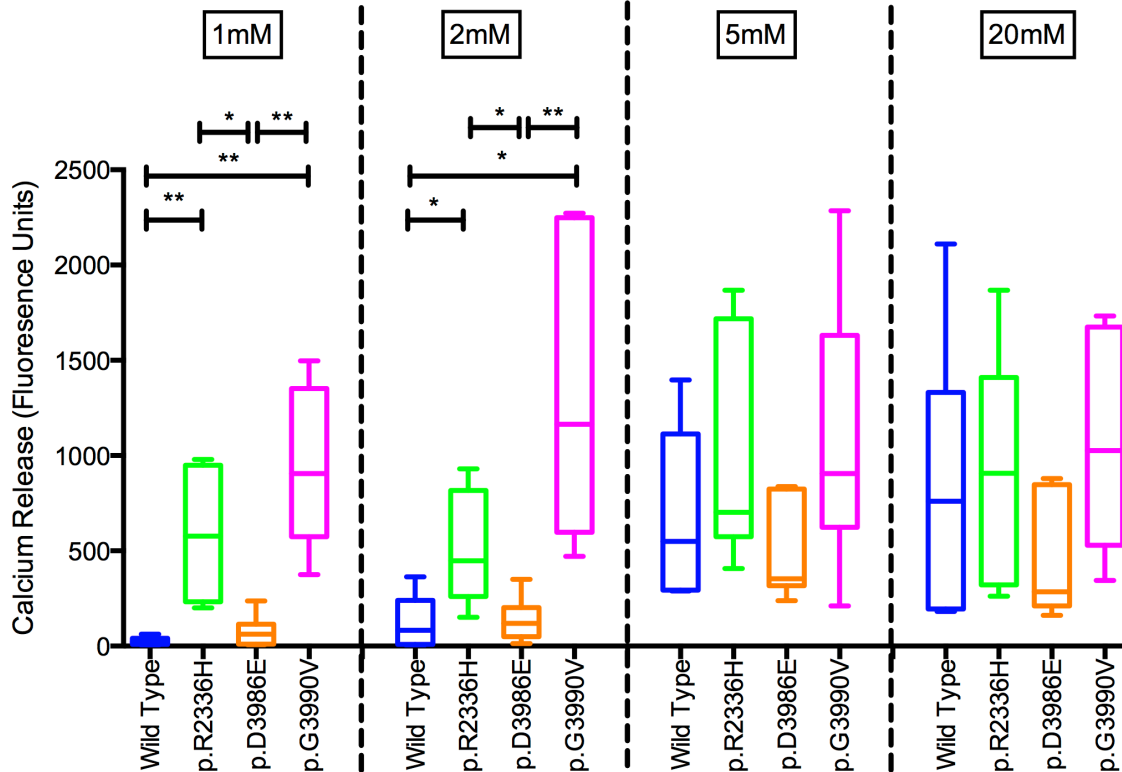


Figure 4.7 – Area under the curve measurements of HEK293 cells stably transfected with *pcRYR1* constructs. Box plots are shown as median, the upper and lower quartiles and the maximum and minimum data points. At 1mM and 2mM caffeine, p.R2336H and p.G3990V transfected cells produced a statistically significant increase in calcium release as compared to both wild type and p.D3986E transfected cells. At these low doses of caffeine, cells transfected with the p.D3986E variant did not produce a response that was significantly different from wild type. At 5mM and 20mM caffeine, no significant difference was observed between any of the constructs under investigation. * $p < 0.05$, ** $p < 0.01$.

4.3.2 HEK293 cells transiently transfected with *pcRYR1* constructs

4.3.2.1 Caffeine-induced calcium release from HEK293 cells transiently transfected with *pcRYR1* constructs

HEK293 cells were transiently transfected with wild type *pcRYR1* and the constructs with the variants p.E3104K, p.G3990V and p.V4849I introduced into them. Transfected cells were exposed to 0.5mM, 1mM, 2mM 4mM, 8mM and 20mM caffeine for p.E3104K and p.V4849I transfected cells and 0.2mM, 0.5mM, 1mM, 2mM, 5mM, 10mM and 20mM caffeine for p.G3990V transfected cells. Each experiment involving

an *RYR1* variant was done in parallel with wild type transfected cells at the same caffeine concentrations. Representative traces produced from each construct are presented in Figure 4.8. No cells responded to either 0.2mM or 0.5mM caffeine. All cells responded to 1mM caffeine but cells transfected with mutant *pcRYR1* constructs tended to produce larger calcium transients. For cells transfected with p.E3104K constructs this reached as high as 60% of the maximum response. At 2mM caffeine, the majority of cells transfected with mutant *pcRYR1* constructs reached a maximum response which was maintained through the remaining doses of caffeine. Wild type transfected cells first reached a maximum at 5mM caffeine with all cells producing 100% of the maximum response at 8mM or 10mM caffeine.

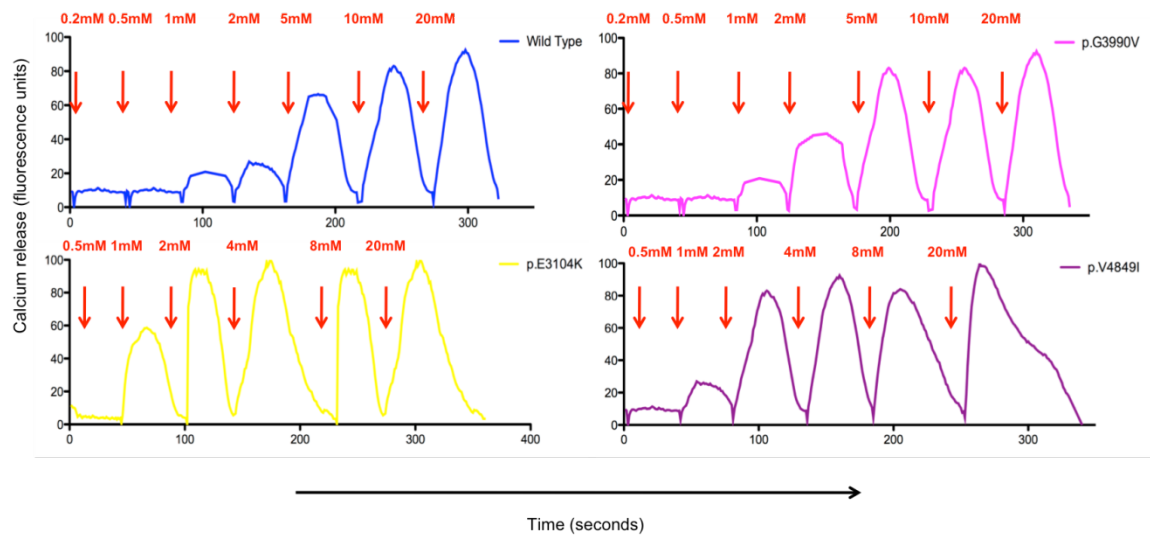


Figure 4.8 – Representative traces of caffeine-induced calcium release of cells transiently transfected with wild type and mutant *pcRYR1* cDNA constructs.

All three of the mutant *pcRYR1* constructs reached a maximum response before the equivalent wild type experiment. All cells responded at 1mM caffeine but this was always more exaggerated in the mutant transfected cells. In some cases, the mutant cells reached a maximum response at caffeine concentrations as low as 2mM whereas it took either 5mM or 8mM caffeine to produce the same response in wild type transfected cells.

Traces obtained from confocal microscopy were normalised where 100% was defined as the peak fluorescence in the entire video and 0% was the baseline fluorescence before the addition of any caffeine. The peak fluorescence obtained after the addition

of each caffeine concentration was taken and plotted on a log x-axis. Non-linear regression was applied to construct dose-response curves for each *RYR1* variant in relation to wild type (Figure 4.9A-C). For each of the *RYR1* variants, the caffeine dose-response curve was shifted to the left indicating an increase in sensitivity to caffeine. From these dose-response curves, the EC_{50} was calculated (Figure 4.9D-E). All three variants transiently transfected into HEK293 cells produced a statistically significant decrease in EC_{50} as compared to wild type. p.E3104K had an EC_{50} of 1.74mM (SEM = 0.287, 95% CI = 1.208-2.615; $p=0.0114$ compared to wild type (EC_{50} for wild type = 4.099mM caffeine, SEM = 0.776, 95% CI = 1.639-5.949) $n=7$), p.G3990V had an EC_{50} of 1.252mM (SEM = 0.1562, 95% CI = 0.758-1.625; $p=0.0111$; $n=6$) and p.V4849I had an EC_{50} of 1.711 (SEM = 0.1693, 95% CI = 1.295-2.213; $p=0.0274$; $n=7$). No statistically significant difference was observed between any of the variants.

The percentage of the maximal response at each caffeine concentration is plotted in Figure 4.9F. At 1mM caffeine, cells transfected with the p.G3990V construct produced a statistically significantly higher percentage of its maximal response as compared to wild type ($P=0.01$; $n=6$). Cells transfected with neither the p.E3104K or p.V4849I variants produced a statistically significant higher percentage of its maximal response at 1mM ($n=7$). At 2mM caffeine, cells transfected with both the p.G3990V and p.V4849I constructs produced a response that was statistically significantly higher as a percentage of its maximum as compared to wild type ($p=0.0001$, $n=6$ and $p=0.0074$, $n=7$ respectively). The p.E3104K variant produced a response that was not statistically significantly higher than wild type at 1mM caffeine but was significantly higher than wild type at 2mM caffeine ($p=0.0522$; $n=7$).

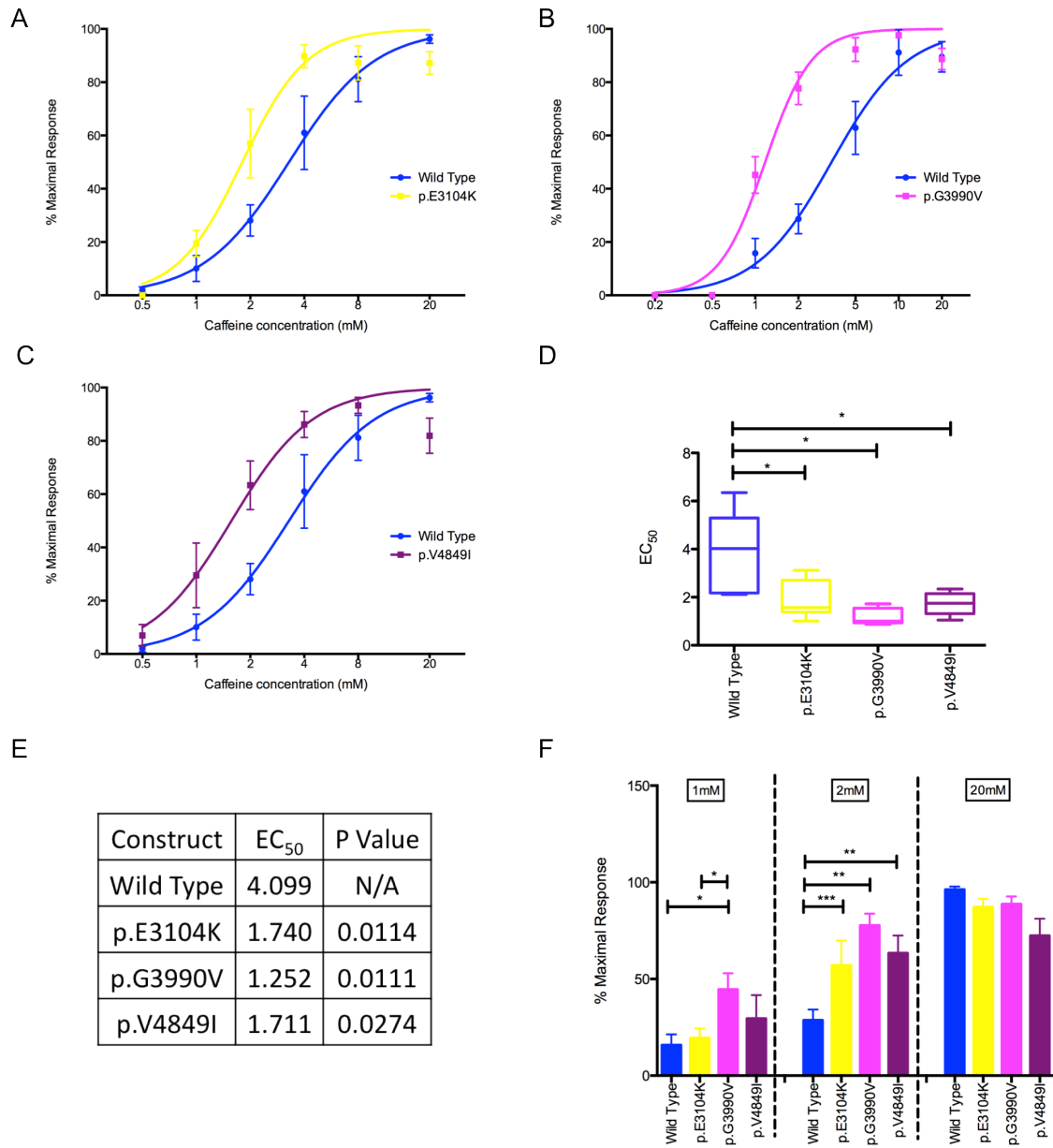


Figure 4.9 – Caffeine dose-response for HEK293 cells transiently transfected with wild type and mutant *pcRYR1* constructs.

(A-C) Dose-response curve for each variant transiently transfected into HEK293 cells plotted with wild type. The curve for all three variants was shifted to the left indicating an increased sensitivity to caffeine. Points are mean plus or minus the standard error of the mean. (D-E) EC₅₀ for each experiment. Box plots are presented as the median, the upper and lower quartiles and the maximum and minimum data points. A two-tailed student's *t*-test showed a statistically significant reduction in EC₅₀ for each variant transiently transfected into HEK293 cells as compared to wild type. (F) Graph showing the percentage of the maximal response produced at 1mM, 2mM and 20mM caffeine for each variant. The data are presented as the mean plus or minus the standard error of the mean. The p.G3990V variant produced a statistically significant higher % of its maximal response as compared to wild type at 1mM caffeine. Both the p.G3990V and p.V4849I produced a statistically significant higher percentage of its maximal response as compared to wild type at 2mM caffeine. No significant difference was seen at 20mM caffeine. **p*<0.05, ***p*<0.01, ****p*<0.001.

At 1mM caffeine, cells transiently transfected with p.G3990V constructs produced a higher response as a percentage of its maximum as compared to cells transfected with p.E3104K ($p=0.0201$; $n=6$). At 20mM caffeine, cells transiently transfected with all constructs had reached a maximum response and no significant difference was observed between any of the constructs.

4.3.2.2 Area under the curve measurements of cells transiently transfected with pcRYR1 constructs

AUC measurements were taken at each caffeine concentration that produced a response (Figure 4.10). The baseline for each experiment was independently assessed from each experiment. At 1mM caffeine wild type produced a calcium release of 80.95 ± 31.11 FU. Cells transfected with p.E3104K, p.G3990V and p.V4849I pcRYR1 constructs produced a statistically significant increase in calcium release as compared to wild type (202.8 ± 46.35 FU; $p=0.0374$, 486.6 ± 58.66 FU; $p=0.0001$ and 587.1 ± 63.09 FU; $p=0.0265$ respectively). The p.G3990V transfected cells also produced a statistically significantly higher calcium release than p.E3104K and p.V4849I transfected cells ($p=0.0027$ and $p=0.0115$ respectively). At 2mM caffeine all three RYR1 variants produced a higher amount of calcium release as compared to wild type transfected cells. Wild type cells released 285.8 ± 100.8 FU compared to 641.7 ± 107.2 for p.E3104K, 667.5 ± 76.46 FU for p.G3990V and 596.1 ± 101 FU for p.V4849I transfected cells. In each case this was a statistically significantly higher amount of calcium release. At 20mM caffeine, on average, cells transfected with mutant pcRYR1 constructs produced a higher amount of calcium release as compared to wild type, but this was not statistically significant. In each comparison $n=6$.

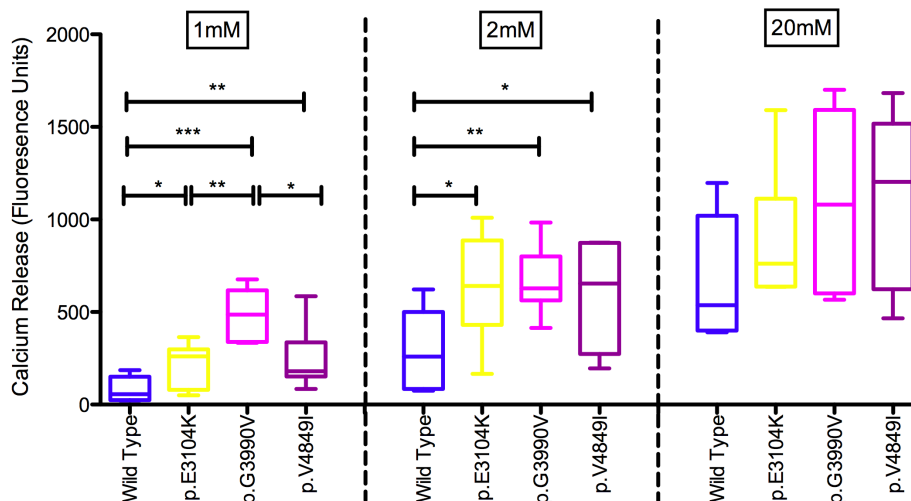


Figure 4.10 – Area under the curve measurements of *pcRYR1* constructs transiently transfected into HEK293 cells. Box plots are presented as the median, the upper and lower quartiles and the maximum and minimum data points. At 1mM and 2mM caffeine, statistically significant increases in calcium release were observed between all variants and wild type. At 1mM caffeine, the p.G3990V variant also produced a statistically significant increase in calcium release as compared to cells transfected with the p.E3104K and p.V4849I constructs. No statistically significant difference was observed between the responses at 20mM caffeine. * p,0.05, ** p<0.01, *** p<0.001

4.3.2.3 Expression analysis of HEK293 cells transfected with *pcRYR1* constructs

HEK293 cells were seeded onto 6-well plates and when at 80% confluence were transiently transfected with wild type and mutant *pcRYR1* constructs. 48 hours post-transfection, whole protein was extracted from the HEK293 cells, quantified and ran on a 4% and 8% SDS polyacrylamide gel. For stable HEK293 cell lines, cells were allowed to grow to confluence on a 10cm dish before extracting whole protein. Proteins on the gel were blotted onto a PVDF membrane and probed with anti-ryanodine receptor (34C) and anti-alpha tubulin antibodies before detection using a secondary HRP-conjugated antibody (Figure 4.11 and Figure 4.12). No RYR1 expression was detected in protein extracts isolated from untransfected HEK293 cells. Alpha tubulin was used as a loading control for all protein samples ran on the gels. Expression of RYR1 was normalised with alpha tubulin set as the relative maximum. The level of RYR1 expression detected in each of the transfected samples was not different from each other (n=3).

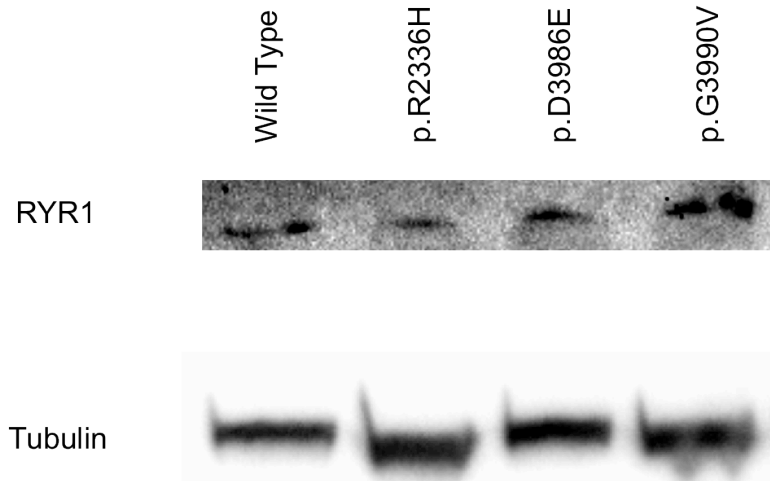


Figure 4.11 – Western blot analysis of HEK293 cells transiently transfected with wild type and mutant pcRYR1 constructs

Protein extracts were run on a SDS-PAGE gel followed by blotting onto a PVDF membrane and probed using anti-ryanodine receptor and anti-alpha tubulin primary antibodies. Proteins were detected using a secondary HRP-conjugated antibody. RYR1 was detected in all stably transfected samples with no apparent difference in expression between constructs.

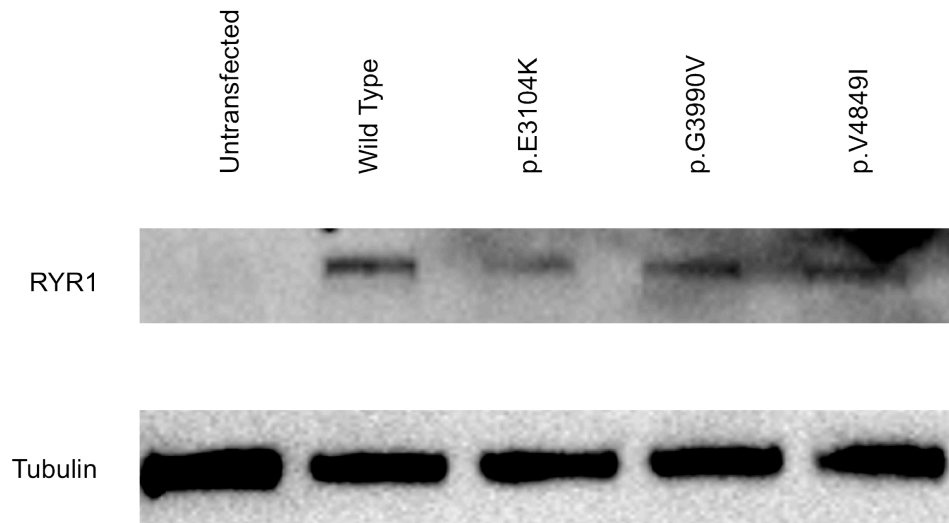


Figure 4.12 – Western blot analysis of HEK293 cells transiently transfected with wild type and mutant pcRYR1 constructs

Protein extracts were run on a SDS-PAGE gel followed by blotting onto a PVDF membrane and probed using anti-ryanodine receptor and anti-alpha tubulin primary antibodies. Proteins were detected using a secondary HRP-conjugated antibody. No RYR1 protein was detected in untransfected HEK293 cells. RYR1 was detected in all transfected samples with no apparent difference in expression between constructs.

4.3.3 Comparison of stable and transient transfection of HEK293 cells

For the wild type and p.G3990V *pcRYR1* constructs experiments were carried out on stable and transiently transfected cells. Results from both sets of experiments are plotted in parallel in Figure 4.13 and Figure 4.14. For each analysis performed $n=6$. The caffeine dose-response curves of cells stably and transiently transfected with both wild type and p.G3990V cells share very similar curves (Figure 4.13A). The EC_{50} calculated for each construct and each transfection method is listed in Figure 4.13C. Stably transfected cells with wild type *pcRYR1* produced an EC_{50} of 4.099mM compared with 3.209mM for transiently transfected cells. This was found not to be statistically significantly different ($p=0.2376$). The same was seen for cells stably and transiently transfected with p.G3990V *pcRYR1* constructs. The EC_{50} of 1.414mM (stable) and 1.252mM (transient) was not significantly different ($p=0.2276$). At 1mM caffeine, cells transiently transfected with p.G3990V constructs produced a statistically significant higher response as a percentage of its maximum as compared with cells stably transfected with p.G3990V constructs ($p=0.0032$). There was no significant difference in response for cells transfected either stably or transiently with wild type *pcRYR1* constructs at 1mM. At 2mM, cells transiently transfected with wild type *pcRYR1* produced a statistically significantly larger response than stably transfected cells ($p=0.0092$). Cells stably or transiently transfected with p.G3990V constructs had reached a response close to the maximum at 2mM caffeine and no significant difference was observed between the two transfection methods. At 20mM caffeine, all cells either stably or transiently transfected with either wild type or p.G3990V constructs had reached a maximum response and so no statistical differences were observed.

AUC measurements taken at corresponding caffeine concentrations were also comparable for cells stably and transiently transfected. No statistically significant differences were observed at any caffeine concentration between either transfection method (stable and transient transfection). There was a trend for cells stably transfected with p.G3990V to have a larger and more varied response at 1mM caffeine

(938.6 ± 180.7 FU) and 2mM caffeine (1326 ± 334.4 FU) compared to transient transfections (486.6 ± 58.66 FU and 667.5 ± 76.47 FU respectively). The opposite was observed with wild type transfected cells. Stably transfected cells produced a smaller calcium transient at both 1mM caffeine (24.81 ± 8.537 FU) and 2mM caffeine (124.1 ± 57.1 FU) than transiently transfected cells (80.95 ± 31.11 FU and 285.8 ± 100.8 FU respectively). Cells stably or transiently transfected with either wild type or p.G3990V constructs all produced a similar response at 20mM. Cells transiently transfected with wild type *pcRYR1* did have a slightly lower amount of calcium release at 20mM compared to stably transfected wild type cells as well as both stably and transiently transfected p.G3990V cells, but this was not statistically significant.

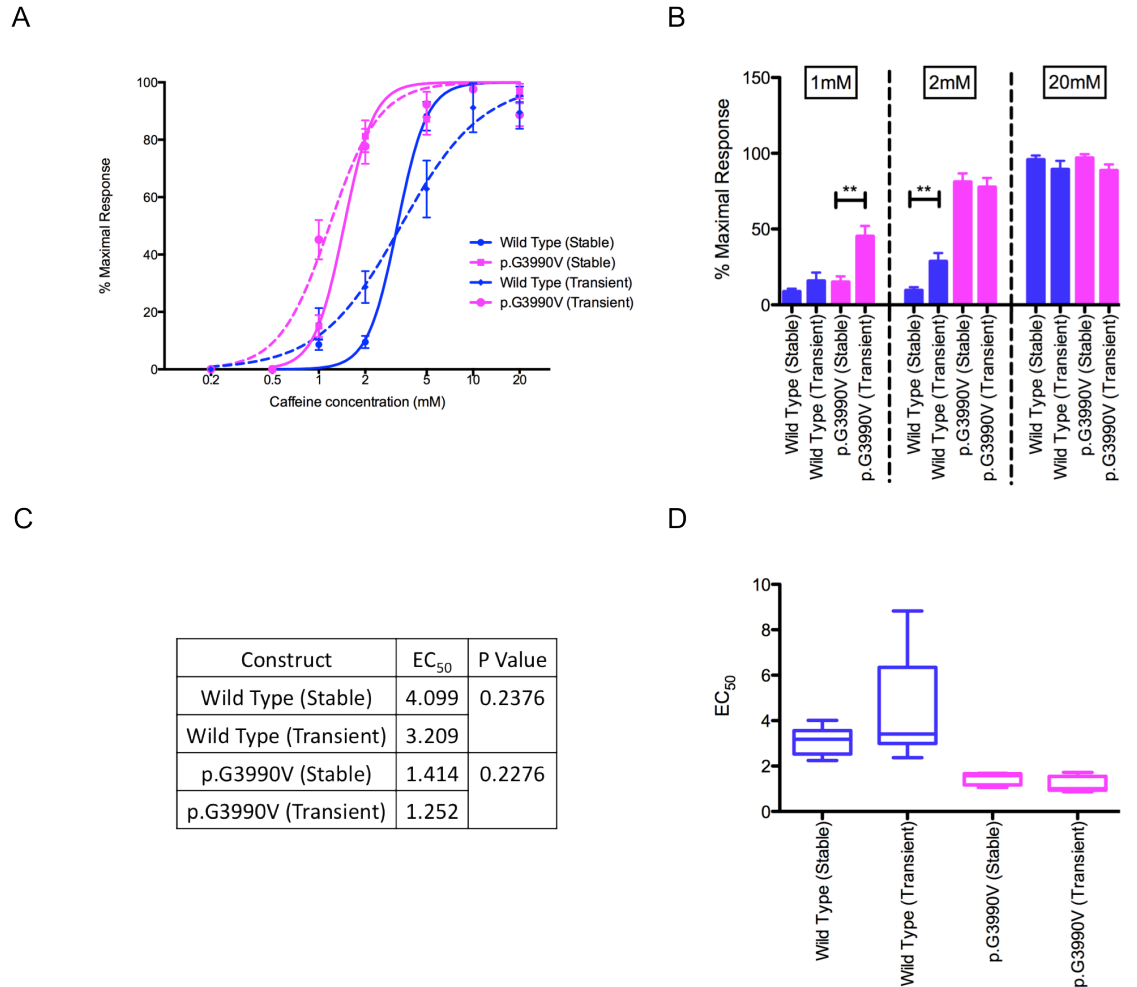


Figure 4.13 – Comparison of the EC₅₀ of HEK293 cells stably or transiently transfected with wild type and p.G3990V pcRYR1 constructs.

(A) Caffeine dose-response for HEK293 cells stably (solid lines) or transiently (dashed lines) transfected with wild type (blue) or p.G3990V (magenta) pcRYR1 constructs. All points are shown as the mean plus or minus the standard error of the mean. (B) Graph showing the % of the maximal response reached at 1mM, 2mM and 20mM for cells either stably or transiently transfected with wild type or p.G3990V RYR1 constructs. Data are presented as the mean plus or minus the standard error of the mean. At 1mM there was no significant difference between wild type constructs but there was for cells either stably or transiently transfected with p.G3990V constructs ($p=0.0032$). At 2mM there was a significant difference observed between the wild type constructs ($p=0.0092$) but no difference was seen between cells stably or transiently transfected with p.G3990V. No differences were observed at 20mM. (C-D) No statistically significant difference between the EC₅₀ of cells stably or transiently transfected with wild type pcRYR1 or p.G3990V pcRYR1. Box plots are the median, the upper and lower quartiles and the maximum and minimum data points. ** $p<0.01$.

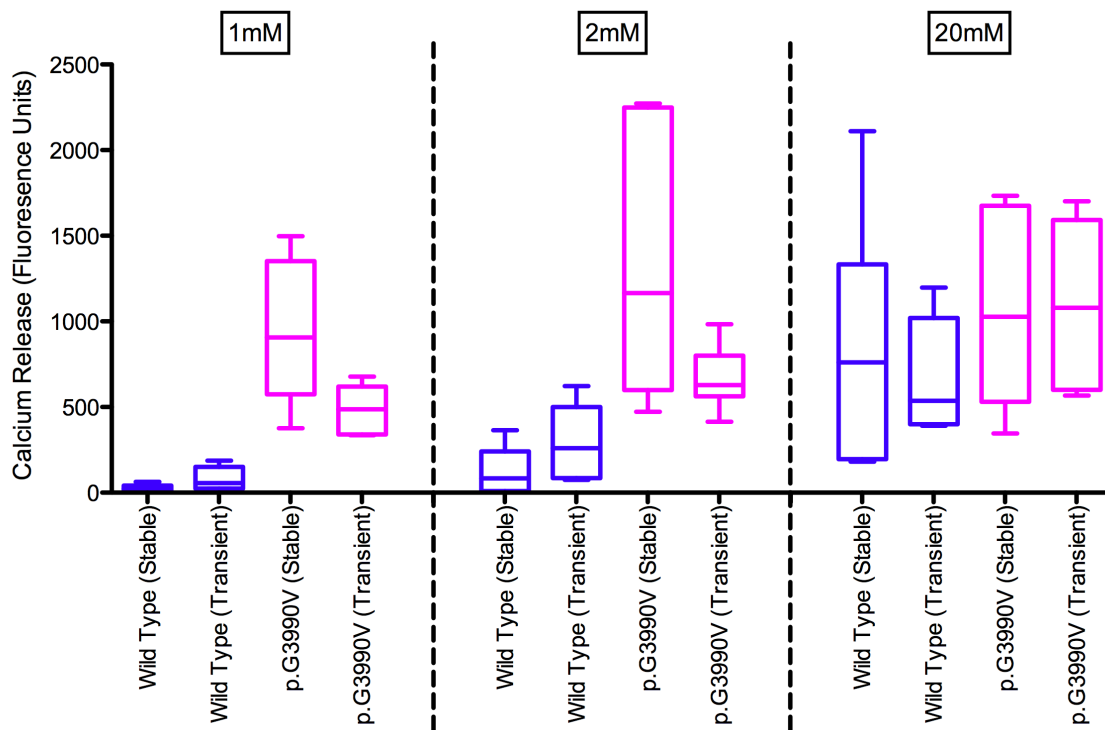


Figure 4.14 – Comparison of the area under the curve responses for cells either transiently or stably transfected with wild type or p.G3990V pcRYR1 cDNA constructs.

Box plots are the median, the upper and lower quartiles and the maximum and minimum data points. No statistically significant difference was observed between cells stably or transiently transfected with either wild type or p.G3990V constructs at the corresponding caffeine concentrations.

4.4 Discussion

The data presented above is supportive of the p.R2336H, p.E3104K, p.G3990V and p.V4948I variants to be added to the genetic diagnostic panel for MH. Cells either stably or transiently transfected with each of these variants produced a statistically significantly reduced EC_{50} as compared to wild type transfected cells as well as a trend to have a higher amount of calcium release and a higher percentage of their maximum response was elicited at lower doses of caffeine. In addition to this, data is presented that indicates that the p.D3986E variant is not causative of MH in the four families it has been identified in.

4.4.1 p.R2336H

The p.R2336H mutation produced the most severe response out of all the variants tested in this chapter. The EC_{50} was reduced by the most with a caffeine concentration of less than 1mM required to produce half of the maximal response (0.91mM). Furthermore, at 1mM caffeine the amount of calcium released was massively more than any other variant under investigation ($p < 0.001$). A maximum response for cells transfected with this variant was reached very early. At 1mM caffeine, 60.7% of the maximum response had been achieved and this increased to 87.68% at 2mM caffeine.

The data from the literature is a little less supportive of the p.R2336H variant being added to the genetic diagnostic panel for MH. Lymphoblastoid cells isolated from patients carrying this variant only produced an MH phenotype when exposed to 4-CmC. The response obtained from these cells when they were exposed to caffeine was similar to that of wild type familial control samples in all 7 families investigated (Levano et al., 2009). The data obtained in this chapter, however, gives clear evidence of the variant's role in the MH phenotype. As previously discussed, the use of patient samples for functional experiments may not be the best method due to unforeseen genetic background issues. In Levano et al. (2009), this problem may be compounded by the use of cells in which RYR1 does not carry out its primary function meaning the results obtained in that study are a reflection of the experimental model used, rather than the pathogenicity of the p.R2336H variant. The variant has been identified in 7 UK families and a further 7 worldwide. It cosegregates with disease and is absent from control samples. Combined with the functional data obtained in this chapter, the p.R2336H variant can be added to the genetic diagnostic panel for MH.

4.4.2 p.E3104K

The p.E3104K variant produced a response that is consistent with being causative of MH. The EC_{50} was significantly reduced to 1.74mM (compared to 4.099mM for wild type transfected cells). At both 1mM and 2mM caffeine a statistically significant

increase in calcium release was observed as compared to wild type. At 1mM caffeine, however, this response was not significantly different to wild type in terms of the percentage of the maximum. At 2mM caffeine, a significant difference was observed in terms of percentage of the maximum. The variant has been identified in 4 families, all of which are in the UK. It cosegregates with disease and is absent from control samples. Combined with the functional data presented above, the p.E3104K variant should be added to the genetic diagnostic panel for MH.

4.4.3 p.G3990V

The p.G3990V variant was both stably and transiently transfected into HEK293 cells. Both sets of experiments showed that cells transfected with p.G3990V had a significantly reduced EC_{50} (stable = 1.44mM and transient = 1.252mM) as compared to wild type transfected cells (stable = 3.209mM and transient = 4.099mM). These values were not significantly different from each other indicating that the data obtained is consistent regardless of the method of transfection. Both sets of experiments showed a significantly increased calcium release at both 1mM and 2mM caffeine. However, only in the transient experiments was this determined to be significantly higher as a percentage of the overall maximum response for 1mM caffeine. The reason for this is unclear but may be due to the nature of the transient experiments. For stable transfections an individual cell is selected and expanded for future experiments. Transient transfections will inherently have more variability in them due to differential uptake of the plasmid between experiments. It is feasible that this variability has caused the differences seen, however, another explanation is that this measurement is not representative of the overall causality of the variant under investigation. The EC_{50} of cells either stably or transiently transfected with this variant was unchanged in terms of being significantly reduced compared to wild type, regardless of the result of that measurement. The p.G3990V variant has been identified in 10 families worldwide, all of which are in the UK. It cosegregates with disease and is not found in

control chromosomes. This knowledge combined with the functional data presented above strongly suggests that the p.G3990V variant should be added to the genetic diagnostic panel for MH.

4.4.4 p.D3986E

The p.D3986E variant was found to have an EC_{50} not significantly different to wild type and a comparable calcium release when exposed to all doses of caffeine. Based on this data it could be concluded that the p.D3986E variant may not be causative of MH in the 4 UK families it has been identified in. At 1mM and 2mM caffeine, cells transfected with p.D3986E did produce a response that was significantly higher as a percentage of its maximum as compared to wild type without altering the overall EC_{50} of the cells, however, as discussed in terms of the p.G3990V variant, this measurement may not be representative of the functional consequences of the variant. Despite this, because of this seemingly exaggerated response at 1mM and 2mM caffeine, the EC_{10} and EC_{25} of the cells containing wild type and the p.D3986E variant were measured from the same dose-response curve as the EC_{50} . Cells transfected with p.D3986E were found to have a statistically significantly decreased EC_{10} as compared to wild type but the EC_{25} was not significantly lowered despite being substantially lower than the wild type cells ($p=0.07$).

Although there is evidence to suggest that MH can be triggered when a certain threshold has been achieved (Jiang et al., 2008) it seems unlikely that an altered EC_{10} would be enough to trigger an MH reaction in these individuals. Moreover, individuals carrying the p.D3986E variant have been found to have a stronger IVCT reaction than most other patients carrying a number of causative or uncharacterised *RYR1* mutations, which could not be explained through a reduction in the EC_{10} of the p.D3986E variant (Carpenter et al., 2009c). A total of 22 *RYR1* variants were screened for in the UK MH population followed by correlating genotyping data with quantitative data obtained through the IVCT tests. The p.D3986E variant produced a caffeine

contracture that was significantly higher than most other *RYR1* variants investigated. Furthermore, individuals carrying the p.D3986E had a higher mean static halothane contracture than all other variants under investigation in this chapter.

Despite individuals carrying the p.D3986E *RYR1* variant appearing to have a more severe IVCT reaction than most other variants the data presented in this chapter indicates that it may be a polymorphism that is segregating with MH phenotype. The families in which the p.D3986E variant has been identified have had the entire coding sequence of *RYR1* and *CACNA1S* sequenced which rules out the presence of another variant within the coding regions of these genes, which has been seen before in a number of families (Monnier et al., 2002). An additional, as yet unidentified variant in another gene that is in linkage disequilibrium with the p.D3986E variant cannot be ruled out. Recent evidence has suggested that individuals who share an *RYR1* variant also possess a common 'high-risk' haplotype that is associated with MH (Carpenter et al., 2009a). Based on this, the families in which the p.D3986E variant has been identified may be good starting points to look for additional variants in other genes as causative agents or potential modifiers to the MH phenotype.

4.4.5 p.V4849I

The p.V4948I variant also had an EC_{50} that was significantly reduced (1.711mM) as compared to wild type (4.099mM). At 1mM caffeine, no significant increase in calcium release was observed when compared with wild type. At 2mM caffeine, however, a significant increase was observed. At 20mM caffeine, there appeared to be a reduced response as a percentage of the maximum for cells transfected with the p.V4849I variant as compared to wild type controls. The p.V4849I variant has been found in both MH and CCD patients (Jungbluth et al., 2002, Monnier et al., 2005, Levano et al., 2009, Ducreux et al., 2006) and although a clear conclusion cannot be drawn directly from this result, the reduction in response may hint at a smaller calcium store as a result of the CCD phenotype. It has been previously reported that CCD mutations can

have a decreased EC_{50} but still present in the patients as a myopathy (Tong et al., 1997, Yang et al., 2003). The p.V4849I variant appears to be a classic MH mutation in terms of the EC_{50} result and there are hints that the same variant is responsible for the CCD phenotype seen in the patients. The p.V4849I variant has been identified in 12 families worldwide, 8 of which are in the UK. The mutation cosegregates with disease and is absent from control chromosomes. This information coupled with the functional data obtained in this chapter indicates that the p.V4849I variant can be added to the genetic diagnostic panel for MH. However, further investigations should be carried out to truly ascertain the role this variant plays in the CCD phenotype. The easiest way in which this could be ascertained is through measuring the resting intracellular calcium level of cells carrying this variant on a defined genetic background to see if the result is consistent with other CCD variants.

4.4.6 Stable vs. Transient transfection

In this chapter, stable HEK293 cell lines were generated carrying wild type pcR $YR1$ and the p.R2336H, p.D3986E and p.G3990V variants. Additionally, the p.E3104K and p.V4849I variants were transiently transfected into HEK293 cells. The p.G3990V was also transiently transfected into HEK293 cells in preliminary experiments designed to generate a firm protocol for calcium imaging and data analysis before the stable clones had been generated. No obvious differences were observed between cells either stably or transiently transfected with wild type and p.G3990V pcR $YR1$ constructs indicating that both methods are equally viable and comparable for these experiments. There were slight discrepancies in the percentage of the maximum response generated at 1mM and 2mM caffeine for p.G3990V and wild type constructs respectively but this had no effect on the EC_{50} or amount of calcium released at these doses of caffeine, further supporting the notion that these measurements are misleading. There was a trend for cells transfected transiently with p.G3990V to have a less varied calcium release when AUC measurements were taken. It is not directly

clear as to why this might be. We would have expected that it would have been the stable clones that produced a more consistent result as they were generated from a single HEK293 cell containing p.G3990V. This may be just due to differential loading of the fluorescent calcium indicator Fluo-4 AM. Fluo-4 is a non-ratiometric calcium indicator meaning that the concentration of calcium released cannot be directly quantified. Differences in loading of the indicator can lead to differences in the observed calcium concentration present in the cells. Instead, the calculations are made relative to a maximum meaning the EC_{50} can be calculated but the concentration of calcium achieved at this dose cannot. Ratiometric calcium indicators such as fura-2 utilise two different excitation and emission wavelengths to create a ratio that can be converted into a concentration of calcium present. However, in this study, it was sufficient to see a trend of an increased calcium release at low doses of caffeine from the mutant *RYR1* variants.

All *RYR1* variants under investigation in this chapter, with the exception of p.D3986E that was discussed earlier, produced a statistically significantly increased calcium release at 1mM and 2mM caffeine. Furthermore, at 20mM caffeine when all variants had reached a maximum response as deduced from the dose-response curves, no significant differences were observed between any construct under investigation. This suggests that the size of the calcium store is not greatly affected by the introduction of either wild type or mutant *RYR1* channels. This was a consistent finding that indicates that any differences in Fluo-4 loading are not significantly altering the data obtained.

4.4.7 G418 selection of stable HEK293 cell lines expressing pcRYR1 constructs

An antibiotic kill curve was produced as a means to deduce the correct concentration of G418 to use in the selective growth medium for HEK293 cells stably transfected with pcRYR1 constructs. After the 10-day selection experiment on untransfected HEK293 cells 98% of cells were dead. Based on this, 1mg/ml G418 was chosen for the initial 10 day selection after transfection. In the kill curve experiment, 88% of untransfected

HEK293 cells had been killed after exposure to 1mg/ml G418 for 10 days. In the preliminary selection of stable clones, this concentration allowed for a high percentage of untransfected HEK293 cells to be killed without going as far as 98% meaning that those that were transfected had a chance to produce the resistance gene before being killed rapidly by the high antibiotic concentration. After the initial 10 day selection, the concentration of G418 in the growth medium was reduced to 0.8mg/ml for a further 10 days to allow for a high level of selection to be maintained but also gave the transfected cells a chance to start to thrive.

4.4.8 Measurement of HEK293 cell background

HEK293 cells are a non-native cell type for *RYR1* to be transfected into. Although any endogenous level of *RYR1* is below the detection capabilities of western blotting, there may be other caffeine-sensitive calcium channels present such as the inositol triphosphate sensitive calcium channels. Because of this, a background rate of calcium release was determined before the calcium release assays were performed. Tong et al. (1999b) have previously reported that 6 out of 200 HEK293 cells responded at 20mM caffeine resulting in an estimated background rate of 3%. No other paper reports any background effect seen from HEK293 cells and in fact, many report that there was either no response seen at all upon exposure to high concentrations of caffeine or make no reference to any control experiments carried out (Lynch et al., 1999, Du et al., 2001, Monnier et al., 2005, Migita et al., 2009). A calcium release assay was carried out on untransfected cells using the same caffeine series that would be used for the experiments involving *RYR1*. Calcium release was observed at high doses of caffeine (8mM-20mM). Ten independent experiments were analysed using ImageJ to count the total number of cells in the field of vision as well as those that responded to caffeine. An average background response of 4.02% was deduced from the 10 experiments, which was close to the background rate observed in Tong et al. (1999b). Based on this, when analysing data obtained from the transfection of HEK293 cells with *RYR1* constructs, cells that only responded to 8mM-20mM caffeine were excluded

from the analysis and assumed to be untransfected. Even though stable cell lines should consist of entirely transfected cells this methodology was also applied to the stable HEK293 cell lines as a precautionary measure to remove the possibility of any untransfected cells entering the analysis.

4.4.9 The calcium transient videos

The calcium release experiments were performed using an 8 channel injector system. Throughout the course of the experiments being carried out, one or more of the channels became unavailable for use meaning the caffeine series had to be altered accordingly. When all 8 channels were available caffeine concentrations of 0.2mM, 0.5mM, 1mM, 2mM, 5mM, 10mM and 20mM were used. The series had to be altered when two channels were out of service. Based on the data already obtained it was decided that 0.2mM caffeine was unnecessary as no cells responded at caffeine concentrations so low and by 5mM, cells transfected with mutant *RYR1* had already reached a maximum meaning that 10mM could also be removed. This was altered further when one of the channels became available again resulting in a final caffeine series of 0.5mM, 1mM, 2mM, 4mM, 8mM and 20mM. In spite of the change in caffeine series no significant differences were observed between the wild type transfected cells in each caffeine series giving us confidence that all the mutant results are accurate.

4.5 Future work

Future work will focus on expanding the number of *RYR1* variants put through this experimental system. The use of the mutations under investigation in this chapter has allowed us to develop a protocol that is highly replicable and relatively straightforward. Coupled with the cloning work carried out in the previous chapter, a production line of *RYR1* variants transfected into HEK293 cells and put through these

experiments is a real possibility allowing us to heavily expand the current number of *RYR1* variants approved for genetic diagnosis.

In the current study, only one *RYR1* channel agonist was used to test the *RYR1* variants. Future work will expand this current protocol to include known channel agonists such as halothane, 4-CmC and ryanodine. All of these have been previously used to investigate the functional consequences of *RYR1* variants (Tong et al., 1997, Lynch et al., 1999, Yang et al., 2003, Migita et al., 2009, Sato et al., 2010, Sato et al., 2013). Halothane is by far the most clinically relevant channel agonist for *RYR1* in terms of the MH phenotype. However, the volatility of halothane has made it difficult to use in such experiments. The exact concentration of halothane reaching the cells is difficult to ascertain accurately. Despite this, retesting the variants under investigation in this study with halothane is of interest, especially with reference to the p.D3986E variant that responded in a similar way to wild type *RYR1*. The likelihood of the p.D3986E responding in a way similar to other causative variants when exposed to halothane remains unclear, especially when considering the fact that IVCT data obtained from patients carrying the same variant responded in a very severe manner when exposed to caffeine.

In this chapter, crude data were presented as a comparison between the results obtained from either stably or transiently transfecting the wild type or p.G3990V variants into HEK293 cells. No discernable difference was seen between the two methods leading to the conclusion that whether or not the experiments are carried out on stably or transiently transfected cells is not important. Although this conclusion was drawn from testing only two constructs it seems highly likely that it is accurate. Based on the simplicity and speed of transiently transfecting HEK293 cells with the constructs future experiments are likely to rely heavily on this method.

By far the most important direction of future work based on this chapter would be the introduction of these variants into a more native cell environment. Our experience with utilising a viral method of transducing a muscle-like cell line that is a functional

knock-out for *RYR1* will be discussed in the next chapter. Although it is widely accepted that ideally these experiments would be carried out in a cellular environment more fitting for the functional purpose of *RYR1*, it remains unclear as to whether there would be a functional difference based on the cellular environment of the channel. With the exception of the p.D3986E variant, an exaggerated response from mutant *RYR1* channels is consistently elicited from experiments carried out in non-native cell types such as HEK293 cells used in this study and others. However, we still feel that confirming that there is no difference between the responses seen in different cell types is important for the future of functional studies of MH variants. It is conceivable that for the p.D3986E variant to display a pathogenic phenotype, it requires the interaction with any one of a number of accessory proteins that are not expressed in HEK293 cells.

4.6 Conclusions

Based on the data obtained in this chapter, it seems clear that the p.R2336H, p.E3104K, p.G3990V and p.V4849I *RYR1* variants are the causative mutation of MH in the families they have been identified in. They all produced a response that has now long been recognised as the hallmark of a causative MH mutation, that is, a reduced EC_{50} when exposed to channel agonists, in this case caffeine. Furthermore, a clear trend in increased calcium release was observed at 1mM and 2mM caffeine which was closer to its maximum response than wild type transfected cells.

The role of the p.D3986E variant remains unclear. Based on the data obtained in this chapter, there is an argument for excluding this variant as the causative factor of MH in the four families it has been identified in. However, the fact that it has only been identified in MH patients, to cosegregate perfectly with disease and that patients carrying this variant have a stronger caffeine contracture during the IVCT test cannot be ignored. These four families that possess this variant may be good starting points for further investigations into new causative variants associated with MH. Recently,

our group has begun sequencing the exome of patients for which no causative variant has been identified. These families would be ideal candidates for such experiments on the basis of their shared MH phenotype and p.D3986E genotype.

Chapter Five - Functional analysis of genetic variants in the *RYR1* gene associated with malignant hyperthermia in 1B5 cells.

5.1 Introduction

5.1.1 EMHG Guidelines and the use of non-native cells for functional analysis

As has been discussed in previous chapters, the majority of the functional analysis of genetic variants in the *RYR1* gene has been carried out using cells in which RYR1 and other EC coupling accessory proteins are not expressed. Some researchers have differentiated primary myoblasts isolated from patients carrying previously identified RYR1 variants in functional studies. Such experiments are therefore performed in the correct cellular environment for RYR1 with all accessory proteins required for EC coupling also being present. However, cells isolated from patients do not possess a defined genetic background meaning that the data obtained is insufficient for inclusion onto the genetic diagnostic panel for MH unless experiments are carried out on more than one family that possess the variant in question (Wehner et al., 2004, Kaufmann et al., 2012). According to Robinson et al. (2006), 106 families possess a unique *RYR1* variant, ruling out the possibility for genetic testing for these families if the primary cell method were to be used alone. Currently, using either a non-native cellular environment of defined genetic background or myotubes isolated from patients are both acceptable according to the EMHG guidelines, however the use of a muscle cell line of defined genetic background would provide the most scientifically accurate method of carrying out functional analysis.

5.1.2 The development of a dyspedic myoblast cell line for use in functional studies of *RYR1* variants

Attempts have been made to use a mouse myoblast cell line as a means of functionally assessing genetic variants in *RYR1* (Otsu et al., 1994). C2C12 cells, a mouse muscle cell line, were transfected using conventional lipid based methods and a difference in the functional consequences of the genetic variants compared to wild type was observed

in terms of sensitivity to channel agonists. However, no difference in expression of *RYR1* was observed in protein extracts when compared with untransfected controls making the estimation of the transfection efficiency of the experiment impossible, as C2C12 cells possess endogenous *RYR1*, and the resulting analysis difficult.

A muscle-like cell line has been developed for use in functional studies of *RYR1* variants (Moore et al., 1998). Mouse embryonic stem cells null for both *RYR1* alleles were injected subcutaneously into an immunodeficient mouse causing teratocarcinoma formation. Fibroblast cells isolated from the tumour were transduced down the muscle differentiation pathway with myoD resulting in a cell line, termed 1B5 cells, that was deficient in all *RYR* isoforms, expressed all the key skeletal muscle triadic proteins and had the ability to form multinucleated myotubes.

5.1.2.1 Development of a viral method of transducing dyspedic myotubes with *RYR1* variants for functional studies

Following on from the development of the 1B5 cell line, a viral method of infecting differentiating myotubes with wild type and mutant *RYR1* constructs was developed for functional experiments (Cunningham and Davison, 1993, Fraefel et al., 1996, Wang et al., 2000, Yang et al., 2003). The entire HSV-1 genome was inserted into a set of five cosmids for functional studies of HSV-1 genes before Fraefel et al. (1996) modified the cosmid set by removing the packaging and cleavage signals from two of the cosmids and placing them into a modified pUC vector (pHSVPrPUC). Rabbit *RyR1* was inserted into the pHSVPrPUC vector creating a highly efficient gene delivery system for 1B5 cells. HSV-1 infection efficiencies of up to 90% were seen compared to almost 0% for standard lipofectamine transfection methods (Wang et al., 2000, Yang et al., 2003). 1B5 cells expressing rabbit *RYR1* variants displayed an increased sensitivity to traditional channel agonists such as caffeine, halothane and 4-CmC as well as KCl. The increase in sensitivity to KCl indicates that MH variants also result in a defect in EC

coupling. Since the development and validation of this system, no further genetic variants in *RYR1* have been functionally characterised utilising this method.

5.1.3 Potential differences between HEK293 cells and 1B5 cells

HEK293 cells have been the primary functional characterisation system employed by researchers examining the effects of *RYR1* variants *in vitro*. However, there is a huge difference in both the structure and function of HEK293 cells and skeletal muscle myotubes. Firstly, no report to date has been able to detect any RYR isoform in HEK293 cells. Whilst it is this characteristic, along with ease of transfection that made HEK293 cells an attractive choice for functional experiments, other key skeletal muscle triadic proteins are also not expressed (Nakai et al., 1996). Perhaps most importantly, $Ca_v1.1$ is not expressed in HEK293 cells. *RYR1* interacts directly with $Ca_v1.1$ (encoded by *CACNA1S*) to initiate calcium release in skeletal muscle after excitation contraction coupling. Additionally, skeletal muscle also possesses a highly organised and specialised structure, which allows efficient calcium release and reuptake. Such organisation is not present in non-native (i.e. non-muscle) cell types such as HEK293 cells.

Although no obvious differences have been observed between the dose-response generated by *RYR1* variants expressed in 1B5 cells and HEK293 cells in response to caffeine, halothane and 4-CmC (Yang et al., 2006), evidence is mounting that the resting calcium levels may differ when the same *RYR1* variants are expressed in the two cell lines. Tong et al. (1999b) expressed 15 *RYR1* mutations previously associated with MH or CCD in HEK293 cells and found that only those mutations associated with the myopathy produced a resting calcium level that was elevated compared to wild type controls as well as all MH mutations under investigation. This directly contradicts work carried out on MHS swine (Lopez et al., 1987a), human muscle preparations (Lopez et al., 1987b, Lopez et al., 2005) and dyspedic myotubes expressing *RYR1* variants (Yang et al., 2007). In Yang et al. (2007), all MH variants expressed in 1B5 cells

produced a resting calcium level significantly higher than that of wild type controls, two of which had been previously expressed in HEK293 cells and resulted in a level similar to wild type (Tong et al., 1999b). One of the variants, p.R615C, is the MH mutation in swine that also produced a significantly higher resting calcium level in the two studies by Lopez and colleagues (Lopez et al., 2005, Lopez et al., 1987b).

The results obtained in these studies hint at a fundamental difference between the biology of HEK293 cells and 1B5 cells when expressing *RYR1* variants. This is not surprising given that myotubes are highly specialised to express *RYR1* and release and sequester calcium. Myotubes have a specialised SR designed for calcium storage, release and reuptake and specific cellular structure for the use of calcium. Conversely, HEK293 cells are largely nuclear and small in comparison to fused, multinucleated myotubes and possess a non-specialised endoplasmic reticulum. In spite of these differences, another factor that may contribute to the difference in results obtained by the above studies is the method of measuring resting calcium. The studies on muscle fibres and cells utilise calcium-sensitive microelectrodes specifically designed and calibrated for the measurement of resting intracellular calcium levels. In comparison, Tong et al. (1999b) utilised the ratiometric calcium dye fura-2 to estimate the resting calcium concentration. Whilst fura-2 has the ability to measure intracellular calcium, the previously mentioned differences in cell structure may make accurately taking these measurements problematic. This is hinted at in a study by Wehner et al. (2004) in which fura-2 was used to measure the resting calcium level of myotubes isolated from patients carrying *RYR1* variants. Two out of the three variants tested had a significantly higher resting calcium level as compared to MHN controls. Whilst the possibility of different *RYR1* mutations producing different levels of resting calcium or the effect of unknown genetic contributors from the patient samples can not be ruled out, the results highlight the possible disadvantages of using fura-2 as a measure of resting calcium.

5.1.4 Variants in pHSVRYR1

Two *RYR1* variants and the wild type construct were shuttled into the pHSVPrPUC vector as described in chapter 3. The two variants successfully transferred were the p.R2336H and the p.D3986E constructs. Whilst the intention of this project was to shuttle all variants under investigation in this thesis into pHSVPrPUC, the only available method of transfer was cloning the entire 15kb *RYR1* coding sequence in a non-directional manner, which limited the success of transfer. In spite of this, these two variants are ideal candidates for further study in 1B5 cells. The p.R2336H variant produced the strongest result in HEK293 cells and can act as a positive control to observe increased sensitivity in the myotubes system compared to wild type. The p.D3986E variant has been identified in 4 UK families and has been associated with a stronger caffeine contracture than other MH variants. However, in the HEK293 system utilised in chapter 4, the p.D3986E variant produced a response that was indistinguishable from wild type transfected cells. Of particular interest in this chapter is the results obtained from 1B5 cells infected with p.D3986E HSV-1 virions, allowing a direct comparison with the results obtained in chapter 4 and forming the basis of an evaluation of the use of HEK293 cells as a system for the functional analysis of genetic variants in *RYR1*.

5.2 Aims of the chapter

The primary aim of this chapter was to express wild type and mutant *RYR1* constructs in the dyspedic myoblast cell line and examine the functional consequences of these variants in the native muscle environment. The data obtained from this chapter would form the basis of an assessment on the use of HEK293 cells as a viable system for the functional analysis of genetic variants in the *RYR1* gene associated with MH.

Additionally, expressing genetic variants of *RYR1* in 1B5 cells would allow us to measure the intracellular resting calcium concentration using calcium-sensitive microelectrodes.

5.3 Results

5.3.1 Titration of HSV-1 virions

5.3.1.1 Titration using immunofluorescence

Titration experiments were carried out to determine the concentration of HSV-1 virions harvested after viral packaging. Monkey Vero (2-2) cells were infected overnight with 1 μ l, 5 μ l and 20 μ l of harvested HSV-1 virions before immunostaining specific for RYR1 (Figure 5.1). A small amount of background staining was observed in uninfected 2-2 cells and a similar pattern was observed in wild type and p.R2336H infected cells. The amount of Cy3 (RYR1) staining observed for wild type and p.R2336H-infected cells was indistinguishable from the background staining seen in uninfected controls. Additionally, the p.D3986E infected cells showed no visible Cy3 staining indicating the absence of RYR1 from the cell samples.

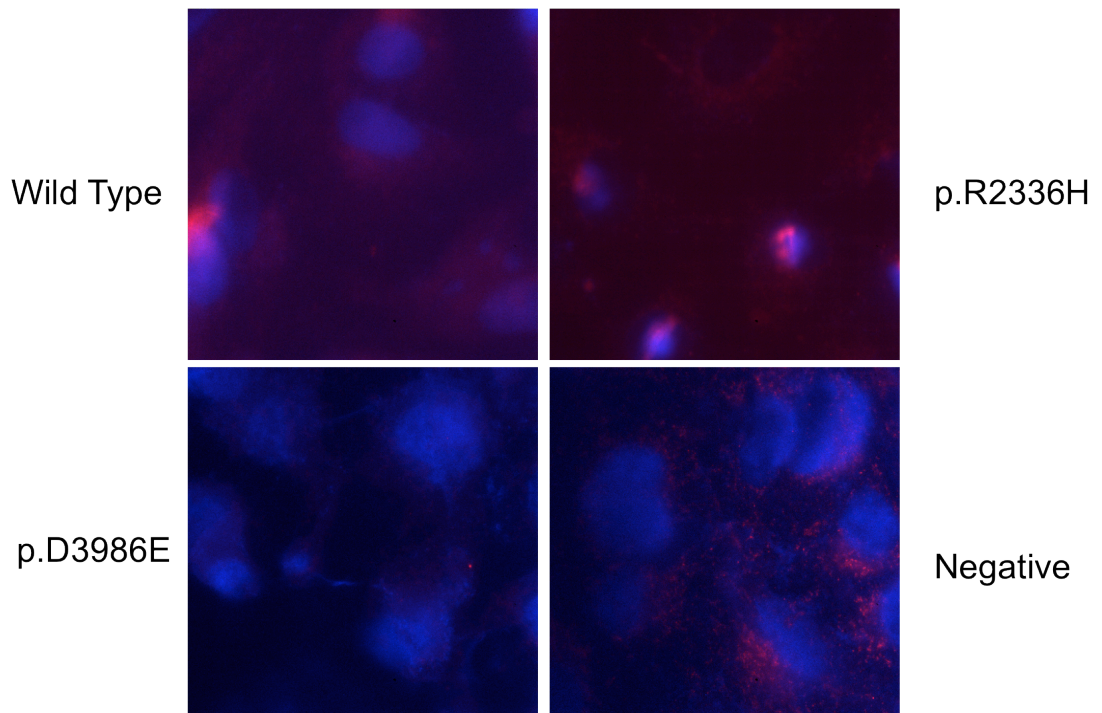


Figure 5.1 – Titration of harvested wild type, p.R2336H and p.D3986E HSV-1 virions using immunocytochemistry on 2-2 cells.

2-2 cells were infected with harvested HSV-1 virions containing wild type, p.R2336H and p.D3986E pHSVRYR1 constructs. Cells were infected overnight before the removal of the virions and incubation in growth medium for a further 24 hours. Cells were fixed with ice-cold methanol before staining with DAPI (blue) and 34C anti-ryanodine receptor antibody (red). Some background was observed in the negative control, uninfected 2-2 cells that were not distinguishable from the wild type or p.R2336H infected cells. Furthermore, the p.D3986E infected cells showed no RYR1 staining.

5.3.1.2 Titration using calcium release assays

Due to the immunocytochemistry experiments showing no apparent RYR1 expression, the harvested virions were also titrated using differentiated 1B5 cells exposed to 1mM, 5mM and 20mM caffeine (Figure 5.2). Differentiating 1B5 cells were exposed to 20 μ l, 50 μ l and 100 μ l of harvested HSV-1 virions overnight before the addition of fresh medium and a further 24-hour incubation before the calcium release assay was performed. None of the infected cells responded to 1mM or 5mM caffeine, however, all wild type and p.R2336H infected cells released calcium when exposed to 20mM caffeine. Wild type infected cells appeared to respond with a larger increase in fluorescence upon exposure to caffeine. The number of cells infected was calculated from the field of view used for the calcium measurements and the percentage of responding cells at 20mM was plotted in Table 5.1. When infected with 20 μ l of virions, 80% of the wild type myotubes in the field of view responded to 20mM caffeine compared with 50% for myotubes infected with the p.R2336H virions. Only 10% of myotubes were successfully infected with *RYR1* when the virion volume increased to 50 μ l and 100 μ l for the p.R2336H construct. Wild type infection efficiency stayed relatively constant throughout the concentration range. Although the efficiency dropped to 40% when 50 μ l of virions was used, it returned to 80% for 100 μ l. For both constructs, as the virion concentration increased, so did the amount of cellular debris visible on the cells. For cells infected with the p.D3986E construct, no response was seen from any of the infected myotubes at any caffeine concentration. Similarly to the wild type and p.R2336H constructs, cellular debris severely increased as the concentration of the p.D3986E virions increased. Cells that did respond to caffeine produced a typical calcium release response from myotubes. The myotubes responded by contracting, releasing calcium as indicated by an increase in fluorescence followed by sequestration back into the intracellular stores (Figure 5.3).

Construct	Concentration of virions	Percentage of cells responding at 20mM caffeine
Wild Type	20µl	80
	50µl	40
	100µl	80
p.R2336H	20µl	50
	50µl	10
	100µl	10
p.D3986E	20µl	0
	50µl	0
	100µl	0

Table 5.1 – Calculation of the efficiency of infection of wild type and p.R2336H pHSVRYR1 virions. For both the wild type and p.R2336H pHSVRYR1 virions, the best infection efficiency was observed at the lowest concentration of virions. For wild type virions, the same efficiency was observed at 100µl virions, however the cellular debris generated from this concentration was higher. As the virion concentration increased for the p.R2336H construct, the infection efficiency dropped dramatically to 10% for both 50µl and 100µl. Myotubes infected with p.D3986E virions did not release calcium at any caffeine concentration for each virion concentration.

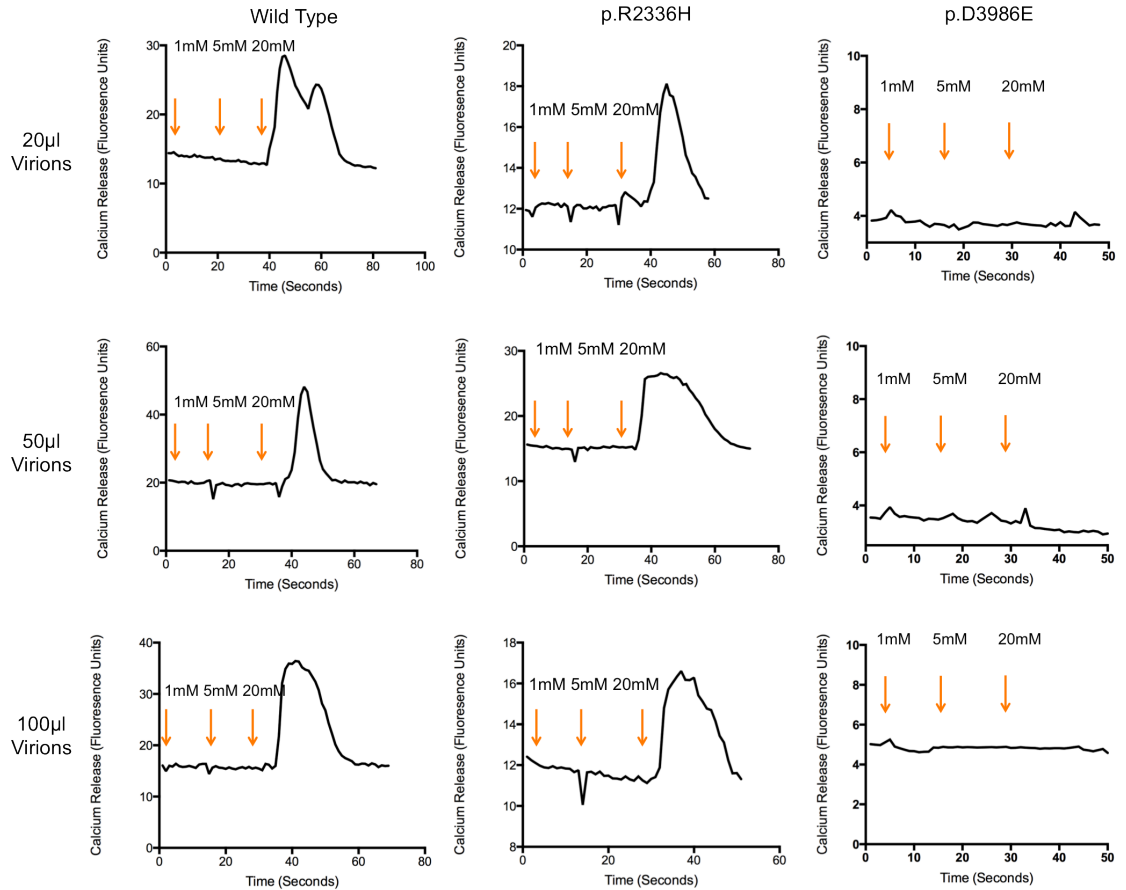


Figure 5.2 – Titration of HSV-1 virions using 1B5 cells exposed to caffeine.

1B5 cells were plated onto 96-well plates and differentiated for 3 days before infection with incremental amounts of harvested wild type, p.R2336H and p.D3986E virions. Infection was carried out overnight before the virions were removed and replaced with differentiation medium and cultured for a further 2 days. Calcium measurements were carried out using 1mM, 5mM and 20mM caffeine. No infected cells responded to 1mM or 5mM caffeine. Cells infected with wild type or p.R2336H HSV-1 virions produced a calcium release at 20mM regardless of the virion concentration used. Cells infected with p.D3986E virions did not respond to any caffeine concentration used in this series.

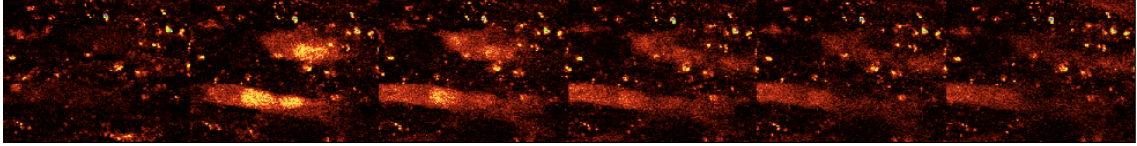


Figure 5.3 – Time lapse image of 1B5 myotubes releasing calcium upon exposure to 20mM caffeine. 1B5 cells were infected with wild type pHSVRYR1 virions and exposed to 20mM caffeine. Upon exposure to caffeine the 1B5 cells contracted and released calcium as visualised by a temporary increase in fluorescence before sequestration back into the calcium stores and fluorescence returned to the baseline.

5.3.2 Caffeine-induced calcium release of 1B5 myotubes infected with HSV-1 virions

Based on the results obtained in the caffeine-induced calcium release titration experiments, 20µl of harvested HSV-1 virions were added to 1B5 cells before being exposed to a more thorough caffeine series for functional assays (Figure 5.4). Unfortunately, the infection efficiency seen in the original titration experiments could not be repeated throughout the caffeine-induced calcium release experiments. On occasion (Figure 5.4 A-B), a calcium release event was observed in a similar manner to the original titration experiments. A response was only ever observed twice out of 10 experiments and only at 20mM caffeine, which was insufficient for a thorough functional examination of the genetic variants in *RYR1* under investigation in this chapter. The vast majority of experiments produced no calcium release at any caffeine concentration used (Figure 5.4C).

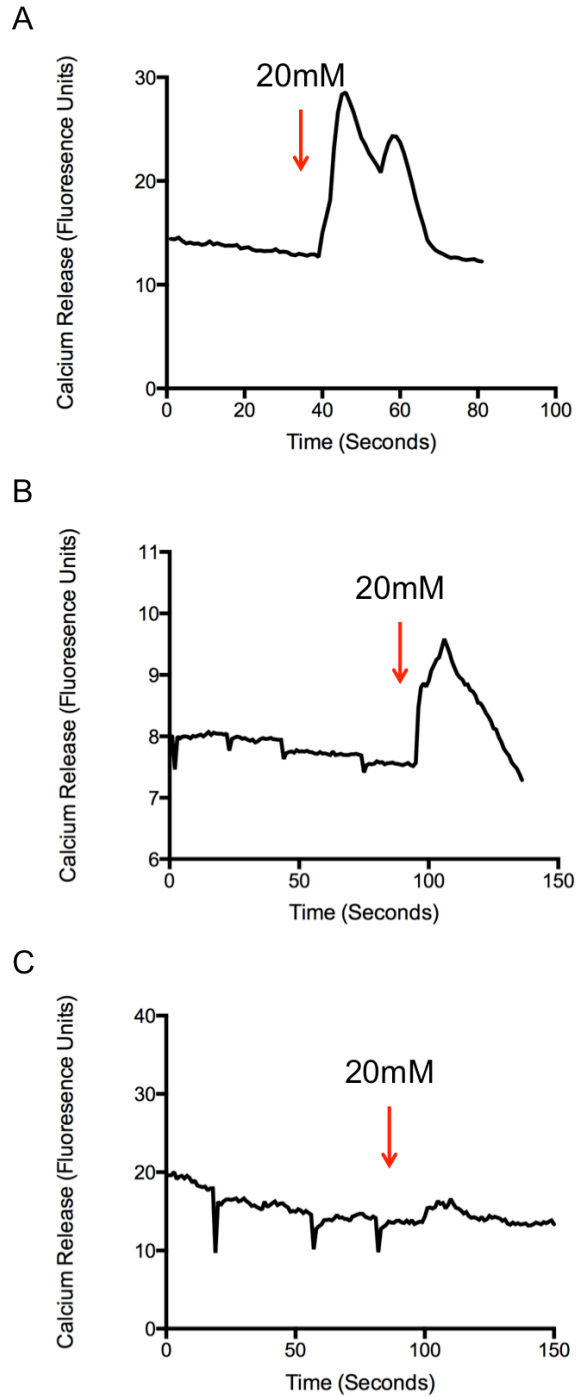


Figure 5.4 – Caffeine-induced calcium release experiments on 1B5 cells infected with HSV-1 virions containing wild type or p.R2336H RYR1

Displayed are examples of the caffeine-induced calcium release experiments carried out on 1B5 cells infected with HSV-1 virions containing *RYR1* constructs. (A-B) On occasion, calcium release events were observed at 20mM caffeine for wild type RYR1 (A) and p.R2336H RYR1 (B). This was, however, a rare event and the two occasions it occurred are displayed above. (C) A representative trace from a caffeine-induced calcium release experiment performed on differentiated 1B5 cells infected with HSV-1 virions containing *RYR1* constructs. No calcium release was observed at any caffeine concentration.

5.3.3 Control experiments to test the ability of 2-2 cells and the cosmid set to package HSV-1 virions

To test the possibility that the anti-RYR1 antibody was not working efficiently, C2C12 cells were also differentiated and stained with the anti-ryanodine receptor antibody (Figure 5.5). Panel A shows multinucleated myotubes clearly showing Cy3 fluorescence, indicating the presence of RYR1. To probe the possibility that the constructs generated in chapter 3 were not being packaged properly due to a fault in the plasmid, a pHSV $RyR1$ plasmid with a green fluorescent protein (GFP) tag was packaged into HSV-1 virions using the same protocol that was used for the pHSV $RyR1$ constructs generated in this thesis. The pHSV $RyR1$ -GFP plasmid had previously been successfully packaged into HSV-1 virions, which had subsequently been used to infect 1B5 cells. Figure 5.5 B shows differentiated 1B5 cells infected with pHSV $RyR1$ -GFP HSV-1 virions. No specific GFP staining was observed indicating that $RyR1$ had not been packaged into the virions.

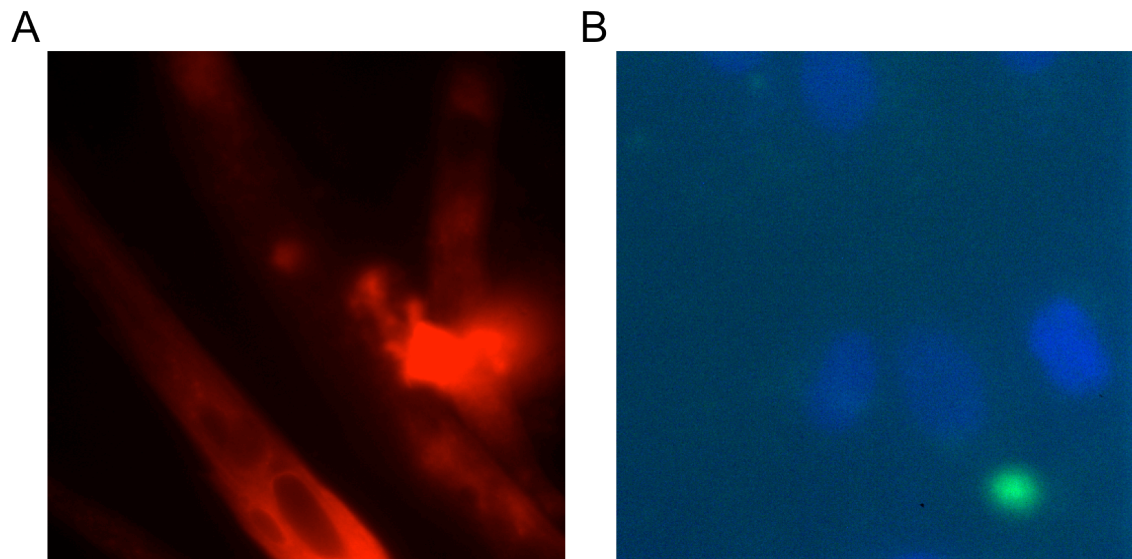


Figure 5.5 – Control experiments carried out to test the 34C antibody and the packaging protocol (A) C2C12 cells fixed and stained with the anti-ryanodine receptor antibody. Clear red (Cy3) staining was observed in all multi-nuclear myotubes examined. (B) GFP fluorescence of myotubes infected with RYR1-GFP HSV-1 virions. No specific GFP staining was observed in the myotubes.

5.3.4 Use of conventional transfection agents on 1B5 dyspedic myotubes

As well as using viral methods, 1B5 cells were transfected with wild type *pcRYR1* using two conventional transfection reagents; LF2000 and Xfect polymer in an attempt to obtain sufficiently high enough RYR1 expression for thorough caffeine-induced calcium release experiments (Figure 5.6). Titration using caffeine-induced calcium release appeared to give a more clear indication of the presence of RYR1 as compared to immunocytochemistry so this method was chosen as the means of testing the conventional transfection reagents. 1B5 cells were transfected and then allowed to differentiate for 3 or 4 days. Additionally, cells were differentiated for 4 days at both low and high cell density. A further experiment was carried out in which cells were transfected midway through a 4-day differentiation period. Cells were exposed to 20mM caffeine followed by 40mM KCl to ascertain whether or not *RYR1* was being expressed in the cells. No cells transfected with either LF2000 or the Xfect polymer responded when exposed to 20mM caffeine. Cells transfected using the Xfect polymer suffered a mild quench in fluorescence when exposed to caffeine. A similar but milder response was seen in some of the experiments utilising LF2000. Cells transfected using LF2000 did not respond to 40mM KCl whereas cells transfected using the Xfect polymer experienced a mild calcium release, which was slowly sequestered back into the intracellular stores. Neither LF2000 or Xfect were able to produce a high enough transfection efficiency for thorough functional analysis so subsequent experiments using mutant *pcRYR1* constructs were not performed.

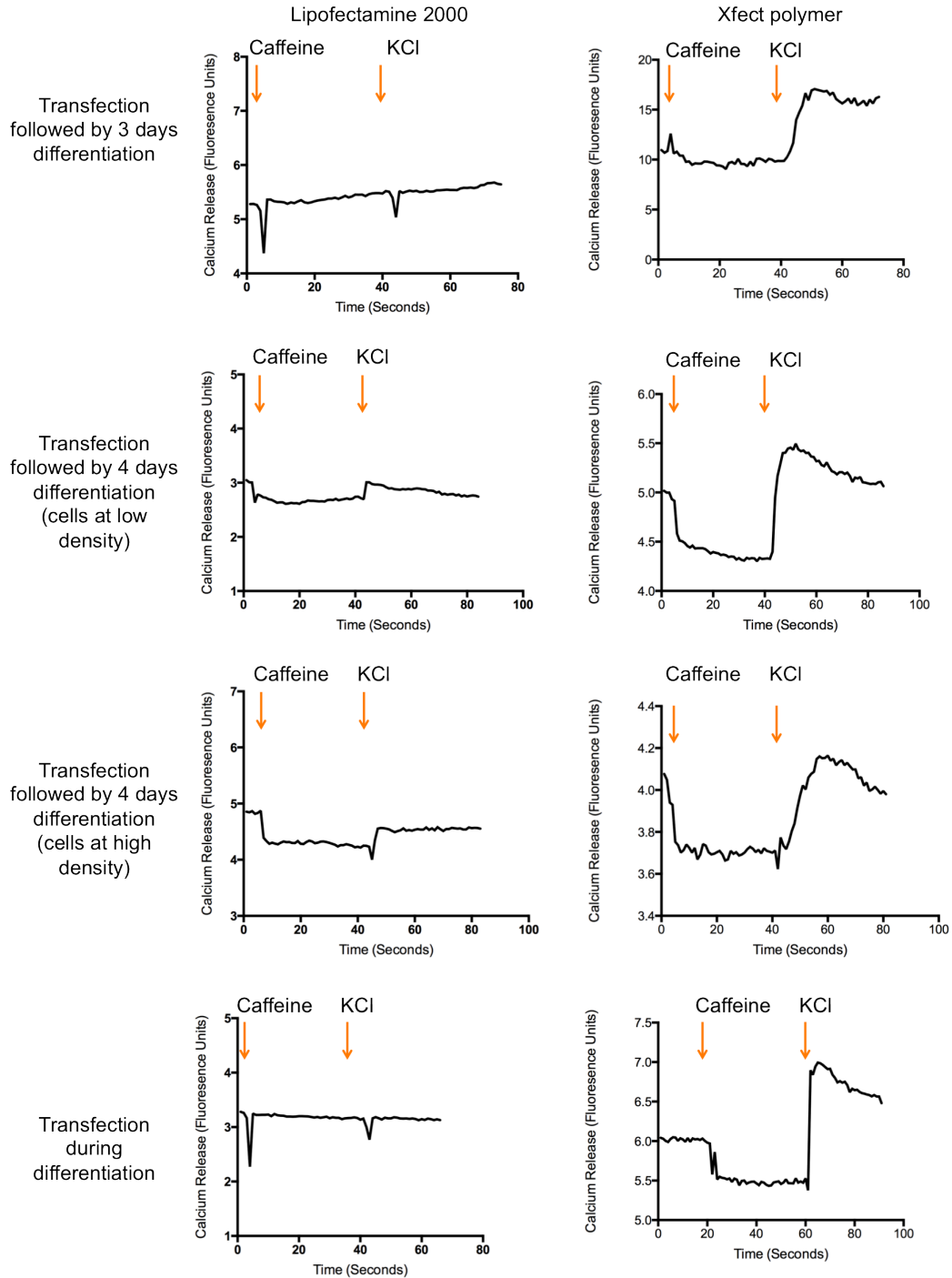


Figure 5.6 – Traces of dyspedic myotubes transfected with wild type *pcRYR1* using LF2000 and Xfect polymer. Transfections were carried out 24 hours prior to the infection of myoblast differentiation. Cells were also plated at high and low density and differentiated for 4 days. Some cells were transfected midway through a 4-day differentiation period. No cells responded when exposed to 20mM caffeine. There appeared to be some quenching of fluorescence when caffeine was added. This was more prominent in cells transfected using the Xfect polymer. Cells transfected using LF2000 did not respond to 40mM KCl whereas cells transfected using the Xfect polymer did have a mild calcium release that was slowly sequestered back into the intracellular stores.

5.4 Discussion

Although the data presented in this chapter does not add to the knowledge of the difference between HEK293 cells and 1B5 cells as a functional experimental system, it does highlight the difficulties encountered by expressing not only large cDNA constructs in cell lines but also more specifically in expressing these constructs in skeletal muscle cells. In this chapter, almost no reliable expression of *RYR1* was observed in 1B5 cells either infected with HSV-1 virions or transfected using the conventional methods of LF2000 and the Xfect polymer.

5.4.1 Difficulties in generating a high titre of HSV-1 virions containing wild type and mutant *RYR1* constructs

The primary reason for the inability to generate data in 1B5 cells in this chapter was the difficulties associated with generating a high titre of HSV-1 virions containing wild type and mutant *RYR1* constructs. Several attempts were made at packaging the wild type, p.R2336H and p.D3986E pHSV*RYR1* constructs into HSV-1 virions. Caffeine-induced calcium release was selected as the primary method of titrating the viral titre obtained in the packaging experiments due to technical difficulties experienced with immunocytochemistry. No response was seen for any of the constructs packaged at 1mM or 5mM caffeine. However, a response was observed in wild type and p.R2336H infected cells upon exposure to 20mM caffeine. The response was specific to the addition of the caffeine and followed a pattern of calcium release and sequestration similar to that reported previously for 1B5 cells (Yang et al., 2003). For wild type infected cells, up to 80% of cells responded to 20mM caffeine. This was observed at a low viral infection volume (20µl of the harvested virions) as well as a high concentration of virions (100µl of the harvested virions). For p.R2336H infected cells the efficiency was not as high and at its peak reached 50%, which was obtained at the lowest virus concentration (20µl of the harvested virions). For p.D3986E infected cells,

no response was observed at any caffeine concentration or viral infection concentration.

For all constructs, as the viral concentration increased so did the amount of cellular debris visible under the microscope. This is likely due to an increase in not only any potential virions in the solution infecting and possibly killing the cells being infected but also an increase in cellular debris left over from the harvesting of the packaged virions. Ideally, this would be reduced by having a high viral titre from the packaging experiments therefore reducing the need for increased volumes of harvested virions. Based on the titration experiments 20 μ l of virus was added to differentiating 1B5 cells for more comprehensive functional experiments involving a wider caffeine series. Unfortunately, the efficiency observed in the original titration experiments was not reproduced and almost no calcium release was observed at any caffeine concentration in any of the experiments. A total of 2 responses were seen throughout the experiments, however, these were always at high doses of caffeine and were not reproduced in different wells of the same experiment meaning no comprehensive functional experiments were completed.

The reason for the extremely low viral titre is unclear. All materials used for the viral packaging experiments were obtained from Professor Paul Allen's laboratory and had been used successfully to package pHSV*RyR1* virions previously. The only difference to the materials was the insertion of the human *RYR1* cDNA constructs generated in this project. The possibility that *RYR1* was not being packaged properly and expressed in the dyspedic myotubes was examined through the use of a positive control pHSV*RyR1*-GFP tagged construct that had been successfully packaged previously. The pHSV*RyR1*-GFP construct was packaged into HSV-1 virions along side the pHSV*RyR1* constructs generated in this project. No GFP-positive cells were observed upon examination under fluorescence microscopy indicating that the defect may be occurring in the packaging process rather than the pHSV*RyR1* constructs, possibly though a defect in one of the five cosmids that contains the entire HSV-1 genome minus the packaging

signals. It is noteworthy that the original laboratory in which the material was acquired from is also currently having difficulties successfully packaging HSV-1 virions.

5.4.2 The use of conventional transfection methods on dyspedic myotubes

Conventional transfection methods were also used in this chapter as an attempt to generate high enough transfection efficiencies for functional experiments. LF2000 is a standard lipid based transfection reagent that has been repeatedly used in functional experiments of *RYR1* variants using HEK293 cells as well as in this thesis (Tong et al., 1997, Tong et al., 1999a, Lynch et al., 1999, Tong et al., 1999b). A second transfection reagent, Xfect, was also used due to claims that muscle cells and primary myoblasts had been previously transfected successfully using it. Unfortunately, neither transfection method produced high enough transfection efficiencies for functional experiments. Based on the findings of Neuhuber et al. (2002) that suggested an increased transfection efficiency when transfecting primary myoblasts compared with differentiating myotubes, several time points during myotubes differentiation were used for the transfection of pc*RYR1* into 1B5 cells as well as different differentiation durations. Transfections were carried out prior to differentiation periods of 3 and 4 days. Furthermore, the effect of cell density was examined by carrying out the 4-day differentiation transfections at a low and a high cell density. A final experiment was set up mimicking the infection method of the HSV-1 virions by transfecting the 1B5 cells mid-differentiation.

No obvious differences were observed between any of the times of transfection. For cells transfected using LF2000, no responses were observed when challenged with 20mM caffeine or 40mM KCl. Cells transfected using the Xfect polymer did not respond to 20mM caffeine, however a slight calcium release was observed upon exposure to 40mM KCl. The reason that the cells responded to 40mM KCl but not 20mM caffeine is not immediately clear. It is unlikely to be a background effect seen in 1B5 cells as untransfected cells or cells transfected with LF2000 did not share this

response and, as reported by Yang et al. (2003), 1B5 cells do not respond to any traditional RYR1 channel agonist. Whatever the reason, the response was not large enough for a comprehensive functional characterisation experiment.

The data obtained using conventional transfection methods in this chapter is consistent with data previously presented by several studies (Wang et al., 2000, Campeau et al., 2001, Neuhuber et al., 2002). Wang et al. (2000) showed that using standard transfection methods was significantly less efficient than the HSV-1 system. The largest plasmid tested in Campeau et al. (2001) was 17kb, 3kb smaller than the pHSVRYR1 and pcRYR1 plasmids constructed in this project and perhaps unsurprisingly, the efficiency generated in this chapter was much lower.

5.5 Future work

Periodically, companies produce transfection reagents that claim to be able to transfect muscle cells with high efficiency. In spite of this there is a wealth of literature showing that different transfection reagents are unsuccessful at transfecting muscle cells to a high efficiency. The problem is exacerbated when the gene of interest is large as transfection efficiency dramatically drops as the size of the cDNA construct increases. Previous reports have obtained up to 90% infection efficiency using the HSV-1 system described above and future work should be aimed at reproducing this success. If this were possible it would allow a thorough comparison to be carried out between the responses of genetic variants of *RYR1* in non-native cell types and 1B5 cells and an argument could be made for the exclusion of the non-native cell types from the EMHG guidelines. If the protocol could be made simpler, more reliable and quicker there would also be the possibility of switching to a guideline protocol that only used muscle cells for the functional characterisation of genetic variants in the *RYR1* gene.

An alternative method of expressing *RYR1* variants in dyspedic muscle cells is the use of microinjection. Experiments have been successfully carried out on dysgenic

(*CACNA1S* null) myotubes for functional assays of Ca_v1.1 (Bannister and Beam, 2009, Eltit et al., 2012a). Utilising this technique for the functional assays involved in *RYR1* variants may avoid the need for viral packaging, potentially making the experiments safer as it would not require HSV-1 virions. However, the number of cells that would need to be manually injected using this process would be high making the process potentially less efficient and more time intensive than if the HSV-1 system was properly optimised.

The use of murine models of MH is increasing. To date, 3 different MH *RYR1* mutations have been knocked in to a mouse model as well as 1 *CACNA1S* mutation (Yang et al., 2006, Chelu et al., 2006, Zvaritch et al., 2007, Eltit et al., 2012b). Although it is still not practical to make a mouse model of every MH mutation, it may be of interest to select individual mutations of interest. For example, in the previous chapter, the p.D3986E variant responded in a way that was indistinguishable from wild type. If the p.D3986E variant still responds in a similar way to wild type in the muscle-like system, it would be of interest to examine the effects of this mutation *in vivo*.

Finally, successful expression of these genetic variants in myotubes would facilitate the possibility of measuring resting intracellular calcium concentrations of wild type and mutant channels that, unfortunately, could not be carried out in this chapter.

5.6 Conclusions

The work presented in this chapter supports a large body of literature highlighting the difficulties associated with expressing genes of interest in muscle cells. These problems were compounded by the size of *RYR1*, which, even in more easily transfected cells has low transfection efficiency due to its 15kb coding sequence. Until the issues surrounding expressing large cDNA constructs in muscle cells are fully resolved it will be impossible to comprehensively deduce whether there is a need to stop the use of non-native cell types for the functional characterisation experiments of genetic variants in the *RYR1* gene.

Chapter Six - Functional analysis of genetic variants in the *RYR1* gene associated with malignant hyperthermia and exertional heat stroke using the pTUNE inducible expression vector.

6.1 Introduction

To date, the majority of the experiments carried out on *RYR1* variants have been dose-response experiments involving known channel agonists such as caffeine, 4-CmC, halothane and ryanodine (Tong et al., 1997, Yang et al., 2003). Further experiments have involved measuring the intracellular resting calcium of cells and muscle specimens known to be carrying variants in *RYR1* (Lopez et al., 1985a, Lopez et al., 1985b, Lopez et al., 1986, Lopez et al., 1987a, Lopez et al., 1988, Tong et al., 1999b, Lopez et al., 2005, Yang et al., 2007). No experiment has looked at the effect of an increased or decreased expression of mutant *RYR1* in terms of its effect on the sensitivity to channel agonists despite a growing body of evidence suggesting that the expression level of *RYR1* may play a role in MH pathogenesis. Grievink and Stowell (2010), carried out allele specific PCR on immortalised lymphoblastoid cells carrying known *RYR1* variants. It was found that patients carrying the *RYR1* variants had a higher expression from the wild type allele, possibly as a compensatory mechanism to protect against the defective allele. This increase in expression may represent some of the variation seen in the clinical presentation of patients undergoing anaesthesia with the same variant but largely differing phenotypes. Perez et al. (2005) carried out a study examining the effect of increasing the expression of *RYR1* in dyspedic myotubes. The resting calcium level of myotubes expressing wild type *RYR1* was not significantly increased when expression level was increased by up to 20-fold. Similarly, no statistically significant effect on caffeine sensitivity was observed within this expression range. Interestingly, when *RYR3* was over-expressed in the same range, the resting calcium level continuously increased and was elevated when compared to wild type at the lowest expression level used. The caffeine sensitivity of *RYR3* also increased as the expression level increased, hinting at the importance of the role of elevated resting calcium in the sensitivity of *RYR1* to channel agonists. Unfortunately,

no variants of *RYR1* were examined in this study. It has, however, long been suggested that patients with MH have an elevated baseline resting calcium level in skeletal muscle (Lopez et al., 1985a) and more specifically, MH-associated *RYR1* and *CACNA1S* variants have been shown to produce a higher resting calcium level in myotubes (Yang et al., 2007, Eltit et al., 2012a). Furthermore, it has been shown that correcting the resting calcium level of cells expressing *RYR1* variants to a wild type level lowers the sensitivity of MHS muscle (Lopez et al., 2005). Reducing this resting calcium level resulted in muscle that responded in a similar way to wild type, indicating that the MH response seen in patients may be, at least in part, due to the chronically elevated resting calcium observed in susceptible individuals.

To facilitate experiments aimed at examining the effect of an increased expression of *RYR1* variants on caffeine sensitivity of transfected HEK293 cells, *RYR1* constructs were cloned into a pTUNE inducible expression vector as described in chapter 3. The p.D1056H, p.R2355W and p.D3986E *RYR1* variants were cloned into the pTUNE vector. These variants have been identified in a total of 13 families in the UK. The p.R2355W variant has also been identified in 2 additional families worldwide.

6.1.1 p.D1056H

The Leeds MH diagnostic centre recently sent patient samples in which no potentially causative genetic variant had been identified for whole exome sequencing. In one family, a novel c.3166 C>T (p.D1056H) *RYR1* variant was identified that had been missed using conventional Sanger sequencing. Subsequent screening in this family found that the variant cosegregated with the MH phenotype in all the family members available for screening. Furthermore, upon routine screening of the rest of the UK MH population for the p.D1056H variant, it was also identified in a patient who experienced an EHS reaction. The individual was a member of the British military and on a training exercise suffered dizziness, excessive sweating and although he did not lose consciousness, he had a temperature of 38.9°C upon examination. Heat tolerance

tests repeatedly showed excessive heat production and he was subsequently referred for MH testing at the Leeds diagnostic centre. The IVCT test diagnosed the patient as MHN and no further family members were tested.

6.1.1.1 Exertional heat stroke and MH

EHS is a disorder in which exercise, usually in warm climates triggers excessive heat production in susceptible individuals that exceeds their body's capability to remove. It has long been suggested that there is a genetic link between MH and EHS, primarily due to the similarity in the symptoms involved in both disorders (Hopkins, 2007, Muldoon et al., 2004, Muldoon et al., 2008) as well as the tendency of animal models of MH to display EHS symptoms when exposed to an increased ambient temperature. Early porcine models of MH all displayed an EHS-like phenotype termed PSS in which pigs that possess a variant in the porcine *RYR1* undergo a hypermetabolic reaction when stressed before slaughter (Heffron et al., 1982, Otsu et al., 1994). More recently, murine models of MH have all displayed an EHS phenotype when the ambient temperature has been elevated to 42°C (Yang et al., 2006, Chelu et al., 2006, Yuen et al., 2012, Lanner et al., 2012).

In recent years, *RYR1* variants have been identified in a number of heat-related illnesses (see table 1.2 in chapter 1). Wappler et al. (2001) reported three families containing an *RYR1* variant in association with exertional rhabdomyolysis as well as MH. Additionally, a common *RYR1* variant was identified in three New Zealand families with exertional rhabdomyolysis (Davis et al., 2002) as well as two variants found associated with a fatal episode of stress-induced MH in two children (Groom et al., 2011). Most significantly, an *RYR1* variant has also been found in association with a classic EHS episode (Tobin et al., 2001). A 12-year-old boy suffered an MH reaction when undergoing surgery but recovered without complications only to die several months later of an EHS episode whilst playing football. Genetic analysis identified a p.R163C *RYR1* mutation that has been consistently associated with MH and has been

found to be functionally relevant in both the HEK293 (Tong et al., 1997) and 1B5 systems (Yang et al., 2003).

A recent study on an MH mouse carrying the p.Y524S RYR1 variant found that pre-treatment with AICAR, a drug that imitates the effect of AMP in the activation of AMPK that has previously been shown to mimic the effects of exercise in sedentary mice (Narkar et al., 2008), completely protected the mice against the EHS phenotype normally associated with MH mice (Lanner et al., 2012). Treatment with AICAR lowered the baseline resting calcium in the MH mice to a level similar to that of wild type littermates. It was postulated that this reduction in resting calcium was responsible for the protection against the EHS phenotype, leading to the suggestion of the use of AICAR as a prophylactic treatment for individuals who are susceptible to EHS. Unfortunately, no experiments were carried out on the effect of AICAR on the sensitivity of the *RYR1* variant through a dose-response curve.

6.1.2 p.R2355W

The p.R2355W variant has been identified in nine families worldwide, seven of which are in the UK. The variant has been found to segregate with MH phenotype and was absent from a panel of control chromosomes. Wehner et al. (2004) differentiated primary myoblasts isolated from patients carrying this variant into myotubes and exposed them to incremental doses of caffeine, 4-CmC and halothane as well as measuring the resting calcium level of the myotubes in comparison with wild type controls. Surprisingly for cells carrying an MH variant, the resting calcium level was not found to be significantly higher than that of wild type controls. However, the EC₅₀ of myotubes containing the p.R2355W variant was consistently significantly lower than that of familial wild type controls. However, as only one family was tested, no firm conclusions could be made on the causality of the variant as outlined in the EMHG guidelines for functional analysis. It cannot be conclusively ruled out that an additional

variant unknown to the investigators is contributing to the MH phenotype in this family. Functional analysis of this variant in the HEK293 cell system established in this thesis would be able to conclusively state whether or not the p.R2355W variant should be added to the genetic diagnostic panel of MH.

6.1.3 p.D3986E

Data was obtained for the p.D3986E variant in chapter 4 that suggested that the p.D3986E variant responds in a similar way to wild type when expressed in HEK293 cells. Based on this, the p.D3986E variant was cloned into the pTUNE inducible vector to further probe its functional consequences through over- or under-expression. Furthermore, the p.D3986E variant is in a region of RYR1 that is important for the maintenance of resting calcium (Claudio Perez, personal communication). When chimeric RYR proteins were expressed in dyspedic myotubes containing a fragment of RYR3 that spans the area of the p.D3986E variant, resting calcium levels increased to levels similar to wild type RYR3 channels and were significantly higher than wild type RYR1 expressing cells. Perez et al. (2005) have previously demonstrated that an increase in *RYR3* expression results in an increase in sensitivity to channel agonists such as caffeine. Experiments performed in this chapter will allow us to examine the effect of an increase in the p.D3986E variant on the sensitivity of transfected HEK293 cells to caffeine.

6.2 Aims of the chapter

The aims of this chapter were to functionally assess the p.D1056H and p.R2355W *RYR1* variants to support their inclusion onto the genetic diagnostic panel for MH. The p.D1056H has been associated with both MH and EHS and functional data would further support the link between the two conditions. Additionally, using the pTUNE inducible expression vector, functional studies were carried out on a defined genetic background as well as with consistent expression levels, allowing us to examine the

effect of *RYR1* expression on the sensitivity of transfected cells to caffeine. Finally, dose-response experiments were carried out on transfected cells pre-treated with AICAR, a compound previously found to be fully preventative of an EHS reaction developing in MH mice. In these experiments, we examined whether or not AICAR acted by reducing the sensitivity of mutant transfected cells to caffeine.

6.3 Results

6.3.1 Caffeine-induced calcium release

HEK293 cells were transfected with full-length wild type, p.D1056H, p.R2355W and p.D3986E pTUNERYR1 variants. Expression of *RYR1* was induced using IPTG at a standard concentration of 25 μ M. 72 hours post-transfection, cells were loaded with Fluo-4 AM, a fluorescent calcium indicator, and exposed to incremental doses of caffeine (0.5mM, 1mM, 2mM, 4mM, 8mM and 20mM). The increase and subsequent decrease in fluorescence was measured using confocal microscopy and the fluorescence data was plotted in Prism6. The background rate of 4.02% estimated in chapter 4 was used again for these experiments. Cells that were untransfected or transfected but not exposed to IPTG were also measured. No difference was observed between the two, confirming no endogenous *RYR1* was being expressed (Figure 6.1). Representative traces from each construct transfected are presented in (Figure 6.2). No cells responded to 0.5mM caffeine. All cells responded to 1mM caffeine but there was a trend for a larger response in cells transfected with p.D1056H. At 2mM caffeine, cells transfected with p.D1056H once again produced a much larger response compared to cells transfected with wild type, p.R2355W and p.D3986E constructs. At 4mM caffeine, cells transfected with the p.D1056H and p.R2355W constructs appeared to reach a maximum response that was maintained when exposed to 8mM and 20mM caffeine. Wild type and p.D3986E transfected cells did not reach a maximum until they were exposed to 8mM caffeine. At 20mM caffeine, all cells had reached a maximum response and produced a large calcium transient.

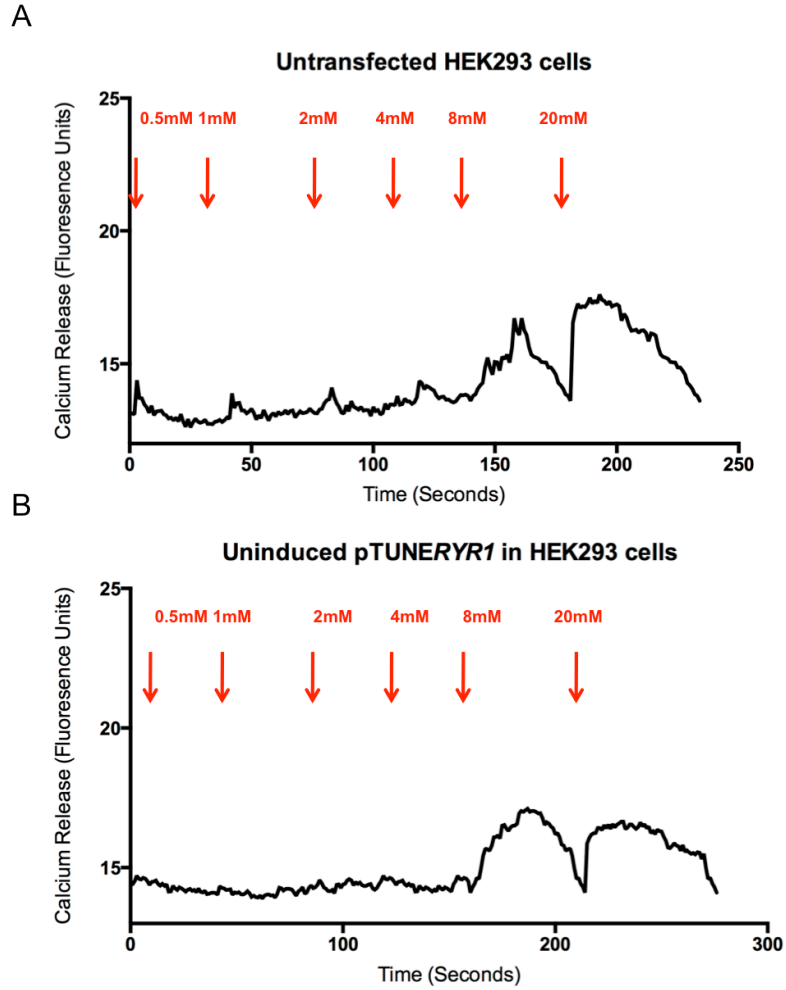


Figure 6.1 – Untransfected HEK293 cells and uninduced pTUNE constructs in HEK293 cells. (A) Untransfected HEK293 cells only responded to high doses of caffeine (8mM-20mM). (B) HEK293 cells transfected with wild type pTUNERYR1 but not exposed to any IPTG were indistinguishable from untransfected HEK293 cells. They also only responded to 8mM and 20mM caffeine.

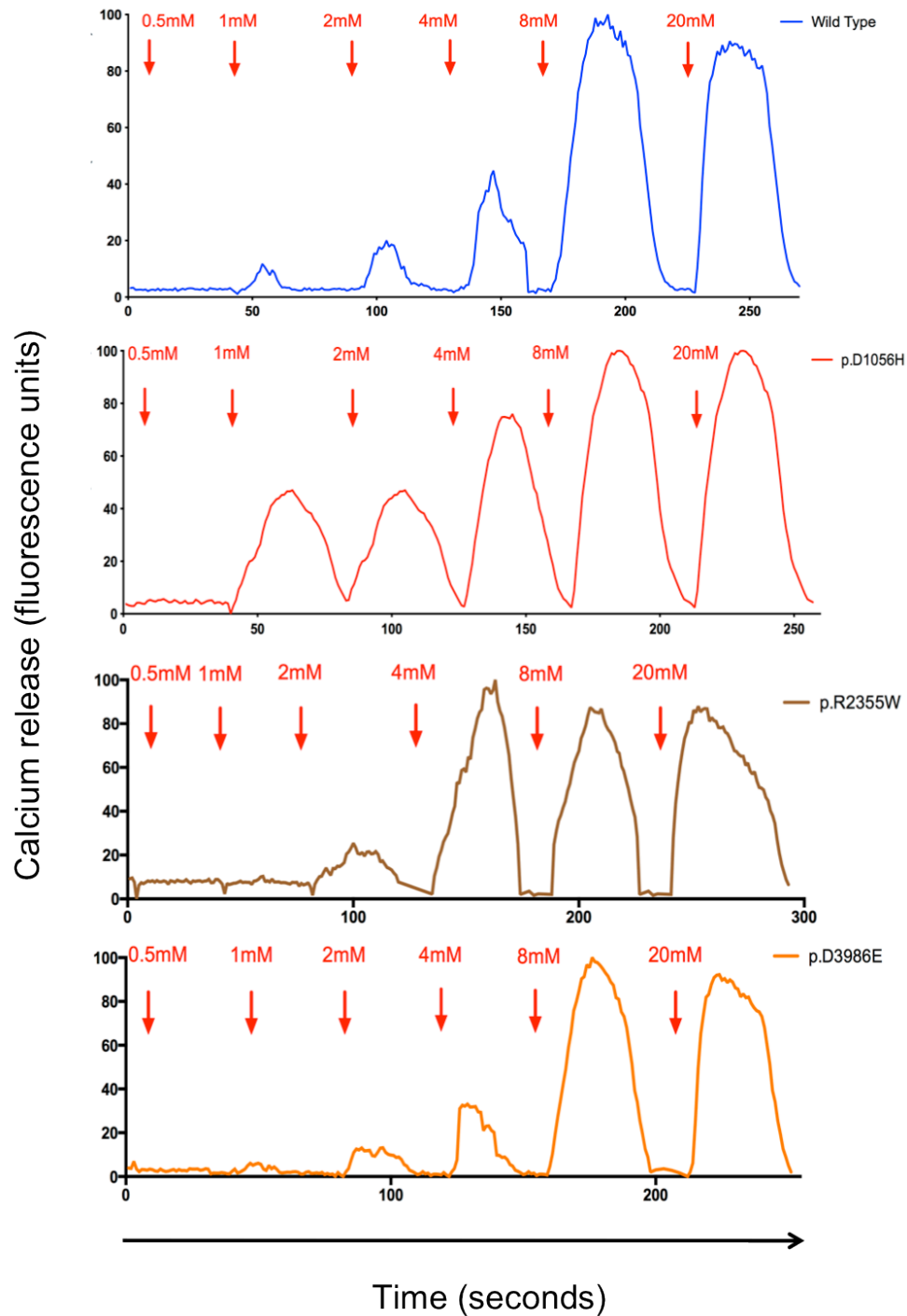


Figure 6.2 – Representative traces of HEK293 cells transfected with different pTUNERYR1 constructs releasing calcium when exposed to incremental doses of caffeine. All transfected cells were induced to express RYR1 using 25 μ M IPTG. Wild type transfected cells responded minimally to 1mM caffeine and had an increased response as the concentration of caffeine increased. A maximum response appeared to be reached at around 8mM caffeine. Cells transfected with p.D3986E responded in a similar way to wild type. Cells transfected with p.D1056H and p.R2355W reached a maximum response at around 4mM caffeine and tended to have a more exaggerated response at doses of caffeine lower than this.

Experiments were normalised with the peak fluorescence obtained in each experiment defined as 100% and the initial baseline fluorescence as 0%. The peak fluorescence generated at each caffeine concentration was taken for each experiment and plotted on a logarithmic scale. A dose-response curve was fitted using the non-linear regression function in Prism6 (Figure 6.3). For the p.D1056H and p.R2355W variants, the dose response curve was shifted to the left indicating an increase in sensitivity to caffeine. The p.D3986E variant produced a similar response to wild type, which is consistent with the results obtained in chapter 4 (Figure 6.3 A-C). The EC₅₀ of the p.D1056H (1.834mM, SEM = 0.278, 95% CI = 1.36-2.792) and p.R2355W (1.378mM, SEM = 0.6186, 95% CI = 0.02-2.298) variants were statistically significantly reduced as compared to wild type (3.804mM, SEM = 0.586, 95% CI = 2.525-5.392) ($p=0.0191$, $n=7$ and $p=0.0477$, $n=4$ respectively) (Figure 6.3 D-E). Consistent with the results obtained in chapter 4, the EC₅₀ of cells transfected with the p.D3986E variant was similar to wild type and was not statistically significantly different (4.667mM, SEM = 0.494, 95% CI = 2.744-5.889; $p=0.6901$, $n=4$). Furthermore, cells transfected with either the p.D1056H or p.R2355W variant had an EC₅₀ that was statistically significantly lower than cells transfected with the p.D3986E variant ($p=0.0027$ and $p=0.0243$ respectively. $n=4$). Cells transfected with the p.D1056H and p.R2355W variants had an EC₅₀ that was not significantly different from each other ($p=0.837$, $n=4$). The percentage of the maximum response generated at each caffeine concentration for each construct under investigation in this chapter was also plotted and analysed (Figure 6.3 F). At 1mM caffeine, no statistically significant differences were observed between each construct under investigation. However, there was a trend for cells transfected with the p.D1056H and p.R2355W variants to produce a response that was higher than wild type or p.D3986E transfected cells.

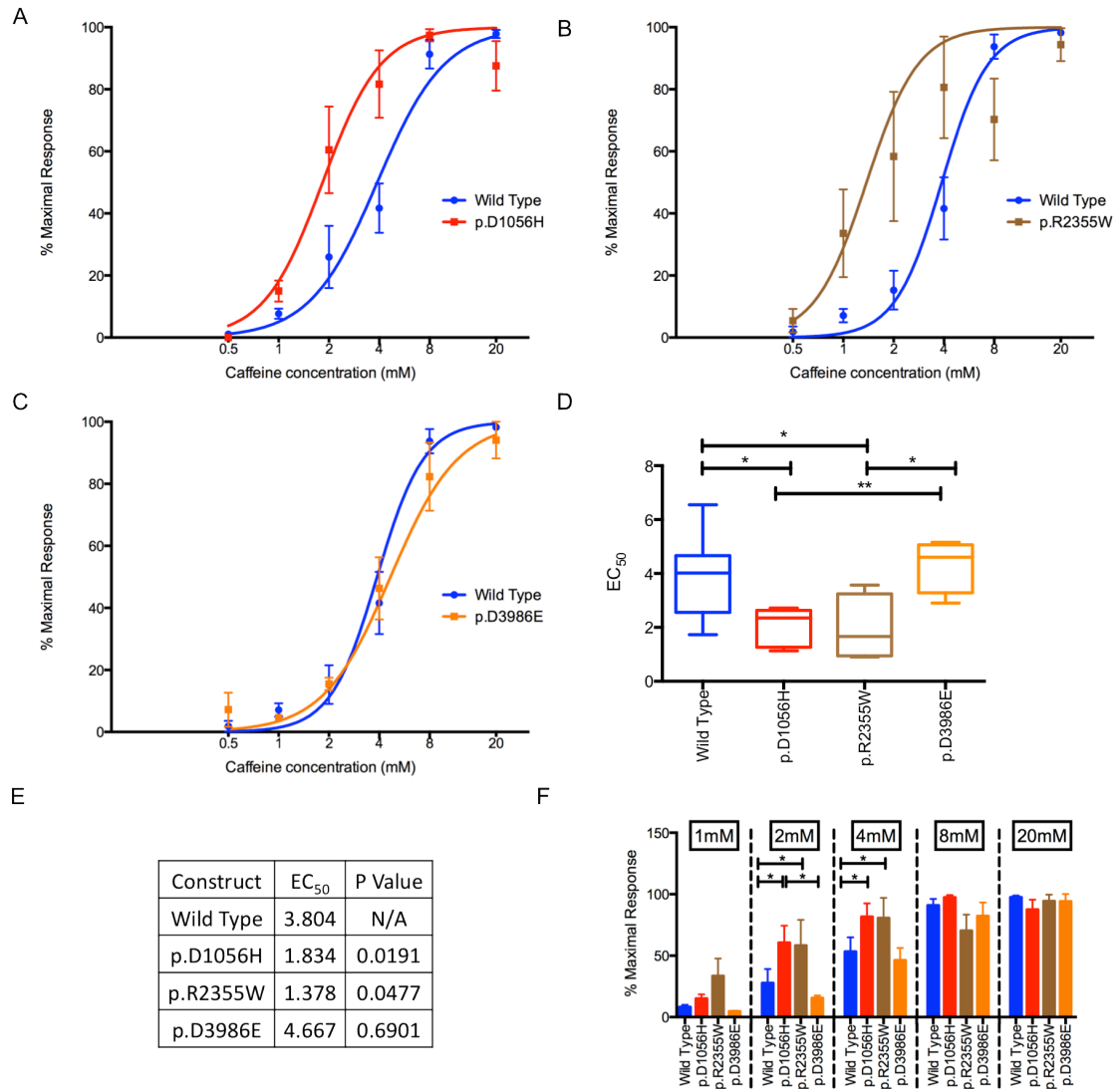


Figure 6.3 – Caffeine dose-response analysis of cells transfected with wild type, p.D1056H, p.R2355W and p.D3986E pTUNERYR1 constructs.

All transfected cells were induced to express RYR1 using 25 μ M IPTG. (A-C) Dose-response curves for the three RYR1 variants under investigation in this chapter plotted with the response from cells transfected with wild type pTUNERYR1. Data points are the mean plus and minus the standard error of the mean. For cells transfected with p.D1056H and p.R2355W the curve was shifted to the left indicating an increase in sensitivity to caffeine. Cells transfected with p.D3986E pTUNERYR1 produced a dose-response curve similar to wild type transfected cells. (D-E) The EC₅₀ was calculated for all constructs. Box plots are presented as the median, the upper and lower quartiles and the maximum and minimum data points. Cells transfected with p.D1056H and p.R2355W constructs had a statistically significantly reduced EC₅₀ as compared to wild type ($p < 0.05$). Cells transfected with p.D3986E pTUNERYR1 had an EC₅₀ similar to wild type transfected cells and was not statistically significantly different ($p = 0.6901$). Furthermore, cells transfected with p.D1056H and p.R2355W constructs had an EC₅₀ that was statistically significantly lower than cells transfected with p.D3986E ($p = 0.0044$ and $p = 0.0243$ respectively). (F) Dose response analysis at each caffeine concentration that produced a response from the transfected cells. Data are presented as the mean plus or minus the standard error of the mean. At 2mM and 4mM caffeine, cells transfected with p.D1056H and p.R2355W produced a statistically significantly increased response as a percentage of the maximum as compared to wild type. At 2mM caffeine, the response produced by p.D1056H transfected cells was also significantly higher than cells transfected with p.D3986E. * $p < 0.05$, ** $p < 0.01$.

At 2mM caffeine, cells transfected with both the p.D1056H and p.R2355W variants produced a response that was statistically significantly greater as a percentage of their maximum as compared to wild type. Cells transfected with p.D1056H and p.R2355W had a mean response of $60.5\% \pm 13.95$ and $58.37\% \pm 20.85$ respectively of the maximum compared to $27.78\% \pm 11.39$ for wild type ($p=0.0471$ and $p=0.0476$ respectively). Cells transfected with the p.D3986E construct produced a response of $13.34\% \pm 2.012$ which was not statistically significantly different to wild type ($p=0.4494$). At 4mM, once again cells transfected with the p.D1056H ($81.69\% \pm 10.87$) and the p.R2355W ($80.64\% \pm 16.37$) constructs produced a response that was statistically significantly higher than the wild type response ($53.37\% \pm 11.56$; $p=0.0498$ and $p=0.0441$ respectively). The p.D3986E transfected cells did not produce a response that was significantly different to wild type ($46.32\% \pm 10.04$; $p=0.7510$). For all analyses of the percentage of the maximum response $n=4$.

6.3.2 EC₁₀ and EC₂₅ of HEK293 cells transfected with the p.D3986E variant

In chapter 4, it was observed that cells transfected with the p.D3986E variant in *pcRYR1* had an EC₁₀ that was statistically significantly lower than that of wild type transfected cells. The EC₂₅ of p.D3986E transfected cells was also substantially reduced as compared to wild type. The same analysis was carried out on HEK293 cells transiently transfected with wild type and p.D3986E *pTUNERYR1* constructs (Figure 6.4). The EC₁₀ of HEK293 cells transfected with wild type *pTUNERYR1* was 2.769mM compared with 2.502mM for p.D3986E transfected cells. This was not statistically significantly different ($p=0.7489$). Similar results were observed for the EC₂₅ of cells transfected with wild type (3.441mM) and p.D3986E (4.297mM; $p=0.05124$). For each analysis $n=4$.

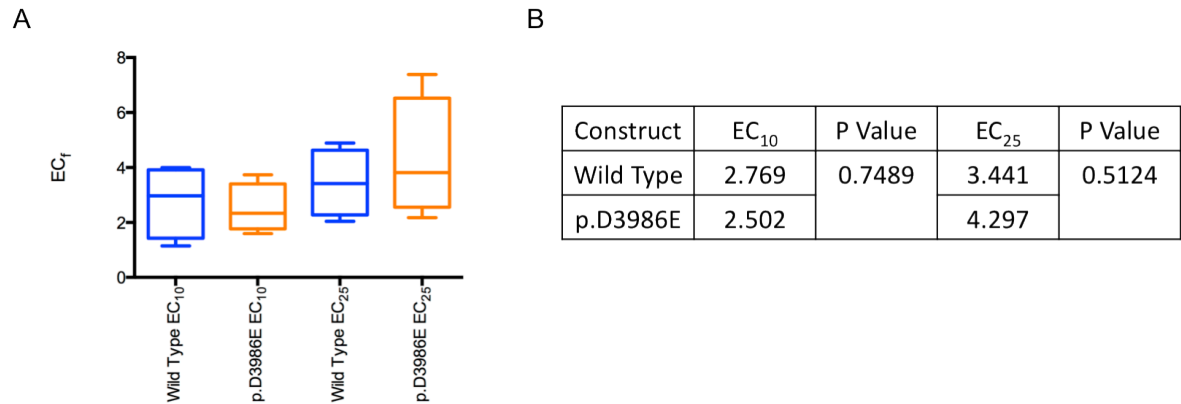


Figure 6.4 – EC₁₀ and EC₂₅ analysis of cells transfected with wild type and p.D3986E pTUNERYR1. All cells were induced to express RYR1 using 25 μ M IPTG. (A) Box plots showing wild type (blue) and p.D3986E (orange) EC₁₀ and EC₂₅. Unlike cells transfected with wild type and p.D3986E pcRYR1, cells transfected with the pTUNERYR1 equivalent constructs showed no difference in either EC₁₀ or EC₂₅. Box plots are presented as the median, the upper and lower quartiles and the maximum and minimum data points. (B) The EC₁₀ of wild type was 2.769mM compared to 2.502mM for p.D3986E transfected cells ($p=0.749$). Similarly, the EC₂₅ of cells transfected with wild type pTUNERYR1 was 3.441mM compared with 4.297mM for cells transfected with p.D3986E pTUNERYR1 ($p=0.5124$).

6.3.3 Area under the curve measurements of HEK293 cells transfected with pTUNERYR1 constructs

AUC measurements were taken from the fluorescence traces obtained in the caffeine-induced calcium release assays as an indirect measure of how much calcium was released at each caffeine concentration (Figure 6.5). For each experiment ($n=4$ for each construct), the baseline was independently ascertained by looking at the fluorescence before the addition of any caffeine. At 1mM caffeine, cells transfected with the p.D1056H and p.R2355W variants produced a statistically significantly higher calcium release than cells transfected with wild type pTUNERYR1.

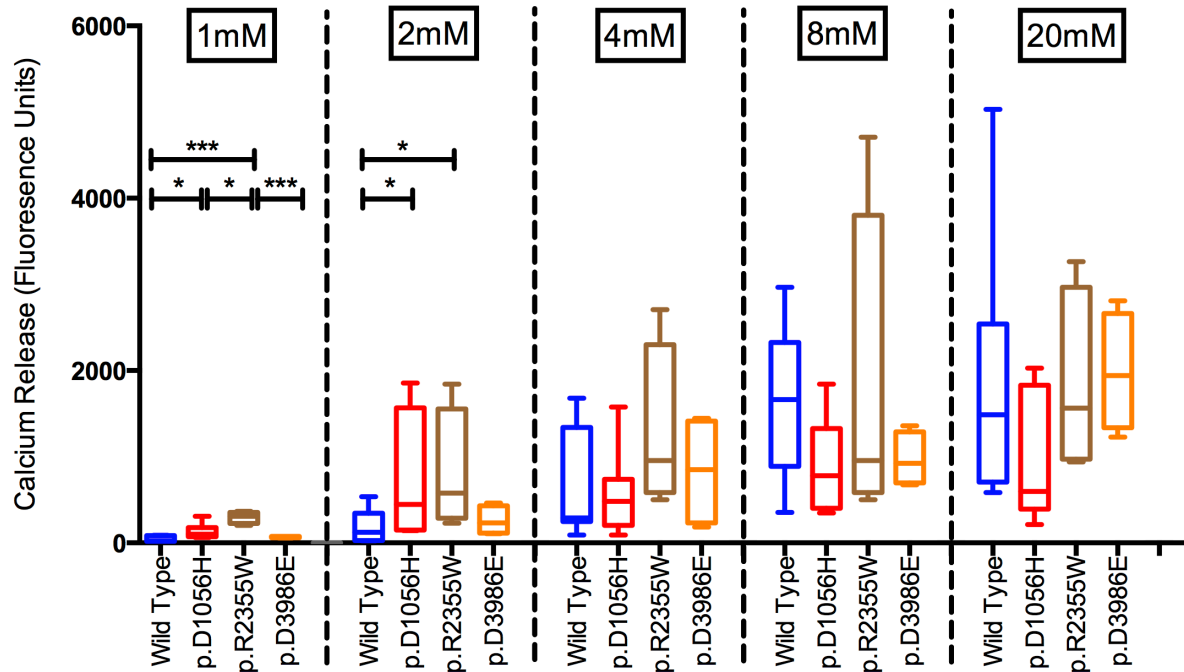


Figure 6.5 – Area under the curve measurements of HEK293 cells transfected with pTUNERYR1 constructs, induced with 25 μ M IPTG for 72 hours and exposed to incremental doses of caffeine.

At 1mM and 2mM caffeine, cells transfected with the p.D1056H and p.R2355W variants had a statistically significantly higher amount of calcium release than cells transfected with wild type pTUNERYR1. Furthermore, cells transfected with the p.R2355W variant had a statistically significantly higher amount of calcium release than either of the other two variants under investigation in this chapter. At 4mM-20mM caffeine, no significant difference in calcium release was observed between any of the constructs under investigation in this chapter.

Box plots are shown as the median, the upper and lower quartiles and the maximum and minimum data points. * $p < 0.05$, ** $p < 0.01$, *** $p < 0.001$.

Cells transfected with the p.D1056H and p.R2355W variants produced a calcium release of 133 FU \pm 32.6 and 295.9 FU \pm 34.04 compared with 45.66 FU \pm 15.87 for cells transfected with the wild type construct ($p = 0.0310$ and $p = 0.0002$ respectively). Furthermore, cells transfected with the p.R2355W variant had a statistically significantly higher calcium release at 1mM caffeine than the p.D1056H variant ($p = 0.0105$). Cells transfected with the p.D3986E variant behaved in a similar way to wild type transfected cells, just as they did in chapter 4. The p.D3986E transfected cells produced a calcium release of 68.23 FU \pm 4.582 which was not statistically significantly different from the wild type response ($p = 0.2605$). The response of the p.D3986E transfected cells was also statistically significantly lower than the p.R2355W response ($p = 0.0006$) but not the p.D1056H response ($p = 0.1772$).

A 2mM caffeine, once again the p.D3986E transfected cells did not produce a response significantly different from wild type (258.9 FU \pm 85.19 and 186 FU \pm 80.43 respectively; $p=0.5636$). Cells transfected with the p.D1056H and p.R2355W variants both produced a calcium release that was statistically significantly different to wild type. p.D1056H transfected cells produced a response of 765.3 FU \pm 273.7 ($p=0.0408$ compared to wild type) and cells transfected with the p.R2355W variant produced a response of 807.5 FU \pm 358.1 ($p=0.0362$ compared to wild type). At the caffeine concentrations of 4mM, 8mM and 20mM, no statistically significantly different amount of calcium release was observed between any of the constructs under investigation in this chapter.

6.3.4 Differential expression of pTUNERYR1 constructs

Experiments were performed to examine the sensitivity of *RYR1* variants at lower and higher expression levels. The expression level of *RYR1* was induced to a lower and a higher expression level than that used in the initial experiments by using 2.5 μ M IPTG and 250 μ M IPTG respectively. For each IPTG concentration and construct examined $n=4$. Cells expressing *RYR1* at a higher and lower level were exposed to the same caffeine series as cells transfected with pTUNERYR1 and induced with 25 μ M IPTG. Dose response curves were created in the same way as before and the EC_{50} was calculated for each expression level (Figure 6.6). The increase or decrease in expression for cells transfected with wild type pTUNERYR1 had no effect on the EC_{50} . The EC_{50} of cells transfected and induced with 25 μ M IPTG was 3.804mM. The EC_{50} did increase slightly to 4.328mM (SEM = 0.871, 95% CI = 1.349-6.893) when the cells were induced with 2.5 μ M IPTG and decrease to 3.05mM (SEM = 0.273, 95% CI = 2.427-3.943) when the cells were induced with 250 μ M IPTG but neither of these reached statistical significance ($p=0.876$ and $p=0.3197$ respectively). Similar results were observed for cells transfected with the p.D1056H variant. The EC_{50} for cells induced with 25 μ M IPTG was 1.834mM compared with 1.914mM (SEM = 0.144, 95% CI = 1.618-2.358) with 2.5 μ M IPTG induction and 2.344mM (SEM = 0.392, 95% CI = 1.86-3.87) for

250 μ M IPTG. Once again, these were not statistically significantly different ($p=0.7846$ and $p=0.1304$ respectively). Cells transfected with the p.R2355W variant and induced with 25 μ M IPTG had an EC_{50} of 1.378mM compared with 3.87mM (SEM = 0.731, 95% CI = 2.237-6.891) for an induction level of 2.5 μ M and 2.842mM (SEM = 0.242, 95% CI = 2.09-3.34) for 250 μ M IPTG. The EC_{50} of cells induced with 2.5 μ M IPTG was statistically significantly higher than cells induced with 25 μ M IPTG ($p=0.0342$) and 250 μ M IPTG ($p=0.0222$). An increase in expression level of the p.R2355W variant from the 25 μ M IPTG level had no significant effect on EC_{50} ($p=0.2184$). The opposite occurred for cells transfected with the p.D3986E variant. A decrease in expression (2.5 μ M IPTG induction) resulted in no significant difference in EC_{50} when compared to the 25 μ M IPTG induction ($EC_{50} = 3.762$ mM and 4.667mM respectively; $p=0.3713$. For the 2.5 μ M induction the SEM = 0.105 and 95% CI = 3.49-4.16). Conversely, cells induced with 250 μ M IPTG had an EC_{50} of 2.724mM (SEM = 0.211, 95% CI = 2.069-3.412), which was statistically significantly lower than for both the 2.5 μ M IPTG level ($p=0.0036$) and the 25 μ M IPTG level ($p=0.0261$).

The EC_{50} of cells transfected with wild type pTUNERYR1 and induced with 2.5 μ M, 25 μ M and 250 μ M IPTG was not statistically significantly different than the EC_{50} of cells transfected with the p.R2355W variant and induced with 2.5 μ M IPTG. ($p=0.7102$, $p=0.541$ and $p=0.943$ respectively) (Figure 6.7). Furthermore, the decreased expression level of the p.R2355W variant produced an EC_{50} that was statistically significantly higher than cells expressing the p.D1056H variant at the 2.5 μ M and 25 μ M IPTG induction levels ($p=0.002$ and $p=0.0061$ respectively) as well as being substantially lower than cells induced at the highest level ($p=0.0556$).

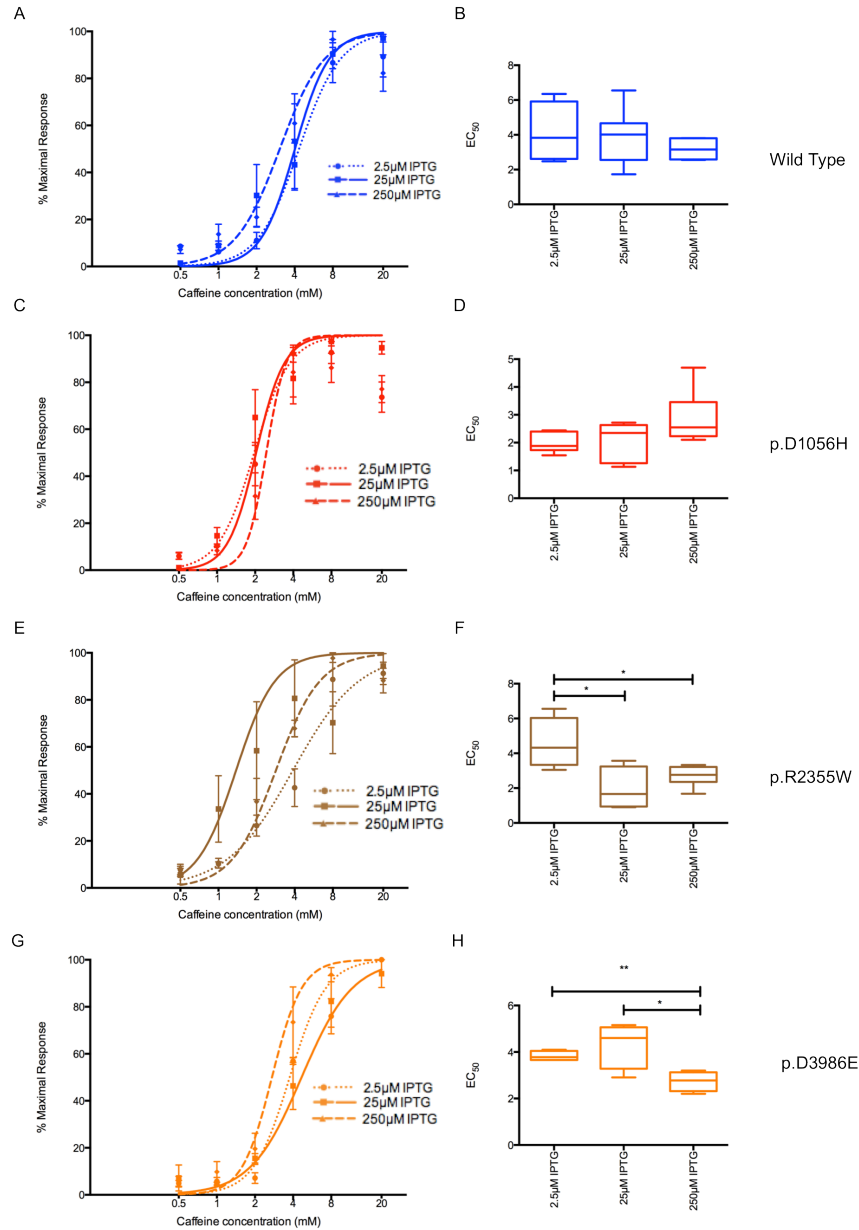


Figure 6.6 – The effect of increased and decreased expression on the EC₅₀ of cells transfected with pTUNERY1 constructs.

(A-B) The EC₅₀ of cells transfected with wild type pTUNERY1. The increase in expression through increased IPTG induction of pTUNE constructs had no effect on the EC₅₀ of cells transfected with wild type pTUNERY1. (C-D) The EC₅₀ of cells transfected with p.D1056H pTUNERY1. The increase in expression had no effect on the EC₅₀ of cells transfected with the p.D1056H construct. (E-F) The EC₅₀ of cells transfected with p.R2355W pTUNERY1. An increased expression of the p.R2355W variant had no effect on the EC₅₀ of the transfected cells. However, a decrease in expression (2.5 μM IPTG induction) resulted in an EC₅₀ that was statistically significantly higher than cells induced with 25 μM and 250 μM IPTG. (G-H) The EC₅₀ of cells transfected with p.D3986E pTUNERY1. A decreased expression of the p.D3986E variant had no effect on the EC₅₀ of transfected cells. However, an increase in expression (250 μM IPTG induction) resulted in an EC₅₀ that was statistically significantly lower than cells induced with 2.5 μM and 25 μM IPTG. For the dose-response graphs, data points are mean plus and minus the standard error of the mean. Box plots are presented as the median, the upper and lower quartiles and the maximum and minimum data points. *p < 0.05, **p < 0.01.

Cells transfected with the p.D3986E variant and induced to a higher level of expression through exposure to 250 μ M IPTG produced an EC₅₀ that was similar to the value observed for causative MH mutations. The EC₅₀ dropped to 2.724mM which was statistically significantly lower than cells transfected with wild type pTUNERYR1 and induced with 25 μ M IPTG (p=0.0398). The EC₅₀ of cells transfected with p.D3986E pTUNERYR1 induced with 250 μ M IPTG was not statistically significantly different from the p.D1056H and p.R2355W variants (p=0.1233 and p=0.2713 respectively).

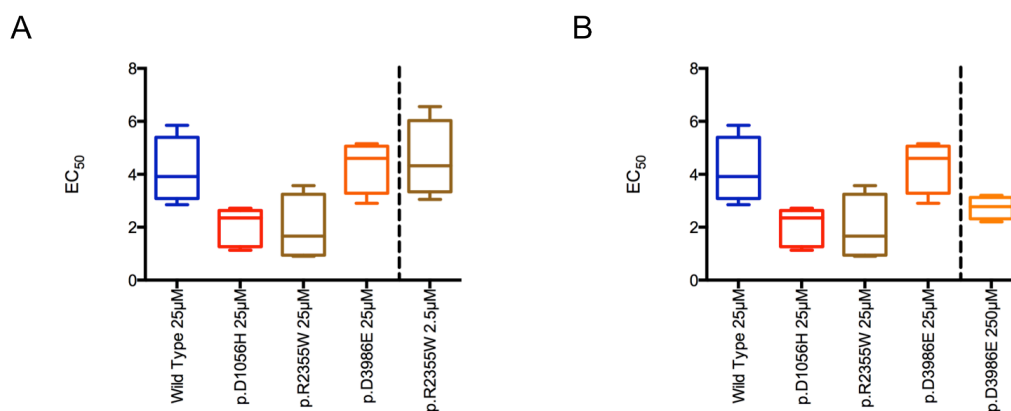


Figure 6.7 – Differential expression of the p.R2355W and p.D3986E variants and the subsequent EC₅₀. (A) Lowering the expression level of the p.R2355W variant causes the EC₅₀ to increase to a level similar to wild type and p.D3986E transfected cells. (B) Increasing the expression level of the p.D3986E variant causes the EC₅₀ to decrease to a level similar to MH mutations. Box plots are shown as the median, the upper and lower quartiles and the maximum and minimum data points.

6.3.5 Area under the curve measurements of HEK293 cells expressing wild type and mutant *RYR1* at different levels

Area under the curve measurements were taken from the traces obtained from the caffeine-induced calcium release experiments carried out on HEK293 cells transiently transfected with pTUNERYR1 and induced with either 2.5 μ M or 250 μ M IPTG (Figure 6.8). Cells transfected with wild type pTUNERYR1 had a trend to release more calcium at every caffeine concentration when they were induced with 250 μ M IPTG. However, at the 1mM and 2mM doses of caffeine, the increase in calcium release was not statistically significantly higher (p=0.348 and p=0.2434 respectively).

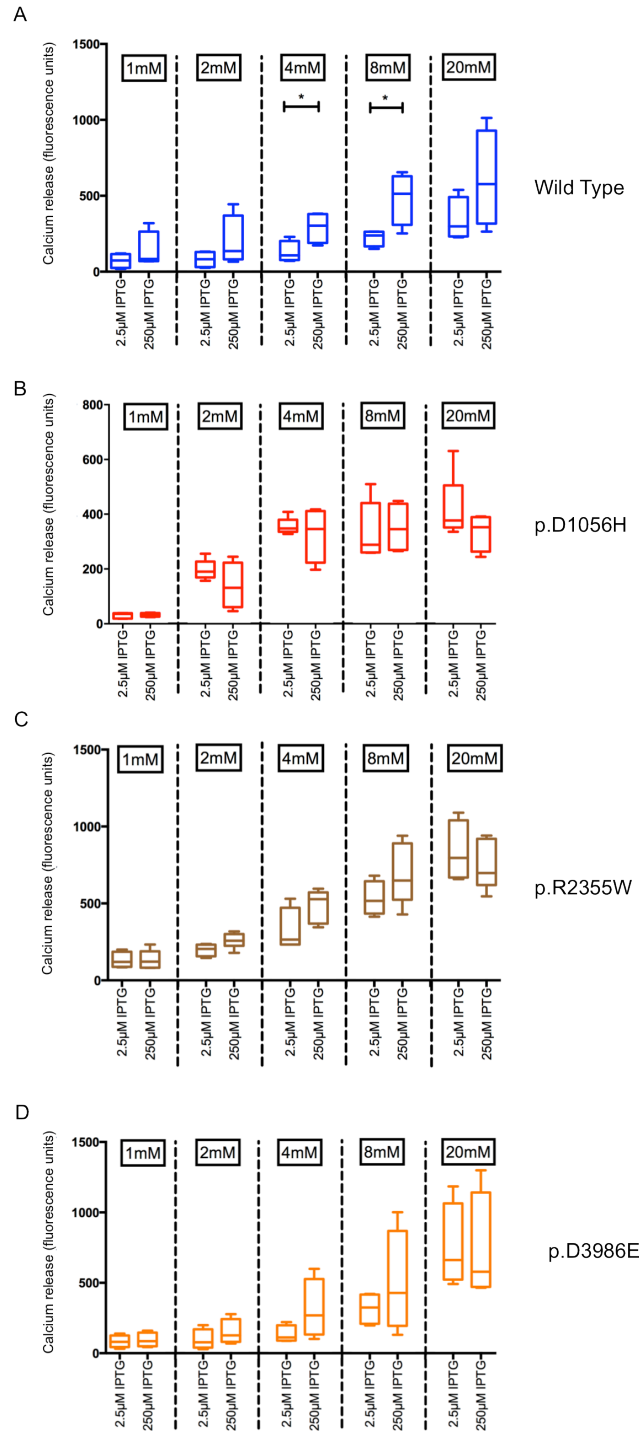


Figure 6.8 – Area under the curve measurements of HEK293 cells transiently transfected with pTUNERYR1 constructs and induced to differing levels of expression.

(A) Wild type pTUNERYR1 induced with 2.5µM and 250µM IPTG. The increase in *RYR1* expression had no effect on the amount of calcium release at 1mM and 2mM caffeine. However, at both 4mM and 8mM caffeine, a statistically significantly higher amount of calcium release was observed in cells expressing *RYR1* to a higher level. This effect was not seen at 20mM caffeine. (B-D) Cells transfected with the mutant pTUNERYR1 constructs did not display a statistically significant amount of calcium release at any caffeine concentration when expression was increased with 250µM IPTG. Box plots are shown as the median, the upper and lower quartiles and the maximum and minimum data points. *p < 0.05.

However, at 4mM and 8mM caffeine, a statistically significant increase in calcium release was observed as expression level increased. At 4mM caffeine, the amount of calcium released by wild type transfected cells increased from $129.1 \text{ FU} \pm 34.94$ to $290 \text{ FU} \pm 50.9$ ($p=0.0396$). At 8mM caffeine, the amount of calcium released by wild type transfected cells increased from $223.3 \text{ FU} \pm 26.46$ to $483.9 \text{ FU} \pm 85.26$ ($p=0.0267$). This trend for increased calcium release was not maintained at 20mM caffeine, where a maximum amount of calcium release appeared to have been reached ($p=0.1770$). For the p.D1056H transfected cells, there appeared to be a trend of more calcium release in cells induced with $2.5\mu\text{M}$ IPTG although this did not reach significance at any caffeine concentration investigated in this experiment. Cells transfected with p.D1056H and induced with $2.5\mu\text{M}$ IPTG also appeared to have a much more consistent response. At 2mM and 4mM caffeine the range of calcium release was from 99.1 FU and 198.09 FU respectively compared with 198.09 FU and 220.5 FU for cells induced with $250\mu\text{M}$ IPTG. For cells transfected with the p.R2355W variant there was once again a trend for cells induced with $250\mu\text{M}$ IPTG to have an increase in calcium release compared to cells induced with only $2.5\mu\text{M}$ IPTG, although this did not reach statistical significance at any caffeine concentration used in this experiment. Cells transfected with the p.D3986E variant did not appear to have a clear trend in the amount of calcium released depending on the level of induction. At each caffeine concentration, no significant difference was observed between cells induced with either $2.5\mu\text{M}$ or $250\mu\text{M}$ IPTG. However, similarly to cells transfected with the p.D1056H variant, cells induced with $2.5\mu\text{M}$ IPTG appeared to have a much more consistent calcium release at 4mM and 8mM caffeine when compared to cells induced with $250\mu\text{M}$ IPTG. At 4mM caffeine, cells induced with $2.5\mu\text{M}$ IPTG had a range of calcium release of 133.52 FU compared with 224.5 FU for the $250\mu\text{M}$ IPTG. Similarly, at 8mM caffeine, cells induced with $2.5\mu\text{M}$ IPTG had a range of 498.7 FU compared with 870.7 FU for cells induced with $250\mu\text{M}$ IPTG.

6.3.6 The effect of AICAR on the sensitivity of HEK293 cells transfected with pTUNERYR1 constructs to caffeine

Experiments were performed to examine the effect of AICAR on the caffeine sensitivity of the *RYR1* variants under investigation in this chapter. HEK293 cells were transfected with pTUNERYR1 constructs and induced with 25 μ M IPTG. Some wells of cells were treated with 1mM AICAR overnight at 37°C and 5% CO₂. For each construct n=4 with and without treatment with AICAR. Transfected cells were exposed to the same caffeine series as with previous experiments to examine the effect of AICAR on the caffeine sensitivity of the various *RYR1* constructs under investigation in this chapter. Dose-response curves were plotted and the EC₅₀ of the transfected were calculated (Figure 6.9). There appeared to be no significant effect of AICAR on cells transfected with wild type pTUNERYR1 with the EC₅₀ of untreated cells being 3.881mM (SEM = 0.626, 95% CI = 2.14-6.128) compared with 4.179mM (SEM = 0.546, 95% CI = 2.333-5.811) for cells exposed to AICAR overnight ($p=0.943$).

All MH mutations were statistically significantly affected by the presence of AICAR in the culture medium overnight. The EC₅₀ of cells transfected with the p.D1056H variant increased from 1.872mM (SEM = 0.159, 95% CI = 1.511-2.527) to 8.684mM (SEM = 0.764, 95% CI = 6.518-11.38) upon exposure to AICAR ($p=0.001$). Similarly, the EC₅₀ of cells transfected with the p.R2355W variant was 4.516mM (SEM = 0.29, 95% CI = 3.918-4.832) when exposed to AICAR compared with 1.34mM (SEM = 0.619, 95% CI = 0.02-2.987) for untreated controls ($p=0.0284$). Finally, cells transfected with the p.D3986E *RYR1* variant had an EC₅₀ of 4.667mM (SEM = 0.494, 95% CI = 2.744-5.889) when cultured in AICAR-free conditions compared with an EC₅₀ of 9.961mM (SEM = 1.182, 95% CI 5.255-12.78) in the presence of AICAR.

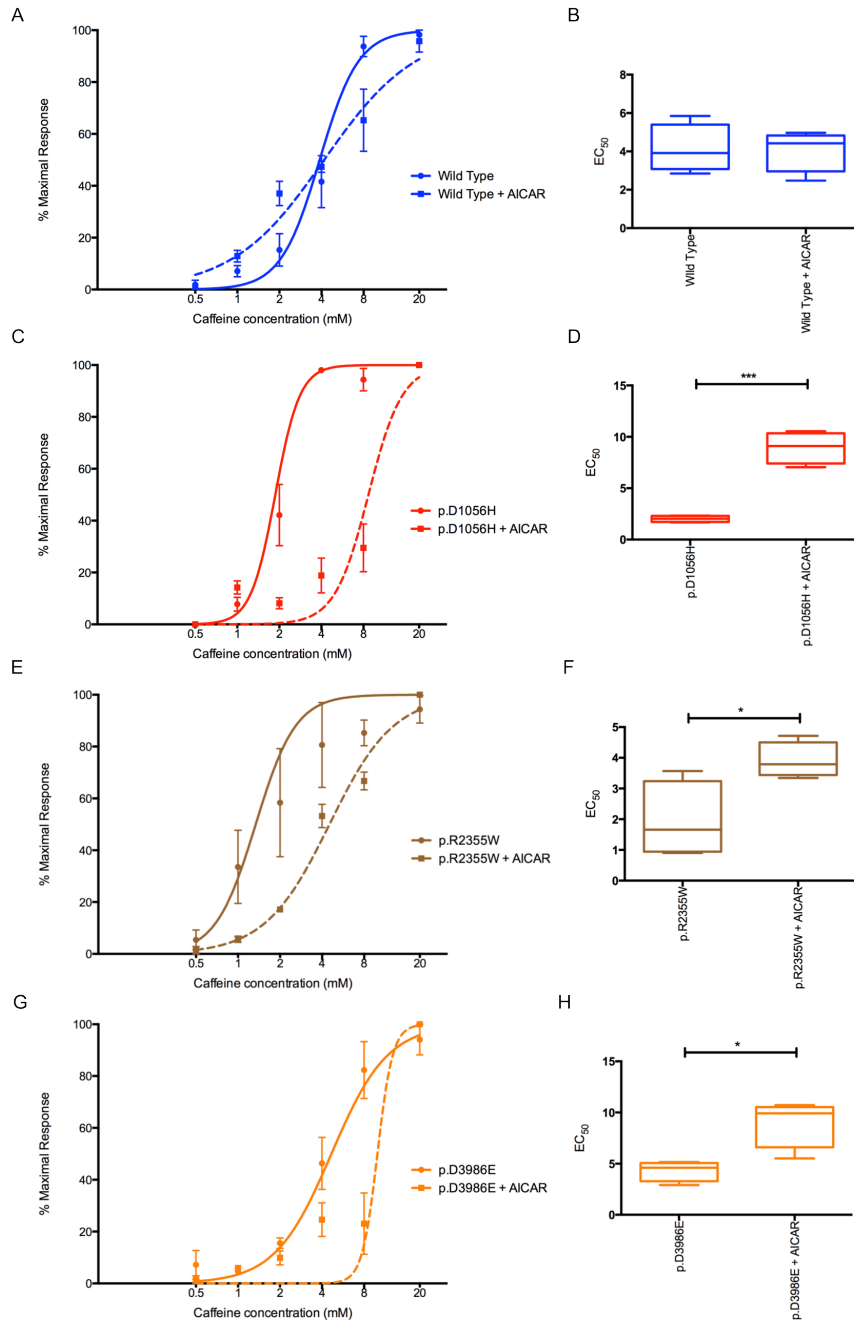


Figure 6.9 – The effect of AICAR on the EC₅₀ of cells transfected with pTUNERYR1 constructs.

(A-B) No statistically significant difference was observed between cells transfected with wild type pTUNERYR1 with or without pre-treatment of AICAR. The EC₅₀ of cells not treated with AICAR was 3.881mM compared with 4.179mM with treatment (p=0.943). (C-H) The treatment of any of the MH variants under investigation in this chapter with AICAR resulted in a statistically significant increase in EC₅₀ as compared with untreated controls. The most dramatic difference was seen in cells transfected with the p.D1056H variant where the EC₅₀ increased from 1.872mM to 8.684mM (p=0.0001). The EC₅₀ of cells transfected with the p.R2355W variant increased to 4.516mM from 1.340mM (p=0.0284) when treated with AICAR and cells transfected with the p.D3986E variant and treated with AICAR saw the EC₅₀ increase from 4.667mM to 9.961mM (p=0.0105). For the dose-response graphs, the data points shown are the mean plus and minus the standard error of the mean. Box plots are shown as the median, the upper and lower quartiles and the maximum and minimum data points. *p<0.05, ***p<0.001.

6.3.7 Viability stain of HEK293 cells transfected with pTUNERYR1 and treated with IPTG and AICAR

To ensure that the presence of AICAR in the culture medium was not causing the effect seen by killing the cells a mutant pTUNERYR1 construct was transfected into HEK293 cells and exposed to either 0 μ M, 25 μ M or 250 μ M IPTG for 72 hours. 48 hours into the experiment some cells were treated with 1mM AICAR overnight in a repeat of the conditions used for the caffeine-induced calcium release experiments. After the 72-hour incubation, cells were pelleted, resuspended in PBS and exposed to a trypan blue viability stain (Figure 6.10). There were no significant differences between the total numbers of cells counted for each of the experimental treatments and there was always substantially more living cells as compared to dead cells. The total percentage of cells alive did appear to decrease with the increasing severity of the experimental treatments with 83.45% of cells alive when untransfected and untreated however the lowest percentage of alive cells was only 77% for the transfected, 250 μ M and 1mM AICAR conditions. Experiments were performed in triplicate and no statistically significant differences were observed between any of the experimental conditions applied.

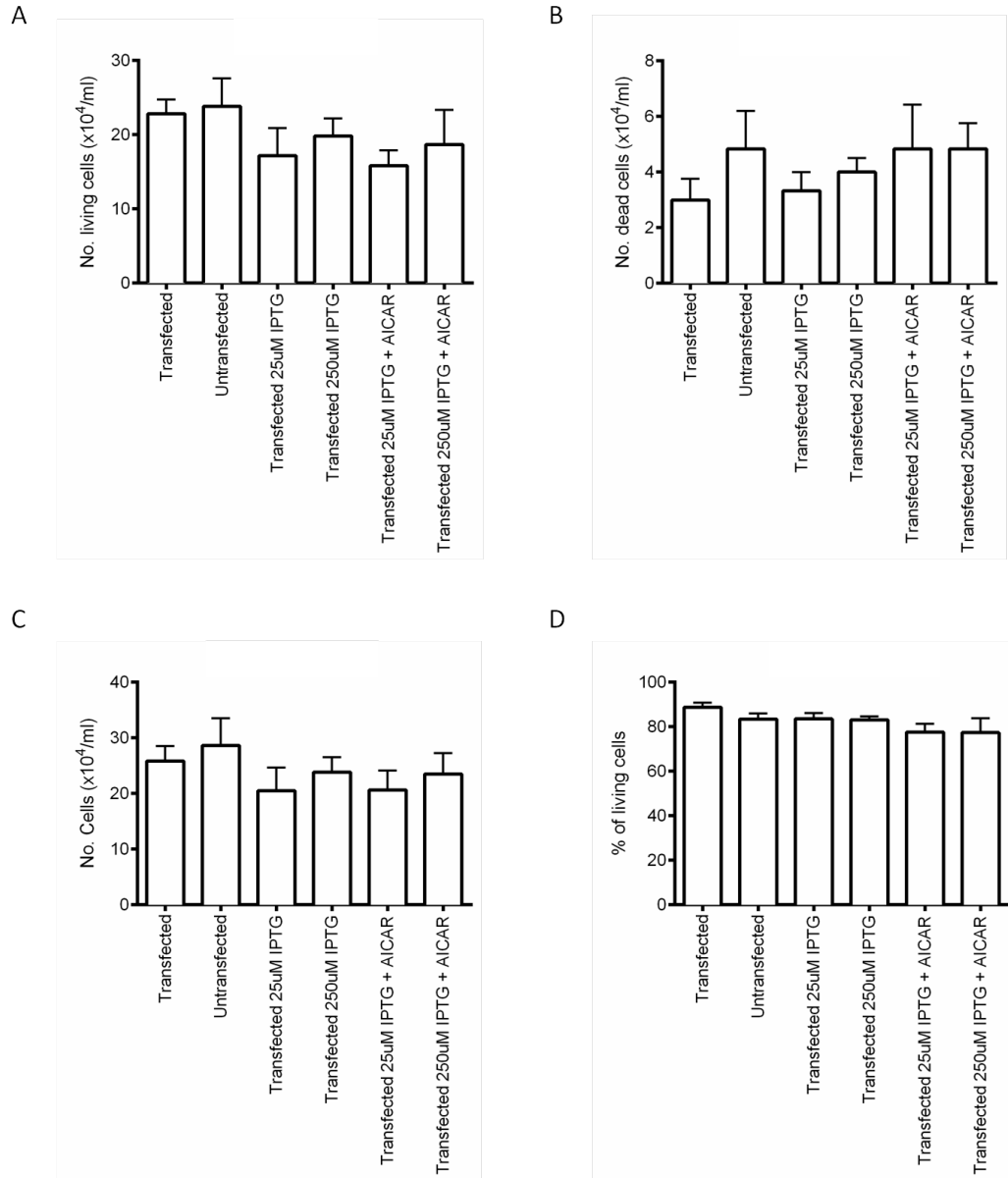


Figure 6.10 – Viability stain of cells transfected with pTUNERY1 and treated with IPTG and AICAR. HEK293 cells were transfected with wild type pTUNERY1. Some cells were induced at a level of 25 μ M IPTG, some were induced with 250 μ M IPTG. Some cells were also exposed to 1mM AICAR overnight before measurements were taken. 72 hours post-transfection and induction with IPTG cells were exposed to a trypan blue viability stain and the number of living and dead cells counted with a haemocytometer (panel A and B). There was a much greater number of living cells compared to dead cells in all experimental conditions and no significant difference between any of experimental conditions in terms of numbers of living or dead cells. Transfection of the pTUNERY1 construct resulted in a slight decrease in the total number of cells which was further reduced upon exposure to either IPTG or AICAR although the difference was not significant (panel C). Panel D shows the percentage of cells that were living after the various treatments. Although there was a trend to have fewer cells alive as the treatments became more extreme this was not statistically significantly different. When cells were transfected, exposed to 250 μ M IPTG and AICAR, 77% of cells were still alive. Data are presented as the mean plus and minus the standard error of the mean.

6.3.8 Comparison between cells transfected with *pcRYR1* and *pTUNERYR1* cDNA constructs

The dose-response curves generated in chapter 4 and this chapter for the wild type and p.D3986E variants in the pcDNA and pTUNE expression vectors are plotted together in Figure 6.11 to examine whether there are any differences in response between the two expression vectors. The EC_{50} of the wild type and p.D3986E variants in both the pcDNA and pTUNE expression vectors were not significantly different. Furthermore, the EC_{50} was not significantly different between the expression vectors. There was a trend for both the pTUNERYR1 constructs to have a slightly elevated EC_{50} but this was not significantly different ($p=0.1213$ for the wild types and $p=0.1781$ for the p.D3986E constructs). There was also no difference between the pcDNA wild type and pTUNE p.D3986E or the pTUNE wild type and the pcDNA p.D3986E ($p=0.1971$ and $p=0.0562$ respectively)

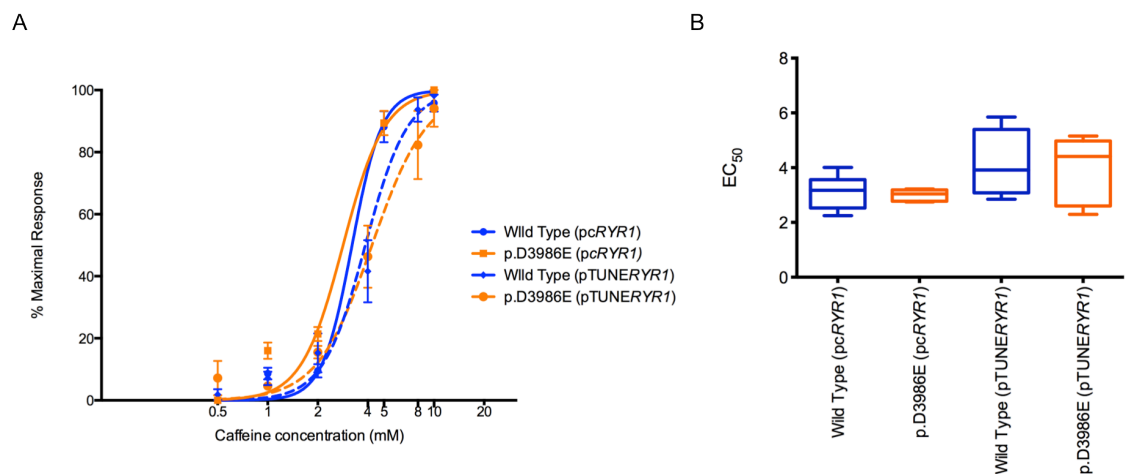


Figure 6.11 – A comparison of the response of wild type and p.D3986E RYR1 in the pcDNA and pTUNE expression vectors.

(A) The dose response curves of wild type and p.D3986E RYR1 in both the pTUNE and pcDNA expression vectors. Data points are the mean plus and minus the standard error of the mean. (B) Box plots of the EC_{50} of each of the wild type and p.D3986E RYR1 constructs in the pTUNE and pcDNA expression vectors. No statistically significant difference in EC_{50} was observed between the two wild type constructs or the two p.D3986E constructs in either expression vector. Box plots are presented as the median, the upper and lower quartiles and the maximum and minimum data points.

6.3.9 Detection of RYR1 expression through western blotting

HEK293 cells were transfected and induced using the same concentrations of IPTG used for the functional experiments. Whole protein was extracted from HEK293 cells 72 hours post-transfection with all pTUNERYR1 constructs. Western blot analysis of the detection of RYR1 at the various IPTG doses is shown in Figure 6.12 and Figure 6.13. Western blots were repeated in triplicate each with a new harvested protein sample. Figure 6.12A shows a representative western blot of RYR1 and tubulin expression when HEK293 cells were transiently transfected with pTUNERYR1 constructs and induced with the incremental doses of IPTG used in this study. Panel B shows the relative intensity of the RYR1 bands detected in comparison to the 'standard' 25 μ M induction level used in the initial experiments. When induced with 2.5 μ M IPTG, RYR1 detection was lowered. Similarly, when 250 μ M IPTG was used to induce the cells, expression was increased.

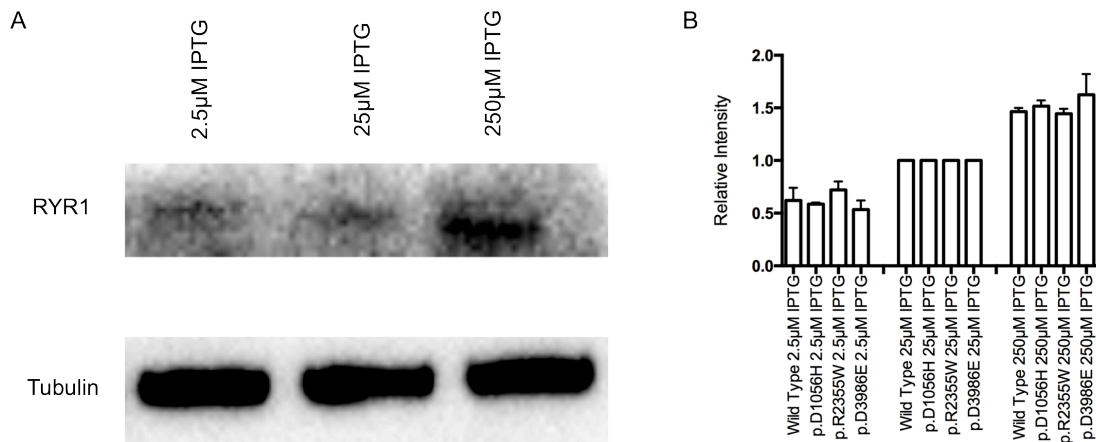


Figure 6.12 – Western blot analysis of HEK293 cells transiently transfected with pTUNERYR1 constructs
(A) Representative western blot image of HEK293 cells transiently transfected with pTUNERYR1 and induced with incremental doses of IPTG. Proteins were run on a 8% polyacrylamide gel and blotted overnight onto a PVDF membrane. The membrane was probed for RYR1 (upper panel) and alpha tubulin (lower panel) using monoclonal antibodies. **(B)** After determining that equal amounts of protein were run using the alpha tubulin control, the relative intensities of the RYR1 protein bands were determined using Image Lab software with the 25 μ M IPTG set as the comparison band. All pTUNERYR1 constructs induced with 2.5 μ M IPTG were expressed at a lower level compared with 25 μ M IPTG and all constructs induced 250 μ M IPTG were expressed at a higher level. No statistically significant difference in protein expression was observed between any of the constructs when induced with the same amount of IPTG. Data are presented as the mean plus and minus the standard error of the mean.

Figure 6.13 shows the combined data for all pTUNERYR1 constructs pooled according to the level of IPTG used to induce RYR1 expression. Cells induced with 25 μ M IPTG were used as the reference band to relatively quantify the cells induced with 2.5 μ M and 250 μ M IPTG. When induced with 2.5 μ M IPTG, a statistically significantly lower amount of RYR1 was detected as compared to both 25 μ M and 250 μ M IPTG ($p < 0.0001$). Similarly, cells induced with 250 μ M IPTG produced a statistically significantly higher amount of RYR1 compared with both 2.5 μ M and 25 μ M IPTG. Pre-treatment with 1mM AICAR overnight had no effect on RYR1 expression in transfected cells (Figure 6.14). Additionally, the presence of AICAR had no effect on untransfected cells.

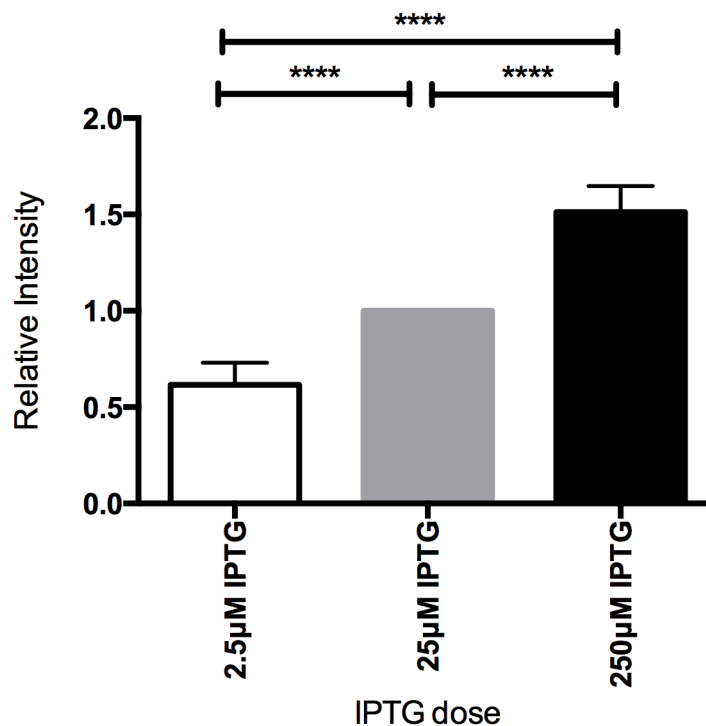


Figure 6.13 – Relative quantity of RYR1 when pTUNERYR1 constructs are pooled into their respective IPTG concentrations.

The data obtained from the western blots on all pTUNERYR1 constructs were pooled according to the concentration of IPTG used to induce expression. 25 μ M IPTG was used as the band for relative quantification of the 2.5 μ M and 250 μ M IPTG inductions. Cells induced with 2.5 μ M IPTG produced a statistically significantly lower amount of RYR1 in comparison to both 25 μ M and 250 μ M IPTG ($p < 0.0001$). Cells induced with 250 μ M IPTG produced a statistically significantly higher amount of RYR1 in comparison to both 2.5 μ M and 25 μ M IPTG. Data points are presented as the mean plus or minus the standard error of the mean. **** $p < 0.0001$.

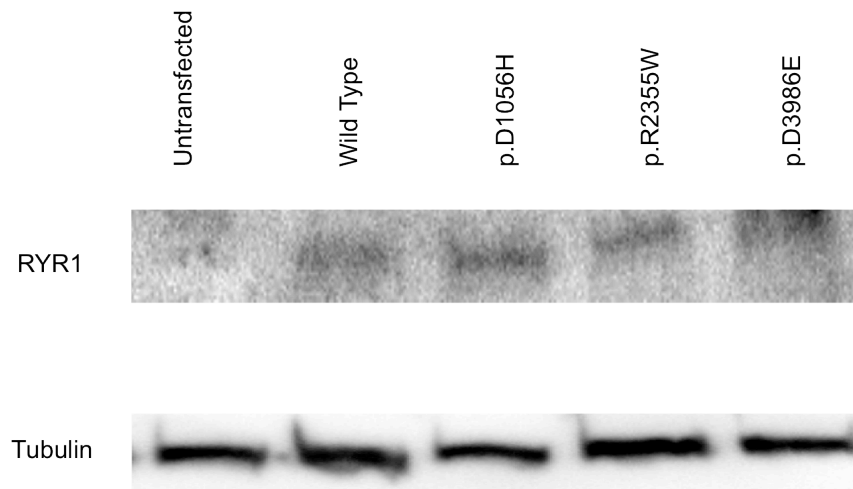


Figure 6.14 – Western blot analysis of HEK293 cells transiently transfected with pTUNERYR1 constructs and exposed to AICAR.

Representative western blot image of HEK293 cells transiently transfected with pTUNERYR1, induced with 25 μ M IPTG and incubated with 1mM AICAR overnight. Proteins were run on a 8% polyacrylamide gel and blotted overnight onto a PVDF membrane. The membrane was probed for RYR1 (upper panel) and alpha tubulin (lower panel) using monoclonal antibodies. RYR1 expression was not affected by the overnight incubation with 1mM AICAR. Additionally, the presence of 1mM AICAR had no affect on untransfected cells.

6.3.9 Comparison of wild type RYR1 in pcDNA and pTUNE expression vectors

All of the dose response experiments that involved wild type *RYR1* were plotted together to examine any differences between the different wild type constructs (Figure 6.15). No statistically significant difference was observed between any of the wild type constructs under investigation in this project (HEK293 cells both stably and transiently transfected with wild type pcRYR1, HEK293 cells transiently transfected with wild type pTUNERYR1 and HEK293 cells transiently transfected with wild type pTUNERYR1 induced to differing levels of expression).

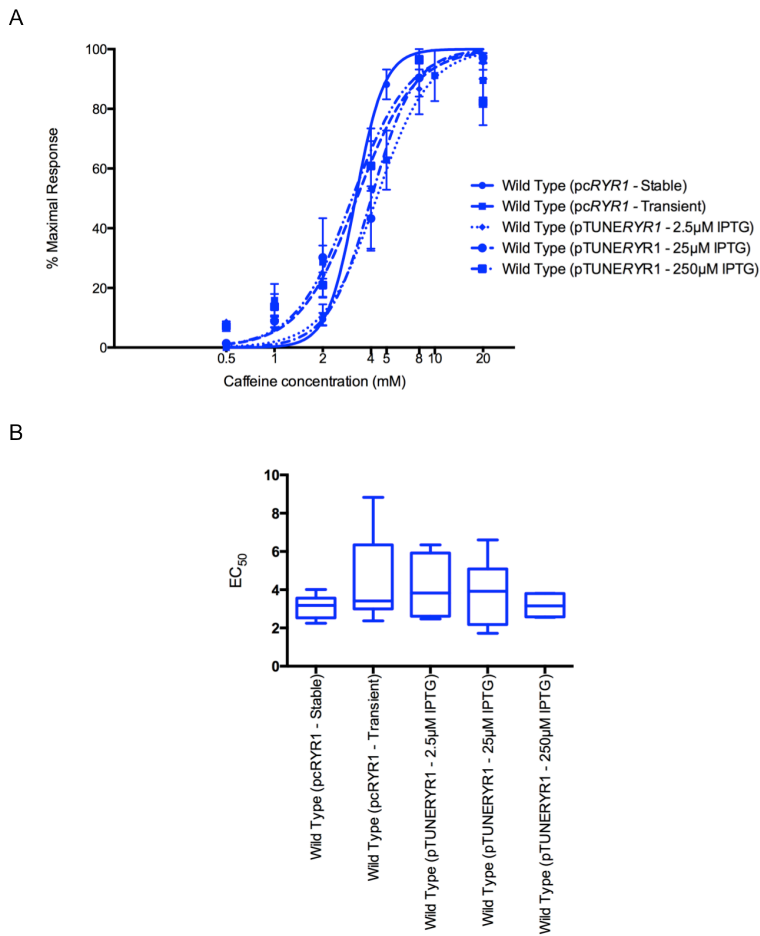


Figure 6.15 – A comparison of all wild type *RYR1* constructs and conditions used in this thesis. (A) Dose response curve for all the wild type constructs and conditions used. The EC_{50} of the various wild types ranged from 3.05mM to 4.328mM. Data points are the mean plus and minus the standard error of the mean. (B) Box plots showing the EC_{50} of all wild type constructs used in this thesis. No statistically significantly different response was seen between any wild type used. Box plots are shown as the median, the upper and lower quartiles and the maximum and minimum data points.

6.4 Discussion

One of the primary goals of this chapter was to functionally assess the consequences of three genetic variants in the *RYR1* gene that have been associated with MH. One variant, the p.D1056H was selected for study based on the occurrence of the mutation in an individual who had suffered an EHS reaction but upon MH testing proved to have a normal IVCT response.

Additionally, the use of the pTUNE inducible expression vector allowed us to carry out experiments examining the effect of an increase or decrease in wild type and mutant *RYR1* expression on the sensitivity of transfected cells to caffeine. This follows on from an accumulation of recent data suggesting that the expression level of *RYR1* may play a role in the variability of MH responses seen in the population.

Finally, in this chapter, the effect of AICAR on the sensitivity of transfected cells to caffeine was also investigated. AICAR has recently become a potential candidate for the prophylactic treatment of EHS and has been proven to play a role in the reduction of baseline resting calcium levels that has previously been implicated as a large contributor to the MH response.

6.4.1 p.D1056H

The p.D1056H *RYR1* variant has been associated with both MH and EHS. Interestingly, the patient who suffered an EHS reaction was tested for MH and diagnosed as MHN. However, in the HEK293 cell system established in this thesis, the p.D1056H variant responds in a typically MH fashion. The EC_{50} of cells transfected with the p.D1056H variant and induced at a level of 25 μ M IPTG was 1.834mM compared with 3.804mM for wild type transfected cells ($p=0.0191$). At 2mM and 4mM caffeine, the response generated from p.D1056H transfected cells as a percentage of the maximum response was statistically significantly higher than the equivalent wild type response ($p=0.0471$ and $p=0.0498$ respectively). Additionally, the amount of calcium released at both 1mM and 2mM caffeine was statistically significantly higher than the wild type response. The above data is indicative of a causative MH variant and it appears as though it should be added to the genetic diagnostic panel for MH. It is possible that there is an additional genetic variant within the EHS patient either preventing the full MH phenotype becoming apparent or driving the phenotype down a specifically EHS route. The *RYR1* variant was identified through exome sequencing, the full results of any potential additional genetic variants that may be responsible for the EHS

phenotype are still pending but may contribute to further understanding the differences between EHS and MH. A further possibility is that the MH family containing this variant may have an additional genetic variant that pushes the phenotype towards full MH however, due to the fact that on a defined genetic background, the p.D1056H variant produces a distinct MH phenotype this seems unlikely. When the expression level of p.D1056H RYR1 was increased or decreased compared with the initial experiments, no differences were observed in either the EC₅₀ or the amount of calcium released, ruling out differential expression as a potential cause in the variability observed in EHS and MH phenotypic presentation.

6.4.2 p.R2355W

Cells transfected with the p.R2355W RYR1 variant and induced with 25 μ M IPTG produced a typical MH phenotype. The EC₅₀ of cells transfected with the p.R2355W variant was 1.378mM compared with 3.804mM for wild type transfected cells (p=0.047). At 2mM caffeine, the response produced by the p.R2355W transfected cells was statistically significantly higher as a percentage of the maximum response than wild type transfected cells. Furthermore, the amount of calcium released at 1mM and 2mM caffeine was statistically significantly higher than the equivalent wild type response. Based on this data, it is clear that the p.R2355W variant is the causative factor of MH in the 14 families it has been identified in. Data previously obtained in primary cells isolated from muscle biopsy specimens carrying this variant had strongly hinted that this variant was causative of MH but failed to place the p.R2355W variant onto the genetic diagnostic panel for MH because cells from only one family were available for testing (Wehner et al., 2004). Cells isolated from patients carrying the mutation displayed an increased sensitivity to caffeine, halothane and 4-CmC but without a second family to test this was insufficient for the inclusion of this variant onto the genetic diagnostic panel. No such problems exist for the work presented in this chapter due to the use of a recombinant system on a defined genetic background

and therefore, the work presented meets the EMHG criteria for adding the p.R2355W variant to the genetic diagnostic panel for MH. Cells transfected with the p.R2355W variant displayed no difference when induced to a higher expression level with IPTG, however, when induced with a smaller concentration of IPTG, the EC_{50} reached a statistically significantly higher level which was in line with the wild type responses at all IPTG concentrations. The reason for this is unclear but may be supportive of the hypothesis put forward by Grievink and Stowell (2010). If a decrease in the p.R2355W variant can cause the sensitivity of the cells expressing it to decrease, then an increase in wild type expression as a compensatory mechanism may provide a similar effect. Such an effect would result in variability seen between patients carrying the p.R2355W variant based on the expression level of each allele.

6.4.3 p.D3986E

The data obtained from cells transfected with the p.D3986E pTUNERYR1 variant and induced with 25 μ M IPTG is consistent with the data obtained in chapter 4 using the pcRYR1 construct. The EC_{50} of cells transfected with the p.D3986E variant was similar to data obtained from wild type transfected cells. The p.D3986E had an EC_{50} of 4.667mM compared with 3.804mM for wild type transfected cells ($p=0.6901$). At every caffeine concentration used in these experiments, the amount of calcium released from p.D3986E transfected cells was not statistically significantly different from wild type transfected cells.

Unlike the data obtained in chapter 4, cells transfected with the p.D3986E pTUNERYR1 construct did not produce a significantly different response as a percentage of the maximum when compared to wild type. HEK293 cells stably transfected with the p.D3986E pcRYR1 construct had displayed a significantly different increase in the response as a percentage of the maximum response at both 1mM and 2mM caffeine ($p=0.046$ and $p=0.0033$ respectively) compared to wild type transfected cells. This increase in response at 1mM and 2mM caffeine resulted in the EC_{25} of cells transfected

with the p.D3986E variant to be dramatically reduced and the EC₁₀ to be statistically significantly reduced. This was not the case in cells transfected with the p.D3986E pTUNERYR1 construct. Both the EC₁₀ (2.502mM) and EC₂₅ (4.297mM) were similar to cells transfected with the wild type pTUNERYR1 construct (EC₁₀ = 2.769mM; p= 0.7849 and EC₂₅ = 3.441mM; p=0.5126). The reason for the difference in EC₁₀ and EC₂₅ for cells transfected with either the pcRYR1 or the pTUNERYR1 construct is not clear. It may be due to differences generated in the cellular environment caused by stable expression of the mutant *RYR1* gene. Evidence suggests that the MH response is exacerbated by a chronic increase in basal resting calcium levels. A HEK293 cell line stably expressing a *RYR1* variant may have an increased resting calcium level due to the prolonged expression over time.

A decrease in expression level for cells transfected with the p.D3986E variant had no effect on the cells' sensitivity to caffeine. However, an increase in induction of expression level resulted in a statistically significant decrease in EC₅₀. Interestingly, this decrease in EC₅₀ brought it in line with that of clear causative MH variants. The data obtained from these experiments may, at least in part, explain how patients carrying the p.D3986E variant can still be MHS despite the variant appearing to produce a wild type phenotype in HEK293 cells as well as further support the suggestion that expression levels of specific alleles of *RYR1* can result in the variable responses seen in patients.

6.4.5 The effect of AICAR on the sensitivity of RYR1 channels

Recently, AICAR, was found to be fully protective of the heat-induced EHS phenotype seen in MH mice (Lanner et al., 2012). The protective effect observed was attributed to a decrease in the resting calcium level in the skeletal muscle fibres of the MH mice. AICAR was, however, seen to have no effect on the anaesthesia-induced MH phenotype in the *RYR1* mutant mice. In Lanner et al. (2012), no experiments were carried out to examine the effect of AICAR on the sensitivity of the mutant *RYR1*

channels. In this project, HEK293 cells were transfected with pTUNERYR1 constructs and induced with 25 μ M IPTG. Cells were incubated with 1mM AICAR overnight, prior to caffeine-induced calcium release experiments. AICAR appeared to have no effect on cells transfected with the wild type pTUNERYR1 construct, as the EC₅₀ remained statistically unchanged. However, for all the mutant pTUNERYR1 constructs, a statistically significant increase in EC₅₀ was observed. AICAR has been found to protect against EHS so it is perhaps not surprising that the most dramatic effect was seen in cells transfected with the p.D1056H variant, which has been implicated in EHS. The EC₅₀ of cells transfected with p.D1056H increased from 1.872mM to 8.684mM. A milder, yet still substantial response was observed in cells transfected with the p.R2355W variant. The EC₅₀ of these cells increased from 1.34mM to 4.516mM, a value very similar to wild type transfected cells. Interestingly, Wehner et al. (2004) reported that this variant did not have a resting calcium level higher than wild type when primary cells were tested. Although this apparently normal resting calcium level may have been observed due to the measurement method employed, the result obtained by Wehner et al. (2004) may help explain why the p.R2355W variant responded in a slightly milder manner to the other variants under investigation in this project. Although wild type transfected cells appeared to have no response, viability experiments were carried out to show that IPTG and AICAR were not killing the cells, resulting in the decrease in sensitivity observed. Furthermore, western blot analysis showed that the level of expression of *RYR1* was not affected by AICAR.

Perhaps most surprising was the result obtained from cells transfected with the p.D3986E variant. The addition of AICAR to cells still resulted in a statistically significant increase in EC₅₀ from 4.667mM to 9.961mM even though the initial experiments indicated that this variant responded in a similar way to wild type transfected cells. This result, combined with the data obtained from an overexpression of the p.D3986E variant through induction with 250 μ M IPTG suggests that the p.D3986E variant may have a more complicated role in MH pathogenesis than was first suspected from the initial experiments.

One possibility is that, although the p.D3986E possesses a seemingly mild sensitivity to caffeine when compared to other MH variants, the resting calcium of cells expressing this variant is still elevated. This theory is supported by data obtained from the Perez laboratory that has hinted that the region that the p.D3986E variant sits in is highly relevant to the maintenance of normal resting calcium. Previous data published by the same group has shown that an increase in *RYR3* expression results in an increase in resting calcium whereas as *RYR1* expression increases, the resting calcium remains constant (Perez et al., 2005). Subsequent experiments using chimeric channels, with sections of *RYR3* inserted into the *RYR1* coding sequence, identified a region containing the 3986 residue as key for maintaining the resting calcium.

A mutation in this region could feasibly cause *RYR1* to start behaving in a similar fashion to *RYR3*, resulting in elevated resting calcium. This is further supported by the data obtained in this chapter regarding the expression level of the p.D3986E variant. Only the p.D3986E variant produced an increased sensitivity to caffeine as the expression level increased, which is analogous to the data obtained from the original Perez study on *RYR3*. An increase in the expression of this variant may be causing the resting calcium level to increase therefore predisposing the cells to be more sensitive to caffeine. Previous studies have hinted that if the resting calcium level is corrected then sensitivity to channel agonists such as caffeine are reduced also. By increasing the resting calcium level through overexpression, the p.D3986E variant may be predisposing the cells to respond in an 'MH positive' manner meaning that this variant may yet be the cause of MH in the families it has been identified in. Data obtained in this chapter shows that an increase in expression level of all constructs under investigation did not result in a significant increase in calcium release meaning that the increase in sensitivity of the p.D3986E variant is being achieved through a different mechanism, possibly an elevated resting calcium level.

6.4.6 Wild types and p.D3986E in pcRYR1 and pTUNERYR1.

With the addition of the data obtained from all induction levels of wild type pTUNERYR1 transfected cells, a total of five different experiments have been carried out using a wild type *RYR1* construct. The data obtained for all of these experiments was plotted together in this chapter and no significant differences were observed. This data confirms the reproducibility of these experiments regardless of the expression vector that wild type *RYR1* is in or the level of expression produced in the cells. Coupled with the fact that the data obtained on the p.D3986E variant in the pTUNERYR1 construct (at a standard 25 μ M IPTG induction level) was also not statistically significantly different from that obtained in the pcRYR1 experiments suggests that the systems utilised in this thesis is robust and reliable. However, as demonstrated through the results obtained in cells expressing p.R2355W at a low level and p.D3986E at a high level, it is important to follow up such experiments with expression analysis through western blotting.

6.5 Future work

The work presented above represents a first step into examining the effect of the expression level of wild type and mutant *RYR1* on the sensitivity to caffeine in HEK293 cells. Three *RYR1* variants have been studied in this chapter and the obvious next step is to expand this to as many *RYR1* variants as possible to get a better understanding of the role of the expression level of *RYR1* in MH pathogenesis. The p.D3986E variant was the only mutation that showed an increase in sensitivity to caffeine as the expression level increased. An obvious next step for this work would be to examine the expression level of the p.D3986E allele in the patients it has been identified in. Allele-specific PCR has previously been used to assess the expression level of each *RYR1* allele and the same could be done with this variant (Grievink and Stowell, 2010). As explained above, the resting calcium level of this variant is of particular interest to us due to the proximity of this variant to an identified region of *RYR1* implicated in resting

calcium levels combined with the data outlined above. It would be of interest to see if all MH-associated variants within this region also cause the sensitivity of *RYR1* to increase, including the p.G3990V variant for which functional data was presented in chapter 4. Future work using the pTUNE inducible vector could also focus on measuring the resting intracellular calcium level of all variants under investigation in this thesis to allow us to get a clearer picture of the role of resting calcium in MH pathogenesis. Of particular interest would be the results of cells expressing p.R2355W at high and low levels to examine whether this is the reason for the reduced sensitivity to caffeine.

The measurement of resting calcium levels in HEK293 cells is difficult to ascertain and conflicting results are present in the literature regarding the resting calcium level of the same MH variants depending on whether they are expressed in HEK293 cells or muscle cells (Tong et al., 1999b, Lopez et al., 2005). Also, an assumption was made in this chapter that AICAR is still acting on HEK293 cells in the same way observed in the Lanner et al. (2012) study. Experiments measuring resting calcium levels should be performed with and without AICAR treatment to confirm this assumption. Ideally, these variants should be transferred to the pHSVPrPUC expression vector, packaged into HSV-1 virions and expressed in dyspedic myotubes to obtain a more accurate resting calcium level.

6.6 Conclusions

Based on the data presented in this chapter, the p.D1056H and p.R2355W variant can be added to the genetic diagnostic panel for MH. The p.R2355W variant has long been suggested as causative of MH as it has been found in association with the MHS phenotype in 7 families in the UK and a total of 9 families worldwide. The functional data presented in this chapter supports work already carried out by Wehner et al. (2004) and confirms its functional role in MH. The p.D1056H variant has what appears to be a more complicated role in MH. The functional data presented above is

supportive of the variant being added to the genetic diagnostic panel for MH and the variant is almost certainly the cause of MH in the family it has been identified in. However, the presence of this variant in an individual who suffered an EHS reaction yet was diagnosed as MHN highlights the complicated genetic nature of MH and strengthens the link between RYR1 variants and EHS.

The work presented in this chapter also supports the growing body of evidence to suggest that the expression level of *RYR1*, at least in part, contributes to the variability seen in the MH experience of susceptible patients. Variations in the expression of the p.R2355W and p.D3986E variants were shown to alter the EC_{50} of transfected HEK293 cells when exposed to caffeine. Reduced expression of the p.R2355W variant resulted in an EC_{50} that decreased from an 'MH-like' range to one that was indistinguishable from the wild type response. Conversely, the p.D3986E variant had been responding in a wild type manner until the expression level was increased. This resulted in the sensitivity of transfected cells to caffeine to increase as seen by the significant decrease in EC_{50} .

The work presented also adds to recent work on the role of AICAR on the sensitivity of mutant RYR1 channels. AICAR caused a significant decrease in caffeine sensitivity for all variants under investigation in this chapter. The effect of AICAR on the p.D3986E was perhaps the most surprising given the fact that it had previously responded in a wild type manner. AICAR works by reducing calcium leak from mutant channels, hinting that the resting calcium level of patients carrying the p.D3986E variant may still be elevated and contributing to the MH phenotype.

Chapter Seven - Final discussion

7.1 Introduction

Since the introduction of the EMHG guidelines for the inclusion of variants in the *RYR1* gene onto a genetic diagnostic panel for MH, one of the main focuses of research has been the functional analysis of the variants found in patients. In over ten years, only 31 variants have met the criteria set out in the guidelines (Urwyler et al., 2001). One of the primary reasons for this are the difficulties associated with cloning, subcloning, performing mutagenesis and expressing large genes *in vitro*. In this thesis, a cloning strategy was employed that resulted in the creation of two subclones of *RYR1* containing the entire coding sequence between them. Furthermore, a protocol was developed for the efficient mutagenesis of these subclones meaning that only one subcloning step is required for the creation of full-length mutant *RYR1* constructs when previously, subclones as small as 4,500bp have been required for mutagenesis (Tong et al., 1997). A total of seven variants were generated and expressed in HEK293 cells, six of which were proven to be causative of MH. One variant, p.D3986E, was found to be indistinguishable from wild type *RYR1*. However, when the expression level of this variant increased, so did the caffeine sensitivity of transfected cells hinting at a more complicated role in MH pathogenesis than was first apparent. Finally, in this thesis, functional analysis of an *RYR1* variant associated with both MH and EHS was performed. This variant, p.D1056H, was identified through exome sequencing of patients in which no variant had previously been identified and was subsequently identified in an EHS patient who had tested negative for MH. The p.D1056H variant responded in the same way as other MH variants did to caffeine stimulation indicating its role as the causative genetic variant of MH in the family in which it was identified. The reason behind the MHN diagnosis upon testing with the IVCT is unclear but the results generated in this thesis highlight the link between the two conditions and the importance of referring EHS patients for MH testing.

7.1.1 Cloning and mutagenesis

244 *RYR1* variants are listed on the EMHG website, only 31 of which are available for use in genetic diagnosis partly due to the difficulties associated with manipulating large cDNA constructs. In this thesis, MEGAWHOP mutagenesis was performed on subclones of 11,128bp and 12,523bp in size. Although MEGAWHOP has been previously used for the mutagenesis of large cDNA templates, the largest reported plasmid successfully mutated using MEGAWHOP is 6,000bp (Sato et al., 2010, Sato et al., 2013). The ability to perform mutagenesis on such large plasmids negated the need to produce further subclones, which, with the lack of unique restriction sites within the *RYR1* coding sequence, would have been problematic. An overall mutagenesis efficiency of 52.9%, although seemingly low, is high for successfully mutating large cDNA constructs. The production and highly efficient mutagenesis of two subclones of *RYR1* that accounts for the entire *RYR1* coding sequence means that future functional studies can be performed without the need for subcloning *RYR1* before being able to perform mutagenesis. With so many as yet uncharacterised *RYR1* variants found in association with MH, the development of a reliable and robust cloning and mutagenesis protocol was essential.

7.1.2 Causative MH variants

In this thesis, the p.D1056H, p.R2336H, p.R2355W, p.E3104K, p.G3990V and p.V4849I variants have been proven to be causative of MH by assessing their functional consequences in an *in vitro*, recombinant expression system. HEK293 cells transfected with each of these variants responded in a typically MH fashion. They displayed an increased sensitivity to caffeine as indicated by a statistically significant decrease in EC_{50} , a measurement in which the dose required to obtain half of the maximal response is calculated. Furthermore, the mutant constructs resulted in a higher amount of intracellular calcium release at lower doses of caffeine when compared to wild type controls. It is the conclusion of this thesis that these variants can be added

to the genetic diagnostic panel of MH, negating the need for the IVCT in patients found to be carrying these mutations.

7.1.3 The role of the p.D3986E variant in MH pathogenesis

The caffeine sensitivity of the p.D3986E variant was no different from that of wild type transfected cells. Furthermore, the amount of calcium released at low doses (1mM and 2mM) of caffeine was not significantly higher than that observed in wild type expressing cells. Based purely on this data it would appear as though the p.D3986E variant is not the causative mutation of MH in the four families in which it has been identified. Whilst we cannot be certain that there is not another, as yet unidentified variant in these patients it is important to note that as a group, patients carrying this variant have been found to have a caffeine contracture that is significantly larger than that of patients carrying other causative MH mutations during the IVCT (Carpenter et al., 2009c). Patients carrying this variant have had the entire *RYR1* gene sequenced and no additional variant was identified, however, there may be an additional variant segregating with this mutant allele through linkage disequilibrium, potentially as part of a 'high risk' haplotype that is contributing to the MH phenotype as a modifier of the overall phenotype (Carpenter et al., 2009a).

The EC₁₀ of cells stably transfected with the p.D3986E variant was statistically significantly higher than that of wild type transfected cells (see section 4.3.1.3). Whilst this result was not repeated in cells transiently transfected with p.D3986E and wild type *RYR1* in the pTUNE expression vector, it hints at the possibility of this variant contributing, at least in part to the overall MH phenotype.

It has long been established that *RYR1* variants that result in MH also confer a higher baseline resting calcium level in cells expressing the mutation (Tong et al., 1999b, Lopez et al., 2005, Yang et al., 2007). The work presented in chapter 6 suggests that the p.D3986E variant may still result in a higher resting calcium level than wild type transfected cells (see section 6.3.6). Treatment with AICAR, a compound proven to

lower baseline resting calcium levels in muscle fibres of MH mice, resulted in a significant decrease in sensitivity to caffeine that was consistent with other MH mutations but not wild type *RYR1*. The suggestion that the p.D3986E variant confers a higher baseline resting calcium level may be consistent with work being performed by Claudio Perez's laboratory in which a 300 amino acid region of *RYR1* has been identified to be important in the maintenance of resting calcium levels (unpublished observations). Substitution of this region with the equivalent region of *RYR3* results in an elevated resting calcium level in line with normal *RYR3* levels. Interestingly, previous work from the same laboratory suggests that an increase in *RYR3* expression results in both an elevated resting calcium level and increased sensitivity to caffeine (Perez et al., 2005). Similar results were obtained from the experiments in chapter 6 looking at the effect of an increase in mutant *RYR1* expression. An increase in p.D3986E expression resulted in a significant increase in sensitivity to caffeine (see section 6.3.4). Whilst a clear answer cannot be given yet on what the p.D3986E variant is doing to the normal resting calcium level of transfected cells, it is interesting that this variant falls in a region so important to resting calcium levels. Looking at all the data obtained on the p.D3986E variant in this thesis, it is apparent that the role of this variant in MH is not as clear as first suspected. Initially it appeared as though this variant was not the causative mutation in the families it has been identified in. However, coupled with the data on increased expression levels and pre-treatment with AICAR, there are suggestions that this variant may still play a role. Future work on this variant will focus on expressing it in myotubes to see if a more native cellular environment and structure for *RYR1* enhance the seemingly mild phenotype observed in HEK293 cells. Furthermore, the families in which this variant has been identified are ideal candidates for exome sequencing to attempt to identify potential modifying loci that could result in the full MH phenotype.

7.1.4 p.D1056H, EHS and MH

In chapter 6, functional analysis of the p.D1056H RYR1 variant was presented. Taken alone, the data obtained indicate a classic MH mutation. The sensitivity of transfected cells to caffeine was statistically significantly reduced and the amount of calcium released at lower doses of caffeine were significantly higher when compared to the equivalent experiment performed on wild type transfected cells (see sections 6.3.1 and 6.3.3 respectively). Additionally, this variant has been found to cosegregate with MH susceptibility in the family it was identified in. However, on subsequent screening of the entire UK MH population, this variant was also found in an individual who suffered an EHS reaction whilst undergoing a military training exercise in a hot climate. The individual was referred for MH testing as per the widely accepted procedure for EHS patients but was diagnosed as MHN after undergoing the IVCT.

The reason for the discrepancy between the EHS and MH phenotype is unknown, however, reports of genotype/phenotype discordance between MH diagnosis through the IVCT and the presence of an *RYR1* variant proven to be causative of MH have been known (Deufel et al., 1995, Fagerlund et al., 1997, Robinson et al., 2003b). The reasons for discordance are unclear but are likely to involve the role of other genetic factors that push the overall phenotype one way or the other. There is evidence to suggest, at least in MH susceptibility and presumably therefore in EHS susceptibility also, that multiple, interacting gene products are responsible for disease (Robinson et al., 2003a, Robinson et al., 2000). Regardless of the exact reason, the work presented in this thesis unequivocally links an *RYR1* variant found in association with both MH and EHS. Furthermore, this variant has been proven to be the causative mutation of MH through the functional studies performed in this project. Whilst the relative lack of *RYR1* variants found in association with EHS may be due to the limited number of studies aimed at identifying genetic variants responsible for the disease, the EHS phenotype is, similarly to MH, likely to be a result of a number of genes and environmental factors. The MHN/EHS patient described in this thesis would be an

ideal candidate for exome sequencing to identify, not only potential contributing genes to the EHS phenotype but also for modifying genes of the MH phenotype.

7.2 Future work

7.2.1 Functional characterisation of further genetic variants

Since the introduction of the EMHG guidelines for the inclusion of variants in *RYR1* onto the genetic diagnostic panel for MH over 10 years ago, only 31 mutations have met the criteria. With 244 variants listed on the EMHG website as potentially causative of MH, the focus of future work will be the further expansion of the availability of genetic diagnosis. The work carried out in this project has provided suitable subclones of *RYR1* and a mutagenesis protocol that can be used to generate any *RYR1* variant associated with MH for functional studies. Currently, the majority of individuals being referred for MH testing are still required to undergo the IVCT for a conclusive diagnosis, however, with suitable resources in place for the generation of cDNA constructs for the functional analysis of many *RYR1* variants, it will eventually mean that genetic diagnosis is the primary method of diagnosis for MH.

7.2.2 Native vs. non-native environment for functional studies

The only project goal that was unfulfilled in this thesis is the successful expression of the *RYR1* variants generated in dyspedic myotubes. Several issues were encountered during this project, the first of which was the lack of suitable restriction sites in the original pc*RYR1* plasmid for efficient and simple transfer into the pHSVPrPUC vector. Due to the fact that there was only one suitable restriction site, non-directional cloning of the full 15kb coding sequence was required, making ligation efficiency in the correct orientation remarkably low. Nevertheless, three constructs were successfully shuttled into the pHSVPrPUC vector; however, sufficiently high viral titres were not obtained for any of the constructs meaning thorough functional experiments could not be performed.

One of the main focuses of future work will be to successfully express the *RYR1* variants generated in this project in dyspedic myotubes to thoroughly evaluate the use of non-native cell types for functional studies. As discussed above, of particular interest are the results obtained from the p.D3986E variant. This variant produced a response that was similar to wild type in the experiments in chapter 4, however increasing the expression of this variant produced a statistically significant increase in caffeine sensitivity. Furthermore, experiments involving AICAR hinted at the possibility that this variant still confers a high resting calcium level on transfected cells. Functional analysis of this variant in myotubes will allow us to further probe the consequences of this mutation in relation to MH. Additionally, expressing these variants in myotubes will allow the measurement of intracellular resting calcium levels, allowing us to confirm the hypothesis that expression of the p.D3986E variant is still resulting in a larger baseline resting calcium level which may be contributing to the MH phenotype.

7.3 Final conclusions

The work presented in this thesis is supportive of the p.D1056H, p.R2336H, p.R2355W, p.E3104K, p.G3990V and p.V4849I *RYR1* variants to be added to the genetic diagnostic panel for MH. The inclusion of these variants expands the availability of initial genetic diagnosis for MH by 19.35%, negating the need for the invasive muscle biopsy associated with the IVCT. The six variants proven to be causative of MH in this thesis have been identified in 52 families worldwide and represent a quarter of the families that possess an as yet uncharacterised *RYR1* variant in the UK. Furthermore, the work presented in this thesis lays the groundwork for the further expansion of the genetic diagnostic panel through the production of suitable *RYR1* subclones covering the entire coding sequence of the gene as well as the development of a robust mutagenesis protocol that reliably produces the desired mutation. On top of the primary goal of expanding the genetic diagnostic panel for MH, work was presented

that further supports the genotypic link between EHS and MH. The functional analysis of the p.D1056H variant highlighted the potential causal role of *RYR1* variants in EHS whilst also suggesting that additional variants are required to either augment the MH reaction or protect against the EHS phenotype. These findings can guide future screening projects for both MH and EHS candidate loci that are currently underway in our laboratory.

Chapter Eight – References

- ALTHOBITI, M., BOOMS, P., FISZER, D., HALSALL, P. J., SHAW, M. A. & HOPKINS, P. M. 2009. Sequencing the JSRP1 gene in patients susceptible to malignant hyperthermia and identification of two novel genetic variants. *Br J Anaesth*, 103, 321-321.
- ANDERSON, A. A., TREVES, S., BIRAL, D., BETTO, R., SANDONA, D., RONJAT, M. & ZORZATO, F. 2003. The novel skeletal muscle sarcoplasmic reticulum JP-45 protein. Molecular cloning, tissue distribution, developmental expression, and interaction with alpha 1.1 subunit of the voltage-gated calcium channel. *J Biol Chem*, 278, 39987-92.
- AVILA, G., O'BRIEN, J. J. & DIRKSEN, R. T. 2001. Excitation--contraction uncoupling by a human central core disease mutation in the ryanodine receptor. *Proc Natl Acad Sci U S A*, 98, 4215-20.
- BANNISTER, R. A. & BEAM, K. G. 2009. Ryanodine modification of RyR1 retrogradely affects L-type Ca(2+) channel gating in skeletal muscle. *J Muscle Res Cell Motil*, 30, 217-23.
- BANNISTER, R. A., ESTEVE, E., ELTIT, J. M., PESSAH, I. N., ALLEN, P. D., LOPEZ, J. R. & BEAM, K. G. 2010. A malignant hyperthermia-inducing mutation in RYR1 (R163C): consequent alterations in the functional properties of DHPR channels. *J Gen Physiol*, 135, 629-40.
- BANNISTER, R. A., PESSAH, I. N. & BEAM, K. G. 2009. The skeletal L-type Ca(2+) current is a major contributor to excitation-coupled Ca(2+) entry. *J Gen Physiol*, 133, 79-91.
- BARRIENTOS, G. C., FENG, W., TRUONG, K., MATTHAEI, K. I., YANG, T., ALLEN, P. D., LOPEZ, J. R. & PESSAH, I. N. 2012. Gene dose influences cellular and calcium channel dysregulation in heterozygous and homozygous T4826I-RYR1 malignant hyperthermia-susceptible muscle. *J Biol Chem*, 287, 2863-76.
- BEVILACQUA, J. A., MONNIER, N., BITOUN, M., EYMARD, B., FERREIRO, A., MONGES, S., LUBIENIECKI, F., TARATUTO, A. L., LAQUERRIERE, A., CLAEYS, K. G., MARTY, I., FARDEAU, M., GUICHENEY, P., LUNARDI, J. & ROMERO, N. B. 2011. Recessive RYR1 mutations cause unusual congenital myopathy with prominent nuclear internalization and large areas of myofibrillar disorganization. *Neuropathol Appl Neurobiol*, 37, 271-84.
- BRANDT, A., SCHLEITHOFF, L., JURKAT-ROTT, K., KLINGLER, W., BAUR, C. & LEHMANN-HORN, F. 1999. Screening of the ryanodine receptor gene in 105 malignant hyperthermia families: novel mutations and concordance with the in vitro contracture test. *Hum Mol Genet*, 8, 2055-62.
- CAMPEAU, P., CHAPDELAINE, P., SEIGNEURIN-VENIN, S., MASSIE, B. & TREMBLAY, J. P. 2001. Transfection of large plasmids in primary human myoblasts. *Gene Ther*, 8, 1387-94.

- CARPENTER, D., MORRIS, A., ROBINSON, R. L., BOOMS, P., ILES, D., HALSALL, P. J., STEELE, D., HOPKINS, P. M. & SHAW, M. A. 2009a. Analysis of RYR1 haplotype profile in patients with malignant hyperthermia. *Ann Hum Genet*, 73, 10-8.
- CARPENTER, D., RINGROSE, C., LEO, V., MORRIS, A., ROBINSON, R. L., HALSALL, P. J., HOPKINS, P. M. & SHAW, M. A. 2009b. The role of CACNA1S in predisposition to malignant hyperthermia. *BMC Med Genet*, 10, 104.
- CARPENTER, D., ROBINSON, R. L., QUINNELL, R. J., RINGROSE, C., HOGG, M., CASSON, F., BOOMS, P., ILES, D. E., HALSALL, P. J., STEELE, D. S., SHAW, M. A. & HOPKINS, P. M. 2009c. Genetic variation in RYR1 and malignant hyperthermia phenotypes. *Br J Anaesth*, 103, 538-48.
- CHELU, M. G., GOONASEKERA, S. A., DURHAM, W. J., TANG, W., LUECK, J. D., RIEHL, J., PESSAH, I. N., ZHANG, P., BHATTACHARJEE, M. B., DIRKSEN, R. T. & HAMILTON, S. L. 2006. Heat- and anesthesia-induced malignant hyperthermia in an RyR1 knock-in mouse. *FASEB J*, 20, 329-30.
- CHEREDNICHENKO, G., HURNE, A. M., FESSENDEN, J. D., LEE, E. H., ALLEN, P. D., BEAM, K. G. & PESSAH, I. N. 2004. Conformational activation of Ca²⁺ entry by depolarization of skeletal myotubes. *Proc Natl Acad Sci U S A*, 101, 15793-8.
- CHEREDNICHENKO, G., WARD, C. W., FENG, W., CABRALES, E., MICHAELSON, L., SAMSO, M., LOPEZ, J. R., ALLEN, P. D. & PESSAH, I. N. 2008. Enhanced excitation-coupled calcium entry in myotubes expressing malignant hyperthermia mutation R163C is attenuated by dantrolene. *Mol Pharmacol*, 73, 1203-12.
- COLLIER, M. L., JI, G., WANG, Y. & KOTLIKOFF, M. I. 2000. Calcium-induced calcium release in smooth muscle: loose coupling between the action potential and calcium release. *J Gen Physiol*, 115, 653-62.
- CORTON, J. M., GILLESPIE, J. G., HAWLEY, S. A. & HARDIE, D. G. 1995. 5-aminoimidazole-4-carboxamide ribonucleoside. A specific method for activating AMP-activated protein kinase in intact cells? *Eur J Biochem*, 229, 558-65.
- CUNNINGHAM, C. & DAVISON, A. J. 1993. A cosmid-based system for constructing mutants of herpes simplex virus type 1. *Virology*, 197, 116-24.
- DAVIS, M., BROWN, R., DICKSON, A., HORTON, H., JAMES, D., LAING, N., MARSTON, R., NORGATE, M., PERLMAN, D., POLLOCK, N. & STOWELL, K. 2002. Malignant hyperthermia associated with exercise-induced rhabdomyolysis or congenital abnormalities and a novel RYR1 mutation in New Zealand and Australian pedigrees. *Br J Anaesth*, 88, 508-15.
- DAVIS, M. R., HAAN, E., JUNGBLUTH, H., SEWRY, C., NORTH, K., MUNTONI, F., KUNTZER, T., LAMONT, P., BANKIER, A., TOMLINSON, P., SANCHEZ, A., WALSH, P., NAGARAJAN, L., OLEY, C., COLLEY, A., GEDEON, A., QUINLIVAN, R., DIXON, J., JAMES, D., MULLER, C. R. & LAING, N. G. 2003. Principal mutation hotspot for central core disease and related myopathies in the C-terminal transmembrane region of the RYR1 gene. *Neuromuscul Disord*, 13, 151-7.

- DEANS, T. L., CANTOR, C. R. & COLLINS, J. J. 2007. A tunable genetic switch based on RNAi and repressor proteins for regulating gene expression in mammalian cells. *Cell*, 130, 363-72.
- DENBOROUGH, M. A., DENNETT, X. & ANDERSON, R. M. 1973. Central-core disease and malignant hyperpyrexia. *Br Med J*, 1, 272-3.
- DENBOROUGH, M. A., FORSTER, J. F., LOVELL, R. R., MAPLESTONE, P. A. & VILLIERS, J. D. 1962. Anaesthetic deaths in a family. *Br J Anaesth*, 34, 395-6.
- DEUFEL, T., GOLLA, A., ILES, D., MEINDL, A., MEITINGER, T., SCHINDELHAUER, D., DEVRIES, A., PONGRATZ, D., MACLENNAN, D. H., JOHNSON, K. J. & ET AL. 1992. Evidence for genetic heterogeneity of malignant hyperthermia susceptibility. *Am J Hum Genet*, 50, 1151-61.
- DEUFEL, T., SUDBRAK, R., FEIST, Y., RUBSAM, B., DU CHESNE, I., SCHAFER, K. L., ROEWER, N., GRIMM, T., LEHMANN-HORN, F., HARTUNG, E. J. & ET AL. 1995. Discordance, in a malignant hyperthermia pedigree, between in vitro contracture-test phenotypes and haplotypes for the MHS1 region on chromosome 19q12-13.2, comprising the C1840T transition in the RYR1 gene. *Am J Hum Genet*, 56, 1334-42.
- DIRKSEN, R. T. & AVILA, G. 2002. Altered ryanodine receptor function in central core disease: leaky or uncoupled Ca(2+) release channels? *Trends Cardiovasc Med*, 12, 189-97.
- DOLPHIN, C. T. & HOPE, I. A. 2006. Caenorhabditis elegans reporter fusion genes generated by seamless modification of large genomic DNA clones. *Nucleic Acids Res*, 34, e72.
- DOWLING, J. J., LILLIS, S., AMBURGEY, K., ZHOU, H., AL-SARRAJ, S., BUK, S. J., WRAIGE, E., CHOW, G., ABBS, S., LEBER, S., LACHLAN, K., BARALLE, D., TAYLOR, A., SEWRY, C., MUNTONI, F. & JUNGBLUTH, H. 2011. King-Denborough syndrome with and without mutations in the skeletal muscle ryanodine receptor (RYR1) gene. *Neuromuscul Disord*, 21, 420-7.
- DU, G. G., OYAMADA, H., KHANNA, V. K. & MACLENNAN, D. H. 2001. Mutations to Gly2370, Gly2373 or Gly2375 in malignant hyperthermia domain 2 decrease caffeine and cresol sensitivity of the rabbit skeletal-muscle Ca²⁺-release channel (ryanodine receptor isoform 1). *Biochem J*, 360, 97-105.
- DU, G. G., SANDHU, B., KHANNA, V. K., GUO, X. H. & MACLENNAN, D. H. 2002. Topology of the Ca²⁺ release channel of skeletal muscle sarcoplasmic reticulum (RyR1). *Proc Natl Acad Sci U S A*, 99, 16725-30.
- DUCREUX, S., ZORZATO, F., FERREIRO, A., JUNGBLUTH, H., MUNTONI, F., MONNIER, N., MULLER, C. R. & TREVES, S. 2006. Functional properties of ryanodine receptors carrying three amino acid substitutions identified in patients affected by multi-minicore disease and central core disease, expressed in immortalized lymphocytes. *Biochem J*, 395, 259-66.
- DUKE, A. M., HOPKINS, P. M., CALAGHAN, S. C., HALSALL, J. P. & STEELE, D. S. 2010. Store-operated Ca²⁺ entry in malignant hyperthermia-susceptible human skeletal muscle. *J Biol Chem*, 285, 25645-53.

- DUKE, A. M., HOPKINS, P. M., HALSAL, J. P. & STEELE, D. S. 2004. Mg²⁺ dependence of halothane-induced Ca²⁺ release from the sarcoplasmic reticulum in skeletal muscle from humans susceptible to malignant hyperthermia. *Anesthesiology*, 101, 1339-46.
- DUKE, A. M., HOPKINS, P. M., HALSALL, P. J. & STEELE, D. S. 2006. Mg²⁺ dependence of Ca²⁺ release from the sarcoplasmic reticulum induced by sevoflurane or halothane in skeletal muscle from humans susceptible to malignant hyperthermia. *Br J Anaesth*, 97, 320-8.
- DUKE, A. M., HOPKINS, P. M. & STEELE, D. S. 2002. Effects of Mg(2+) and SR luminal Ca(2+) on caffeine-induced Ca(2+) release in skeletal muscle from humans susceptible to malignant hyperthermia. *J Physiol*, 544, 85-95.
- DUKE, A. M., HOPKINS, P. M. & STEELE, D. S. 2003. Mg²⁺ dependence of halothane-induced Ca²⁺ release from the sarcoplasmic reticulum in rat skeletal muscle. *J Physiol*, 551, 447-54.
- DUKE, A. M. & STEELE, D. S. 2008. The presence of a functional t-tubule network increases the sensitivity of RyR1 to agonists in skinned rat skeletal muscle fibres. *Cell Calcium*, 44, 411-21.
- ELLIS, F. R. 1984. European Malignant Hyperpyrexia Group. *Br J Anaesth*, 56, 1181-2.
- ELLIS, F. R., HARRIMAN, D. G., KEANEY, N. P., KYEI-MENSAH, K. & TYRRELL, J. H. 1971. Halothane-induced muscle contracture as a cause of hyperpyrexia. *Br J Anaesth*, 43, 721-2.
- ELTIT, J. M., BANNISTER, R. A., MOUA, O., ALTAMIRANO, F., HOPKINS, P. M., PESSAH, I. N., MOLINSKI, T. F., LOPEZ, J. R., BEAM, K. G. & ALLEN, P. D. 2012a. Malignant hyperthermia susceptibility arising from altered resting coupling between the skeletal muscle L-type Ca²⁺ channel and the type 1 ryanodine receptor. *Proc Natl Acad Sci U S A*, 109, 7923-8.
- ELTIT, J. M., DING, X., PESSAH, I. N., ALLEN, P. D. & LOPEZ, J. R. 2012b. Nonspecific sarcolemmal cation channels are critical for the pathogenesis of malignant hyperthermia. *FASEB J*, 27, 991-1000.
- ENDO, M. 2009. Calcium-induced calcium release in skeletal muscle. *Physiol Rev*, 89, 1153-76.
- ESTEVE, E., ELTIT, J. M., BANNISTER, R. A., LIU, K., PESSAH, I. N., BEAM, K. G., ALLEN, P. D. & LOPEZ, J. R. 2010. A malignant hyperthermia-inducing mutation in RYR1 (R163C): alterations in Ca²⁺ entry, release, and retrograde signaling to the DHPR. *J Gen Physiol*, 135, 619-28.
- FAGERLUND, T. H., ORDING, H., BENDIXEN, D., ISLANDER, G., RANKLEV TWETMAN, E. & BERG, K. 1997. Discordance between malignant hyperthermia susceptibility and RYR1 mutation C1840T in two Scandinavian MH families exhibiting this mutation. *Clin Genet*, 52, 416-21.
- FERREIRO, A., MONNIER, N., ROMERO, N. B., LEROY, J. P., BONNEMANN, C., HAENGGELI, C. A., STRAUB, V., VOSS, W. D., NIVOCHÉ, Y., JUNGBLUTH, H., LEMAINQUE, A., VOIT, T., LUNARDI, J., FARDEAU, M. & GUICHENEY, P. 2002. A recessive form of central core disease, transiently presenting as multi-minicore

- disease, is associated with a homozygous mutation in the ryanodine receptor type 1 gene. *Ann Neurol*, 51, 750-9.
- FRAEFEL, C., SONG, S., LIM, F., LANG, P., YU, L., WANG, Y., WILD, P. & GELLER, A. I. 1996. Helper virus-free transfer of herpes simplex virus type 1 plasmid vectors into neural cells. *J Virol*, 70, 7190-7.
- FUJII, J., OTSU, K., ZORZATO, F., DE LEON, S., KHANNA, V. K., WEILER, J. E., O'BRIEN, P. J. & MACLENNAN, D. H. 1991. Identification of a mutation in porcine ryanodine receptor associated with malignant hyperthermia. *Science*, 253, 448-51.
- GILLARD, E. F., OTSU, K., FUJII, J., KHANNA, V. K., DE LEON, S., DERDEMEZI, J., BRITT, B. A., DUFF, C. L., WORTON, R. G. & MACLENNAN, D. H. 1991. A substitution of cysteine for arginine 614 in the ryanodine receptor is potentially causative of human malignant hyperthermia. *Genomics*, 11, 751-5.
- GIRARD, T., CAVAGNA, D., PADOVAN, E., SPAGNOLI, G., URWYLER, A., ZORZATO, F. & TREVES, S. 2001a. B-lymphocytes from malignant hyperthermia-susceptible patients have an increased sensitivity to skeletal muscle ryanodine receptor activators. *J Biol Chem*, 276, 48077-82.
- GIRARD, T., URWYLER, A., CENSIER, K., MUELLER, C. R., ZORZATO, F. & TREVES, S. 2001b. Genotype-phenotype comparison of the Swiss malignant hyperthermia population. *Hum Mutat*, 18, 357-8.
- GRIEVINK, H. & STOWELL, K. M. 2010. Allele-specific differences in ryanodine receptor 1 mRNA expression levels may contribute to phenotypic variability in malignant hyperthermia. *Orphanet J Rare Dis*, 5, 10.
- GROOM, L., MULDOON, S. M., TANG, Z. Z., BRANDOM, B. W., BAYARSAIKHAN, M., BINA, S., LEE, H. S., QIU, X., SAMBUUGHIN, N. & DIRKSEN, R. T. 2011. Identical de novo mutation in the type 1 ryanodine receptor gene associated with fatal, stress-induced malignant hyperthermia in two unrelated families. *Anesthesiology*, 115, 938-45.
- HACKL, W., WINKLER, M., MAURITZ, W., SPORN, P. & STEINBEREITHNER, K. 1991. Muscle biopsy for diagnosis of malignant hyperthermia susceptibility in two patients with severe exercise-induced myolysis. *Br J Anaesth*, 66, 138-40.
- HARBITZ, I., CHOWDHARY, B., THOMSEN, P. D., DAVIES, W., KAUFMANN, U., KRAN, S., GUSTAVSSON, I., CHRISTENSEN, K. & HAUGE, J. G. 1990. Assignment of the porcine calcium release channel gene, a candidate for the malignant hyperthermia locus, to the 6p11---q21 segment of chromosome 6. *Genomics*, 8, 243-8.
- HEFFRON, J. J., MITCHELL, G. & DREYER, J. H. 1982. Muscle fibre type, fibre diameter and pH1 values of M. longissimus dorsi of normal, malignant hyperthermia- and PSE-susceptible pigs. *Br Vet J*, 138, 45-50.
- HOLMES, B. F., KURTH-KRACZEK, E. J. & WINDER, W. W. 1999. Chronic activation of 5'-AMP-activated protein kinase increases GLUT-4, hexokinase, and glycogen in muscle. *J Appl Physiol*, 87, 1990-5.
- HOPKINS, P. M. 2000. Malignant hyperthermia: advances in clinical management and diagnosis. *Br J Anaesth*, 85, 118-28.

- HOPKINS, P. M. 2007. Is there a link between malignant hyperthermia and exertional heat illness? *Br J Sports Med*, 41, 283-4; discussion 284.
- HOPKINS, P. M., ELLIS, F. R. & HALSALL, P. J. 1991a. Evidence for related myopathies in exertional heat stroke and malignant hyperthermia. *Lancet*, 338, 1491-2.
- HOPKINS, P. M., ELLIS, F. R. & HALSALL, P. J. 1991b. Ryanodine contracture: a potentially specific in vitro diagnostic test for malignant hyperthermia. *Br J Anaesth*, 66, 611-3.
- HURNE, A. M., O'BRIEN, J. J., WINGROVE, D., CHEREDNICHENKO, G., ALLEN, P. D., BEAM, K. G. & PESSAH, I. N. 2005. Ryanodine receptor type 1 (RyR1) mutations C4958S and C4961S reveal excitation-coupled calcium entry (ECCE) is independent of sarcoplasmic reticulum store depletion. *J Biol Chem*, 280, 36994-7004.
- ILES, D. E., LEHMANN-HORN, F., SCHERER, S. W., TSUI, L. C., OLDE WEGHUIS, D., SUIJKERBUIJK, R. F., HEYTENS, L., MIKALA, G., SCHWARTZ, A., ELLIS, F. R. & ET AL. 1994. Localization of the gene encoding the alpha 2/delta-subunits of the L-type voltage-dependent calcium channel to chromosome 7q and analysis of the segregation of flanking markers in malignant hyperthermia susceptible families. *Hum Mol Genet*, 3, 969-75.
- ILES, D. E., SEGERS, B., HEYTENS, L., SENGERS, R. C. & WIERINGA, B. 1992. High-resolution physical mapping of four microsatellite repeat markers near the RYR1 locus on chromosome 19q13.1 and apparent exclusion of the MHS locus from this region in two malignant hyperthermia susceptible families. *Genomics*, 14, 749-54.
- JIANG, D., CHEN, W., XIAO, J., WANG, R., KONG, H., JONES, P. P., ZHANG, L., FRUEN, B. & CHEN, S. R. 2008. Reduced threshold for luminal Ca²⁺ activation of RyR1 underlies a causal mechanism of porcine malignant hyperthermia. *J Biol Chem*, 283, 20813-20.
- JUNGBLUTH, H., DOWLING, J. J., FERREIRO, A. & MUNTONI, F. 2012. 182nd ENMC International Workshop: RYR1-related myopathies, 15-17th April 2011, Naarden, The Netherlands. *Neuromuscul Disord*, 22, 453-62.
- JUNGBLUTH, H., MULLER, C. R., HALLIGER-KELLER, B., BROCKINGTON, M., BROWN, S. C., FENG, L., CHATTOPADHYAY, A., MERCURI, E., MANZUR, A. Y., FERREIRO, A., LAING, N. G., DAVIS, M. R., ROPER, H. P., DUBOWITZ, V., BYDDER, G., SEWRY, C. A. & MUNTONI, F. 2002. Autosomal recessive inheritance of RYR1 mutations in a congenital myopathy with cores. *Neurology*, 59, 284-7.
- JURKAT-ROTT, K., MCCARTHY, T. & LEHMANN-HORN, F. 2000. Genetics and pathogenesis of malignant hyperthermia. *Muscle Nerve*, 23, 4-17.
- KALOW, W. 1970. Malignant hyperthermia. *Proc R Soc Med*, 63, 178-80.
- KAUFMANN, A., KRAFT, B., MICHALEK-SAUBERER, A., WEINDLMAYR, M., KRESS, H. G., STEINBOECK, F. & WEIGL, L. G. 2012. Novel double and single ryanodine receptor 1 variants in two Austrian malignant hyperthermia families. *Anesth Analg*, 114, 1017-25.

- KAWANA, Y., IINO, M., OYAMADA, H. & ENDO, M. 1992. Effects of halothane, caffeine and ryanodine on the intracellular calcium store in blood mononuclear cells. *Masui*, 41, 727-32.
- KOCHLING, A., WAPPLER, F., WINKLER, G. & SCHULTE AM ESCH, J. S. 1998. Rhabdomyolysis following severe physical exercise in a patient with predisposition to malignant hyperthermia. *Anaesth Intensive Care*, 26, 315-8.
- KOLB, M. E., HORNE, M. L. & MARTZ, R. 1982. Dantrolene in human malignant hyperthermia. *Anesthesiology*, 56, 254-62.
- KREISS, P., CAMERON, B., RANGARA, R., MAILHE, P., AGUERRE-CHARRIOL, O., AIRIAU, M., SCHERMAN, D., CROUZET, J. & PITARD, B. 1999. Plasmid DNA size does not affect the physicochemical properties of lipoplexes but modulates gene transfer efficiency. *Nucleic Acids Res*, 27, 3792-8.
- LANNER, J. T., GEORGIU, D. K., DAGNINO-ACOSTA, A., AINBINDER, A., CHENG, Q., JOSHI, A. D., CHEN, Z., YAROTSKYY, V., OAKES, J. M., LEE, C. S., MONROE, T. O., SANTILLAN, A., DONG, K., GOODYEAR, L., ISMAILOV, II, RODNEY, G. G., DIRKSEN, R. T. & HAMILTON, S. L. 2012. AICAR prevents heat-induced sudden death in RyR1 mutant mice independent of AMPK activation. *Nat Med*, 18, 244-51.
- LARACH, M. G. 1989. Standardization of the caffeine halothane muscle contracture test. North American Malignant Hyperthermia Group. *Anesth Analg*, 69, 511-5.
- LARACH, M. G., GRONERT, G. A., ALLEN, G. C., BRANDOM, B. W. & LEHMAN, E. B. 2010. Clinical presentation, treatment, and complications of malignant hyperthermia in North America from 1987 to 2006. *Anesth Analg*, 110, 498-507.
- LEVANO, S., VUKCEVIC, M., SINGER, M., MATTER, A., TREVES, S., URWYLER, A. & GIRARD, T. 2009. Increasing the number of diagnostic mutations in malignant hyperthermia. *Hum Mutat*, 30, 590-8.
- LEVITT, R. C., NOURI, N., JEDLICKA, A. E., MCKUSICK, V. A., MARKS, A. R., SHUTACK, J. G., FLETCHER, J. E., ROSENBERG, H. & MEYERS, D. A. 1991. Evidence for genetic heterogeneity in malignant hyperthermia susceptibility. *Genomics*, 11, 543-7.
- LEVITT, R. C., OLCKERS, A., MEYERS, S., FLETCHER, J. E., ROSENBERG, H., ISAACS, H. & MEYERS, D. A. 1992. Evidence for the localization of a malignant hyperthermia susceptibility locus (MHS2) to human chromosome 17q. *Genomics*, 14, 562-6.
- LEWIS, R. S. 2007. The molecular choreography of a store-operated calcium channel. *Nature*, 446, 284-7.
- LOBO, P. A. & VAN PETEGEM, F. 2009. Crystal structures of the N-terminal domains of cardiac and skeletal muscle ryanodine receptors: insights into disease mutations. *Structure*, 17, 1505-14.
- LOKE, J., KRAEVA, N. & MACLENNAN, D. 2007. Mutations in ryr1 gene associated with malignant hyperthermia and a non-anaesthetic phenotype. *Can J Anaesth*, 54, 44609.
- LOPEZ, J. R., ALAMO, L., CAPUTO, C., WIKINSKI, J. & LEDEZMA, D. 1985a. Intracellular ionized calcium concentration in muscles from humans with malignant hyperthermia. *Muscle Nerve*, 8, 355-8.

- LOPEZ, J. R., ALAMO, L. A., JONES, D., PAPP, L., ALLEN, P., GERGELY, J. & STRETER, F. 1985b. [Determination of intracellular free calcium concentration, in vivo, in swine susceptible to malignant hyperthermia syndrome]. *Acta Cient Venez*, 36, 102-4.
- LOPEZ, J. R., ALAMO, L. A., JONES, D. E., PAPP, L., ALLEN, P. D., GERGELY, J. & SRETER, F. A. 1986. $[Ca^{2+}]_i$ in muscles of malignant hyperthermia susceptible pigs determined in vivo with Ca^{2+} selective microelectrodes. *Muscle Nerve*, 9, 85-6.
- LOPEZ, J. R., ALLEN, P., ALAMO, L., RYAN, J. F., JONES, D. E. & SRETER, F. 1987a. Dantrolene prevents the malignant hyperthermic syndrome by reducing free intracellular calcium concentration in skeletal muscle of susceptible swine. *Cell Calcium*, 8, 385-96.
- LOPEZ, J. R., ALLEN, P. D., ALAMO, L., JONES, D. & SRETER, F. A. 1988. Myoplasmic free $[Ca^{2+}]$ during a malignant hyperthermia episode in swine. *Muscle Nerve*, 11, 82-8.
- LOPEZ, J. R., CONTRERAS, J., LINARES, N. & ALLEN, P. D. 2000. Hypersensitivity of malignant hyperthermia-susceptible swine skeletal muscle to caffeine is mediated by high resting myoplasmic $[Ca^{2+}]$. *Anesthesiology*, 92, 1799-806.
- LOPEZ, J. R., GERARDI, A., LOPEZ, M. J. & ALLEN, P. D. 1992. Effects of dantrolene on myoplasmic free $[Ca^{2+}]$ measured in vivo in patients susceptible to malignant hyperthermia. *Anesthesiology*, 76, 711-9.
- LOPEZ, J. R., LINARES, N., PESSAH, I. N. & ALLEN, P. D. 2005. Enhanced response to caffeine and 4-chloro-m-cresol in malignant hyperthermia-susceptible muscle is related in part to chronically elevated resting $[Ca^{2+}]_i$. *Am J Physiol Cell Physiol*, 288, C606-12.
- LOPEZ, J. R., MEDINA, P. & ALAMO, L. 1987b. Dantrolene sodium is able to reduce the resting ionic $[Ca^{2+}]_i$ in muscle from humans with malignant hyperthermia. *Muscle Nerve*, 10, 77-9.
- LUDTKE, S. J., SERYSHEVA, II, HAMILTON, S. L. & CHIU, W. 2005. The pore structure of the closed RyR1 channel. *Structure*, 13, 1203-11.
- LYNCH, P. J., KRIVOSIC-HORBER, R., REYFORD, H., MONNIER, N., QUANE, K., ADNET, P., HAUDECOEUR, G., KRIVOSIC, I., MCCARTHY, T. & LUNARDI, J. 1997. Identification of heterozygous and homozygous individuals with the novel RYR1 mutation Cys35Arg in a large kindred. *Anesthesiology*, 86, 620-6.
- LYNCH, P. J., TONG, J., LEHANE, M., MALLETT, A., GIBLIN, L., HEFFRON, J. J., VAUGHAN, P., ZAFRA, G., MACLENNAN, D. H. & MCCARTHY, T. V. 1999. A mutation in the transmembrane/luminal domain of the ryanodine receptor is associated with abnormal Ca^{2+} release channel function and severe central core disease. *Proc Natl Acad Sci U S A*, 96, 4164-9.
- MACLENNAN, D. H., DUFF, C., ZORZATO, F., FUJII, J., PHILLIPS, M., KORNELUK, R. G., FRODIS, W., BRITT, B. A. & WORTON, R. G. 1990. Ryanodine receptor gene is a candidate for predisposition to malignant hyperthermia. *Nature*, 343, 559-61.
- MACLENNAN, D. H. & PHILLIPS, M. S. 1992. Malignant hyperthermia. *Science*, 256, 789-94.

- MCCARTHY, T. V., HEALY, J. M., HEFFRON, J. J., LEHANE, M., DEUFEL, T., LEHMANN-HORN, F., FARRALL, M. & JOHNSON, K. 1990. Localization of the malignant hyperthermia susceptibility locus to human chromosome 19q12-13.2. *Nature*, 343, 562-4.
- MELTON, A. T., MARTUCCI, R. W., KIEN, N. D. & GRONERT, G. A. 1989. Malignant hyperthermia in humans--standardization of contracture testing protocol. *Anesth Analg*, 69, 437-43.
- MERRILL, G. F., KURTH, E. J., HARDIE, D. G. & WINDER, W. W. 1997. AICA riboside increases AMP-activated protein kinase, fatty acid oxidation, and glucose uptake in rat muscle. *Am J Physiol*, 273, E1107-12.
- MIGITA, T., MUKAIDA, K., HAMADA, H., YASUDA, T., HARAOKI, T., NISHINO, I., MURAKAMI, N. & KAWAMOTO, M. 2009. Functional analysis of ryanodine receptor type 1 p.R2508C mutation in exon 47. *J Anesth*, 23, 341-6.
- MITCHELL, G. & HEFFRON, J. J. 1982. Porcine stress syndromes. *Adv Food Res*, 28, 167-230.
- MIYAZAKI, K. 2003. Creating Random Mutagenesis Libraries by Megaprimer PCR of Whole Plasmid (MEGAWHOP). In: ARNOLD, F. & GEORGIU, G. (eds.) *Directed Evolution Library Creation*. Humana Press.
- MONNIER, N., FERREIRO, A., MARTY, I., LABARRE-VILA, A., MEZIN, P. & LUNARDI, J. 2003. A homozygous splicing mutation causing a depletion of skeletal muscle RYR1 is associated with multi-minicore disease congenital myopathy with ophthalmoplegia. *Hum Mol Genet*, 12, 1171-8.
- MONNIER, N., KOZAK-RIBBENS, G., KRIVOSIC-HORBER, R., NIVOCHÉ, Y., QI, D., KRAEV, N., LOKE, J., SHARMA, P., TEGAZZIN, V., FIGARELLA-BRANGER, D., ROMERO, N., MEZIN, P., BENDAHAN, D., PAYEN, J. F., DEPRET, T., MACLENNAN, D. H. & LUNARDI, J. 2005. Correlations between genotype and pharmacological, histological, functional, and clinical phenotypes in malignant hyperthermia susceptibility. *Hum Mutat*, 26, 413-25.
- MONNIER, N., KRIVOSIC-HORBER, R., PAYEN, J. F., KOZAK-RIBBENS, G., NIVOCHÉ, Y., ADNET, P., REYFORD, H. & LUNARDI, J. 2002. Presence of two different genetic traits in malignant hyperthermia families: implication for genetic analysis, diagnosis, and incidence of malignant hyperthermia susceptibility. *Anesthesiology*, 97, 1067-74.
- MONNIER, N., PROCACCIO, V., STIEGLITZ, P. & LUNARDI, J. 1997. Malignant-hyperthermia susceptibility is associated with a mutation of the alpha 1-subunit of the human dihydropyridine-sensitive L-type voltage-dependent calcium-channel receptor in skeletal muscle. *Am J Hum Genet*, 60, 1316-25.
- MONNIER, N., ROMERO, N. B., LERALE, J., LANDRIEU, P., NIVOCHÉ, Y., FARDEAU, M. & LUNARDI, J. 2001. Familial and sporadic forms of central core disease are associated with mutations in the C-terminal domain of the skeletal muscle ryanodine receptor. *Hum Mol Genet*, 10, 2581-92.
- MONNIER, N., ROMERO, N. B., LERALE, J., NIVOCHÉ, Y., QI, D., MACLENNAN, D. H., FARDEAU, M. & LUNARDI, J. 2000. An autosomal dominant congenital myopathy with cores and rods is associated with a neomutation in the RYR1

- gene encoding the skeletal muscle ryanodine receptor. *Hum Mol Genet*, 9, 2599-608.
- MOORE, R. A., NGUYEN, H., GALCERAN, J., PESSAH, I. N. & ALLEN, P. D. 1998. A transgenic myogenic cell line lacking ryanodine receptor protein for homologous expression studies: reconstitution of Ry1R protein and function. *J Cell Biol*, 140, 843-51.
- MULDOON, S., BUNGER, R., DEUSTER, P. & SAMBUUGHIN, N. 2007. Identification of risk factors for exertional heat illness: a brief commentary on genetic testing. *J Sport Rehabil*, 16, 222-6.
- MULDOON, S., DEUSTER, P., BRANDOM, B. & BUNGER, R. 2004. Is there a link between malignant hyperthermia and exertional heat illness? *Exerc Sport Sci Rev*, 32, 174-9.
- MULDOON, S., DEUSTER, P., VOELKEL, M., CAPACCHIONE, J. & BUNGER, R. 2008. Exertional heat illness, exertional rhabdomyolysis, and malignant hyperthermia: is there a link? *Curr Sports Med Rep*, 7, 74-80.
- NAKAI, J., DIRKSEN, R. T., NGUYEN, H. T., PESSAH, I. N., BEAM, K. G. & ALLEN, P. D. 1996. Enhanced dihydropyridine receptor channel activity in the presence of ryanodine receptor. *Nature*, 380, 72-5.
- NARKAR, V. A., DOWNES, M., YU, R. T., EMBLER, E., WANG, Y. X., BANAYO, E., MIHAYLOVA, M. M., NELSON, M. C., ZOU, Y., JUGUILON, H., KANG, H., SHAW, R. J. & EVANS, R. M. 2008. AMPK and PPARdelta agonists are exercise mimetics. *Cell*, 134, 405-15.
- NEUHUBER, B., HUANG, D. I., DANIELS, M. P. & TORGAN, C. E. 2002. High efficiency transfection of primary skeletal muscle cells with lipid-based reagents. *Muscle Nerve*, 26, 136-40.
- O'BRIEN, P. J. 1986a. Porcine malignant hyperthermia susceptibility: hypersensitive calcium-release mechanism of skeletal muscle sarcoplasmic reticulum. *Can J Vet Res*, 50, 318-28.
- O'BRIEN, P. J. 1986b. Porcine malignant hyperthermia susceptibility: increased calcium-sequestering activity of skeletal muscle sarcoplasmic reticulum. *Can J Vet Res*, 50, 329-37.
- OLCKERS, A., MEYERS, D. A., MEYERS, S., TAYLOR, E. W., FLETCHER, J. E., ROSENBERG, H., ISAACS, H. & LEVITT, R. C. 1992. Adult muscle sodium channel alpha-subunit is a gene candidate for malignant hyperthermia susceptibility. *Genomics*, 14, 829-31.
- OTSU, K., KHANNA, V. K., ARCHIBALD, A. L. & MACLENNAN, D. H. 1991. Cosegregation of porcine malignant hyperthermia and a probable causal mutation in the skeletal muscle ryanodine receptor gene in backcross families. *Genomics*, 11, 744-50.
- OTSU, K., NISHIDA, K., KIMURA, Y., KUZUYA, T., HORI, M., KAMADA, T. & TADA, M. 1994. The point mutation Arg615-->Cys in the Ca²⁺ release channel of skeletal sarcoplasmic reticulum is responsible for hypersensitivity to caffeine and halothane in malignant hyperthermia. *J Biol Chem*, 269, 9413-5.

- OWEN, V. J., TASKE, N. L. & LAMB, G. D. 1997. Reduced Mg²⁺ inhibition of Ca²⁺ release in muscle fibers of pigs susceptible to malignant hyperthermia. *Am J Physiol*, 272, C203-11.
- OYAMADA, H., OGUCHI, K., SAITOH, N., YAMAZAWA, T., HIROSE, K., KAWANA, Y., WAKATSUKI, K., OGUCHI, K., TAGAMI, M., HANAOKA, K., ENDO, M. & IINO, M. 2002. Novel mutations in C-terminal channel region of the ryanodine receptor in malignant hyperthermia patients. *Jpn J Pharmacol*, 88, 159-66.
- PEREZ, C. F., LOPEZ, J. R. & ALLEN, P. D. 2005. Expression levels of RyR1 and RyR3 control resting free Ca²⁺ in skeletal muscle. *Am J Physiol Cell Physiol*, 288, C640-9.
- PHILLIPS, M. S., FUJII, J., KHANNA, V. K., DELEON, S., YOKOBATA, K., DE JONG, P. J. & MACLENNAN, D. H. 1996. The structural organization of the human skeletal muscle ryanodine receptor (RYR1) gene. *Genomics*, 34, 24-41.
- POLD, R., JENSEN, L. S., JESSEN, N., BUHL, E. S., SCHMITZ, O., FLYVBJERG, A., FUJII, N., GOODYEAR, L. J., GOTFREDSEN, C. F., BRAND, C. L. & LUND, S. 2005. Long-term AICAR administration and exercise prevents diabetes in ZDF rats. *Diabetes*, 54, 928-34.
- QUANE, K. A., HEALY, J. M., KEATING, K. E., MANNING, B. M., COUCH, F. J., PALMUCCI, L. M., DORIGUZZI, C., FAGERLUND, T. H., BERG, K., ORDING, H. & ET AL. 1993. Mutations in the ryanodine receptor gene in central core disease and malignant hyperthermia. *Nat Genet*, 5, 51-5.
- QUINLIVAN, R. M., MULLER, C. R., DAVIS, M., LAING, N. G., EVANS, G. A., DWYER, J., DOVE, J., ROBERTS, A. P. & SEWRY, C. A. 2003. Central core disease: clinical, pathological, and genetic features. *Arch Dis Child*, 88, 1051-5.
- RICHTER, M., SCHLEITHOFF, L., DEUFEL, T., LEHMANN-HORN, F. & HERRMANN-FRANK, A. 1997. Functional characterization of a distinct ryanodine receptor mutation in human malignant hyperthermia-susceptible muscle. *J Biol Chem*, 272, 5256-60.
- ROBINSON, R., CARPENTER, D., SHAW, M. A., HALSALL, J. & HOPKINS, P. 2006. Mutations in RYR1 in malignant hyperthermia and central core disease. *Hum Mutat*, 27, 977-89.
- ROBINSON, R., HOPKINS, P., CARSANA, A., GILLY, H., HALSALL, J., HEYTENS, L., ISLANDER, G., JURKAT-ROTT, K., MULLER, C. & SHAW, M. A. 2003a. Several interacting genes influence the malignant hyperthermia phenotype. *Hum Genet*, 112, 217-8.
- ROBINSON, R. L., ANETSEDER, M. J., BRANCADORO, V., VAN BROEKHOVEN, C., CARSANA, A., CENSIER, K., FORTUNATO, G., GIRARD, T., HEYTENS, L., HOPKINS, P. M., JURKAT-ROTT, K., KLINGER, W., KOZAK-RIBBENS, G., KRIVOSIC, R., MONNIER, N., NIVOCHÉ, Y., OLTHOFF, D., RUEFFERT, H., SORRENTINO, V., TEGAZZIN, V. & MUELLER, C. R. 2003b. Recent advances in the diagnosis of malignant hyperthermia susceptibility: how confident can we be of genetic testing? *Eur J Hum Genet*, 11, 342-8.

- ROBINSON, R. L., CARPENTER, D., HALSALL, P. J., ILES, D. E., BOOMS, P., STEELE, D., HOPKINS, P. M. & SHAW, M. A. 2009. Epigenetic allele silencing and variable penetrance of malignant hyperthermia susceptibility. *Br J Anaesth*, 103, 220-5.
- ROBINSON, R. L., CURRAN, J. L., ELLIS, F. R., HALSALL, P. J., HALL, W. J., HOPKINS, P. M., ILES, D. E., WEST, S. P. & SHAW, M. A. 2000. Multiple interacting gene products may influence susceptibility to malignant hyperthermia. *Ann Hum Genet*, 64, 307-20.
- ROBINSON, R. L. & HOPKINS, P. M. 2001. A breakthrough in the genetic diagnosis of malignant hyperthermia. *Br J Anaesth*, 86, 166-8.
- ROBINSON, R. L., MONNIER, N., WOLZ, W., JUNG, M., REIS, A., NUERNBERG, G., CURRAN, J. L., MONSIEURS, K., STIEGLITZ, P., HEYTENS, L., FRICKER, R., VAN BROECKHOVEN, C., DEUFEL, T., HOPKINS, P. M., LUNARDI, J. & MUELLER, C. R. 1997. A genome wide search for susceptibility loci in three European malignant hyperthermia pedigrees. *Hum Mol Genet*, 6, 953-61.
- ROSENBERG, H. 1989. Standards for halothane/caffeine contracture test. *Anesth Analg*, 69, 429-30.
- ROSENBERG, P. B. 2009. Calcium entry in skeletal muscle. *J Physiol*, 587, 3149-51.
- ROSSI, D., SIMEONI, I., MICHELI, M., BOOTMAN, M., LIPP, P., ALLEN, P. D. & SORRENTINO, V. 2002. RyR1 and RyR3 isoforms provide distinct intracellular Ca²⁺ signals in HEK 293 cells. *J Cell Sci*, 115, 2497-504.
- RYAN, J. F., LOPEZ, J. R., SANCHEZ, V. B., SRETER, F. A. & ALLEN, P. D. 1994. Myoplasmic calcium changes precede metabolic and clinical signs of porcine malignant hyperthermia. *Anesth Analg*, 79, 1007-11.
- SAMBUUGHIN, N., MCWILLIAMS, S., DE BANTEL, A., SIVAKUMAR, K. & NELSON, T. E. 2001a. Single-amino-acid deletion in the RYR1 gene, associated with malignant hyperthermia susceptibility and unusual contraction phenotype. *Am J Hum Genet*, 69, 204-8.
- SAMBUUGHIN, N., NELSON, T. E., JANKOVIC, J., XIN, C., MEISSNER, G., MULLAKANDOV, M., JI, J., ROSENBERG, H., SIVAKUMAR, K. & GOLDFARB, L. G. 2001b. Identification and functional characterization of a novel ryanodine receptor mutation causing malignant hyperthermia in North American and South American families. *Neuromuscul Disord*, 11, 530-7.
- SAMSO, M., FENG, W., PESSAH, I. N. & ALLEN, P. D. 2009. Coordinated movement of cytoplasmic and transmembrane domains of RyR1 upon gating. *PLoS Biol*, 7, e85.
- SAMSO, M., WAGENKNECHT, T. & ALLEN, P. D. 2005. Internal structure and visualization of transmembrane domains of the RyR1 calcium release channel by cryo-EM. *Nat Struct Mol Biol*, 12, 539-44.
- SATO, K., POLLOCK, N. & STOWELL, K. M. 2010. Functional studies of RYR1 mutations in the skeletal muscle ryanodine receptor using human RYR1 complementary DNA. *Anesthesiology*, 112, 1350-4.
- SATO, K., ROESL, C., POLLOCK, N. & STOWELL, K. M. 2013. Skeletal Muscle Ryanodine Receptor Mutations Associated with Malignant Hyperthermia Showed

- Enhanced Intensity and Sensitivity to Triggering Drugs when Expressed in Human Embryonic Kidney Cells. *Anesthesiology*, 119, 111-8.
- SCHLEITHOFF, L., MEHRKE, G., REUTLINGER, B. & LEHMANN-HORN, F. 1999. Genomic structure and functional expression of a human alpha(2)/delta calcium channel subunit gene (CACNA2). *Genomics*, 61, 201-9.
- SEI, Y., GALLAGHER, K. L. & BASILE, A. S. 1999. Skeletal muscle type ryanodine receptor is involved in calcium signaling in human B lymphocytes. *J Biol Chem*, 274, 5995-6002.
- SEI, Y., SAMBUUGHIN, N. N., DAVIS, E. J., SACHS, D., CUENCA, P. B., BRANDOM, B. W., TAUTZ, T., ROSENBERG, H., NELSON, T. E. & MULDOON, S. M. 2004. Malignant hyperthermia in North America: genetic screening of the three hot spots in the type I ryanodine receptor gene. *Anesthesiology*, 101, 824-30.
- SERYSHEVA, II, HAMILTON, S. L., CHIU, W. & LUDTKE, S. J. 2005. Structure of Ca²⁺ release channel at 14 Å resolution. *J Mol Biol*, 345, 427-31.
- SERYSHEVA, II, SCHATZ, M., VAN HEEL, M., CHIU, W. & HAMILTON, S. L. 1999. Structure of the skeletal muscle calcium release channel activated with Ca²⁺ and AMP-PCP. *Biophys J*, 77, 1936-44.
- SHEPHERD, S., ELLIS, F., HALSALL, J., HOPKINS, P. & ROBINSON, R. 2004. RYR1 mutations in UK central core disease patients: more than just the C-terminal transmembrane region of the RYR1 gene. *J Med Genet*, 41, e33.
- SHUAIB, A., PAASUKE, R. T. & BROWNELL, K. W. 1987. Central core disease. Clinical features in 13 patients. *Medicine (Baltimore)*, 66, 389-96.
- SMYTH, J. T., HWANG, S. Y., TOMITA, T., DEHAVEN, W. I., MERCER, J. C. & PUTNEY, J. W. 2010. Activation and regulation of store-operated calcium entry. *J Cell Mol Med*, 14, 2337-49.
- SUDBRAK, R., PROCACCIO, V., KLAUSNITZER, M., CURRAN, J. L., MONSIEURS, K., VAN BROECKHOVEN, C., ELLIS, R., HEYETENS, L., HARTUNG, E. J., KOZAK-RIBBENS, G. & ET AL. 1995. Mapping of a further malignant hyperthermia susceptibility locus to chromosome 3q13.1. *Am J Hum Genet*, 56, 684-91.
- SUTKO, J. L., AIREY, J. A., WELCH, W. & RUEST, L. 1997. The pharmacology of ryanodine and related compounds. *Pharmacol Rev*, 49, 53-98.
- TOBIN, J. R., JASON, D. R., CHALLA, V. R., NELSON, T. E. & SAMBUUGHIN, N. 2001. Malignant hyperthermia and apparent heat stroke. *JAMA*, 286, 168-9.
- TONG, J., DU, G. G., CHEN, S. R. & MACLENNAN, D. H. 1999a. HEK-293 cells possess a carbachol- and thapsigargin-sensitive intracellular Ca²⁺ store that is responsive to stop-flow medium changes and insensitive to caffeine and ryanodine. *Biochem J*, 343 Pt 1, 39-44.
- TONG, J., MCCARTHY, T. V. & MACLENNAN, D. H. 1999b. Measurement of resting cytosolic Ca²⁺ concentrations and Ca²⁺ store size in HEK-293 cells transfected with malignant hyperthermia or central core disease mutant Ca²⁺ release channels. *J Biol Chem*, 274, 693-702.
- TONG, J., OYAMADA, H., DEMAUREX, N., GRINSTEIN, S., MCCARTHY, T. V. & MACLENNAN, D. H. 1997. Caffeine and halothane sensitivity of intracellular Ca²⁺ release is altered by 15 calcium release channel (ryanodine receptor)

- mutations associated with malignant hyperthermia and/or central core disease. *J Biol Chem*, 272, 26332-9.
- TREVES, S., LARINI, F., MENEGAZZI, P., STEINBERG, T. H., KOVAL, M., VILSEN, B., ANDERSEN, J. P. & ZORZATO, F. 1994. Alteration of intracellular Ca²⁺ transients in COS-7 cells transfected with the cDNA encoding skeletal-muscle ryanodine receptor carrying a mutation associated with malignant hyperthermia. *Biochem J*, 301 (Pt 3), 661-5.
- TREVES, S., VUKCEVIC, M., JEANNET, P. Y., LEVANO, S., GIRARD, T., URWYLER, A., FISCHER, D., VOIT, T., JUNGBLUTH, H., LILLIS, S., MUNTONI, F., QUINLIVAN, R., SARKOZY, A., BUSHBY, K. & ZORZATO, F. 2011. Enhanced excitation-coupled Ca(2+) entry induces nuclear translocation of NFAT and contributes to IL-6 release from myotubes from patients with central core disease. *Hum Mol Genet*, 20, 589-600.
- TUNG, C. C., LOBO, P. A., KIMLICKA, L. & VAN PETEGEM, F. 2010. The amino-terminal disease hotspot of ryanodine receptors forms a cytoplasmic vestibule. *Nature*, 468, 585-8.
- URWYLER, A., DEUFEL, T., MCCARTHY, T. & WEST, S. 2001. Guidelines for molecular genetic detection of susceptibility to malignant hyperthermia. *Br J Anaesth*, 86, 283-7.
- WANG, Y., FRAEFEL, C., PROTASI, F., MOORE, R. A., FESSENDEN, J. D., PESSAH, I. N., DIFRANCESCO, A., BREAKFIELD, X. & ALLEN, P. D. 2000. HSV-1 amplicon vectors are a highly efficient gene delivery system for skeletal muscle myoblasts and myotubes. *Am J Physiol Cell Physiol*, 278, C619-26.
- WAPPLER, F., FIEGE, M., STEINFATH, M., AGARWAL, K., SCHOLZ, J., SINGH, S., MATSCHKE, J. & SCHULTE AM ESCH, J. 2001. Evidence for susceptibility to malignant hyperthermia in patients with exercise-induced rhabdomyolysis. *Anesthesiology*, 94, 95-100.
- WEHNER, M., RUEFFERT, H., KOENIG, F., NEUHAUS, J. & OLTHOFF, D. 2002. Increased sensitivity to 4-chloro-m-cresol and caffeine in primary myotubes from malignant hyperthermia susceptible individuals carrying the ryanodine receptor 1 Thr2206Met (C6617T) mutation. *Clin Genet*, 62, 135-46.
- WEHNER, M., RUEFFERT, H., KOENIG, F. & OLTHOFF, D. 2004. Functional characterization of malignant hyperthermia-associated RyR1 mutations in exon 44, using the human myotube model. *Neuromuscul Disord*, 14, 429-37.
- WEISS, R. G., O'CONNELL, K. M., FLUCHER, B. E., ALLEN, P. D., GRABNER, M. & DIRKSEN, R. T. 2004. Functional analysis of the R1086H malignant hyperthermia mutation in the DHPR reveals an unexpected influence of the III-IV loop on skeletal muscle EC coupling. *Am J Physiol Cell Physiol*, 287, C1094-102.
- WILMSHURST, J. M., LILLIS, S., ZHOU, H., PILLAY, K., HENDERSON, H., KRESS, W., MULLER, C. R., NDONDO, A., CLOKE, V., CULLUP, T., BERTINI, E., BOENNEMANN, C., STRAUB, V., QUINLIVAN, R., DOWLING, J. J., AL-SARRAJ, S., TREVES, S., ABBS, S., MANZUR, A. Y., SEWRY, C. A., MUNTONI, F. & JUNGBLUTH, H. 2010. RYR1 mutations are a common cause of congenital myopathies with central nuclei. *Ann Neurol*, 68, 717-26.

- WINDER, W. W. & HARDIE, D. G. 1999. AMP-activated protein kinase, a metabolic master switch: possible roles in type 2 diabetes. *Am J Physiol*, 277, E1-10.
- WINDER, W. W., HOLMES, B. F., RUBINK, D. S., JENSEN, E. B., CHEN, M. & HOLLOSZY, J. O. 2000. Activation of AMP-activated protein kinase increases mitochondrial enzymes in skeletal muscle. *J Appl Physiol*, 88, 2219-26.
- YAMAMOTO, T., EL-HAYEK, R. & IKEMOTO, N. 2000. Postulated role of interdomain interaction within the ryanodine receptor in Ca(2+) channel regulation. *J Biol Chem*, 275, 11618-25.
- YANG, T., ESTEVE, E., PESSAH, I. N., MOLINSKI, T. F., ALLEN, P. D. & LOPEZ, J. R. 2007. Elevated resting [Ca(2+)]_i in myotubes expressing malignant hyperthermia RyR1 cDNAs is partially restored by modulation of passive calcium leak from the SR. *Am J Physiol Cell Physiol*, 292, C1591-8.
- YANG, T., RIEHL, J., ESTEVE, E., MATTHAEI, K. I., GOTH, S., ALLEN, P. D., PESSAH, I. N. & LOPEZ, J. R. 2006. Pharmacologic and functional characterization of malignant hyperthermia in the R163C RyR1 knock-in mouse. *Anesthesiology*, 105, 1164-75.
- YANG, T., TA, T. A., PESSAH, I. N. & ALLEN, P. D. 2003. Functional defects in six ryanodine receptor isoform-1 (RyR1) mutations associated with malignant hyperthermia and their impact on skeletal excitation-contraction coupling. *J Biol Chem*, 278, 25722-30.
- YASUDA, T., DELBONO, O., WANG, Z. M., MESSI, M. L., GIRARD, T., URWYLER, A., TREVES, S. & ZORZATO, F. 2013. JP-45/JSRP1 variants affect skeletal muscle excitation-contraction coupling by decreasing the sensitivity of the dihydropyridine receptor. *Hum Mutat*, 34, 184-90.
- YEH, H. M., TSAI, M. C., SU, Y. N., SHEN, R. C., HWANG, J. J., SUN, W. Z. & LAI, L. P. 2005. Denaturing high performance liquid chromatography screening of ryanodine receptor type 1 gene in patients with malignant hyperthermia in Taiwan and identification of a novel mutation (Y522C). *Anesth Analg*, 101, 1401-6.
- YIN, W., XIANG, P. & LI, Q. 2005. Investigations of the effect of DNA size in transient transfection assay using dual luciferase system. *Anal Biochem*, 346, 289-94.
- YUCHI, Z., LAU, K. & VAN PETEGEM, F. 2012. Disease mutations in the ryanodine receptor central region: crystal structures of a phosphorylation hot spot domain. *Structure*, 20, 1201-11.
- YUEN, B., BONCOMPAGNI, S., FENG, W., YANG, T., LOPEZ, J. R., MATTHAEI, K. I., GOTH, S. R., PROTASI, F., FRANZINI-ARMSTRONG, C., ALLEN, P. D. & PESSAH, I. N. 2012. Mice expressing T4826I-RYR1 are viable but exhibit sex- and genotype-dependent susceptibility to malignant hyperthermia and muscle damage. *FASEB J*, 26, 1311-22.
- ZHANG, Y., CHEN, H. S., KHANNA, V. K., DE LEON, S., PHILLIPS, M. S., SCHAPPERT, K., BRITT, B. A., BROWELL, A. K. & MACLENNAN, D. H. 1993. A mutation in the human ryanodine receptor gene associated with central core disease. *Nat Genet*, 5, 46-50.

- ZHOU, H., BROCKINGTON, M., JUNGBLUTH, H., MONK, D., STANIER, P., SEWRY, C. A., MOORE, G. E. & MUNTONI, F. 2006a. Epigenetic allele silencing unveils recessive RYR1 mutations in core myopathies. *Am J Hum Genet*, 79, 859-68.
- ZHOU, H., YAMAGUCHI, N., XU, L., WANG, Y., SEWRY, C., JUNGBLUTH, H., ZORZATO, F., BERTINI, E., MUNTONI, F., MEISSNER, G. & TREVES, S. 2006b. Characterization of recessive RYR1 mutations in core myopathies. *Hum Mol Genet*, 15, 2791-803.
- ZVARITCH, E., DEPREUX, F., KRAEVA, N., LOY, R. E., GOONASEKERA, S. A., BONCOMPAGNI, S., KRAEV, A., GRAMOLINI, A. O., DIRKSEN, R. T., FRANZINI-ARMSTRONG, C., SEIDMAN, C. E., SEIDMAN, J. G. & MACLENNAN, D. H. 2007. An Ryr1I4895T mutation abolishes Ca²⁺ release channel function and delays development in homozygous offspring of a mutant mouse line. *Proc Natl Acad Sci U S A*, 104, 18537-42.